HEREDITARY OPTIC NEUROPATHIES: A NEW PERSPECTIVE

EDITED BY: Chiara La Morgia, Valerio Carelli and Rustum Karanjia

frontiers Research Topics

About Frontiers

Frontiers is more than just an open-access publisher of scholarly articles: it is a pioneering approach to the world of academia, radically improving the way scholarly research is managed. The grand vision of Frontiers is a world where all people have an equal opportunity to seek, share and generate knowledge. Frontiers provides immediate and permanent online open access to all its publications, but this alone is not enough to realize our grand goals.

Frontiers Journal Series

The Frontiers Journal Series is a multi-tier and interdisciplinary set of open-access, online journals, promising a paradigm shift from the current review, selection and dissemination processes in academic publishing. All Frontiers journals are driven by researchers for researchers; therefore, they constitute a service to the scholarly community. At the same time, the Frontiers Journal Series operates on a revolutionary invention, the tiered publishing system, initially addressing specific communities of scholars, and gradually climbing up to broader public understanding, thus serving the interests of the lay society, too.

Dedication to Quality

Each Frontiers article is a landmark of the highest quality, thanks to genuinely collaborative interactions between authors and review editors, who include some of the world's best academicians. Research must be certified by peers before entering a stream of knowledge that may eventually reach the public - and shape society; therefore, Frontiers only applies the most rigorous and unbiased reviews.
Frontiers revolutionizes research publishing by freely delivering the most outstanding research, evaluated with no bias from both the academic and social point of view. By applying the most advanced information technologies, Frontiers is catapulting scholarly publishing into a new generation.

What are Frontiers Research Topics?

Frontiers Research Topics are very popular trademarks of the Frontiers Journals Series: they are collections of at least ten articles, all centered on a particular subject. With their unique mix of varied contributions from Original Research to Review Articles, Frontiers Research Topics unify the most influential researchers, the latest key findings and historical advances in a hot research area! Find out more on how to host your own Frontiers Research Topic or contribute to one as an author by contacting the Frontiers Editorial Office: frontiersin.org/about/contact

HEREDITARY OPTIC NEUROPATHIES: A NEW PERSPECTIVE

Topic Editors:
Chiara La Morgia, IRCCS Institute of Neurological Sciences of Bologna (ISNB), Italy
Valerio Carelli, University of Bologna, Italy
Rustum Karanjia, University of Ottawa, Canada

Table of Contents

Editorial: Hereditary Optic Neuropathies: A New Perspective

Valerio Carelli[1,2], Rustum Karanjia[3,4,5,6] and Chiara La Morgia[1,7]

[1] Istituto di Ricerca e Cura a Carattere Scientifico Istituto delle Scienze Neurologiche di Bologna, Programma di Neurogenetica, Bologna, Italy, [2] Department of Biomedical and Neuromotor Sciences (DIBINEM), University of Bologna, Bologna, Italy, [3] Doheny Eye Institute, Los Angeles, CA, United States, [4] Department of Ophthalmology, Doheny Eye Center, David Geffen School of Medicine, University of California, Los Angeles, Los Angeles, CA, United States, [5] Department of Ophthalmology, Ottawa Eye Institute, University of Ottawa, Ottawa, ON, Canada, [6] Ottawa Hospital Research Institute, Ottawa, ON, Canada, [7] Istituto di Ricerca e Cura a Carattere Scientifico Istituto delle Scienze Neurologiche di Bologna, UOC Clinica Neurologica, Bologna, Italy

Editorial on the Research Topic

Hereditary Optic Neuropathies: A New Perspective

Over 30 years have elapsed from the landmark finding of the first point mutation in mitochondrial DNA (mtDNA) associated with Leber's hereditary optic neuropathy (LHON) by Doug Wallace and his team in 1988 (1). Twelve years later came the identification of the nuclear *OPA1* gene, which encodes for a mitochondrial dynamin-like protein, whose pathogenic mutations cause Dominant Optic Atrophy (DOA) (2, 3). This was a predictable convergence, as both nuclear and mtDNA mutations may cause a similar mitochondrial disorder resulting in vision loss, identifying DOA as a mitochondrial disease similar to LHON (4, 5). We are delighted to have compiled this special issue of Frontiers in Neurology on hereditary optic neuropathies, to highlight how lively the field of inherited optic neuropathies is in 2021.

Three of the papers published in this series deal with new mtDNA variants affecting complex I in association with LHON, highlighting the emergence of the *MT-ND5* gene as a new hot spot for LHON mutations (Sun et al.; Engvall et al.; Peverelli et al.). Thus, quoting Salvatore DiMauro, these findings clearly indicate that "*we are not scraping the bottom of the barrel*" yet (6). Complex I remains the most frequent biochemical defect and LHON-like phenotypes may frequently overlap with more complex phenotypes combining MELAS and Leigh syndrome features in a continuum (7).

LHON remains a paradigm for mitochondrial disorders and neurodegeneration, thus continuous efforts are directed to the intimate understanding of its pathogenic mechanism. The *in vitro* modeling of disease has become key to preclinical science, and the use of reprogrammed pluripotent stem cells (iPSCs) derived from primary LHON patient's cells, into differentiated neuronal cellular types including retinal ganglion cells (RGCs) is expanding our toolbox to understand and treat this and other diseases (Peron et al.). This emergent biotechnology to model rare disorders such as LHON, also overcomes some of the difficulties of using animal models, which do not always faithfully reproduce mitochondrial diseases. The innovative models like iPSCs-derived organoids have helped to untangling the details of the pathogenic mechanisms allowing multiomic approaches at single cell type level (8), truly applying the principles of personalized medicine, as summarized in a perspective article in this special issue (Peron et al.).

RGCs are special neurons that are functionally asymmetric and metabolically skewed by the architecture of their axons (4, 5). The need to keep the inner retina transparent to light requires the RGC axons to remain unmyelinated for their long intra-retinal segment, before converging at the optic disc to form the myelinated optic nerve. Understanding this special neuronal cell type is essential to dissect hereditary optic neuropathies and this aspect is comprehensively covered in a complete review of the 18 RGCs subtypes and their morphological and functional characteristics as part of this special issue (Kim et al.). This review also looks at the tools to explore RGCs and how they are eventually lost in different pathological conditions including inherited and acquired optic neuropathies.

DOA, as previously stated, is a companion disease to LHON, which in the large majority of cases is due to various types of pathogenic mutations in the OPA1 gene (2, 3). This gene encodes a protein that comes in 8 isoforms further processed from long to short forms, providing a "kaleidoscopic" spectrum of functions, a concept which is comprehensively reviewed in this special issue, covering the wide range of models used to study OPA1 to date (Del Dotto and Carelli) The complexities of OPA1 function and dysfunction may include mechanisms regulating the cellular resilience during development and adulthood, such as adaptations to OPA1 deficiency that may be reflected in mitochondrial motility or inflammatory responses, which ultimately impinge on cell aging, as argued in a dedicated article in this special issue (Erchova et al.).

Understanding the clinical presentation of these diseases continues to evolve and the use of new objective clinical metrics, such as the photopic negative response (PhNR), are becoming more important as new treatments are being developed (Botelho et al.). Again, LHON is on the frontline of new treatment strategies with gene therapy trials, which have been recently concluded, and the first and up to now the only therapy approved for a mitochondrial disorder by the European Medicines Agency, the quinone analog idebenone. These clinical topics have been reviewed in a contribution to this special issue (Hage andVignal-Clermont). Moreover, a comparison between the recently published results of gene therapy trials and the natural history of LHON is included in this special issue and provides an interesting perspective on the success of these treatments (Newman et al.).

Overall, the field of hereditary optic neuropathies remains extremely dynamic and lively. By presenting the "tip of the neurodegeneration iceberg" in this special issue we hope to demonstrate the importance of these diseases as an informative model to make key observation of relevance to other neurodegenerative disorders (9). From the genetic foundation, to the clinical and preclinical research, and ultimately ending with new therapeutic strategies, we look forward to further groundbreaking progress in hereditary optic neuropathies, leading to the ultimate goal of an effective cure for these patients, preserving vision.

AUTHOR CONTRIBUTIONS

All authors listed have made a substantial, direct and intellectual contribution to the work, and approved it for publication.

FUNDING

REFERENCES

1. Wallace DC, Singh G, Lott MT, Hodge JA, Schurr TG, Lezza AM, et al. Mitochondrial DNA mutation associated with Leber's hereditary optic neuropathy. Science. (1988) 242:1427–30. doi: 10.1126/science.3201231
2. Delettre C, Lenaers G, Griffoin JM, Gigarel N, Lorenzo C, Belenguer P, et al. Nuclear gene OPA1, encoding a mitochondrial dynamin-related protein, is mutated in dominant optic atrophy. Nat Genet. (2000) 26:207–10. doi: 10.1038/79936
3. Alexander C, Votruba M, Pesch UE, Thiselton DL, Mayer S, Moore A, et al. OPA1, encoding a dynamin-related GTPase, is mutated in autosomal dominant optic atrophy linked to chromosome 3q28. Nat Genet. (2000) 26:211–5. doi: 10.1038/79944
4. Carelli V, Ross-Cisneros FN, Sadun AA. Mitochondrial dysfunction as a cause of optic neuropathies. Prog Retin Eye Res. (2004) 23:53–89. doi: 10.1016/j.preteyeres.2003.10.003
5. Yu-Wai-Man P, Griffiths PG, Chinnery PF. Mitochondrial optic neuropathies - disease mechanisms and therapeutic strategies. Prog Retin Eye Res. (2011) 30:81–114. doi: 10.1016/j.preteyeres.2010.11.002
6. DiMauro S, Andreu AL. Mutations in mtDNA: are we scraping the bottom of the barrel? Brain Pathol. (2000) 10:431–41. doi: 10.1111/j.1750-3639.2000.tb00275.x
7. Carelli V, La Morgia C, Valentino ML, Barboni P, Ross-Cisneros FN, Sadun AA. Retinal ganglion cell neurodegeneration in mitochondrial inherited disorders. Biochim Biophys Acta. (2009) 1787:518–28. doi: 10.1016/j.bbabio.2009.02.024
8. Cowan CS, Renner M, De Gennaro M, Gross-Scherf B, Goldblum D, Hou Y, et al. Cell types of the human retina and its organoids at single-cell resolution. Cell. (2020) 182:1623–40.e34. doi: 10.1016/j.cell.2020.08.013

9. Carelli V, La Morgia C, Ross-Cisneros FN, Sadun AA. Optic neuropathies: the tip of the neurodegeneration iceberg. *Hum Mol Genet.* (2017) 26:R139–50. doi: 10.1093/hmg/ddx273

Publisher's Note: All claims expressed in this article are solely those of the authors and do not necessarily represent those of their affiliated organizations, or those of the publisher, the editors and the reviewers. Any product that may be evaluated in this article, or claim that may be made by its manufacturer, is not guaranteed or endorsed by the publisher.

Impaired Ganglion Cell Function Objectively Assessed by the Photopic Negative Response in Affected and Asymptomatic Members From Brazilian Families With Leber's Hereditary Optic Neuropathy

Gabriel Izan Santos Botelho[1], Solange Rios Salomão[1], Célia Harumi Tengan[2], Rustum Karanjia[3,4,5,6], Felipo Victor Moura[2], Daniel Martins Rocha[1], Paula Baptista Eliseo da Silva[1], Arthur Gustavo Fernandes[1], Sung Eun Song Watanabe[1], Paula Yuri Sacai[1], Rubens Belfort Jr.[1,7], Valerio Carelli[8], Alfredo Arrigo Sadun[3,4] and Adriana Berezovsky[1]*

[1] Departamento de Oftalmologia e Ciências Visuais, Escola Paulista de Medicina, Universidade Federal de São Paulo, São Paulo, Brazil, [2] Departamento de Neurologia e Neurocirurgia, Escola Paulista de Medicina, Universidade Federal de São Paulo, São Paulo, Brazil, [3] Doheny Eye Institute, University of California Los Angeles, Los Angeles, CA, United States, [4] Department of Ophthalmology, Doheny Eye Center, David Geffen School of Medicine at UCLA, Los Angeles, CA, United States, [5] Ottawa Eye Institute, University of Ottawa, Ottawa, ON, Canada, [6] Ottawa Hospital Research Institute, Ottawa, ON, Canada, [7] Instituto da Visão-IPEPO, São Paulo, Brazil, [8] Department of Biomedical and NeuroMotor Sciences (DIBINEM), University of Bologna School of Medicine, Bologna, Italy

Purpose: The photopic negative response (PhNR) is an electrophysiological method that provides retinal ganglion cell function assessment using full-field stimulation that does not require clear optics or refractive correction. The purpose of this study was to assess ganglion cell function by PhNR in affected and asymptomatic carriers from Brazilian families with LHON.

Methods: Individuals either under suspicion or previously diagnosed with LHON and their family members were invited to participate in this cross-sectional study. Screening for the most frequent LHON mtDNA mutations was performed. Visual acuity, color discrimination, visual fields, pattern-reversal visual evoked potentials (PRVEP), full-field electroretinography and PhNR were tested. A control group of healthy subjects was included. Full-field ERG PhNR were recorded using red (640 nm) flashes at $1 \, \text{cd.s/m}^2$, on blue (470 nm) rod saturating background. PhNR amplitude (μV) was measured using baseline-to-trough (BT). Optical coherence tomography scans of both the retinal nerve fiber layer (RNFL) and ganglion cell complex (GCC) were measured. PhNR amplitudes among affected, carriers and controls were compared by Kruskal-Wallis test followed by *post-hoc* Dunn test. The associations between PhNR amplitude and OCT parameters were analyzed by Spearman rank correlation.

Results: Participants were 24 LHON affected patients (23 males, mean age=30.5 ± 11.4 yrs) from 19 families with the following genotype: m.11778G>A [$N = 15$ (62%), 14 males]; m.14484T>C [$N = 5$ (21%), all males] and m.3460G>A [$N = 4$ (17%), all males]

and 14 carriers [13 females, mean age: 43.2 ± 13.3 yrs; m.11778G>A ($N = 11$); m.3460G>A ($N = 2$) and m.14484T>C ($N = 1$)]. Controls were eight females and seven males (mean age: 32.6 ± 11.5 yrs). PhNR amplitudes were significantly reduced ($p = 0.0001$) in LHON affected (-5.96 ± 3.37 μV) compared to carriers (-16.53 ± 3.40 μV) and controls (-23.91 ± 4.83; $p < 0.0001$) and in carriers compared to controls ($p = 0.01$). A significant negative correlation was found between PhNR amplitude and total macular ganglion cell thickness ($r = -0.62$, $p < 0.05$). Severe abnormalities in color discrimination, visual fields and PRVEPs were found in affected and subclinical abnormalities in carriers.

Conclusions: In this cohort of Brazilian families with LHON the photopic negative response was severely reduced in affected patients and mildly reduced in asymptomatic carriers suggesting possible subclinical abnormalities in the latter. These findings were similar among pathogenic mutations.

Keywords: leber's hereditary optic neuropathy, photopic negative response, retinal ganglion cell, visual evoked cortical potentials, electroretinography

INTRODUCTION

Leber's hereditary optic neuropathy (LHON) is a disease characterized by a sub-acute, painless loss of central vision, either simultaneously or in one eye followed by the other eye within weeks to months, affecting mainly young male adults between 15 and 35 years of age (1). The loss of vision is due to selective vulnerability of retinal ganglion cells (RGCs) in the papillomacular bundle that causes central scotoma and subsequent optic atrophy (2, 3).

The disease is caused by mutations in the mitochondrial DNA (mtDNA) that disrupt critical complex I subunits of the mitochondrial respiratory chain, causing impaired cellular ATP synthesis and increased production of reactive oxygen species (4, 5). The main mutations are m.11778G>A (ND4), m.14484T>C (ND6) and m.3460G>A (ND1) considered the three primary variations and representing over 90% of all LHON cases (5).

LHON is the most common of the mtDNA diseases, but epidemiological studies on prevalence and incidence involving different countries are scarce. A recent meta-analysis in Europe, estimated LHON prevalence of one in 40,000 (6). LHON is more frequent in males with the male/female ratio varying from 3:1 to 8:1, depending on the LHON mutation and the population studied (1, 7). The penetrance of the disease is incomplete with

only about 50% of males and 10% of females carrying a genetic defect becoming affected and a substantial number of individuals along the maternal line carrying the genetic defect remaining asymptomatic lifelong (1).

A very large Brazilian pedigree with m.11778G>A/haplogroup J LHON (SOA-BR) has been extensively studied (3, 8–32) but information on other Brazilian LHON families has not been thoroughly investigated. A major obstacle in a developing country is the poor access to genetic analysis which provides confirmation of one of the three primary LHON mtDNA mutations, even though a strong clinical suspicion of the disease was present based on symptoms and neuro-ophthalmological assessment (33).

The involvement of RGCs on the LHON pathophysiology has been confirmed by fundoscopy, optical coherence tomography (OCT) and histopathological studies (23, 33–35). Recently, it was discovered that RGCs also generate a slow negative wave response observable on the full-field electroretinogram (ff-ERG) immediately following the b-wave of the cone response. This component of the ERG is referred to as the photopic negative response (PhNR) (36) and it has not been fully incorporated in conventional full-field ERG protocols as it is recommended as an expanded testing protocol by the ISCEV (37, 38). Reduced PhNR amplitudes have been reported in patients with RGCs pathologies such as glaucoma (39–42), optic atrophy (43, 44), childhood optic glioma (45), retinal vascular diseases (46–50) and idiopathic intracranial hypertension (51, 52).

A previous study including only members from the SOA-BR pedigree reported that PhNR amplitude is significantly decreased in patients affected by LHON compared to carriers and there was also a decrease in PhNR in carriers, suggesting potential subclinical RGC dysfunction (32). Electrophysiological assessment including PhNR performed in LHON families from the United Kingdom harboring one of the three common mtDNA mutations, was attenuated in affected individuals (53).

Abbreviations: BT, Baseline to trough; SOA-BR, Brazilian pedigree with m.11778G>A/haplogroup J LHON; DTL-Plus™, Dawson-Trick-Litzkow; ETDRS, Early Treatment Diabetic Retinopathy Study; UNIFESP, Federal University of São Paulo; N75, First negative deflection; P100, First positive deflection; FVEP, Flash Visually Evoked Potential; ff-ERG, Full-field electroretinogram; GCC, Ganglion cell complex; GCL, Ganglion cell layer; IPL, Inner plexiform layer; ISCEV, International Society of Clinical Electrophysiology of Vision; kΩ, Kilo Ohms; LHON, Leber's hereditary optic neuropathy; logMAR, Logarithm of the minimum angle of resolution; MD, Mean deviation; μV, Microvolt; ms, Milisecond; mtDNA, Mitochondrial DNA; nm, Nanometer; OPL, Outer plexiform layer; PRVEP, Pattern-Reversal Visually Evoked Potential; PT, Peak to trough; PhNR, Photopic negative response; ROC, Receiver operating characteristic; RGCs, Retinal ganglion cells.

Our purpose was to prospectively investigate a cohort of Brazilian families other than the extensively studied SOA-BR pedigree, aiming to assess ganglion cell function by PhNR in affected and asymptomatic carriers. Additionally, other clinical features were studied by comprehensive ophthalmic and electrophysiological testing including visual acuity, fundus exam, optical coherence tomography, color discrimination, visual fields, visually evoked potentials and full-field electroretinography.

METHODS

In this prospective, observational, cross-sectional study, patients with a clinical suspicion or diagnosis of LHON and their family members were invited for a free-of-charge assessment in the Clinical Electrophysiology of Vision Laboratory of the Federal University of São Paulo (UNIFESP) from August 2018 to January 2020. The inclusion criteria were the presence of the following features: (a) clinical symptoms suggesting LHON including painless and subacute blurred vision either bilateral or in one eye followed by the other; (b) vascular tortuosity of the central retinal vessels, swelling of the retinal nerve fiber layer and peripapillary telangiectatic microangiopathy and optic disc atrophy or paleness; (c) dyschromatopsia or color blindness and central scotoma, and (d) family history of individuals with bilateral sequential visual loss in the maternal line. Subjects with macular degeneration or signs of pathology of the optic nerve other than LHON were excluded.

A control group was included with healthy volunteers recruited among students and employees from the Federal University of São Paulo. Inclusion criteria for the control group were: visual acuity with current correction in either eye = 0.0 logMAR and normal ophthalmic examination. The exclusion criteria were: high ametropia (spherical equivalent = ±5.00 diopters), any systemic disease, family history of glaucoma, history of previous eye surgery and history of hereditary eye diseases.

This study has been approved by the Committee of Ethics in Research of the Federal University of São Paulo and adhered to the tenets of the Declaration of Helsinki. All participants provided informed consent.

PROCEDURES

Clinical Parameters

A thorough history was taken to determine demographic features as age, sex, associated symptoms, age at onset of vision loss and time between the first and second affected eyes. Family history of LHON was collected and a family pedigree was elaborated. Any known exposure to environmental toxins, tobacco, alcohol, and drugs was also noted. Additional information included whether patients were currently being treated with idebenone.

Visual Electrophysiological Assessment
Pattern-Reversal Visually Evoked Potential and Flash Visually Evoked Potential

PRVEP and FVEP were done with natural pupils in a darkened room using the UTAS E-3000 Electrodiagnostic System (LKC

Technologies Inc., Gaithersburg, MD, USA), in accordance with International Society of Clinical Electrophysiology of Vision (ISCEV) guidelines (54). PRVEP of each eye were obtained using electrodes placed according to the 10–20 system. The active, reference, and ground electrodes were placed at O_z, FP_z, and C_z respectively. Stimuli were presented in a monochromatic CRT display at a 1 m distance using two check sizes subtending 15' and 60' visual angles.

The PRVEP waveforms were triphasic. The main positive deflection was the P100, the preceding and following negative deflections were the N75 and the N135, respectively. Peak-to-peak amplitudes were measured from the first negative deflection (N75) to the following positive deflection (P100) and expressed in microvolts (μV). Peak times were measured for P100 in milliseconds (ms). Amplitudes were classified as normal or reduced and P100 peak times as normal or delayed in relation to normative cutoffs obtained from normal values of our own laboratory (55).

FVEP was presented inside a Ganzfeld dome and the waveforms were composed by successive deflections and named in order of appearance. The first and the second positive deflections were named P1 and P2, respectively, and their preceding negative deflections, N1 and N2. Peak-to-peak amplitudes (μV) were measured for N1–P1 and N2–P2 complexes. Peak times (ms) were measured for all deflections (N1, P1, N2, and P2).

Full-field ERG
ERGs were performed following ISCEV standardized protocol in both eyes (37). Both pupils were dilated (pupil diameter >7 mm) after administering a drop of tropicamide 1% and a drop of phenylephrine 10%, and all subjects were dark-adapted for 30 min. The corneal surface was anesthetized with two drops of tetracaine 1.0% and a bipolar contact lens electrode (Burian-Allen bipolar electrode, Hansen Ophthalmic Development Lab, Coralville, IA, USA) was placed on the corneal surface with a drop of methylcellulose 2%. A gold cup ground electrode was applied to the earlobe. All stimuli were presented in a Ganzfeld dome. Dark-adapted responses from rods, combined rod and cone and oscillatory potentials followed by light-adapted photopic responses from single-flash cone and 30-Hz flicker were recorded. Signals were amplified, digitized, averaged and saved by a digital plotter (UTAS E-3000 System, LKC Technologies Inc., Gaithersburg, MD, USA). The peak-to-peak amplitude (μV) and the implicit time (ms) from each step of the ISCEV standard protocol were determined. The oscillatory potential amplitude was calculated as the sum of each wavelet and automatically analyzed by the UTAS E-3000 system (56). Amplitudes and peak times were classified in relation to normal values obtained in our own laboratory (57).

PhNR of the Light-Adapted ERG
Both pupils were dilated (pupil diameter >7 mm) with one drop each of tropicamide 1% and phenylephrine 10% and then light-adapted for 10 min followed by 1 min of preadaptation to the blue background light before the first stimulus. The corneal surface was anesthetized with two drops of tetracaine 1%.

ERGs were registered with Dawson-Trick-Litzkow (DTL-Plus™) micro conductors (Diagnosys LLC, Lowell, MA, USA) attached to the nasal and temporal canthus with the fiber positioned on the lower border of the cornea. Gold cup electrodes were used in the temple for reference and Fz for ground. Electrode impedance was checked and set at 5 kilo Ohms (kΩ) or less. All stimuli were presented in a LED-based ColorBurst™ mini-ganzfeld handheld stimulator (Diagnosys LLC, Lowell, MA, USA) as previously described (58).

A flash of a red stimulus (640 nm) lasting 4 ms was recorded at a rate of 2 Hz against a blue (470 nm) background saturation. The flashing red stimulus was presented at $1 \, cd.s/m^2$, while the blue background remained at $10 \, cd/m^2$. Three sets of 50 sweeps lasting 150 ms were recorded using a bandpass filter between 0.3 and 300 Hz. The PhNR waveforms were amplified, digitized and saved by an Espion e2™ (Diagnosys LLC, Lowell, MA, USA). Each of the three repetitions was edited to eliminate artifacts and determine a constant average value. The records were obtained and analyzed from both eyes (58).

The a-wave, b-wave and PhNR were determined for each peak time (ms) and amplitudes (μV) by two experienced examiners (AB, GISB). PhNR was specified as a negative-going wave that occurs after the b-wave. PhNR can be measured from baseline to trough (BT, the amplitude to the trough of the PhNR measured from pre-stimulus baseline of 0 μV) or from peak to trough (PT, the amplitude between the peak of the b-wave and the trough of the PhNR). Wave ratios BT/b and PT/b were also evaluated (58).

Fundus Photography and OCT Imaging

Dilated indirect ophthalmoscopy and fundus photography (iCam Camera, Optovue, Fremont, CA, USA) were performed. Spectral-domain OCT (iVue SD-OCT, Optovue, Fremont, CA, USA) was used for imaging of the macula and the optic nerve head from both eyes under pupil dilation. Automated segmentation (manually confirmed) and thickness analyses were performed for macular ganglion cell complex (GCC) and peripapillary retinal nerve fiber layer (RNFL) thickness. For peripapillary RNFL measurement, a 3.45 mm diameter circular scan centered on the optic disc was used and the data of four sectors (temporal, superior, nasal and inferior) were collected. Scans with a 6 × 6 mm circular field were used for acquire global macular GCC (comprised of retinal ganglion cell layer, inner plexiform layer and RNFL). The normal range of global macular GCC and RNFL thickness were considered from database of SD-OCT Optovue. The image acquisition software had its own quality indicator based on the signal power index (SQI), which classifies the mappings as "good" (if SQI ≥ 60) or "bad" (if SQI < 60). Images with segmentation failures, significant motion artifacts, or signal strength <60 were excluded.

Psychophysical Testing: Visual Acuity, Color Vision, and Visual Fields

Visual acuity was measured with current correction by using a retro-illuminated Early Treatment Diabetic Retinopathy Study (ETDRS) chart positioned at 4 m, expressed as a logarithm of the minimum angle of resolution (logMAR). Counting fingers, hand movements, light perception and no light perception, were respectively, converted to 1.8; 2.3; 2.8, and 3.0 logMAR (59).

Color discrimination was estimated by two distinct tests: The Pseudo-Isochromatic Plates for Testing Color Perception (American Optical Corporation) and the Farnsworth-Munsell 100 Hue Color Test (13). The Pseudo-Isochromatic Test is composed by 15 plates of numeric patterns of one or two digits and the score was set as the number of plates identified. Farnsworth-Munsell 100-hue color test was used for monocular color vision assessment and the scoring software was used to evaluate subject's color vision discrimination providing error score and axis.

Visual field testing was performed in either eye of affected and unaffected subjects according to the visual status. For eyes with VA <20/200 the Goldmann kinetic perimetry was performed whereas eyes with VA ≥20/200 had their visual fields tested with the Humphrey visual field analyzer (HVFA)with SITA-Standard 30-2 protocol (HFAII 750 Threshold Test, Carl Zeiss Meditec, Jena, Germany). Visual field defects were quantified by measurement of mean deviation (MD) in Humphrey visual field test and the occurrence of central scotoma (defined as isolated scotoma in the circular area between 0 and 10 degrees), cecocentral scotoma or full-field defect in both perimeters.

Molecular Analysis

Genomic DNA was extracted from blood samples using the QIAamp DNA Mini Kit (Qiagen®). Screening of the m.11778G>A, m.3460G>A, and m.14484 T>C mutations was performed by Sanger Sequencing. We amplified the regions encompassing these mutations by polymerase chain reaction (PCR) with the following pairs of primers: (from mtDNA position 11,640 to 12,413) 5'- TAGCCCTCGTAGTAACAG CCATT-3' and 5'- GGGTTAACGAGGGTGGTAAGG-3'; (from mtDNA position 3,130 to 3,751) 5'- AGGACAAGAGAA ATAAGGCC-3' and 5'- TGATGGCTAGGGGTGACTTCAT-3'; (from mtDNA position 14,150 to 14,810) 5' – CTATTCCCC GAGCAATCTCAATT-3' and 5' CCACATCATTCATCGACCT CC-3'. PCR products were purified with the QIAEX II Gel Extraction Kit (Qiagen®), and 90 ng of the purified product was used for sequencing reactions with BigDye™ Terminator v3.1 Cycle Sequencing kit (Applied Biosystems ™), and according to manufacturer's instructions. Sequencing PCR products were electrophoresed in a 3,130 Genetic Analyzer (Applied Biosystems TM), and the obtained sequences compared to the revised Cambridge Reference Sequence (NC_12920).

The presence of heteroplasmy was confirmed by restriction fragment length polymorphism analysis (RFLP). For the m.11778G>A mutation, we amplified a region between mtDNA positions 11,640 and 12,898, which was digested with *Bms*I (*SfaN*I isoschizomer; Invitrogen™). This fragment contains restriction sites for *Bms*I at positions 11,787, 12,466, and 12,813, giving rise to fragments with 147 bp, 679 bp, 347 bp, and 85 bp. The mutation abolishes the restriction site located at position 11787, generating fragments with 826 bp, 347 bp, and 85 bp. In the case of the m.3460G>A mutation, the fragment between positions 3,130 and 3,751 was digested

with *Hin*1I (*Bsa*HI isoschizomer; Thermo Scientific). This fragment contains a restriction site for *Hin*1I, at position 3,459, generating two fragments: with 329 bp and 292 bp. The m.3460G>A mutation abolishes this restriction site. In both cases, digested products were run in a 2% agarose gel, stained with ethidium bromide, and visualized under UV light (60).

Statistical Analysis

Statistical analyses were performed using Stata/SE Statistical Software, Release 14.0, 2015 (Stata Corp, College Station, Texas, USA). Frequency tables were used for descriptive

analysis. The association of continuous results with categorical predictors was evaluated through Kruskal-Wallis test followed by *post-hoc* analysis of Dunn. Receiver operating characteristic (ROC) curve was constructed to determine the best cut-off of PhNR BT amplitudes for detecting affected participants as well as to determine sensitivity and specificity. Correlations between different continuous parameters were evaluated using Spearman correlation test. *P*-values ≤0.05 were considered statistically significant.

Both eyes from each participant were tested for all procedures. However, for statistical analysis, only data from one eye of each

TABLE 1 | Demographics, visual acuity, substance usage and idebenone therapy from 24 genotyped affected LHON participants.

Subject	Family #	Age (years)	Sex	Genotype	VA (logMAR)		Age onset (years)	Interval between eyes (months)	Substance usage	Idebenone
					RE	LE				
A1	1	14	M	m.11778G>A homoplasmic	1.9	**HM**	12	2	None	N
A2	2	16	M	m.11778G>A homoplasmic	1.2	**1.4**	11	0.5	None	N
A3	3[+]	17	M	m.11778G>A homoplasmic	0.2	**0.9**	16	0	None	Y
A4	4	19	M	m.11778G>A homoplasmic	**1.9**	1.9	15	1	None	Y
A5	3[+]	21	M	m.11778G>A homoplasmic	0.5	**CF**	20	0.5	None	N
A6	5	24	M	m.11778G>A homoplasmic	**1.3**	1.0	17	0.25	A	N
A7	6[+]	25	M	m.11778G>A homoplasmic	**0.7**	0	20	0	None	N
A8	6[+]	27	M	m.11778G>A homoplasmic	1.0	**1.2**	19	0	None	N
A9	7	27	M	m.11778G>A homoplasmic	1.6	**1.5**	25	4.5	A	N
A10	8	31	M	m.11778G>A homoplasmic	**HM**	HM	20	0	None	N
A11	9	33	M	m.11778G>A heteroplasmic	**1.5**	1.4	27	12	A	Y
A12	10	33	M	m.11778G>A homoplasmic	CF	**HM**	15	0	None	N
A13	11	33	M	m.11778G>A homoplasmic	**HM**	HM	25	5	None	N
A14	12[§]	39	F	m.11778G>A homoplasmic	CF	**CF**	11	0.25	None	N
A15	12[§]	62	M	m.11778G>A homoplasmic	**HM**	HM	18	6	A, T	N
		$\overline{X} = 28.5 \pm 27.4$					$\overline{X} = 18.3 \pm 4.8$	$\overline{X} = 2.1 \pm 3.4$		
A16	13	28	M	m.14484T>C homoplasmic	0.9	**1.0**	14	3	None	N
A17	14	39	M	m.14484T>C homoplasmic	**1.5**	1.0	38	5	A, T	N
A18	15	43	M	m.14484T>C homoplasmic	**1.4**	1.1	28	6	A	N
A19	16[+]	44	M	m.14484T>C homoplasmic	0.8	**0.9**	14	2	None	N
A20	16[+]	48	M	m.14484T>C homoplasmic	**0.4**	0.3	25	0.5	A, T	N
		$\overline{X} = 40.9 \pm 7.6$					$\overline{X} = 24.1 \pm 9.8$	$\overline{X} = 3.2 \pm 2.2$		
A21	17*	21	M	m.3460G>A heteroplasmic	**1.6**	1.8	14	0	A, T, C	N
A22	17*	21	M	m.3460G>A heteroplasmic	**1.8**	1.6	15	1	A, C	N
A23	18	25	M	m.3460G>A homoplasmic	**1.1**	1.3	22	2	None	Y
A24	19	31	M	m.3460G>A homoplasmic	1.8	**CF**	29	1	A, T	N
		$\overline{X} = 24.7 \pm 4.8$					$\overline{X} = 20.5 \pm 7.0$	$\overline{X} = 1.0 \pm 0.8$		
Overall		$\overline{X} = 30.5 \pm 11.4$					$\overline{X} = 20.4 \pm 6.4$	$\overline{X} = 2.0 \pm 2.9$		

*index (A21) and twin brother; §index (A14) & maternal uncle; +index (A3, A20) and brother.
A, alcohol; C, Cannabis; CF, counting fingers; F, female; HM, hand movements; M, male; N, no; T, tobacco; Y, yes. Visual acuity from first affected eye is shown in bold; $\overline{X}$, mean value followed by ±standard deviation.

participant were included. In the affected group only data from the first affected eye were used whereas for carriers and controls only data from the right eye were used.

RESULTS

Demographics, Genotype, Clinical Features, Color Vision, and Visual Field

A total of 41 individuals with suspected mutation of LHON were referred, from different geographical regions of Brazil (28 cities) and were genotyped for one of the three LHON pathogenic mtDNA mutations. Out of these, 38 (92.6%) participants (24 affected and 14 carriers of 19 families) had the confirmation of one of the three LHON pathogenic mtDNA mutations (m.11778G>A; m.14484T>C and m. 3460 G>A). In **Table 1** demographics, genotype, clinical features (age at onset, visual acuity, interval between first and second affected eye and idebenone usage) for affected patients are shown. Demographics, genotype and visual acuity for unaffected carriers are shown in **Table 2**.

In the 24 LHON affected subjects (23 males, mean age = 30.5 ± 11.4 years; median: 28 years) the genotype was m.11778G>A [N = 15 (62.5%)]; m.14484T>C [N = 5 (20.8%)] and m.3460G>A [N = 4 (16.7%)]. Carriers (mean age: 43.2 ± 13.3 years) were 13 females and one male [m.11778G>A – N = 12 (78.5%), m.14484T>C – N = 1 (7.2%), and m.3460G>A – N = 2 (14.3%)]. Controls were eight females and seven males (mean age: 32.6 ± 11.5 years).

The age onset vision loss ranged from 11.8 to 38.0 (mean 20.4 ± 6.4 years; median: 19.8). The duration of symptoms ranged from 5 to 516 months (mean 120 ± 129.6 months; median: 78.4 months) and the visual acuity was severely impaired in both eyes in most cases (mean logMAR 1.65 ± 0.90; median: 1.5). The right eye was first affected in 54% of subjects, with 4 (16%) affected subjects on continuous use of idebenone.

Color discrimination tests were performed in 22 affected, with two affected not able to be tested due to severe vision loss (subjects A15 and A24). All tested affected subjects showed severe diffuse dyschromatopsia. All asymptomatic carriers had normal Pseudo-Isochromatic test scores in both eyes, with 10 showing low color discrimination scores in at least one eye in Farnsworth-Munsell 100 Hue Color Test (error scores ranging from 40 to 400 losses were detected in 10/14 LHON asymptomatic carriers).

Ten affected subjects had both eyes tested with HVFA, with reliable results in five subjects (A3, A7, A16, A19, and A20); in two subjects (A3 and A16) absolute central scotoma were found in both eyes; cecocentral scotoma in one eye and central scotoma in the contralateral eye were found in two brothers with m.m.3460G>AT>C mutation (A19 and A20) and in one subject (A7) there was a central scotoma in the right eye and normal exam in the left eye. In 13 affected subjects the visual fields were tested by Goldmann perimetry, with 11 of them showing absolute central scotoma in both eyes (A1, A2, A4, A8, A9, A12, A13, A14, A21, A22, and A23), one subject with only small peripheric island of vision in both eyes (A15) and one subject (A10) with a peripheric island of vision in one eye and central scotoma in

TABLE 2 | Demographics and visual acuity from 14 carrier LHON participants.

Subject	Family #	Age (years)	Sex	Genotype	VA (logMAR)	
					RE	LE
C1	12	14	F	m.11778G>A homoplasmic	0	0
C2	11	18	M	m.11778G>A heteroplasmic	−0.2	−0.2
C3	3	36	F	m.11778G>A homoplasmic	0	0
C4	12	36	F	m.11778G>A homoplasmic	0	0
C5	11	38	F	m.11778G>A heteroplasmic	−0.1	−0.1
C6	6	44	F	m.11778G>A homoplasmic	0.6	0
C7	6	45	F	m.11778G>A homoplasmic	0	1
C8	11	48	F	m.11778G>A heteroplasmic	0	0
C9	2	48	F	m.11778G>A homoplasmic	0	0
C10	11	56	F	m.11778G>A homoplasmic	0.1	0.2
C11	12	57	F	m.11778G>A homoplasmic	0.2	0.2
C12	13	58	F	m.14484T>C homoplasmic	−0.1	0
C13	18	47	F	m.3460G>A homoplasmic	0	0
C14	17	52	F	m.3460G>A heteroplasmic	0	0
	$\overline{X}$ = 43.2 ± 13.3					

F, female; M, male; logMAR, logarithm of the minimum angle of resolution; RE, right eye; LE, left eye; VA, visual acuity.
$\overline{X}$, mean followed by ± standard deviation.

the contralateral eye (A10). In one subject (A17) HVF disclosing ceco-central scotoma in left eye and central scotoma in his right eye by Goldmann perimetry.

All 14 carriers had both eyes tested by HVFA with reliable results in 12 subjects. In 10 subjects the visual fields were completely normal in both eyes (C1, C2, C3, C4, C5, C8, C9, C11, C12, and C13). Central scotoma in the right eye and normal VF was found in one subject (C6) and normal VF in the right eye with central scotoma in the left eye (C7).

Photopic Negative Response

The PhNR parameters (a-wave, b-wave, BT, PT, BT/b and PT/b) for the LHON affected, LHON carrier and control subjects are summarized and compared in **Table 3** and shown in **Figure 1**. PhNR (BT, BT/b and PT/b) amplitudes were significantly reduced ($p < 0.0001$) in LHON affected (BT = −5.96 ± 3.37 μV) compared to carriers (BT = −16.53 ± 3.4 μV) and controls (BT = −23.91 ± 4.83 μV), and in carriers compared to controls ($p < 0.0001$). PhNR amplitudes

TABLE 3 | Mean, median and respective standard deviations PhNR amplitudes (BT and PT), PhNR amplitude ratios (PT/b and BT/b) and PhNR peak times of affected, carrier and controls.

	Affected Mean ± SD (median)	Carrier Mean ± SD (median)	Control Mean ± SD (median)	p-value[I]
Amplitude (μV)				
PhNR (BT)	−5.96 ± 3.37 (5.20)*	−16.53 ± 3.41 (15.78)**	−23.91 ± 4.83 (22.54)	**0.0001**
PhNR (PT)	−105.53 ± 28.43 (105.98)*	−138.27 ± 35.63 (127.92)	−121.64 ± 30.27 (117.07)	**0.0002**
PhNR Amplitudes ratios				
BT/B (μV)	0.06 ± 0.04 (0.06)*	0.14 ± 0.02 (0.14)**	0.27 ± 0.11 (0.24)	**0.0001**
PT/B (μV)	1.06 ± 0.04 (1.06)*	1.14 ± 0.02 (1.14)**	1.27 ± 0.11 (1.24)	**0.0001**
Peak times (ms)				
PhNR	62.54 ± 2.03 (60.07)	63.58 ± 2.95 (63.63)	62.79 ± 3.38 (62.98)	0.6677

[I]Kruskal-Wallis test.

BT, baseline to trough; μV, microvolts, ms, milliseconds; PhNR, photopic negative response; PT, peak-to-trough; SD, standard deviation.

*p < 0.05 by Dunn test, comparing affected with carrier and affected with control.

**p < 0.05 by Dunn test, comparing carrier with control.

FIGURE 1 | Photopic negative response amplitude (BT) from LHON affected patients, LHON asymptomatic carriers and controls (each box shows the median, quartiles, and extreme values; circles represent the subjects).
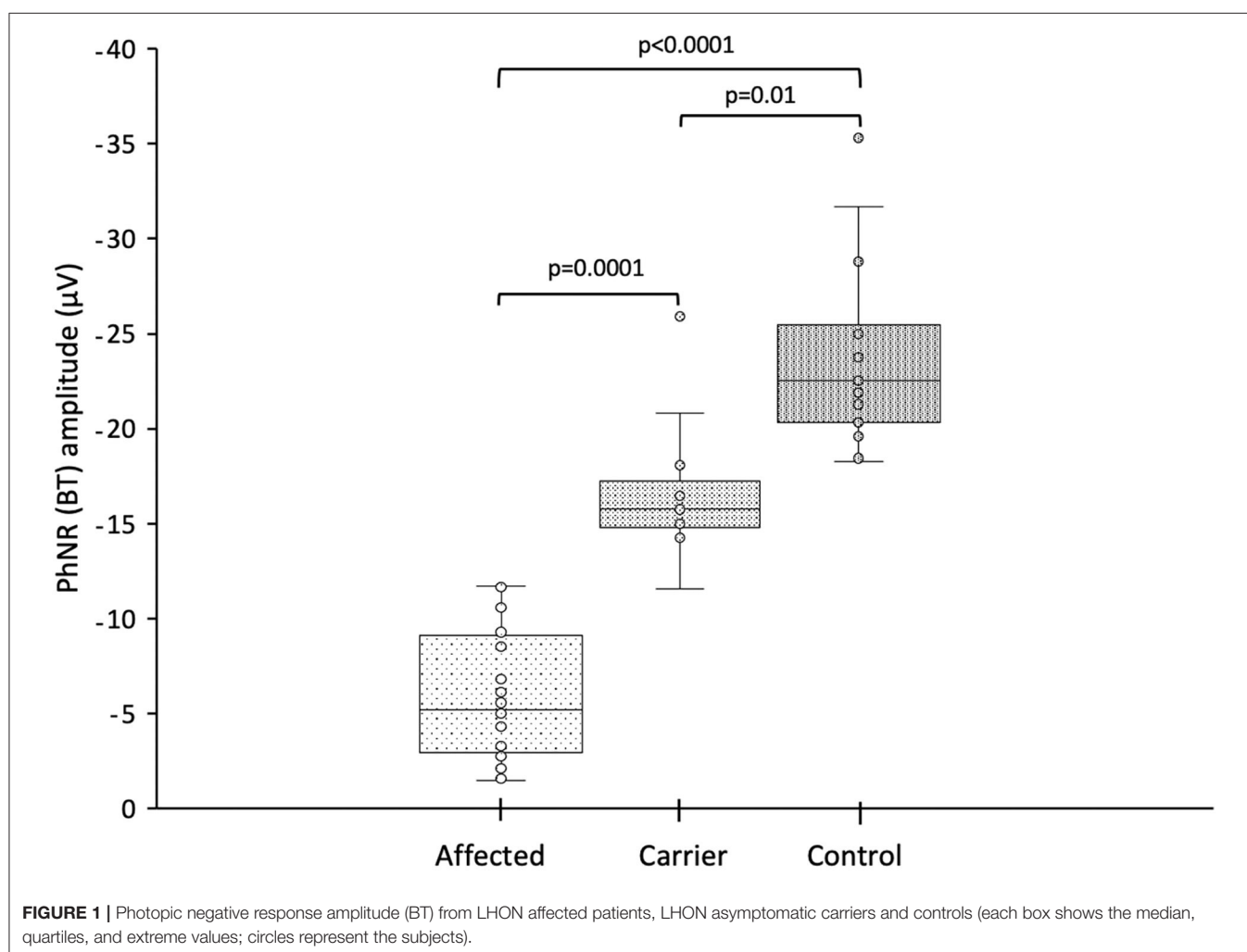
either by BT or PT were comparable among the three LHON mtDNA pathogenic mutations. There was no correlation between PhNR amplitude (BT) with age, use of idebenone or duration of symptoms.

Representative PhNR amplitudes for affected, carrier and control individuals are shown in **Figure 2**. ROC curve analysis revealed PhNR amplitude of BT to be a good parameter (**Figure 3**) to detect cases yielding a positive predictive value of

FIGURE 2 | Representative PhNR recordings with amplitudes measured by both BT (left panels) and PT (right panels) from an m.11778G>A LHON affected (A13–upper panels), his unaffected carrier sister (C 5–middle panels) and a healthy 41-year-old male control (lower panels).
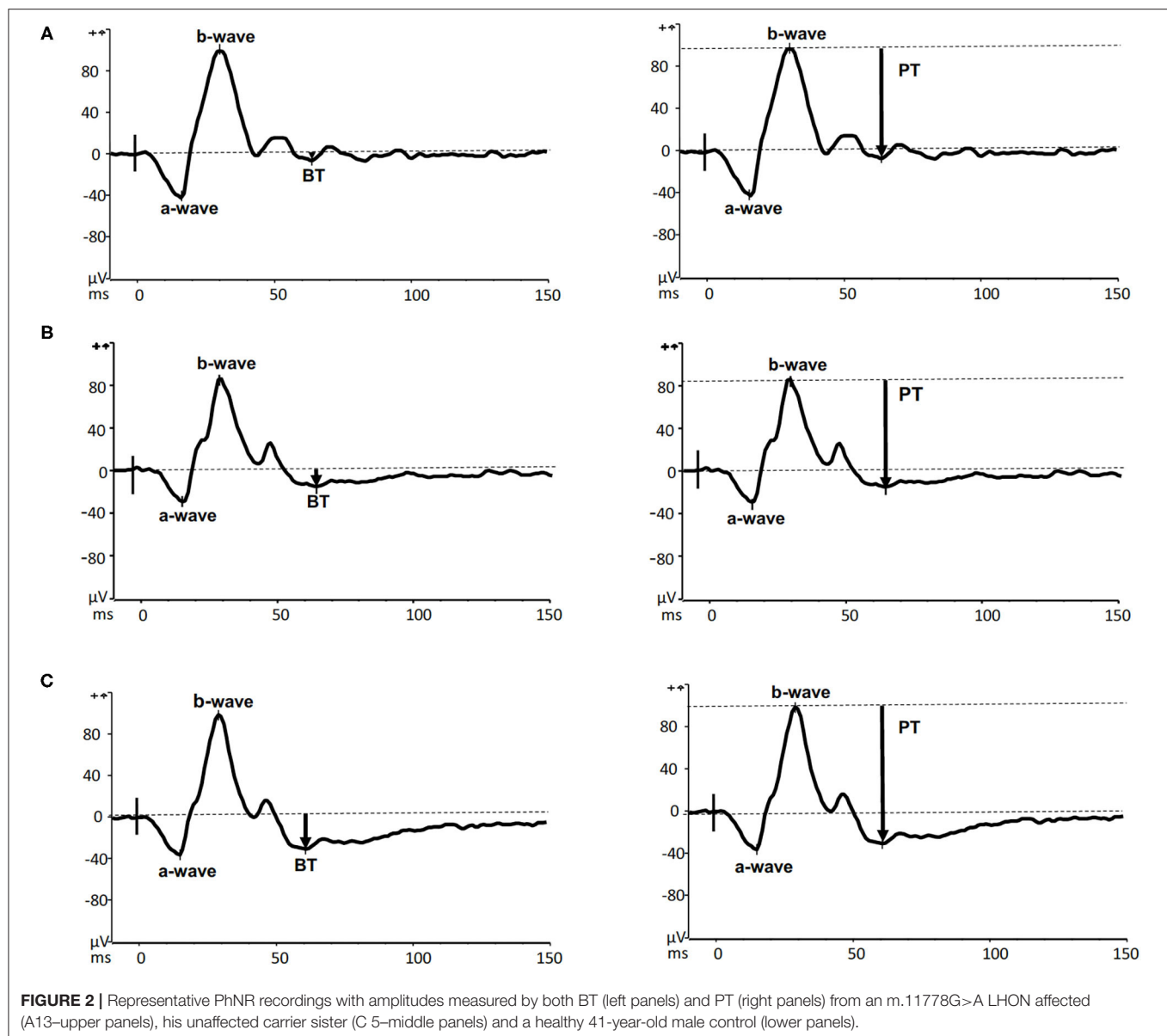
100%, a sensitivity of 96.5% and specificity of 100% at the cutoff of 11.72 µV. PhNR amplitude (BT) was significantly correlated ($r = -0.62$; $p < 0.05$) with the macular GCC thickness in affected, carrier and control as shown in **Figure 4**.

Fundoscopy and OCT Imaging

Bilateral optic atrophy was found LHON affected subjects, except subject A5 who presented in the acute phase of the disease with optic disk edema and peripapillary telangiectasia in his right eye and mild temporal optic disk pallor in his left eye.

Macular SD-OCT revealed selective loss of the global macular GCC thickness in affected LHON compared with carrier and control as shown in **Table 4** and **Figure 5** ($p < 0.001$). Global macular GCC thickness did not show significant changes in unaffected carrier compared to control. This occurred in parallel

with loss of the average peripapillary RNFL thickness and was similar in temporal, nasal, inferior, and superior quadrants ($p < 0.001$) (**Figure 6**). In one particular family (#6) macular microcysts were found (**Figure 7**). The unaffected mother (C7) had strabismic amblyopia in her left eye (VA 20/200) and 20/20 vision in her right eye, with few microcysts in the macular innermost retina in the left eye. Her two affected sons (A7 and A8) had macular microcysts, A7 in right eye and A8 in both eyes.

PRVEP, FVEP, and ff-ERG

Abnormalities in PRVEPs were found in all affected individuals, with 12 (50%) showing undetectable PRVEP for both 15' and 60'check sizes (A1, A4, A9, A10, A11, A12, A13, A14, A15, A21, A22, and A24). In 4 affected patients (17%) there were abnormal responses (reduced amplitudes and delayed latencies)
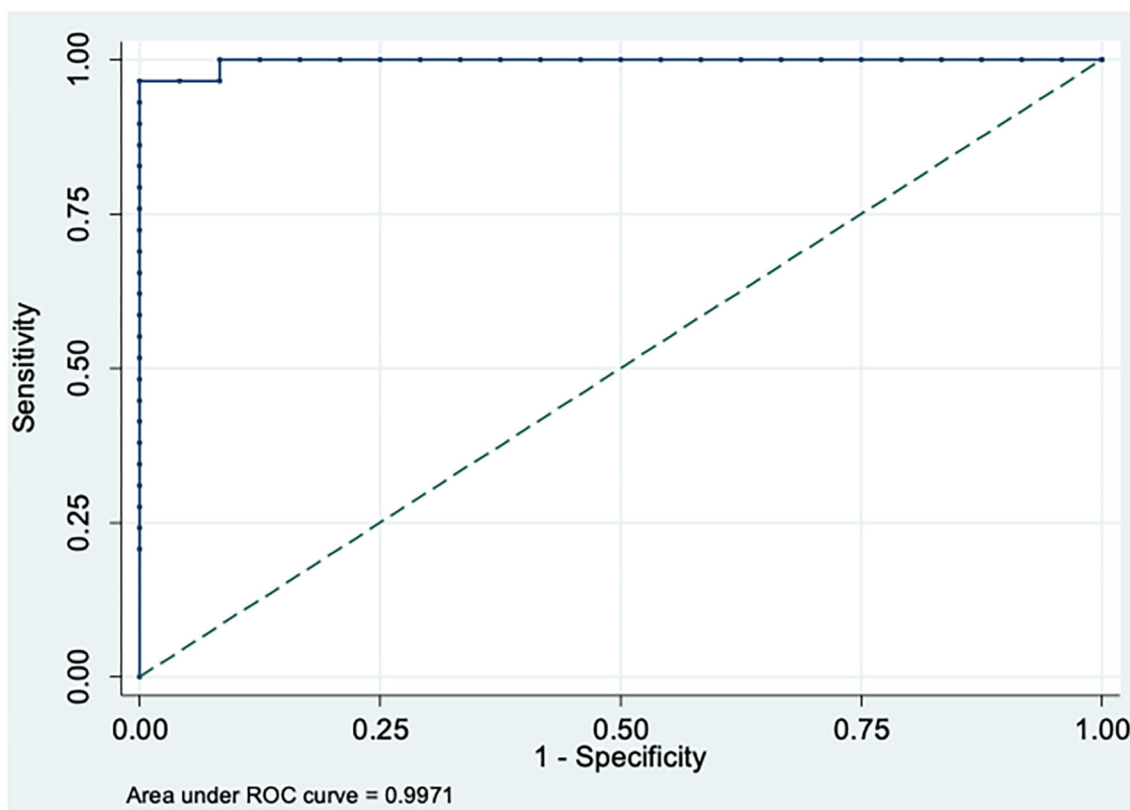
FIGURE 3 | Receiver Operating Characteristic (ROC) curve for affected vs. controls plotted at best cut-off at 11.72 μV for PhNR amplitude (BT) showing high sensitivity and specificity with area under the curve (AUC) = 0.997 (95%CI: 0.990–1.000).

for both check sizes in both eyes (A3, A8, A16, and A20). Non-detectable responses only for the smaller checks along with abnormal responses for larger checks in both eyes were found in 3 (13%) affected (A6, A19, and A23). Responses for smaller checks with either reduced amplitude or delayed latencies in at least one eye were found in 4 (17%) affected (A2, A5, A17, and A7). One patient (A10) showed undetectable responses for both check sizes in one eye and abnormal response for the larger checks in the contralateral eye.

For those 12 affected patients with undetectable pattern-reversal responses in both eyes for both check sizes, normal flash VEPs in both eyes were found in seven (A4, A9, A12, A13, A15, A21, and A22) whereas abnormal responses in both eyes were found in the remaining (A1, A10, A11, A14, and A24). In 12 patients with PRVEP recordable responses, FVEP normal responses for both eyes were found in 6 participants (A7, A16, A17, A19, A20, and A23), two patients showed normal response in one eye and delayed latencies in the contralateral eye (A3, A5) and in three patients (A6, A8, and A18) abnormal flash VEPs were found in both eyes.

All carriers had normal pattern-reversal and flash VEPs in both eyes, except two participants with previous strabismic amblyopia (C6 and C7) disclosing only abnormalities (reduced PRVEP P100 amplitudes) in their amblyopic eyes.

Normal scotopic and photopic ff-ERGs in both eyes (ISCEV standard protocol) were found in 38 participants with two affected (A7 and A8) showing reduced b/a ratio for the maximal response in both eyes consistent with OCT findings of macular microcysts in both eyes.

DISCUSSION

The assessment of the ganglion cell function by PhNR in LHON carrier and affected subjects confirmed and extended previous findings with significantly reduced mean PhNR amplitude (BT) and the PhNR/bwave amplitudes ratios (BT/b and PT/b) in both affected and carriers compared to the responses from the normal controls (32, 53). Accordingly, the ROC analysis also confirmed that the PhNR (BT) amplitude showed the best discrimination between control, LHON carrier and affected groups confirming findings from the SOA-BR pedigree (32). The current findings suggest that the PhNR amplitude can reveal functional abnormality in LHON carriers with normal vision while the SD-OCT decreases later in the course of the chronic disease in affected subjects. Our study also indicated severe RGC dysfunction in LHON affected subjects. The amplitude of PhNR in LHON does not seem to be influenced by
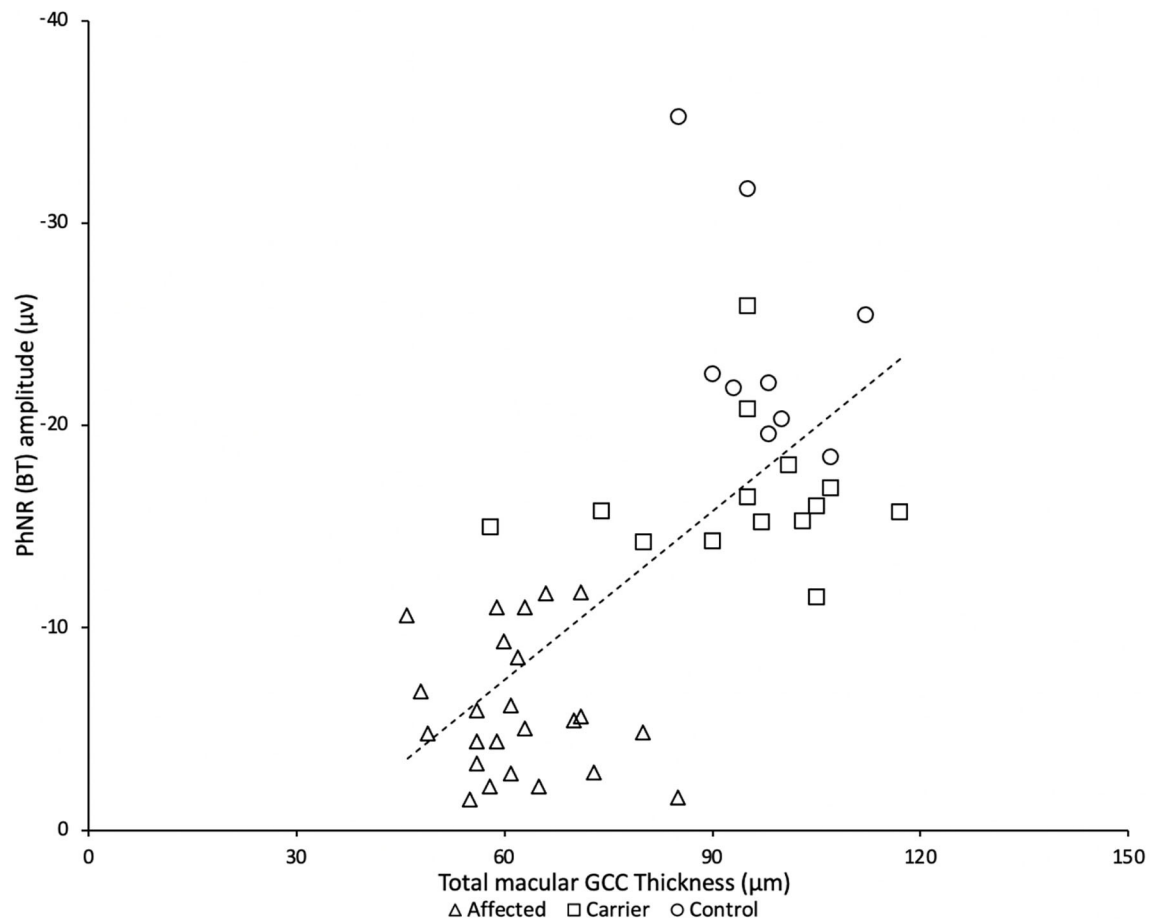
FIGURE 4 | There was a significant correlation between PhNR (BT) and total macular ganglion cell complex (GCC) from LHON affected patients ($N = 24$), asymptomatic carriers ($N = 14$) and controls ($N = 8$).

the specific mtDNA mutation, visual acuity, age or duration of symptoms.

Our results demonstrate the usefulness of the PhNR in both clinical care and research of diseases affecting RGCs, as LHON. Since the PhNR objectively and quantitatively reflects the overall function of the RGCs, it seemed a suitable quantitative test to monitor disease severity and could also represent a useful additional tool in clinical trials to investigate new therapeutic approaches for these conditions. This can be confirmed by the significant correlation found between PhNR amplitude and macular GCC thickness assessed by OCT. Furthermore, the PhNR offers advantages over other electrophysiological tests based on pattern stimuli, since it is a full field test that does not require clear optics or refractive correction. To note, PhNR, as other electrophysiological tests, might precede structural changes or even monitor changes at a different rate than changes in visual structure and function.

The affected LHON subjects showed a significant reduction in macular GCC and RNFL thickness in all quadrants compared with carriers and control subjects. The present study provides

key corroboration with previous investigations that reveal OCT an important feature in structural analyses of LHON including optic disk size, RNFL and GCC (22, 23, 61). Furthermore, it has been showed that RGCs loss occurs before RNFL in time of LHON visual loss in acute vision loss, whereas in our study mostly chronic LHON affected subjects were included and we found diffuse reduction of RGCs and RFNL thickness (34). A statistically significant association between the PhNR BT amplitude and total macular ganglion cell complex thickness using SD-OCT was found. Since PhNR is likely to reflect the activity of RGCs, this linear relationship between function and structure was already described in previous studies and indicates that RGCs function declines proportionately with neural loss (32).

In Family#6 (homoplasmic m.11778G>A), macular microcysts were found in a carrier (C7) and her two sons (A7 and A8), consistent with previous findings including the SOA-BR pedigree which demonstrate that macular microcysts occur in about 5.6% of patients with LHON (29). Some authors have proposed that the young age of these patients supports the

TABLE 4 | Peripapillary retinal nerve fiber layer thickness and macular ganglion cell complex, as measured by optical coherence tomography.

	Affected Mean ± sd (median)	Carrier Mean ± sd (median)	Control Mean ± sd (median)	p-value[I]
RFNL thickness (μm)				
Average	61.58 ± 15.24 (56.50)*	101.86 ± 15.08 (101.50)	105.67 ± 9.87 (105.00)	0.0001
Superior	75.42 ± 25.19 (71.00)*	125.79 ± 21.51 (128.00)	132.56 ± 20.12 (128.00)	0.0001
Temporal	42.46 ± 9.62 (41.00)*	73.43 ± 16.07 (75.50)	76.00 ± 6.56 (77.00)	0.0001
Inferior	76.08 ± 18.42 (74.00)*	127.64 ± 21.71 (132.00)	138.78 ± 14.45 (139.00)	0.0001
Nasal	52.21 ± 15.88 (49.50)*	81.14 ± 9.28 (80.00)	77.67 ± 8.73 (79.00)	0.0001
Macular GCC thickness (μm)	62.21 ± 9.43 (61.00)*	94.43 ± 15.16 (96.00)	97.56 ± 8.26 (98.00)	0.0001

[I]Kruskal-Wallis test.

RFNL, retinal nerve fiber layer; GCC, macular ganglion cell complex; μm, micra.

*$p < 0.05$ by Dunn test, comparing affected with carrier and affected with control.

FIGURE 5 | **(A)** Retinal nerve fiber layer thickness in the 360-degree average from LHON affected patients, LHON asymptomatic carriers and controls (each box shows the median, quartiles, and extreme values; circles represent individual subjects); **(B)** Total macular ganglion cell complex thickness from LHON affected (each box shows the median, quartiles, and extreme values; circles represent individual subjects).
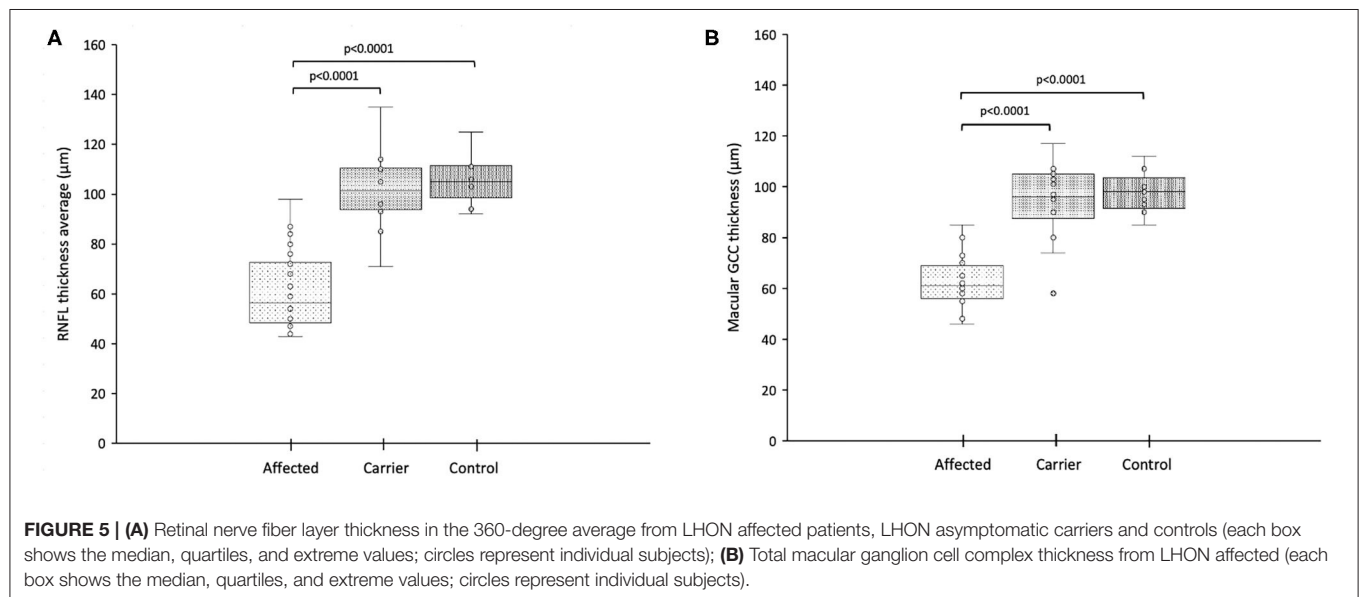
hypothesis of vitreoretinal adhesion and traction, as vitreous is known to be more firmly adherent in youth (62). It has also been proposed that macular microcysts are caused by the effects of trans-synaptic retrograde degeneration (63, 64).

Other Tests and Demographics

Since currently mtDNA testing is not available in the Brazilian public health system (Sistema Único de Saúde – SUS), the opportunity to have genotype provided free-of-charge, as part of this study, was of assistance to patients. Out of the 24 affected subjects, 12 (A1, A2, A3, A4, A5, A6, A7, A8, A9, A12, A17, and A24) were from very low-income sociodemographic background and anxious for the diagnosis confirmation, with a waiting time up to 18 years (mean = 4.5 years). Limitations of this study were the genotype testing including only the three more frequently found mtDNA mutations, which excluded three recruited individuals that might harbor other mutations and the restrict recruitment interval that might have impacted the sample size.

In this group of 19 Brazilian families genotyped for LHON the distribution of the three most common mtDNA mutations found was comparable to previous reports from other parts of the world with 62% of m.11778G>A, 21% of m.14484T>C and 16% of m.3460G>A (6, 7). While it is known that LHON affects prevalently males and in the studied sample there was only one female (4%) affected at 11 years of age among the 24 affected subjects compared to 15% affected females in the original description of the SOA-BR pedigree (8). We believe that this male:female ratio is an underestimation related to the recruitment interval and the small sample size. Longitudinal studies with larger samples could provide a better representation of the disease in Brazil.

An international consensus has recommended idebenone as the standard therapy for LHON, mainly in the acute phase of the disease (65). However, this substance is not registered in the Brazilian regulatory agency (Agência Nacional de Vigilância Sanitária – ANVISA) as a therapy for LHON and consequently is not available in the market. In our sample only 17% of
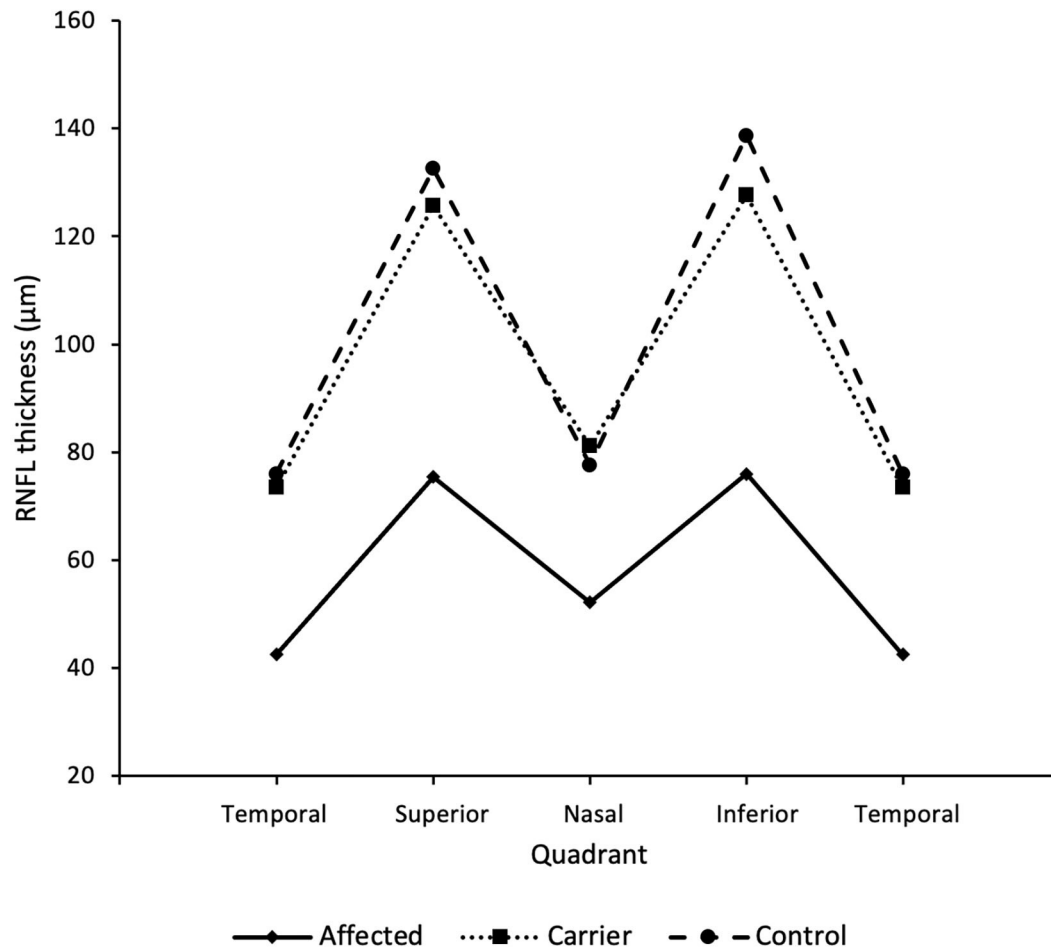
FIGURE 6 | RNFL thickness in each quadrant of LHON affected, LHON asymptomatic carriers and controls, showing a significantly thinner RNFL in all quadrants for LHON affected compared to carriers and controls ($p < 0.0001$).
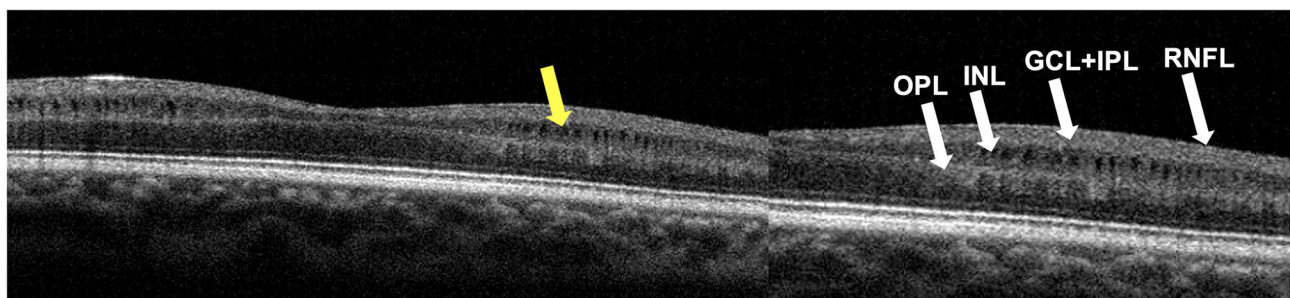
FIGURE 7 | Foveal OCT scan from subject A8's right eye. Segmentation identifies macular microcysts of inner nuclear layer (INL) as pointed by the yellow arrow. Retinal nerve fiber layer (RNFL), ganglion cell layer (GCL), inner plexiform layer (IPL) and outer plexiform layer (OPL) are shown on the right panel.

affected subjects reported idebenone treatment, with some of them obtaining the medication after legal appeal. To note, one patient who was not under idebenone therapy (A7 m.11778G>A) referred spontaneous recovery of vision in his left eye, with 20/20 visual acuity, relative central scotoma and reduced responses only for the smaller check size in the PRVEP. This particular case

points out that recovery might have implications in therapeutic approaches (66).

A pair of monozygotic twin brothers harboring the m.3460G>A mutation presented the disease onset quite closely from each other (**Table 1** subjects A21 and A22). Subject A21 developed visual loss at the age of 14 years in his right

eye being affected firstly followed by left eye less than a month later, whereas the twin brother (A22) had visual loss at 15 years of age also in his right followed by left eye a month later. This concordant LHON cases in monozygotic twin brothers had already being reported with m.11778G>A (67) and m.14484T>C (68) mutations with the patients showing similar genotypic and clinical features as the pair of Brazilian twin brothers.

Our study shows the severe abnormalities in psychophysical and electrophysiological tests found in affected subjects as diffuse dyschromatopsia, central scotoma and reduced or non-recordable PRVEPs. A number of studies have reported abnormal PRVEP and flash VEP responses in LHON affected subjects (11, 69). Subclinical abnormalities in PhNR, color discrimination and PRVEPs were present in some carriers, confirming findings from the SOA-BR pedigree (12, 13, 21, 32).

In this representative cohort of Brazilian families with LHON the impairment of the ganglion cell function assessed by photopic negative response was found in both affected and carrier subjects harboring one of the three most frequent pathogenic mutations. These results show that PhNR is a promising tool for future clinical trials and function-structure studies in this disease. The present study provided important demographic features of LHON in Brazilian families as the distribution of the three major mtDNA mutations and gender prevalence along with the clinical and electrophysiological characterization of affected and carrier individuals.

DATA AVAILABILITY STATEMENT

The raw data supporting the conclusions of this article will be made available by the authors, without undue reservation.

ETHICS STATEMENT

The studies involving human participants were reviewed and approved by the Committee of Ethics in Research of Federal University of São Paulo. All procedures performed in studies involving human participants were in accordance with the ethical standards of the institutional and/or national research committee and with the 1964 Helsinki declaration, its later amendments or comparable ethical standards. All participants provided informed consent. (Reference of ethics committee approval: UNIFESP-Hospital São Paulo - CAAE: 89695718.0.0000.55.05). Written informed consent to participate in this study was provided by the participants' legal guardian/next of kin.

AUTHOR CONTRIBUTIONS

AB, SS, CT, RK, VC, RB, and AS: conceptualization. AB, GB, PSa, DR, PSi, FM, SS, and SW: data collection. AB, GB, SS, CT, and AF: data analysis. AB, GB, SS, CT, RK, FM, DR, PSi, AF, SW, PSa, RB, VC, and AS: writing and review of manuscript. AB, SS, RB, RK, VC, and AS: funding acquisition. All authors contributed to the article and approved the submitted version.

FUNDING

REFERENCES

1. Barboni P, Sadun AA, Balducci N, Carelli V. Natural history. Atlas of LHON. In: Barboni P, Sadun AA, editors. *Chapter I*. Netherlands: MEDonline International (2019). p. 6–29.

2. Carelli V, La Morgia C, Valentino ML, Barboni P, Ross-Cisneros FN, Sadun AA. Retinal ganglion cell neurodegeneration in mitochondrial inherited disorders. *Biochim Biophys Acta*. (2009) 1787:518–28. doi: 10.1016/j.bbabio.2009.02.024

3. Hwang TJ, Karanjia R, Moraes-Filho MN, Gale J, Tran JS, Chu ER, et al. Natural history of conversion of leber's hereditary optic neuropathy: a prospective case series. *Ophthalmology*. (2017) 124:843–50. doi: 10.1016/j.ophtha.2017.01.002

4. Yu-Wai-Man P, Griffiths PG, Chinnery PF. Mitochondrial optic neuropathies: disease mechanisms and therapeutic strategies. *Prog Retin Eye Res*. (2011) 30:81–114. doi: 10.1016/j.preteyeres.2010.11.002

5. Meyerson C, Van Stavern G, McClelland C. Leber hereditary optic neuropathy: current perspectives. *Clin Ophthalmol*. (2015) 9:1165–76. doi: 10.2147/OPTH.S62021

6. Mascialino B, Leinonen M, Meier T. Meta-analysis of the prevalence of Leber hereditary optic neuropathy mtDNA mutations in Europe. *Eur J Ophthalmol*. (2012) 22:461–5. doi: 10.5301/ejo.5000055

7. Poincenot L, Pearson AL, Karanjia R. Demographics of a large international population of patients affected by leber's hereditary optic neuropathy. *Ophthalmology*. (2020) 127:679–88. doi: 10.1016/j.ophtha.2019.11.014

8. Sadun AA, Carelli V, Salomao SR, Berezovsky A, Quiros P, Sadun F, et al. A very large Brazilian pedigree with m.11778G>A Leber's hereditary optic neuropathy. *Trans Am Ophthalmol Soc*. (2002) 100:169–79.

9. Sadun AA, Carelli V, Salomao SR, Berezovsky A, Quiros PA, Sadun F, et al. Extensive investigation of a large Brazilian pedigree of m.11778G>A/haplogroup J Leber hereditary optic neuropathy. *Am J Ophthalmol*. (2003) 136:231–8. doi: 10.1016/S0002-9394(03)00099-0

10. Sadun F, De Negri AM, Carelli V, Salomao SR, Berezovsky A, Andrade R, et al. Ophthalmologic findings in a large pedigree of m.11778G>A/Haplogroup J Leber hereditary optic neuropathy. *Am J Ophthalmol*. (2004) 137:271–7. doi: 10.1016/j.ajo.2003.08.010

11. Salomão SR, Berezovsky A, Andrade RE, Belfort R Jr, Carelli V, Sadun AA. Visual electrophysiologic findings in patients from an extensive Brazilian family with Leber's hereditary optic neuropathy. *Doc Ophthalmol*. (2004) 108:147–55. doi: 10.1023/B:DOOP.0000036829.37053.31

12. Ventura DF, Quiros P, Carelli V, Salomão SR, Gualtieri M, Oliveira AG, et al. Chromatic and luminance contrast sensitivities in asymptomatic carriers from a large Brazilian pedigree of m.11778G>A Leber hereditary optic neuropathy. *Invest Ophthalmol Vis Sci*. (2005) 46:4809–14. doi: 10.1167/iovs.05-0455

13. Quiros PA, Torres RJ, Salomao S, Berezovsky A, Carelli V, Sherman J, et al. Colour vision defects in asymptomatic carriers of the Leber's hereditary optic neuropathy (LHON) mtDNA m.11778G>A mutation from a large Brazilian LHON pedigree: a case-control study. *Br J Ophthalmol*. (2006) 90:150–3. doi: 10.1136/bjo.2005.074526

14. Sadun AA, Salomao SR, Berezovsky A, Sadun F, Denegri AM, Quiros PA, et al. Subclinical carriers and conversions in Leber hereditary optic

neuropathy: a prospective psychophysical study. *Trans Am Ophthalmol Soc.* (2006) 104:51–61.

15. Hudson G, Carelli V, Spruijt L, Gerards M, Mowbray C, Achilli A, et al. Clinical expression of Leber hereditary optic neuropathy is affected by the mitochondrial DNA-haplogroup background. *Am J Hum Genet.* (2007) 81:228–33. doi: 10.1086/519394

16. Ventura DF, Gualtieri M, Oliveira AG, Costa MF, Quiros P, Sadun F, et al. Male prevalence of acquired color vision defects in asymptomatic carriers of Leber's hereditary optic neuropathy. *Invest Ophthalmol Vis.* (2007) 48:2362–70. doi: 10.1167/iovs.06-0331

17. Gualtieri M, Bandeira M, Hamer RD, Costa MF, Oliveira AG, Moura AL, et al. Psychophysical analysis of contrast processing segregated into magnocellular and parvocellular systems in asymptomatic carriers of m.11778G>A Leber's hereditary optic neuropathy. *Vis Neurosci.* (2008) 25:469–74. doi: 10.1017/S0952523808080462

18. Guy J, Shaw G, Ross-Cisneros FN, Quiros P, Salomao SR, Berezovsky A, et al. Phosphorylated neurofilament heavy chain is a marker of neurodegeneration in Leber hereditary optic neuropathy (LHON). *Mol Vis.* (2008) 14:2443–50.

19. Shankar SP, Fingert JH, Carelli V, Valentino ML, King TM, Daiger SP, et al. Evidence for a novel x-linked modifier locus for leber hereditary optic neuropathy. *Ophthalmic Genet.* (2008) 29:17–24. doi: 10.1080/13816810701867607

20. Ramos Cdo V, Bellusci C, Savini G, Carbonelli M, Berezovsky A, Tamaki C, et al. Association of optic disc size with development and prognosis of Leber's hereditary optic neuropathy. *Invest Ophthalmol Vis Sci.* (2009) 50:1666–74. doi: 10.1167/iovs.08-2695

21. Sacai PY, Salomão SR, Carelli V, Pereira JM, Belfort R Jr, Sadun AA, et al. Visual evoked potentials findings in non-affected subjects from a large Brazilian pedigree of m.11778G>A Leber's hereditary optic neuropathy. *Doc Ophthalmol.* (2010) 121:147–54. doi: 10.1007/s10633-010-9241-2

22. La Morgia C, Ross-Cisneros FN, Sadun AA, Hannibal J, Munarini A, Mantovani V, et al. Melanopsin retinal ganglion cells are resistant to neurodegeneration in mitochondrial optic neuropathies. *Brain.* (2010) 133:2426–38. doi: 10.1093/brain/awq155

23. Barboni P, Carbonelli M, Savini G, Ramos Cdo V, Carta A, Berezovsky A, et al. Natural history of Leber's hereditary optic neuropathy: longitudinal analysis of the retinal nerve fiber layer by optical coherence tomography. *Ophthalmology.* (2010) 117:623–7. doi: 10.1016/j.ophtha.2009.07.026

24. Barboni P, Savini G, Feuer WJ, Budenz DL, Carbonelli M, Chicani F, et al. Retinal nerve fiber layer thickness variability in Leber hereditary optic neuropathy carriers. *Eur J Ophthalmol.* (2012) 22:985–91. doi: 10.5301/ejo.5000154

25. Pan BX, Ross-Cisneros FN, Carelli V, Rue KS, Salomao SR, Moraes-Filho MN, et al. Mathematically modeling the involvement of axons in Leber's hereditary optic neuropathy. *Invest Ophthalmol Vis Sci.* (2012) 53:7608–17. doi: 10.1167/iovs.12-10452

26. Yee KM, Ross-Cisneros FN, Lee JG, Da Rosa AB, Salomao SR, Berezovsky A, et al. Neuron-specific enolase is elevated in asymptomatic carriers of Leber's hereditary optic neuropathy. *Invest Ophthalmol Vis Sci.* (2012) 53:6389–92. doi: 10.1167/iovs.12-9677

27. Moura AL, Nagy BV, La Morgia C, Barboni P, Oliveira AG, Salomão SR, et al. The pupil light reflex in Leber's hereditary optic neuropathy: evidence for preservation of melanopsin-expressing retinal ganglion cells. *Invest Ophthalmol Vis Sci.* (2013) 54:4471–7. doi: 10.1167/iovs.12-11137

28. Giordano C, Iommarini L, Giordano L, Maresca A, Pisano A, Valentino ML, et al. Efficient mitochondrial biogenesis drives incomplete penetrance in Leber's hereditary optic neuropathy. *Brain.* (2014) 137:335–53. doi: 10.1093/brain/awt343

29. Carbonelli M, La Morgia C, Savini G, Cascavilla ML, Borrelli E, Chicani F, et al. Macular microcysts in mitochondrial optic neuropathies: prevalence and retinal layer thickness measurements. *PLoS ONE.* (2015) 10:e0127906. doi: 10.1371/journal.pone.0127906

30. Giordano L, Deceglie S, d'Adamo P, Valentino ML, La Morgia C, Fracasso F, et al. Cigarette toxicity triggers Leber's hereditary optic neuropathy by affecting mtDNA copy number, oxidative phosphorylation and ROS detoxification pathways. *Cell Death Dis.* (2015) 6:e2021. doi: 10.1038/cddis.2015.364

31. Carelli V, d'Adamo P, Valentino ML, La Morgia C, Ross-Cisneros FN, Caporali L, et al. Parsing the differences in affected with LHON: genetic vs. environmental triggers of disease conversion. *Brain.* (2016) 139:e17. doi: 10.1093/brain/awv339

32. Karanjia R, Berezovsky A, Sacai PY, Cavascan NN, Liu HY, Nazarali S, et al. The photopic negative response: an objective measure of retinal ganglion cell function in patients with Leber's hereditary optic neuropathy. *Invest Ophthalmol Vis Sci.* (2017) 58:8527–33. doi: 10.1167/iovs.17-21773

33. Carelli V, Ross-Cisneros FN, Sadun AA. Optic nerve degeneration and mitochondrial dysfunction: genetic and acquired optic neuropathies. *Neurochem Int.* (2002) 40:573–84. doi: 10.1016/S0197-0186(01)00129-2

34. Balducci N, Savini G, Cascavilla ML, La Morgia C, Triolo G, Giglio R, et al. Macular nerve fibre and ganglion cell layer changes in acute Leber's hereditary optic neuropathy. *Br J Ophthalmol.* (2016) 100:1232–7. doi: 10.1136/bjophthalmol-2015-307326

35. Asanad S, Tian JJ, Frousiakis S, Jiang JP, Kogachi K, Felix CM, et al. Optical coherence tomography of the retinal ganglion cell complex in leber's hereditary optic neuropathy and dominant optic atrophy. *Curr Eye Res.* (2019) 44:638–44. doi: 10.1080/02713683.2019.1567792

36. Viswanathan S, Frishman LJ, Robson JG, Harwerth RS, Smith EL III. The photopic negative response of the macaque electroretinogram: reduction by experimental glaucoma. *Invest Ophthalmol Vis Sci.* (1999) 40:1124–36.

37. McCulloch DL, Marmor MF, Brigell MG, Hamilton R, Holder GE, Tzekov R, et al. ISCEV Standard for full-field clinical electroretinography (2015 update). *Doc Ophthalmol.* (2015) 130:1–12. doi: 10.1007/s10633-014-9473-7

38. Frishman L, Sustar M, Kremers J, McAnany JJ, Sarossy M, Tzekov R, et al. ISCEV extended protocol for the photopic negative response (PhNR) of the full-field electroretinogram. *Doc Ophthalmol.* (2018) 136:207–11. doi: 10.1007/s10633-018-9638-x

39. Viswanathan S, Frishman LJ, Robson JG, Walters JW. The photopic negative response of the flash electroretinogram in primary open angle glaucoma. *Invest Ophthalmol Vis Sci.* (2001) 42:514–22.

40. Wakili N, Horn FK, Jünemann AG, Nguyen NX, Mardin CY, Korth M, et al. The photopic negative response of the blue-on-yellow flash-electroretinogram in glaucomas and normal subjects. *Doc Ophthalmol.* (2008) 117:147–54. doi: 10.1007/s10633-008-9116-y

41. Senger C, Moreto R, Watanabe S, Matos AG, Paula JS. Electrophysiology in glaucoma. *J Glaucoma.* (2020) 29:147–53. doi: 10.1097/IJG.0000000000001422

42. North RV, Jones AL, Drasdo N, Wild JM, Morgan JE. Electrophysiological evidence of early functional damage in glaucoma and ocular hypertension. *Invest Ophthalmol Vis Sci.* (2010) 51:1216–22. doi: 10.1167/iovs.09-3409

43. Gotoh Y, Machida S, Tazawa Y. Selective loss of the photopic negative response in patients with optic nerve atrophy. *Arch Ophthalmol.* (2004) 122:341–6. doi: 10.1001/archopht.122.3.341

44. Tamada K, Machida S, Yokoyama D, Kurosaka D. Photopic negative response of full-field and focal macular electroretinograms in patients with optic nerve atrophy. *Jpn J Ophthalmol.* (2009) 53:608–14. doi: 10.1007/s10384-009-0731-2

45. Abed E, Piccardi M, Rizzo D, Chiaretti A, Ambrosio L, Petroni S, et al. Functional loss of the inner retina in childhood optic gliomas detected by photopic negative response. *Invest Ophthalmol Vis Sci.* (2015) 56:2469–74. doi: 10.1167/iovs.14-16235

46. Chen H, Wu D, Huang S, Yan H. The photopic negative response of the flash electroretinogram in retinal vein occlusion. *Doc Ophthalmol.* (2006) 113:53–9. doi: 10.1007/s10633-006-9015-z

47. Matsumoto CS, Shinoda K, Yamada K, Nakatsuka K. Photopic negative response reflects severity of ocular circulatory damage after central retinal artery occlusion. *Ophthalmologica.* (2009) 223:362–9. doi: 10.1159/000227782

48. Moon CH, Ahn SI, Ohn YH, Kwak HW, Park TK. Visual prognostic value of photopic negative response and optical coherence tomography in central retinal vein occlusion after anti-VEGF treatment. *Doc Ophthalmol.* (2013) 126:211–9. doi: 10.1007/s10633-013-9379-9

49. Noma H, Mimura T, Kuse M, Yasuda K, Shimura M. Photopic negative response in branch retinal vein occlusion with macular edema. *Int Ophthalmol.* (2015) 35:19–26. doi: 10.1007/s10792-014-0012-z

50. Park JC, Chau FY, Lim JI, McAnany JJ. Electrophysiological and pupillometric measures of inner retina function in nonproliferative diabetic retinopathy. *Doc Ophthalmol.* (2019) 139:99–111. doi: 10.1007/s10633-019-09699-2

51. Moss HE, Park JC, McAnany JJ. The photopic negative response in idiopathic intracranial hypertension. *Invest Ophthalmol Vis Sci.* (2015) 56:3709–14. doi: 10.1167/iovs.15-16586

52. Park JC, Moss HE, McAnany JJ. Electroretinography in idiopathic intracranial hypertension: comparison of the pattern ERG and the photopic negative response. *Doc Ophthalmol.* (2018) 136:45–55. doi: 10.1007/s10633-017-9620-z

53. Majander A, Robson AG, João C, Holder GE, Chinnery PF, Moore AT, et al. The pattern of retinal ganglion cell dysfunction in Leber hereditary optic neuropathy. *Mitochondrion.* (2017) 36:138–49. doi: 10.1016/j.mito.2017.07.006

54. Odom JV, Bach M, Brigell M, Holder GE, McCulloch DL, Mizota A, et al. International society for clinical electrophysiology of vision. ISCEV standard for clinical visual evoked potentials: (2016 update). *Doc Ophthalmol.* (2016) 133:1–9. doi: 10.1007/s10633-016-9553-y

55. Dotto PF, Berezovsky A, Sacai PY, Rocha DM, Salomão SR. Gender-based normative values for pattern-reversal and flash visually evoked potentials under binocular and monocular stimulation in healthy adults. *Doc Ophthalmol.* (2017) 135:53–67. doi: 10.1007/s10633-017-9594-x

56. Berezovsky A, Rocha DM, Sacai PY, Watanabe SS, Cavascan NN, Salomão SR. Visual acuity and retinal function in patients with Bardet-Biedl syndrome. *Clinics (São Paulo).* (2012) 67:145–9. doi: 10.6061/clinics/2012(02)09

57. Pereira JM, Mendieta L, Sacai PY, Salomão SR, Berezovsky A. Normative values for full-field electroretinogram in healthy young adults. *Arq Bras Oftalmol.* (2003) 66:137–44. doi: 10.1590/S0004-27492003000200005

58. Berezovsky A, Karanjia R, Fernandes AG, Botelho GIS, Bueno TLN, Ferraz NN, et al. Photopic negative response using a handheld mini-ganzfeld stimulator in healthy adults: normative values, intra- and inter-session variability. *Doc Ophthalmol.* (2020). doi: 10.1007/s10633-020-09784-x

59. Schulze-Bonsel K, Feltgen N, Burau H, Hansen L, Bach M. Visual acuities "hand motion" and "counting fingers" can be quantified with the freiburg visual acuity test. *Invest Ophthalmol Vis Sci.* (2006) 47:1236–40. doi: 10.1167/iovs.05-0981

60. Moraes CT, Atencio DP, Oca-Cossio J, Diaz F. Techniques and pitfalls in the detection of pathogenic mitochondrial DNA mutations. *J Mol Diagn.* (2003) 5:197–208. doi: 10.1016/S1525-1578(10)60474-6

61. Akiyama H, Kashima T, Li D, Shimoda Y, Mukai R, Kishi S. Retinal ganglion cell analysis in Leber's hereditary optic neuropathy. *Ophthalmology.* (2013) 120:1943–4. doi: 10.1016/j.ophtha.2013.05.031

62. Gupta P, Yee KMP, Garcia P, Rosen RB, Parikh J, Hageman GS, et al. Vitreoschisis in macular diseases. *Br J Ophthalmol.* (2011) 95:376–80. doi: 10.1136/bjo.2009.175109

63. Abegg M, Zinkernagel M, Wolf S. Microcystic macular degeneration from optic neuropathy. *Brain.* (2012) 135:e225. doi: 10.1093/brain/aws215

64. Abegg M, Dysli M, Wolf S, Kowal J, Dufour P, Zinkernagel M. Microcystic macular edema. Retrograde maculopathy caused by optic neuropathy. *Ophthalmol.* (2014) 121:142–9. doi: 10.1016/j.ophtha.2013.08.045

65. Carelli V, Carbonelli M, de Coo IF, Kawasaki A, Klopstock T, Lagrèze WA, et al. International consensus statement on the clinical and therapeutic management of leber hereditary optic neuropathy. *J Neuroophthalmol.* (2017) 37:371–81. doi: 10.1097/WNO.0000000000000570

66. Newman NJ. Hereditary optic neuropathies: from the mitochondria to the optic nerve. *Am J Ophthalmol.* (2005) 140:517–23. doi: 10.1016/j.ajo.2005.03.017

67. Lam BL. Identical twins no longer discordant for Leber's hereditary optic neuropathy. *Arch Ophthalmol.* (1998) 116:956–7.

68. Biousse V, Brown MD, Newman NJ, Allen JC, Rosenfeld J, Meola G, et al. De novo 14484 mitochondrial DNA mutation in monozygotic twins discordant for Leber's hereditary optic neuropathy. *Neurology.* (1997) 49:1136–8. doi: 10.1212/WNL.49.4.1136

69. Ziccardi L, Sadun F, De Negri AM, Barboni P, Savini G, Borrelli E, et al. Retinal function and neural conduction along the visual pathways in affected and unaffected carriers with Leber's hereditary optic neuropathy. *Invest Ophthalmol Vis Sci.* (2013) 54:6893–901. doi: 10.1167/iovs.13-12894

Mitochondrial 13513G>A Mutation With Low Mutant Load Presenting as Isolated Leber's Hereditary Optic Neuropathy Assessed by Next Generation Sequencing

Chuan-bin Sun[1], Hai-xia Bai[1], Dan-ni Xu[1], Qing Xiao[1] and Zhe Liu[2]*

[1] Eye Center, Second Affiliated Hospital of Zhejiang University School of Medicine, Hangzhou, China, [2] Department of Ophthalmology, Zhejiang Provincial People's Hospital, People's Hospital of Hangzhou Medical College, Hangzhou, China

Objective: Mitochondrial 13513G>A mutation presenting as isolated Leber's hereditary optic neuropathy (LHON) without any extraocular pathology has not been reported in literature. We herein evaluate the clinical characteristics and heteroplasmy of m.13513G>A mutation manifesting as isolated LHON.

Methods: Seven members of a Chinese family were enrolled in this study. All subjects underwent detailed systemic and ophthalmic examinations. Mitochondrial DNA in their blood was assessed by targeted PCR amplifications, next generation sequencing (NGS), and pyrosequencing. One hundred of blood samples from ethnic-matched healthy volunteers were tested by NGS and pyrosequencing as normal controls.

Results: Isolated LHON without any other ocular or extraocular pathology was identified in a 16 year old patient in this family. Heteroplasmic m.13513G>A mutation was detected by NGS of the full mtDNA genome in the patient with mutant load of 33.56%, and of 26% 3 months and 3 years after the onset of LHON, respectively. No m.13513G>A mutation was detected in all his relatives by NGS. Pyrosequencing revealed the mutant load of m.13513G>A mutation of the LHON patient, his mother, father and sister were 22.4, 1.9, 0, and 0%, respectively. None of 100 healthy control subjects was detected to harbor m.13513G>A mutation either by NGS or by pyrosequencing of the full mt DNA genome.

Conclusions: We first report m.13513G>A mutation with low mutant load presenting as isolated LHON. NGS of the full mitochondrial DNA genome is highly recommended for LHON suspects when targeted PCR amplification for main primary point mutations of LHON was negative.

Keywords: Leber's hereditary optic neuropathy, mitochondrial DNA, gene mutation, m13513G>A, optic atrophy

INTRODUCTION

As one of the most common mitochondrial inherited diseases, Leber's hereditary optic neuropathy (LHON) is typically characterized by acute painless bilateral central vision loss in adolescents and young adults, predominantly in males (1–4). Previous investigations have revealed that more than 90% of LHON cases are related to one of three primary point mutations in the mitochondrial

DNA (mtDNA): m.11778G>A, m.3460G>A, and m.14484T>C, which encode the ND4, ND1, and ND6 subunits of Complex I in the mitochondrial respiratory chain, respectively (5–7). However, other rare primary mtDNA mutaions such as m.3635G>A in ND1, m.14495A>G in ND6, and m.13513G>A in ND5 have also been reported to cause LHON independently (1–7).

Since first identified as a gene mutation causative for mitochondrial encephalomyopathy with lactic acidosis and stroke-like episodes (MELAS), m.13513G>A mutation has been mostly reported in Leigh syndrome (LS), MELAS, as well as MELAS/LHON and MELAS/LS overlap syndromes (5, 6). Ophthalmic manifestations related to m.13513G>A mutation including optic atrophy, ptosis, and chronic progressive external ophthalmoplegia (CPEO) are mostly accompanied by MELAS or LS, and classified as MELAS /LHON, LS/LHON, or MELAS/CPEO overlap syndromes (5–8).

Until now, m.13513G>A mutation-related LHON without LS or MELAS has been reported in only three cases (9–11). However, all above 3 cases were accompanied by other extraocular pathology such as hypertrophic myocardiopathy, myopathy, Wolff-Parkinson White syndrome, chronic kidney disease, diabetes mellitus, or hearing loss. To our knowledge, m.13513G>A mutation presenting as isolated LHON without any extraocular pathology has not been reported. We herein evaluate the clinical characteristics and heteroplasmy of the m.13513G>A mutation manifesting as isolated LHON without any other ocular or extraocular pathology.

METHODS

Subjects and Clinical Examinations

Six maternal family members (including one half-brother and one half-sister) and the farther of the LHON patient of Han population in a Chinese family were enrolled in this study (**Figure 1**). Detailed medical records of the patient visiting different hospitals were collected. All subjects underwent detailed systemic and ophthalmic examinations including consciousness, hearing, articulation, superficial and deep sensation, muscle strength, tone and reflexes, best corrected visual acuity (BCVA), slit-lamp microscopy, color fundus photography, and visual field test, as well as blood test for cardiac enzymes, blood lactate fluctuation during exercise test, electrocardiogram and Doppler echocardiography. Gadolinium enhanced orbital MRI, and magnetic resonance spectroscopy were performed only in the LHON patient.

Mitochondrial DNA Assessment

Peripheral blood was collected from the patient and his relatives for mtDNA sequencing after informed consents were signed. One hundred of blood samples from ethnic-matched healthy volunteers were used as normal controls. Targeted PCR amplifications and Sanger DNA sequencing of three main primary point mutations of LHON in mt DNA, i.e.: m.11778G>A, m.3460G>A, and m.14484T>C, were first assessed in the LHON patient according to procedures described previously (12, 13). In brief, QIAamp

DNA Blood Mini kits were employed for genomic DNA extraction (Qiagen, NO.51104). Three main primary mutations of LHON including m.11778G>A, m.3460G>A, and m.14484T>C were assessed by targeted PCR amplifications of DNA fragments, using oligodeoxynucleotides that correspond to mitochondrial DNA at 11,654–11,865 for m.11778G>A mutations; 3,108-3,717 for m.3460G>A mutations, and 14,260–14,510 for m.14484T>C mutations (12). Fragments were isolated and analyzed in an ABI 3700 automated DNA sequencer (Applied Biosystems; Thermo Fisher Scientific, Inc.) using Big Dye Terminator Cycle sequencing kits. Comparisons of the fragments were performed through Cambridge sequencing (Gen-Bank accession number: NC_012920).

Since none of above three primary point mutations in mt DNA was detected in the LHON patient. Next generation sequencing (NGS) of the whole mtDNA genome and DNA sequence analysis were then performed in the patient based on procedures described previously (14, 15). In brief, whole genomic DNA was extracted with the Purgene DNA isolation kit (Qiagen), and the entire genome of mitochondrial was amplified total of three pooled reactions by PCR as 99 separate fragments, using primers for the light and heavy stranded DNA. Then the DNA was purified using magnetic beads and a library was made for directly sequenced on a sequencer using a NGS reaction kit (MiniSeq, Illumina). To identify mutations within the obtained genome, the consensus Cambridge sequence (Gen-Bank accession number: NC_012920) was used as a reference (14, 15). To detect m.13513G>A mutation in the mitochondrial ND5 gene in the patient, his relatives and normal controls, 13,319–14,287 region was amplified using: forward 5′-ACA TCT GTA CCC ACG CCT TC—3, and reverse 5′- AGA GGG GTC AGG GTT GAT TC-3′, as described previously (12, 14), and analyzed as mentioned in the context.

To further detect and quantify the mutant load of the m.13513G4A mutation in the LHON patient, his relatives and normal controls, specific single nucleotide polymorphism assays using pyrosequencing which is more sensitive in detecting low-level DNA mutations were performed as described previously (16, 17). In brief, PCR amplification of a mtDNA fragment containing the m.13513 position was carried out on Pyrosequencer PSQ96MA platform using the following primers: forward 5′-CTTCAACCTCCCT CACC-3′, reverse 5′-AGCGCTGCTCCGGTTCATAGATTGCTCAGGCGTTT GTG TATGA-3′, and sequencing A(G/A)ACCACAT (nt. 13512–13520). Sequence identification was performed by the PSQ SQA software (Biotage AB), and the percentage of mutant load was determined using the quantification function of the software.

Mitochondrial DNA sequences of 17 vertebrates were assessed for interspecific analysis (13, 18). The confidence interval (CI) was measured through the comparison of human nucleotide variants to other vertebrates ($n = 16$). The CI indicates the percentage of species with wild type nucleotides at an identical position. The mitochondrial haplogroups of the Asian were also determined as described previously (19, 20).
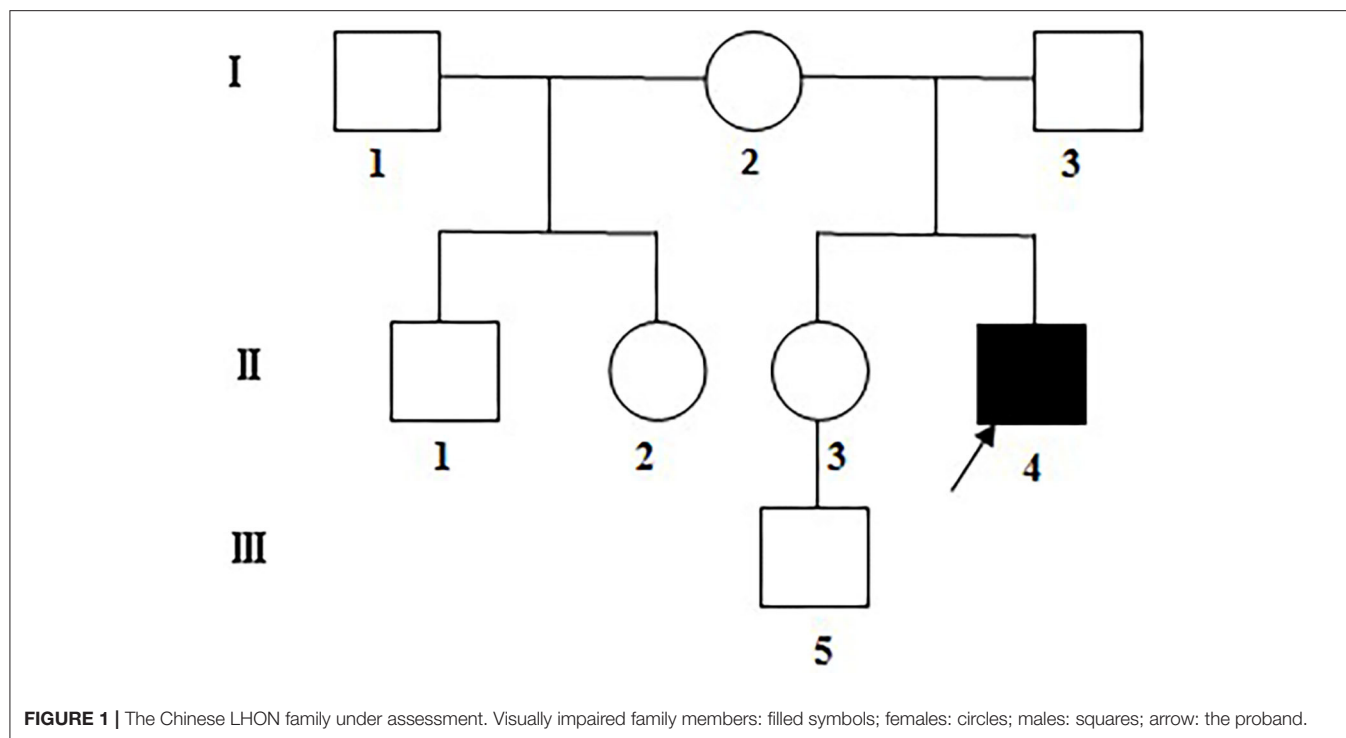
FIGURE 1 | The Chinese LHON family under assessment. Visually impaired family members: filled symbols; females: circles; males: squares; arrow: the proband.

RESULTS

Clinical Characteristics of m.13513G>A Mutation-Related LHON

Isolated LHON without any other ocular or extraocular pathology was identified in one patient in this family. The patient was a 16 years old male presenting with a complaint of sequential painless bilateral central vision loss. He first experienced a blurred vision in the left eye, unfortunately he did not pay any attention until another sudden vision loss in the right eye 1 month later, he was then taken to the local hospital for ophthalmic examination. Medical record revealed a BCVA of 20/100 and counting fingers in the right and left eye, respectively, fundus photography revealed congested optic disc edema in the right eye, and pale temporal optic disc with congested nasal optic disc edema in the left eye (**Figures 2A,B**). Octopus visual field test showed large centrocecal scotoma in the right eye and diffuse field constriction in the left eye (**Figures 2C,D**).

His past medical history was unremarkable, and he denied any other ocular or extraocular symptoms such as ptosis, extraocular muscle paralysis, sensation or movement disorders, epilepsy episode, or hearing loss. His physical examination was normal. Blood test for basic metabolic panel was unremarkable. Gadolinium enhanced orbital MRI examination showed normal signals of bilateral optic nerves and brain. He was initially diagnosed as bilateral idiopathic demyelinating optic neuritis, and treated with intravenous methylprednisolone pulse therapy (500 mg qd × 3d) followed by gradual tapering of oral methylprednisolone. Unfortunately, the patient showed no response to steroid therapy, and his vision progressively deteriorated in both eyes.

When the patient first came to our eye center another 2 weeks later, his vision was counting fingers in the right and hand motion in left eye, pupil size was 5 mm and pupillary light reflex was sluggish in both eyes with a relative afferent pupil defect in the left eye, and temporal optic disc was pale in both eyes (**Figures 3A,B**). Blood test for neuromyelitis optica-IgG antibody and myelin oligodendrocyte glycoprotein antibody were both negative. Bilateral LHON was suspected and mtDNA assessment was highly recommended. The patient initially refused our suggestion, but finally accepted and underwent mtDNA assessment 1 month later when he visited another neuro-ophthalmologist in another hospital and was clinically diagnosed as LHON.

None of three main primary point mutations in mtDNA related to LHON was detected by targeted PCR amplifications and Sanger DNA sequencing in the patient. However, heteroplasmic m.13513G>A mutation was detected by NGS and pyrosequencing of the full mt DNA genome in this paient (**Figures 4A,B**). Hence, his diagnosis was corrected to m.13513G>A mutation-related LHON.

To further exclude other possible mitochondrial diseases, the patient was referred to a neurologist and a cardiologist for consultation. However, his neurological examinations were all normal including consciousness, hearing, articulation, superficial and deep sensation, as well as muscle strength, tone, and reflexes. Blood test for cardiac enzymes including creatine kinase and lactate dehydrogenase were both unremarkable. Blood lactate fluctuation was within normal limits during exercise test. Electrocardiogram was normal and Doppler echocardiography revealed normal cardiac morphology and hemodynamics. There
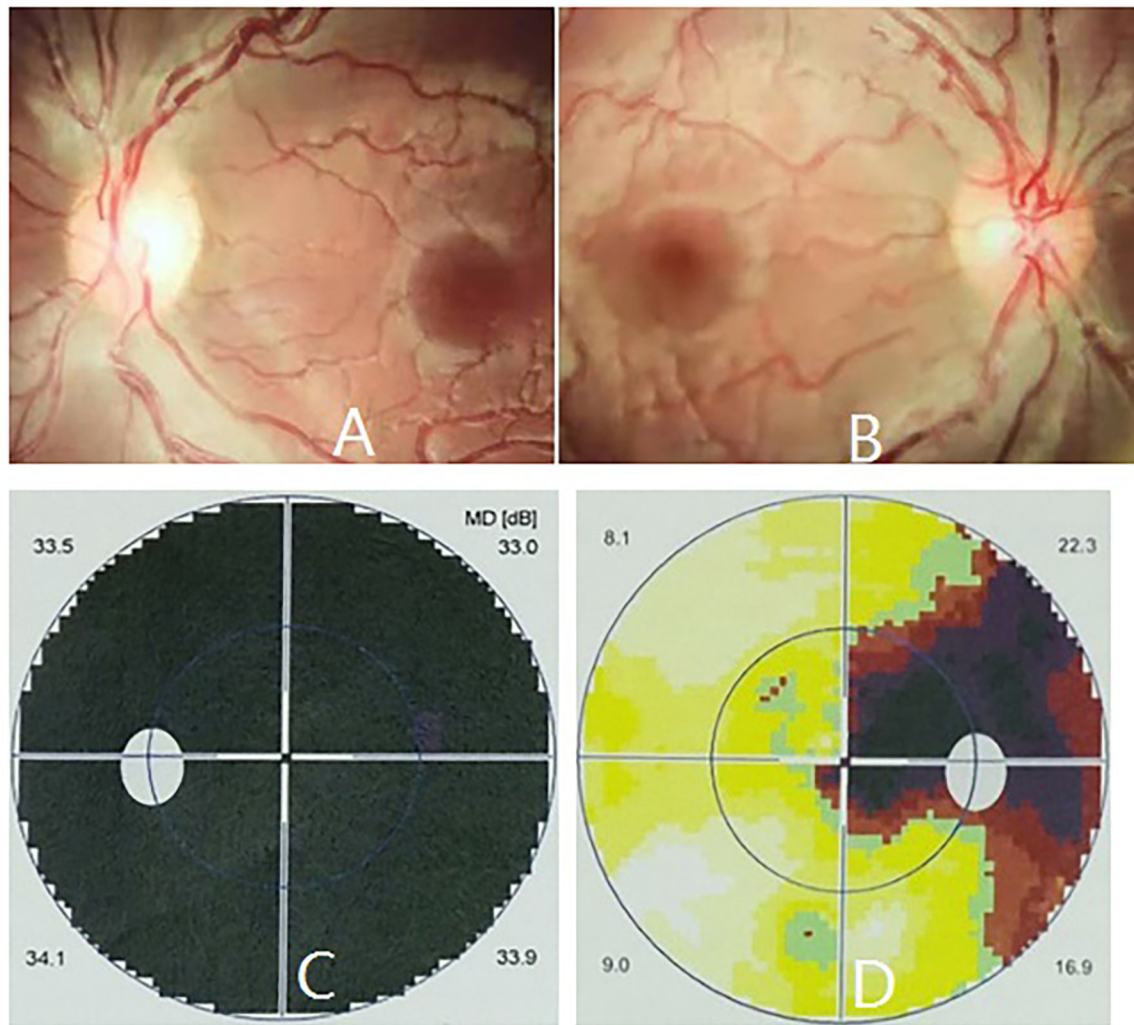
FIGURE 2 | Ophthalmic manifestations of m.13513G>A mutation-related LHON at presentation. Fundus photography revealed pale temporal optic disc with congested nasal optic disc edema in the left eye **(A)**, and congested optic disc edema in the right eye **(B)**, respectively. Octopus visual field test showed full field blindness in the left eye **(C)** and large centrocecal scotoma in the right eye **(D)**, respectively.

was no lactic acid peak found in the brain by magnetic resonance spectroscopy.

The patient was regularly followed up for 4 years, ophthalmic examination at last follow-up revealed spontaneously slight increase in his vision (20/320 in the right eye and counting fingers in the left eye), and pale optic disc in both eyes (**Figures 3C,D**). However, no other ocular or extraocular pathology was found during his follow-up.

Although all relatives of the patient underwent detailed systemic and ophthalmic examinations, no abnormal findings in consciousness, hearing, articulation, superficial and deep sensation, muscle strength, tone, and reflexes, BCVA, anterior segment and fundus examination, visual field test, as well as blood test for cardiac enzymes, blood lactate fluctuation during exercise test, electrocardiogram and Doppler echocardiography, were found during 4 years' follow-up.

Mitochondrial DNA Assessment of m.13513G>A Mutation-Related LHON

None of three main primary point mutations of LHON, i.e., m.11778G>A, m.3460G>A, and m.14484T>C, were detected by targeted PCR amplifications and Sanger DNA sequencing in the patient. However, heteroplasmic m.13513G>A mutation in the mitochondrial ND5 gene was detected by NGS of the full mtDNA genome and further confirmed by Sanger DNA sequencing in the patient (**Figure 4A**).

Mutant load of m.13513G>A mutation in the patient assessed by NGS was 33.56% (Mygenostics Company, Beijing, China) 3 months after the onset of bilateral vision loss, and 26% (Amplicon Gene Company, Shanghai, China) 3 years after the onset of bilateral vision loss. Nevertheless, no m.13513G>A mutation was detected in all his relatives by either of above twice NGS tests.
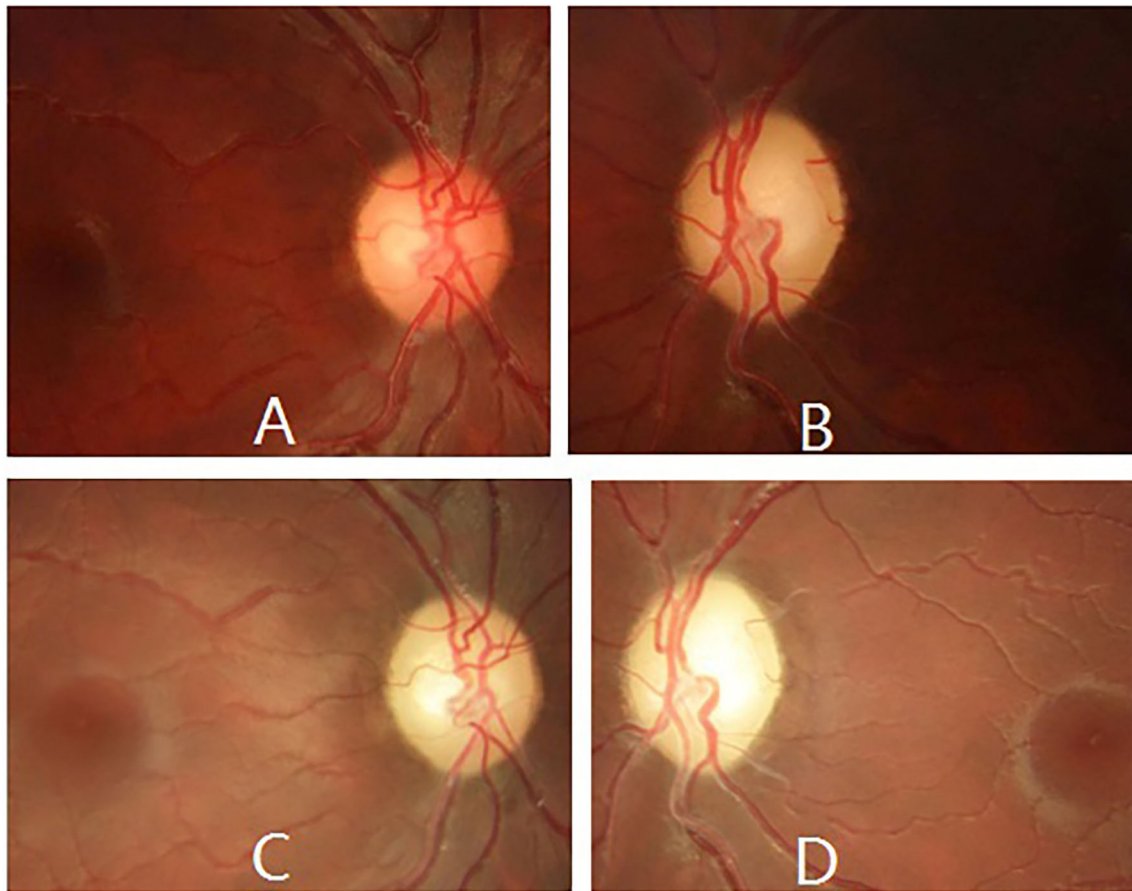
FIGURE 3 | Ophthalmic manifestations of m.13513G>A mutation-related LHON during follow-up. Fundus photography revealed temporal optic disc was pale in both eyes 2 weeks later **(A,B)**, and pale optic disc in both eyes 4 years later **(C,D)**.

Pyrosequencing of the full mt DNA genome was assessed 3 years after the onset of bilateral vision loss in this patient, and m.13513G>A mutation with a mutant load of 22.4, 1.9, 0, and 0% was detected in the patient, his mother, father and other maternal relatives, respectively (**Figure 4B**). None of 100 healthy control subjects were detected to harbor m.13513G>A mutation either by NGS or by pyrosequencing of the full mt DNA genome.

Based on crystal-structures of complex I in mammals, m.13513 encoded the residue D393 of ND5 protein (**Figure 5**). This residue was found to be highly conserved amongst ND5 proteins of the 17 organisms. The array of polymorphic loci in the mitochondrial DNA of the family investigated in this study was shown in **Table 1**, there were 2 variants detected in 12S rRNA gene, 2 variants in 16S rRNA gene, 11 variants in D-loop, one variant in tRNA, and 9 missense mutations and 17 silent variants in protein- encoding genes. The phylogeny of variants were investigated through comparisons to mice (21), cows (22), and Xenopus laevis (23), whereas none of them showed obvious evolutionary conservation. Moreover, according to the nomenclature of mitochondrial haplogroups, these mtDNA polymorphic variations in this pedigree belonged to the Eastern Asian haplogroups D4a.

DISCUSSION

Although ∼90% of the mtDNA mutations related to LHON was one of three primary mutations, i.e., m.11778G>A, m.3460G>A, and m.14484 T>C, other rare primary mtDNA mutaions including m.13513G>A have also been reported to cause LHON independently (1–7). As the most frequently reported mutation in the mitochondrial ND5 gene, m.13513G>A mutation was identified as a causative gene mutation mostly related to LS, MELAS, and LS or MELAS related overlap syndromes (7–11, 24, 25). Until now, LHON caused by m.13513G>A mutation yet not accompanied by LS or MELAS was reported in only three cases (9–11). However, all above three LHON cases were accompanied by other ocular and (or) extraocular pathology (9–11). To our knowledge, this is the first report of the m.13513G>A mutation presenting as isolated LHON yet without any other ocular or extraocular pathology.

In mitochondrial diseases, it is not unusual for the same mutation in the same gene to result in different manifestations. Previous study indicated that germ-line mtDNA bottleneck existed during oogenesis and caused significant heteroplasmy frequency shifts between generations. As for a pathogenic

FIGURE 4 | Mutant load of the m.13513G>A mutation in this Chinese LHON family. Test results of m.13513G>A mutation in the LHON patient (II-4), his mother (I-2), his sister (II-3), and his father (I-3) assessed by next generation sequencing **(A)** and by pyrosequencing **(B)**, respectively.
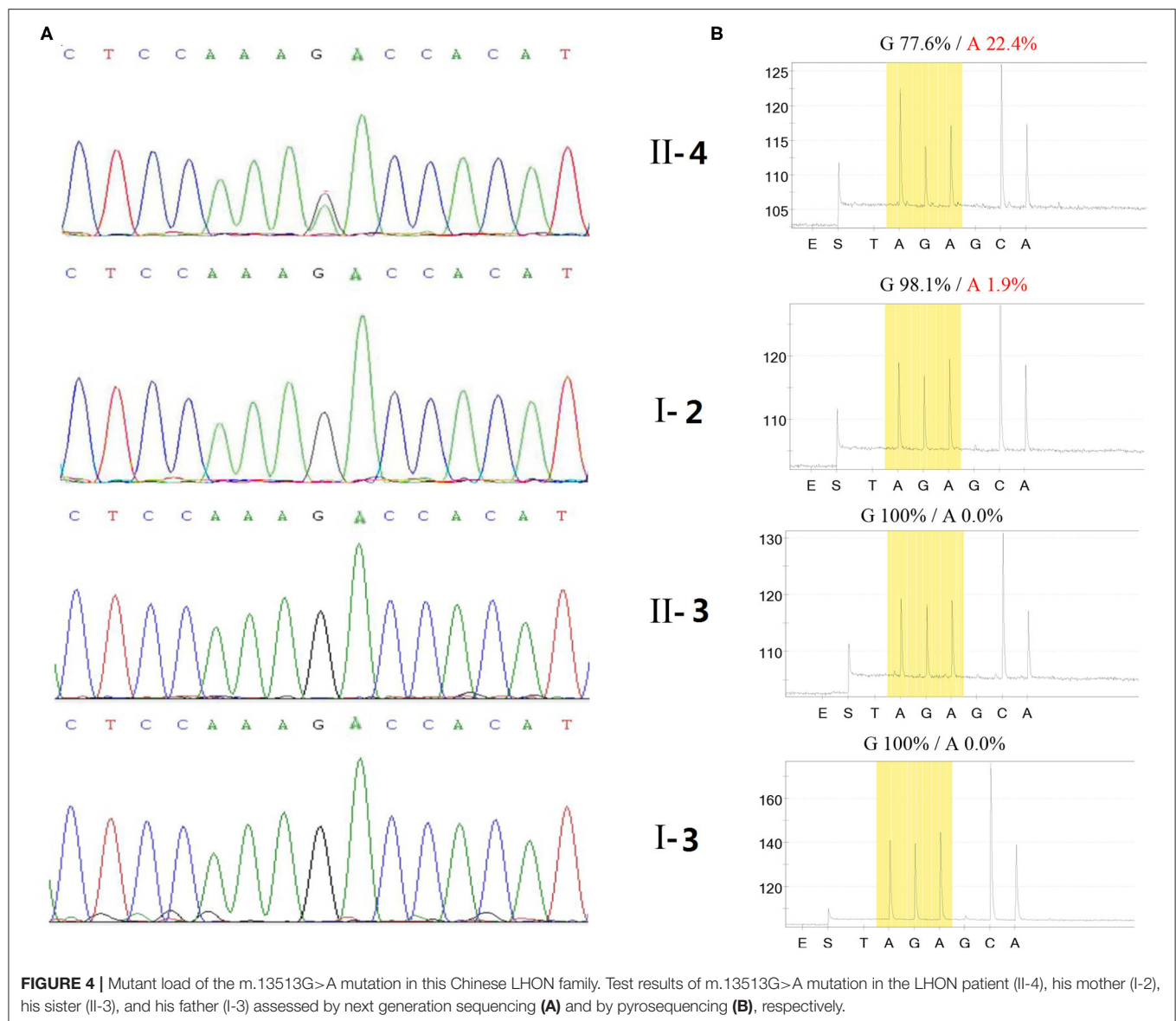
heteroplasmy, a severe bottleneck might abruptly transform a benign (low) frequency in a mother into a disease-causing (high) frequency in her children (26). It is also hypothesized that the drastic changes of heteroplasmy frequency between generations contribute to non-disease mutant load or higher disease severity. In this study, the LHON patient presented 22.4% mutant load, compared to his mother only 1.9% in blood cells by pyrosequencing assessment, which might be explained by the genetic drift due to germ-line bottleneck effect.

The m.13513G>A is a point mutation in mitochondrial ND5 gene which can cause severe oxidative phosphorylation defect (26). The amino acid at position 393 of ND5 subunit encoded by m.13513 is located at an evolutionarily conserved part of a putative quinone-reactive site of the enzyme, and the D393N amino acid change caused by m.13513 G>A mutation may lead to loss of the quinine reactive site and a subsequent negative effect on the activity of the oxidative phosphorylation system, followed by significant mitochondrial impairment, as well as an increased reactive oxygen species generation and reduced ATP production, which finally resulting in the development of LHON (24, 25, 27).

In cultured cells, the threshold for m.13513G>A mutation causing a complex I defect is a mutant load of ~30%, and its impairment increased in a mutant-load dependent way (24, 28). The mutant load of the m.13513G>A mutation which is 22.4 ~33.56% in blood cells in the LHON patient in our study is consistent with above finding. Previous investigations about the mutant load in patients with m.13513G>A mutation revealed much lower mutant load of 4~6% in blood cells, 1~5% in fibroblasts, and 13~15% in muscle in one patient, and of 11~17% in blood, hair and muscle tissues in another patient (24). Among all human tissues, optic nerve head is most susceptible to mitochondrial dysfunction, since mitochondria are most

FIGURE 5 | Altered complex I assembly. Structural interactions of ND5-D393 (5XTD in the protein bank). The hydroxyl group of D393 forms specific electrostatic interactions with G388, F389, I396, and E397 in MT-ND5.
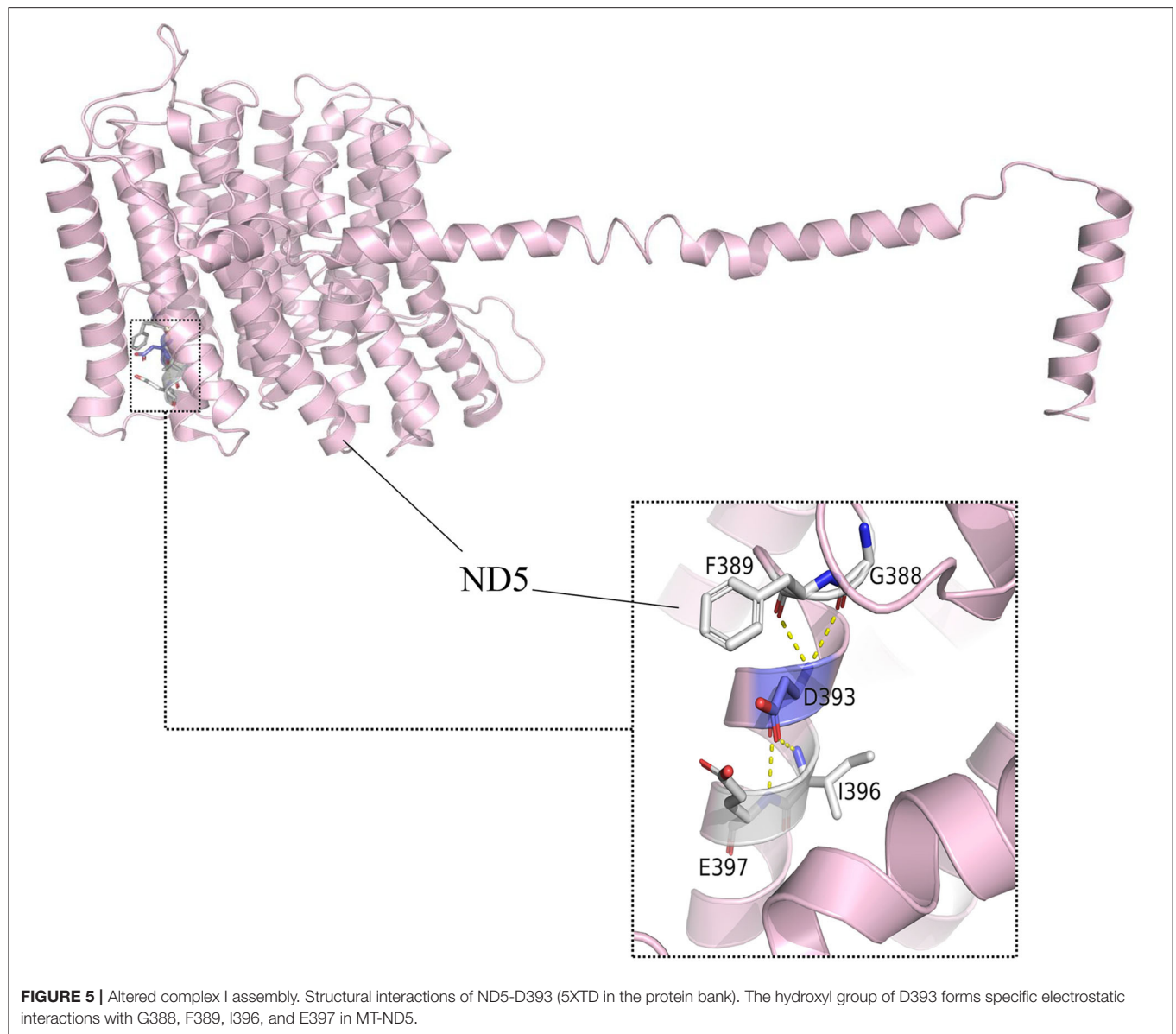
abundantly clustered in retinal nerve fibers at optic nerve head. On the other hand, previous investigations have demonstrated that ND5 synthesis is probably the rate-limiting step for the activity of complex I and consequently of respiration (24). Hence, contrary to most pathogenic mtDNA mutations which only result in the outbreak of a oxidative phosphorylation defect disease when presenting at high mutant loads in target tissues, the m.13513G>A mutation may cause significant complex I defect at optic nerve head and induce an isolated LHON without any other tissue involvement even at unusually low mutant loads.

Our study revealed that the mitochondrial genomes of this pedigree belongs to the Eastern Asian haplogroups D4a. Although many other mtDNA variants were also detected in this study, there were no functionally significant mutations in this pedigree. Hence, these mtDNA variants may not

have a potential modifying role in the development of visual impairment associated with m.13513G>A mutation. This implied that m.13513G>A mutation, similar to three primary mt.DNA mutations related to LHON, occurred sporadically and multiplied through evolution of the mtDNA.

There are several limitations in this study. First, only peripheral blood cells were collected for genome assessment. Considering that the percentage of m.13513G>A mutation may vary in different tissues, it would greatly benefit if the percentage of heteroplasmy of m.13513G>A mutation in other tissues such as urine, hair, buccal mucosa, and muscles were assessed. Unfortunately, the patient declined further genome assessment, for no other tissues except optic nerves were involved. Second, although no other ocular or extraocular pathology was found in

TABLE 1 | mtDNA variants in a Chinese family with Leber's hereditary optic neuropathy.

Gene	Position	Replacement	AA change	Conservation (H/B/M/X)	Previously reported
D-loop	73	A-G			Yes
	152	T-C			Yes
	263	A-G			Yes
	298	C-T			Yes
	489	T-C			Yes
	514	C-/			Yes
	515	A-/			Yes
	16092	T-C			Yes
	16223	C-T			Yes
	16274	G-A			Yes
	16362	T-C			Yes
12S rRNA	750	A-G		A/A/A/-	Yes
	1438	A-G		C/C/A/-	Yes
16S rRNA	2706	A-G			Yes
	3010	G-A			Yes
ND1	3969	C-A			Yes
tRNA Gln	4393	C-T			Yes
ND2	4769	A-G			Yes
	4883	C-T			Yes
	5178	C-A	Leu-Met	L/T/T/T	Yes
	5231	G-A			Yes
CO1	7028	C-T			Yes
ATP8	8414	C-T	Leu-Phe		Yes
ATP6	8701	A-G	Thr-Ala	T/S/L/Q	Yes
	8860	A-G	Thr-Ala	T/A/A/T	Yes
CO3	9355	A-G	Asn-Ser		Yes
	9380	G-A			Yes
	9540	T-C			Yes
ND3	10398	A-G	Thr-Ala	T/T/T/A	Yes
	10400	C-T			Yes
ND4	10873	T-C			Yes
	11059	C-T			Yes
	11719	G-A			Yes
ND5	12705	C-T			Yes
	13104	A-G			Yes
	13513	G-A	Asp-Asn		Yes
	13708	G-A	Ala-Thr		Yes
ND6	14668	C-T			Yes
Cytb	14766	C-T	Thr-Ile	T/S/T/S	Yes
	14783	T-C			Yes
	15043	G-A			Yes
	15301	G-A			Yes
	15326	A-G	Thr-Ala	T/M/I/I	Yes

this young-adult patient during 4 years' follow-up, other tissues involvement can not be excluded if follow-up time is much longer. Hence, regular ophthalmic and systemic examinations, as well as long-term follow-up have been highly recommended to this patient.

In summary, low mutant load of m.13513G>A mutation was detected in the LHON patient by both NGS and pyrosequencing of the full mt DNA genome in this study, indicating that NGS and pyrosequencing are both sensitive to detect low-level DNA mutation. Hence, patients with typical ophthalmic manifestations of LHON but with negative results of three primary point mutations related to LHON tested by targeted PCR amplification, may need to be further assessed by NGS or pyrosequencing.

DATA AVAILABILITY STATEMENT

The raw data supporting the conclusions of this article will be made available by the authors, without undue reservation.

ETHICS STATEMENT

The studies involving human participants were reviewed and approved by Second Affiliated Hospital of Zhejiang University School of Medicine. Written informed consent to participate in this study was provided by the participants' legal guardian/next of kin.

AUTHOR CONTRIBUTIONS

C-bS and ZL wrote and reviewed the manuscript. C-bS, H-xB, and D-nX collected the patient data. C-bS, D-nX, and QX performed literature research. C-bS, H-xB, and ZL analyzed and interpreted the clinical data. C-bS performed medical treatment. All authors read and approved the final manuscript.

FUNDING

REFERENCES

1. Rasool N, Lessell S, Cestari DM. Leber hereditary optic neuropathy: bringing the lab to the clinic. *Semin Ophthalmol.* (2016) 31:107–16. doi: 10.3109/08820538.2015.1115251

2. Chun BY, Rizzo JF III. Dominant optic atrophy and leber's hereditary optic neuropathy: update on clinical features and current therapeutic approaches. Semin *Pediatr Neurol.* (2017) 24:129–34. doi: 10.1016/j.spen.2017.06.001

3. Jurkute N, Yu-Wai-Man P. Leber hereditary optic neuropathy: bridging the translational gap. *Curr Opin Ophthalmol.* (2017) 28:403–9. doi: 10.1097/ICU.0000000000000410

4. Kirches E. LHON: mitochondrial mutations and more. *Curr Genomics.* (2011) 12:44–54. doi: 10.2174/138920211794520150

5. Yahata N, Matsumoto Y, Omi M, Yamamoto N, Hata R. TALEN-mediated shift of mitochondrial DNA heteroplasmy in MELAS-iPSCs with m.13513G>A mutation [published correction appears in Sci Rep. (2018). Mar 13;8:4683]. *Sci Rep.* (2017) 7:15557. doi: 10.1038/s41598-017-15871-y

6. Brecht M, Richardson M, Taranath A, Grist S, Thorburn D, Bratkovic D. Leigh syndrome caused by the MT-ND5 m.13513G>A mutation: a case presenting with WPW-like conduction defect, cardiomyopathy, hypertension and hyponatraemia. *JIMD Rep.* (2015) 19:95–100. doi: 10.1007/8904_2014_375

7. Pulkes T, Eunson L, Patterson V, Siddiqui A, Wood NW, Nelson IP, et al. The mitochondrial DNA G13513A transition in ND5 is associated with a LHON/MELAS overlap syndrome and may be a frequent cause of MELAS. *Ann Neurol.* (1999) 46:916–9. doi: 10.1002/1531-8249(199912)46:6<916::AID-ANA16>3.0.CO;2-R

8. Han J, Lee YM, Kim SM, Han SY, Lee JB, Han SH. Ophthalmological manifestations in patients with Leigh syndrome. *Br J Ophthalmol.* (2015) 99:528–35. doi: 10.1136/bjophthalmol-2014-305704

9. Vázquez-Justes D, Carreño-Gago L, García-Arumi E, et al. Mitochondrial m.13513G>A point mutation in ND5 in a 16-year-old man with leber hereditary optic neuropathy detected by next-generation sequencing. *J Pediatr Genet.* (2019) 8:231–4. doi: 10.1055/s-0039-1691812

10. Ahmad KE, Fraser CL, Sue CM, Barton JJ. Beyond what the eye can see. *Surv Ophthalmol.* (2016) 61:674–9. doi: 10.1016/j.survophthal.2016.02.003

11. Chen BS, Biousse V, Newman NJ. Mitochondrial DNA 13513G>A mutation presenting with Leber's hereditary optic neuropathy. *Clin Exp Ophthalmol.* (2019) 47:1202–4. doi: 10.1111/ceo.13603

12. Andrews RM, Kubacka I, Chinnery PF, Lightowlers RN, Turnbull DM, Howell N. Reanalysis and revision of the Cambridge reference sequence for human mitochondrial DNA. *Nat Genet.* (1999) 23:147. doi: 10.1038/13779

13. Liang M, Jiang P, Li F, et al. Frequency and spectrum of mitochondrial ND6 mutations in 1218. Han Chinese subjects with Leber's hereditary optic neuropathy. *Invest Ophthalmol Vis Sci.* (2014) 55:1321–31. doi: 10.1167/iovs.13-13011

14. Wang J, Zhao N, Mao X, Meng F, Huang K, Dong G, et al. Obesity associated with a novel mitochondrial tRNACys 5802A>G mutation in a Chinese family. *Biosci Rep.* (2020) 40:BSR20192153. doi: 10.1042/BSR20200131

15. Lott MT, Leipzig JN, Derbeneva O, Xie HM, Chalkia D, Sarmady M, et al. mtDNA variation and analysis using mitomap and mitomaster. *Curr Protoc Bioinformatics.* (2013) 44:1.23.1-26. doi: 10.1002/0471250953.bi0123s44

16. Ballana E, Govea N, de Cid R, Garcia C, Arribas C, Rosell J, et al. Detection of unrecognized low-level mtDNA heteroplasmy may explain the variable phenotypic expressivity of apparently homoplasmic mtDNA mutations. *Hum Mutat.* (2008) 29:248–57. doi: 10.1002/humu.20639

17. Ruiter EM, Siers MH, van den Elzen C, et al. The mitochondrial 13513G>A mutation is most frequent in Leigh syndrome combined with reduced complex I activity, optic atrophy and/or Wolff-Parkinson- White. *Eur J Hum Genet.* (2007) 15:155–61. doi: 10.1038/sj.ejhg.5201735

18. Jiang P, Jin X, Peng Y, Wang M, Liu H, Liu X, et al. The exome sequencing identified the mutation in YARS2 encoding the mitochondrial tyrosyl-tRNA synthetase as a nuclear modifier for the phenotypic manifestation of Leber's hereditary optic neuropathy-associated mitochondrial DNA mutation. *Hum Mol Genet.* (2016) 25:584–96. doi: 10.1093/hmg/ddv498

19. Kong QP, Bandelt HJ, Sun C, Yao YG, Salas A, Achilli A, et al. Updating the East Asian mtDNA phylogeny: a prerequisite for the identification of pathogenic mutations. *Hum Mol Genet.* (2006) 15:2076–86. doi: 10.1093/hmg/ddl130

20. Tanaka M, Cabrera VM, González AM, Larruga JM, Takeyasu T, Fuku N, et al. Mitochondrial genome variation in eastern Asia and the peopling of Japan. *Genome Res.* (2004) 14:1832–50. doi: 10.1101/gr.2286304

21. Bibb MJ, Van Etten RA, Wright CT, Walberg MW, Clayton DA. Sequence and gene organization of mouse mitochondrial DNA. *Cell.* (1981) 26:167–80. doi: 10.1016/0092-8674(81)90300-7

22. Gadaleta G, Pepe G, De Candia G, Quagliariello C, Sbisà E, Saccone C. The complete nucleotide sequence of the Rattus norvegicus mitochondrial genome: cryptic signals revealed by comparative analysis between vertebrates. *J Mol Evol.* (1989) 28:497–516. doi: 10.1007/BF02602930

23. Roe BA, Ma DP, Wilson RK, Wong JF. The complete nucleotide sequence of the Xenopus laevis mitochondrial genome. *J Biol Chem.* (1985) 260:9759–74. doi: 10.1016/S0021-9258(17)39303-1

24. Blok MJ, Spruijt L, de Coo IF, Schoonderwoerd K, Hendrickx A, Smeets HJ. Mutations in the ND5 subunit of complex I of the mitochondrial DNA are a frequent cause of oxidative phosphorylation disease. *J Med Genet.* (2007) 44:e74. doi: 10.1136/jmg.2006.045716

25. Monlleo-Neila L, Toro MD, Bornstein B, Garcia-Arumi E, Sarrias A, Roig-Quilis M, et al. Leigh syndrome and the mitochondrial m.13513G>A mutation: expanding the clinical spectrum. *J Child Neurol.* (2013) 28:1531–4. doi: 10.1177/0883073812460580

26. Rebolledo-Jaramillo B, Su MS, Stoler N, McElhoe JA, Dickins B, Blankenberg D, et al. Maternal age effect and severe germ-line bottleneck in the inheritance of human mitochondrial DNA. *Proc*

Natl Acad Sci USA. (2014) 111:15474–9. doi: 10.1073/pnas.14093
28111

27. Petruzzella V, Di Giacinto G, Scacco S, Piemonte F, Torraco A, Carrozzo R, et al. Atypical Leigh syndrome associated with the D393N mutation in the mitochondrial ND5 subunit. *Neurology.* (2003) 61:1017–8. doi: 10.1212/01.WNL.0000080363.10902.E9

28. Galera-Monge T, Zurita-Díaz F, Garesse R, Gallardo ME. The mutation m.13513G>A impairs cardiac function, favoring a neuroectoderm commitment, in a mutant-load dependent way. *J Cell Physiol.* (2019) 234:19511–2. doi: 10.1002/jcp.28549

frontiers
in Neurology

Case Report: A Novel Mutation in the Mitochondrial *MT-ND5* Gene Is Associated With Leber Hereditary Optic Neuropathy (LHON)

Martin Engvall [1,2], Aki Kawasaki [3], Valerio Carelli [4,5], Rolf Wibom [2,6], Helene Bruhn [2,6], Nicole Lesko [1,2], Florian A. Schober [1], Anna Wredenberg [2,6], Anna Wedell [1,2] and Frank Träisk [7,8]*

[1] Department of Molecular Medicine and Surgery, Karolinska Institutet, Stockholm, Sweden, [2] Centre for Inherited Metabolic Diseases, Karolinska University Hospital, Stockholm, Sweden, [3] Hopital Ophtalmique Jules Gonin, Fondation Asile des Aveugles, University of Lausanne, Lausanne, Switzerland, [4] Programma di Neurogenetica, IRCCS Istituto delle Scienze Neurologiche di Bologna, Bologna, Italy, [5] Department of Biomedical and Neuromotor Sciences (DIBINEM), University of Bologna, Bologna, Italy, [6] Department of Medical Biochemistry and Biophysics, Karolinska Institutet, Stockholm, Sweden, [7] Department of Clinical Neuroscience, Division of Eye and Vision, St. Erik Eye Hospital, Karolinska Institutet, Solna, Sweden, [8] Department of Neuro-Ophthalmology, St.Erik Eye Hospital, Solna, Sweden

Leber hereditary optic neuropathy (LHON) is a mitochondrial disease causing severe bilateral visual loss, typically in young adults. The disorder is commonly caused by one of three primary point mutations in mitochondrial DNA, but a number of other rare mutations causing or associated with the clinical syndrome of LHON have been reported. The mutations in LHON are almost exclusively located in genes encoding subunits of complex I in the mitochondrial respiratory chain. Here we report two patients, a mother and her son, with the typical LHON phenotype. Genetic investigations for the three common mutations were negative, instead we found a new and previously unreported mutation in mitochondrial DNA. This homoplasmic mutation, m.13345G>A, is located in the *MT-ND5* gene, encoding a core subunit in complex I in the mitochondrial respiratory chain. Investigation of the patients mitochondrial respiratory chain in muscle found a mild defect in the combined activity of complex I+III. In the literature six other mutations in the *MT-ND5* gene have been associated with LHON and by this report a new putative mutation in the *MT-ND5* can be added.

Keywords: leber hereditary optic neuropathy, optic neuropathy, MT-ND5, mitochondrial DNA, case report, complex 1, LHON

INTRODUCTION

Leber hereditary optic neuropathy (LHON) usually manifests as a sequential subacute optic neuropathy. A pathogenic mutation in the mitochondrial DNA (mtDNA), in conjunction with environmental and possibly other genetic factors, leads to the disruption and progressive loss of small caliber retinal ganglion cells in the papillo-macular bundle (1–3). Typically the patient with LHON presents with monocular loss of visual acuity in parts of the central visual field. Involvement of the second eye occurs within 1 year, in most cases already within 6–8 weeks. The optic disc appearance may at first assessment be normal or show blurred margins and telangiectatic

microangiopathy. Over the following weeks or months vision continues to deteriorate as a result of the progressive loss of retinal ganglion cells and atrophy of the optic nerves (3). LHON is a rare cause of optic neuropathy, with a prevalence of about 1 in 30,000 to 1 in 50,000 people in the population (4–6). Male gender is clearly associated with an increased risk of the disease, as roughly 50% of males and only 10% of female LHON carriers develop visual loss (7). Other likely risk-factors are exposure to tobacco and alcohol (8) as well as modifying genetic factors that may regulate disease penetrance (2, 9). If there is no family history of LHON, there is an inherent risk that the clinician will falsely suspect the patient with LHON to have optic neuritis since both disorders often manifest at age 15–35 years. However, the painless continuous progression of visual loss without recovery does not follow the evolution of a typical optic neuritis, and therefore such a presentation requires an early and thorough work-up to exclude other causes of acute optic neuropathy.

In LHON three common point mutations in mtDNA constitute the primary pathogenic mutations, m.11778G>A (*MT-ND4*), m.3460G>A (*MT-ND1*) and m.14484T>C (*MT-ND6*). Together they account for 90% of symptomatic patients with LHON. The proteins encoded by these genes are crucial subunits for complex I of the mitochondrial respiratory chain (7, 10).

Progress in DNA-sequencing techniques of both nuclear and mitochondrial genes, in conjunction with increasing awareness of mitochondrial disease, has led to many new mutations reported in association with clinically recognized phenotypes of mitochondrial diseases, including LHON. The collective prevalence of adult mitochondrial disease now makes them among the most common adult form of inherited neurological disorders, when including disease-causing mutations in both the mitochondrial and nuclear genome (11). More information is continuously being reported about previously undescribed mtDNA mutations and their phenotypic features.

Mitomap, a database of human mitochondrial DNA variations, reports 19 primary mtDNA mutations which are now associated with the LHON phenotype and 18 others which are candidate mutations for singleton or single families (12).

Herein, we report a mother and her adult son who presented in the same year with a severe bilateral optic neuropathy. There was no known family history of optic neuropathy. Testing for the three primary LHON mutations was negative, but whole genome sequencing (WGS) analysis of DNA from muscle targeting both nuclear genes causing mitochondrial and other metabolic diseases and mtDNA identified the same unique homoplasmic mutation in both subjects, m.13345G>A, p.(Ala337Thr) in *MT-ND5*. No other disease-causing mutation was found that could explain the phenotype.

CASE REPORT

Case 1 (Proband)

A 49 year old woman came to the eye clinic for rapid and painless visual loss in her right eye (RE) over 3 weeks. Prior to right eye visual loss, she had noted deteriorating vision in her left eye (LE) but could not be more specific about the time of

onset. Review of prior records showed that 1 month prior to presentation, her optician had documented best corrected visual acuity (BCVA) as 0.8 in the RE and 0.05 in the LE. She was a consumer of tobacco mainly in the form of snuff (oral smokeless tobacco) and she occasionally smoked 5–10 cigarettes a day. She denied regular use of alcohol but according to medical records she had a history of periodic high consumption of alcohol. She had also been prescribed vitamin B12 daily. Past medical history was otherwise unremarkable. The patient has one son and two sisters of which one has a daughter. The patient's mother had died from malignant melanoma and the maternal grandmother from ruptured aortic aneurysm. None of the relatives known to the patient had any history of visual problems, dementia, muscle disease, diabetes or hearing problems apart from one sister having some hearing loss after a rubella infection in childhood. On examination, BCVA was 0.13 in the RE and hand motion in the LE Humphrey® automated visual fields 24-2 (Carl Zeiss Meditec.Inc®, Jena) showed a temporal defect encroaching fixation in the RE and a large central scotoma in the LE (**Figure 1**). A relative afferent pupillary defect was observed in the LE. Funduscopy showed slight temporal pallor of the optic disk and there was an epiretinal membrane in the LE.

The rapidly progressing deep central scotoma in one eye combined with a temporal hemidefect in the other eye suggested pathology at the chiasm. The MRI showed increased signal on T2 and FLAIR sequences without contrast enhancement in the central optic chiasm, in the optic tracts and in the intracranial portion of both optic nerves. There was no signal abnormality in the brain or brainstem. The patient underwent extensive investigations for various causes of an acute optic neuropathy and corticosteroid therapy was initiated for presumed neuromyelitis optica. A lumbar puncture was performed for analysis of cerebrospinal fluid including electrophoresis. Other work-up for inflammatory neuropathy included CT scan of the thorax and serum analysis for angiotensin converting enzyme and many autoantibodies: S-ANA, antibodies against the S-nucleosome, S-Ribosomal P, S-RNP68, S-Scl-70, S-Sm, S-SmRNP, SS-A, SS-B, Centromer, Jo-1, dsDNA, antiMOG and Aquaporin 4 in serum, of which all were negative. Since the patient's vision did not improve after 5 days of corticosteroids, the severity of visual loss prompted further treatment with plasmapheresis. This also failed to improve vision.

The history of tobacco/alcohol use and vitamin B12 vitamin substitution raised consideration for malnutritional optic neuropathy, but levels of folic acid, vitamin B6 and cobalamin were found to be within normal limits. Intravenous multivitamin injections were however given *ex juvantibus*. Three weeks after presentation, OCT (Carl Zeiss Meditec.Inc®, Jena) showed significant thinning of the ganglion cell-internal plexiform layer thickness predominantly in the nasal parts with the average thickness of 65 μm in the RE and 82 μm in the LE. The peripapillary retinal nerve fiber layer (pRNFL) thickness was still preserved (96 μm in RE and 122 μm in LE) but artefactually augmented in the LE due to missegmentation due to the epiretinal membrane. A fullfield ERG was normal, confirming intact retinal photoreceptor function.

FIGURE 1 | Automated Humphrey visual field of patient described in Case 1 performed 3 weeks from symptomatic decline of vision in the second eye, i.e., the right eye. A temporal defect is noted in the RE and a central defect in the LE.
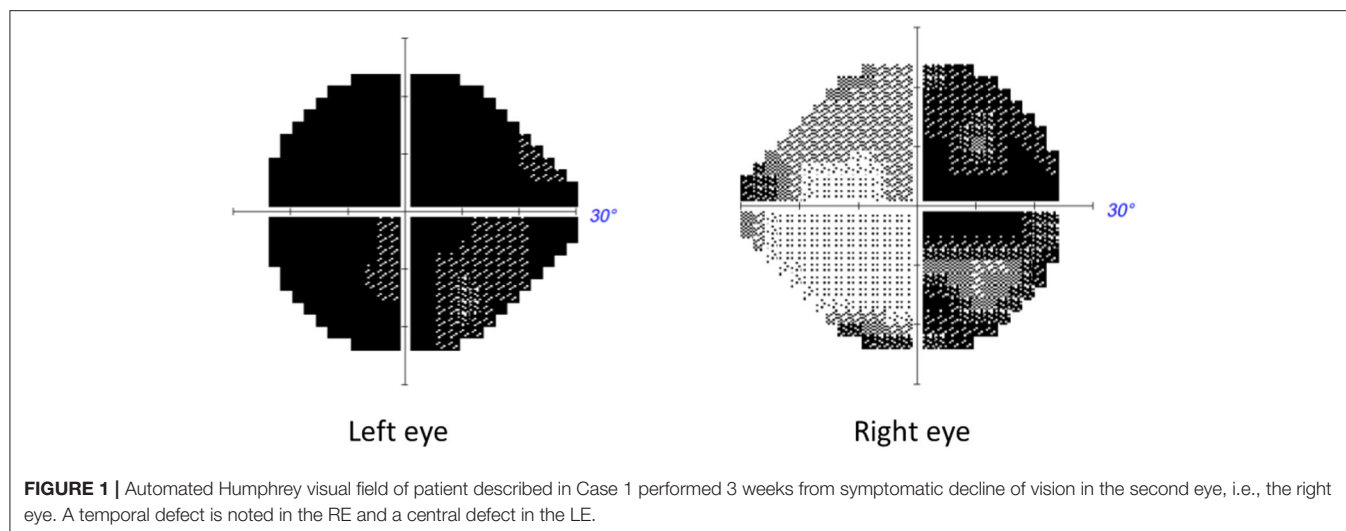
Even though the family history was negative, the sequential visual loss and absence of response to treatment for optic neuritis suggested mitochondrial origin, but since the three most common mutations associated with LHON were negative we pursued more extensive molecular analysis, see below.

Case 2: Son

The 19 year old son of the proband was referred to the eye clinic in a neighboring town. He had not been in contact with his mother for several years, but had heard through a relative that she was under investigation for loss of vision. In the preceding 2 months he had experienced progressive painless visual deterioration in both eyes and the news of similar symptoms in his mother prompted him to seek medical advice. The patient was smoking ∼10 cigarettes a day and had a history of recreational drug use. During the few months prior to visual loss, he had consumed more alcohol than usual and had used cannabis more than once a week. He denied ingestion of other toxic substances in the months preceding visual loss.

On examination BCVA was 0.04 in the RE and 0.02 in the LE with bilateral central scotomas and temporal pallor of both optic nerves. There was no significant temporal thinning in the pRNFL on OCT but at this stage the average pRNFL was still relatviely preserved at 92 μm in the RE and 94 μm in the LE.

When the treating ophthalmologist discovered that the patient's mother was under investigation for LHON, there was an immediate suspicion of the same diagnosis. MRI of the brain and orbit was normal. Routine laboratory tests including serum vitamin B screening, ANA and antibodies against aquaporin-4 and myelin oligodendrocyte glycoprotein were normal. The three most common mutations for LHON were negative.

In both cases we suspected mitochondrial optic neuropathy and extended investigations by performing muscle biopsies for mitochondrial biochemical investigations and targeted whole genome sequencing (WGS) to look for mitochondrial as well as all other inherited optic neuropathies. A percutaneous muscle specimen was obtained from the anterior tibial muscle using a conchotome. Mitochondria were isolated from muscle

and mitochondrial ATP production rate and respiratory chain enzyme activities were determined as previously described (13). The muscle biopsy showed normal mitochondrial ATP production rates (data not shown). Measurements of the respiratory chain enzyme activities revealed a mild reduction in complex I+III in both the patient and her son while all other activities (including complex I) were found to be within the reference range (**Figure 2**).

Blue Native Gel Electrophoresis showed normal amount and composition of complexes I-V (data not shown). WGS of DNA extracted from skeletal muscle was performed to a sequencing depth of 30x mean coverage using a NovaSeq 6000 sequencing instrument (Illumina) after library preparation with NxSeq AmpFREE Low DNA Library Kit (Lucigen). This was followed by in-house bioinformatics analysis, using the mutation identification pipeline (MIP) as earlier described (14). Analysis of all known nuclear disease genes associated with optic neuropathies (for gene list see **Supplementary File 1**), mitochondrial and metabolic diseases and mtDNA detected the mutation m.13345G>A, p.(Ala 337Thr) in the mitochondrially encoded NADH:ubiquinone oxidoreductase core subunit 5 (*MT-ND5*) in homoplasmy and was assumed to be related to the optic neuropathy (**Figure 3A**). No other disease-causing mutations that could explain the phenotype were identified. Sanger sequencing of DNA extracted from urinary epithelial cells and blood also showed the mutation in homoplasmy.

After the detection of a homoplasmic mtDNA mutation, additional investigations for other clinical manifestations of mitochondrial disease including echocardiography, electrocardiography, audiography and electromyography were performed. All were normal apart from a slight sublinical decline in the high frequencies in the audiogram of both ears in the mother.

At this stage both mother and son were diagnosed with LHON. They were advised to refrain from smoking and use of alcohol and also prescribed Idebenone 900 mg daily. Regrettably this did not improve vision and after a year the treatment was stopped. During the months following onset, optic atrophy

FIGURE 2 | Graphic of respiratory chain enzyme activities in the muscle biopsy of the two patients described in Case 1 and Case 2, as compared to normal controls. There is a mild reduction in complex I + III.
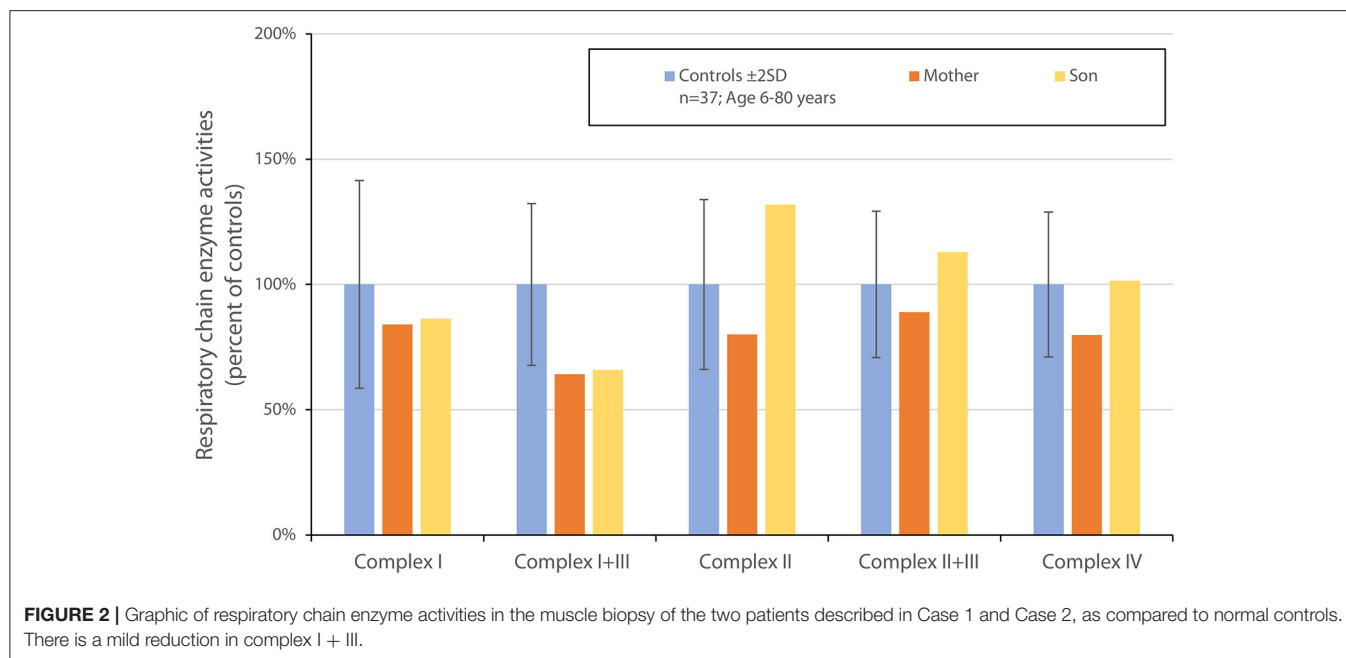
developed (**Figure 4**). Sixteen months from presentation, the BCVA of the mother was 0.04 in the RE and 0.02 in the LE and deep central scotomas were present on Humphrey perimetry 20 months after the first visit, BCVA of the son was in the RE 0.04 and in the LE 0.04 with deep central scotomas still present. OCT (Topcon®, Dublin, CA) showed severe thinning of the pRNFL; 50 microm in the RE and 48 microm in the LE consistent with bilateral optic atrophy.

DISCUSSION

Although the age at symptomatic onset is broad, patients with LHON typically lose vision between the ages of 15 and 35 years. In this report of a familial optic neuropathy, the mother at age 49 years and her son at age 19 years experienced onset of visual loss within the same 6 month period. Because of this curious coincidence, a shared external factor which might have precipitated symptomatic expression of the mtDNA mutation was suspected. Specifically, we wondered about exposure to similar toxic substances or illicit drugs. We investigated the background of tobacco, alcohol and other drug consumption in both patients. There was no evidence of home-distilled alcohol consumption from a mutual supplier nor corroboration of purchase of similar recreational drugs from the same source. In fact, the son was living in Spain for several months just before and at the time of his visual decline, while his mother had stayed in Sweden. Thus, the only identified shared external factor was tobacco use (snuff and cigarettes in the mother and cigarettes in the son) and commercially-purchased alcohol consumption. The striking similarity and timing of the visual loss in our patients suggest that the tobacco and alcohol use could influence penetrance of the same underlying mtDNA mutation.

The homoplasmic mutation m.13345G>A, p.(Ala337Thr) in the *MT-ND5* gene found in our two patients is not previously

described in patients with LHON or other mitochondrial disorders. The mutation is reported in heteroplasmy in one individual in the Helix mitochondrial database of 195,983 sequences (16), but is not present in 51673 GenBank sequences according to Mitomap (12) and not in 2,704 sequences in the Human Mitochondrial Genome Database (mtDB) (17). The mtSNP Database mtSAP (18) shows that the amino acid residue affected by the mutation is evolutionarily very well conserved. All 61 mammals in the database have alanine in that position (**Figure 3B**). The mutation is located in the membrane arm of complex I (**Figure 3C**) and is predicted to be pathogenic by the prediction tools PROVEAN (19), Rhapsody (20), Polyphen-2 (21), EVmutation (22) and SIFT (23) (**Figure 3D**). Ala337 is buried inside the ND5 protein structure (**Figure 3C**) in a human cryogenic electron microscopy (cryo-EM) structure of complex I (24). Alanine is a small apolar amino acid, and Ala337 is in close proximity to at least two highly hydrophobic residues Val96 and Leu457 in ND5 (**Figure 3E**). We suggest that any other amino acid at this position will be too large and will affect the apolar environment, thus changing the conformation of surrounding side chains.

Mutations in *MT-ND5* have been associated with the LHON phenotype in several other families or single patients (25–28) and also in other phenotypic syndromes including Leigh syndrome, mitochondrial encephalopathy with lactic acidosis and stroke-like episodes (MELAS) and myoclonic epilepsy with ragged red Fibers (MERRF) (29, 30). In other cases of *MT-ND5* mutations in LHON defective assembly could be demonstrated (31). Given the high energy demand of retinal cells, including ganglion cells, visual loss is a common manifestation of various mitochondrial disorders (18). Among patients having optic neuropathy, most are associated with mutations affecting complex I subunits. *MT-ND5*, the subunit affected in our two patients, is one of the core subunits of complex I and is closely associated with
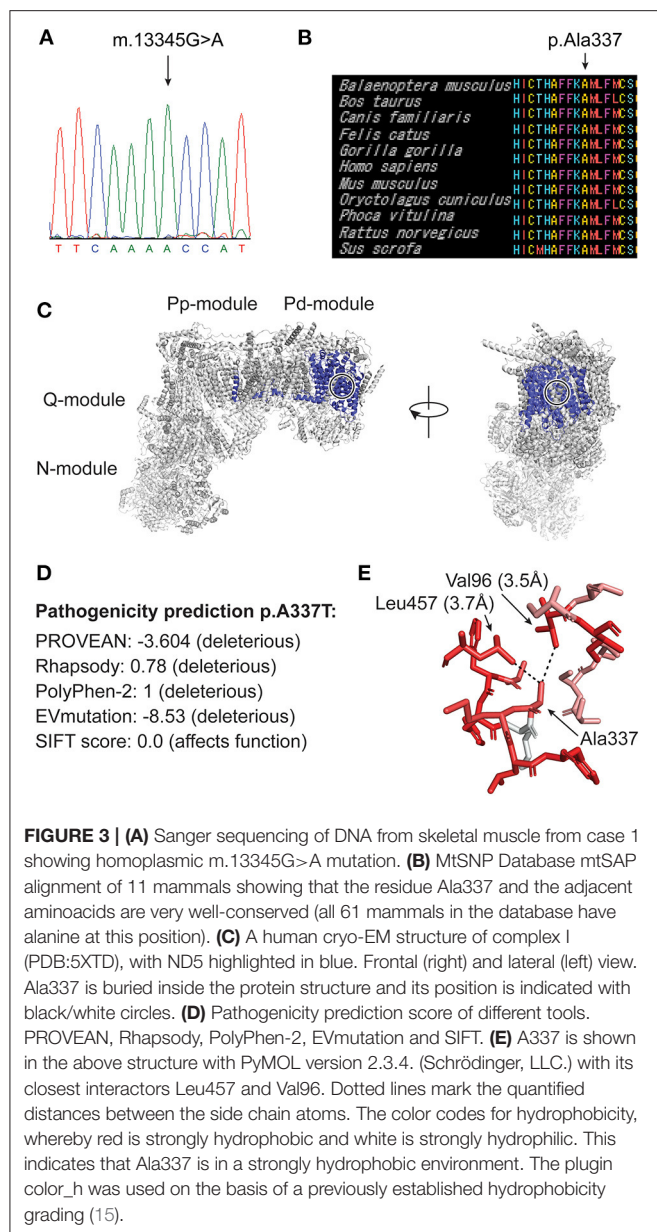
FIGURE 3 | (A) Sanger sequencing of DNA from skeletal muscle from case 1 showing homoplasmic m.13345G>A mutation. (B) MtSNP Database mtSAP alignment of 11 mammals showing that the residue Ala337 and the adjacent aminoacids are very well-conserved (all 61 mammals in the database have alanine at this position). (C) A human cryo-EM structure of complex I (PDB:5XTD), with ND5 highlighted in blue. Frontal (right) and lateral (left) view. Ala337 is buried inside the protein structure and its position is indicated with black/white circles. (D) Pathogenicity prediction score of different tools. PROVEAN, Rhapsody, PolyPhen-2, EVmutation and SIFT. (E) A337 is shown in the above structure with PyMOL version 2.3.4. (Schrödinger, LLC.) with its closest interactors Leu457 and Val96. Dotted lines mark the quantified distances between the side chain atoms. The color codes for hydrophobicity, whereby red is strongly hydrophobic and white is strongly hydrophilic. This indicates that Ala337 is in a strongly hydrophobic environment. The plugin color_h was used on the basis of a previously established hydrophobicity grading (15).

FIGURE 4 | Fundus-photography of patient described in Case 1 taken 5 months from presentation to the ophthalmic clinic. There is bilateral pallor of the optic disk and a non-related epiretinal membrane in the left eye 5 months after presentation.

DATA AVAILABILITY STATEMENT

The datasets presented in this article are not readily available because this would jeopardize patient integrity. Requests to access the datasets should be directed to the corresponding author.

ETHICS STATEMENT

Ethical review and approval was not required for the study on human participants in accordance with the local legislation and institutional requirements. The patients/participants provided their written informed consent to participate in this study. Written informed consent was obtained from the individual(s) for the publication of any potentially identifiable images or data included in this article.

AUTHOR CONTRIBUTIONS

AK, FT, ME, and VC contributed to conception of the manuscript. AK, FT, and ME collected the original data. HB, NL, and ME performed the genetic and bioinformatic analysis. RW, HB, and NL performed the mitochondrial biochemical investigations. ME performed the muscle biopsies. AK, ME, FT, RW, HB, and VC drafted the manuscript with table and figures. AWe and AWr developed the sequencing and bioinformatic platforms and revised the manuscript critically. All authors contributed to the article and approved the submitted version.

one of the proton pumping pores (10). In our subjects we could document a modest but significant reduction of the combined activity of complex I + III, but not when complex I was measured in isolation. Blue native gel electrophoresis showed no signs of deficiency or disruption of neither complex I or of complex II-V. Our two patients did not have any other symptoms apart from visual loss and all laboratory investigations showed no indication of dysfunction of other organ systems.

In summary, we report a novel mtDNA mutation associated with subacute onset of bilateral optic neuropathy in a mother and her adult son. This mutation in combination with the typical clinical findings suggests it is a new putative LHON-mutation.

REFERENCES

1. Kirkman MA, Yu-Wai-Man P, Korsten A, Leonhardt M, Dimitriadis K, De Coo IF, et al. Gene-environment interactions in Leber hereditary optic neuropathy. *Brain.* (2009) 132 (Pt 9):2317–26. doi: 10.1093/brain/awp158

2. Hudson G, Carelli V, Spruijt L, Gerards M, Mowbray C, Achilli A, et al. Clinical expression of Leber hereditary optic neuropathy is affected by the mitochondrial DNA-haplogroup background. *Am J Hum Genet.* (2007) 81:228–33. doi: 10.1086/519394

3. La Morgia C, Carbonelli M, Barboni P, Sadun AA, Carelli V. Medical management of hereditary optic neuropathies. *Front Neurol.* (2014) 5:141. doi: 10.3389/fneur.2014.00141

4. Yu-Wai-Man P, Griffiths PG, Brown DT, Howell N, Turnbull DM, Chinnery PF. The epidemiology of Leber hereditary optic neuropathy in the North East of England. *Am J Hum Genet.* (2003) 72:333–9. doi: 10.1086/346066

5. Rosenberg T, Nørby S, Schwartz M, Saillard J, Magalhães PJ, Leroy D, et al. Prevalence and genetics of leber hereditary optic neuropathy in the danish population. *Invest Ophthalmol Vis Sci.* (2016) 57:1370–5. doi: 10.1167/iovs.15-18306

6. Puomila A, Hamalainen P, Kivioja S, Savontaus ML, Koivumaki S, Huoponen K, et al. Epidemiology and penetrance of Leber hereditary optic neuropathy in Finland. *Eur J Hum Genet.* (2007) 15:1079–89. doi: 10.1038/sj.ejhg.5201828

7. Yu-Wai-Man P, Griffiths PG, Hudson G, Chinnery PF. Inherited mitochondrial optic neuropathies. *J Med Genet.* (2009) 46:145–58. doi: 10.1136/jmg.2007.054270

8. Sadun AA, Carelli V, Salomao SR, Berezovsky A, Quiros PA, Sadun F, et al. Extensive investigation of a large Brazilian pedigree of 11778/haplogroup J Leber hereditary optic neuropathy. *Am J Ophthalmol.* (2003) 136:231–8. doi: 10.1016/S0002-9394(03)00099-0
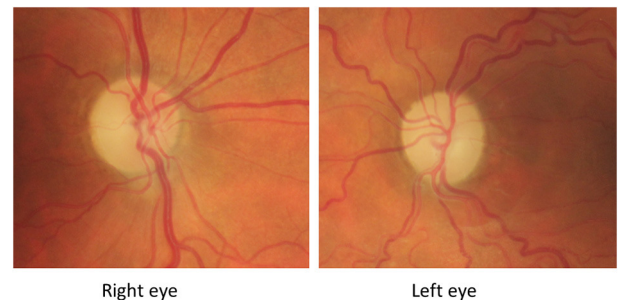
9. Yu-Wai-Man P, Griffiths PG, Chinnery PF. Mitochondrial optic neuropathies - disease mechanisms and therapeutic strategies. *Prog Retin Eye Res.* (2011) 30:81–114. doi: 10.1016/j.preteyeres.2010.11.002

10. Wirth C, Brandt U, Hunte C, Zickermann V. Structure and function of mitochondrial complex I. *Biochim Biophys Acta.* (2016) 1857:902–14. doi: 10.1016/j.bbabio.2016.02.013

11. Gorman GS, Schaefer AM, Ng Y, Gomez N, Blakely EL, Alston CL, et al. Prevalence of nuclear and mitochondrial DNA mutations related to adult mitochondrial disease. *Ann Neurol.* (2015) 77:753–9. doi: 10.1002/ana.24362

12. *MITOMAP: A Human Mitochondrial Genome Database.* (2018). Available from: http://www.mitomap.org/ (accessed October 21, 2020).

13. Wibom R, Hagenfeldt L, von Dobeln U. Measurement of ATP production and respiratory chain enzyme activities in mitochondria isolated from small muscle biopsy samples. *Anal Biochem.* (2002) 311:139–51. doi: 10.1016/S0003-2697(02)00424-4

14. Stranneheim H, Engvall M, Naess K, Lesko N, Larsson P, Dahlberg M, et al. Rapid pulsed whole genome sequencing for comprehensive acute diagnostics of inborn errors of metabolism. *BMC Genomics.* (2014) 15:1090. doi: 10.1186/1471-2164-15-1090

15. Eisenberg D, Schwarz E, Komaromy M, Wall R. Analysis of membrane and surface protein sequences with the hydrophobic moment plot. *J Mol Biol.* (1984) 179:125–42. doi: 10.1016/0022-2836(84)90309-7

16. Bolze, A., Mendez, F., White, S., Tanudjaja, F., Isaksson, M., Jiang, R., et al. (2020). A catalog of homoplasmic and heteroplasmic mitochondrial DNA variants in humans. *bioRxiv 798264.* doi: 10.1101/798264

17. Ingman M, Gyllensten U. mtDB: human mitochondrial genome database, a resource for population genetics and medical sciences. *Nucleic Acids Res.* (2006) 34:D749–51. doi: 10.1093/nar/gkj010

18. Tanaka M, Takeyasu T, Fuku N, Li-Jun G, Kurata M. Mitochondrial genome single nucleotide polymorphisms and their phenotypes in the Japanese. *Ann N Y Acad Sci.* (2004) 1011:7–20. doi: 10.1196/annals.1293.002

19. Choi Y, Chan AP. PROVEAN web server: a tool to predict the functional effect of amino acid substitutions and indels. *Bioinformatics.* (2015) 31:2745–7. doi: 10.1093/bioinformatics/btv195

20. Ponzoni L, Penaherrera DA, Oltvai ZN, Bahar I. Rhapsody: predicting the pathogenicity of human missense variants. *Bioinformatics.* (2020) 36:3084–92. doi: 10.1093/bioinformatics/btaa127

21. Adzhubei I, Jordan DM, Sunyaev SR. Predicting functional effect of human missense mutations using PolyPhen-2. *Curr Protoc Hum Genet.* (2013) Chapter 7:Unit7 20. doi: 10.1002/0471142905.hg0720s76

22. Hopf TA, Ingraham JB, Poelwijk FJ, Scharfe CP, Springer M, Sander C, et al. Mutation effects predicted from sequence co-variation. *Nat Biotechnol.* (2017) 35:128–35. doi: 10.1038/nbt.3769

23. Sim NL, Kumar P, Hu J, Henikoff S, Schneider G, Ng PC. SIFT web server: predicting effects of amino acid substitutions on proteins. *Nucleic Acids Res.* (2012) 40:W452–7. doi: 10.1093/nar/gks539

24. Guo R, Zong S, Wu M, Gu J, Yang M. Architecture of human mitochondrial respiratory megacomplex I2III2IV2. *Cell.* (2017) 170:1247–57 e12. doi: 10.1016/j.cell.2017.07.050

25. Dombi E, Diot A, Morten K, Carver J, Lodge T, Fratter C, et al. The m.13051G>A mitochondrial DNA mutation results in variable neurology and activated mitophagy. *Neurology.* (2016) 86:1921–3. doi: 10.1212/WNL.0000000000002688

26. Howell N, Oostra RJ, Bolhuis PA, Spruijt L, Clarke LA, Mackey DA, et al. Sequence analysis of the mitochondrial genomes from Dutch pedigrees with Leber hereditary optic neuropathy. *Am J Hum Genet.* (2003) 72:1460–9. doi: 10.1086/375537

27. Huoponen K, Lamminen T, Juvonen V, Aula P, Nikoskelainen E, Savontaus ML. The spectrum of mitochondrial DNA mutations in families with Leber hereditary optic neuroretinopathy. *Hum Genet.* (1993) 92:379–84. doi: 10.1007/BF01247339

28. Valentino ML, Barboni P, Rengo C, Achilli A, Torroni A, Lodi R, et al. The 13042G –> A/ND5 mutation in mtDNA is pathogenic and can be associated also with a prevalent ocular phenotype. *J Med Genet.* (2006) 43:e38. doi: 10.1136/jmg.2005.037507

29. Blok MJ, Spruijt L, de Coo IF, Schoonderwoerd K, Hendrickx A, Smeets HJ. Mutations in the ND5 subunit of complex I of the mitochondrial DNA are a frequent cause of oxidative phosphorylation disease. *J Med Genet.* (2007) 44:e74. doi: 10.1136/jmg.2006.045716

30. Ng YS, Lax NZ, Maddison P, Alston CL, Blakely EL, Hepplewhite PD, et al. MT-ND5 mutation exhibits highly variable neurological manifestations at low mutant load. *EBioMedicine.* (2018) 30:86–93. doi: 10.1016/j.ebiom.2018.02.010

31. Zhang J, Ji Y, Lu Y, Fu R, Xu M, Liu X, et al. Leber's hereditary optic neuropathy (LHON)-associated ND5 12338T > C mutation altered the assembly and function of complex I, apoptosis and mitophagy. *Hum Mol Genet.* (2018) 27:1999–2011. doi: 10.1093/hmg/ddy107

A Perspective on Accelerated Aging Caused by the Genetic Deficiency of the Metabolic Protein, OPA1

Irina Erchova[1], Shanshan Sun[1] and Marcela Votruba[1,2]*

[1] *Mitochondria and Vision Lab, School of Optometry and Vision Sciences, Cardiff University, Cardiff, United Kingdom,*
[2] *Cardiff Eye Unit, University Hospital of Wales, Cardiff, United Kingdom*

Autosomal Dominant Optic Atrophy (ADOA) is an ophthalmological condition associated primarily with mutations in the *OPA1* gene. It has variable onset, sometimes juvenile, but in other patients, the disease does not manifest until adult middle age despite the presence of a pathological mutation. Thus, individuals carrying mutations are considered healthy before the onset of clinical symptoms. Our research, nonetheless, indicates that on the cellular level pathology is evident from birth and mutant cells are different from controls. We argue that the adaptation and early recruitment of cytoprotective responses allows normal development and functioning but leads to an exhaustion of cellular reserves, leading to premature cellular aging, especially in neurons and skeletal muscle cells. The appearance of clinical symptoms, thus, indicates the overwhelming of natural cellular defenses and break-down of native protective mechanisms.

Keywords: mitochondria, OPA1, mitochondrial dynamics, aging, cellular adaptation

INTRODUCTION

Autosomal Dominant Optic Atrophy (ADOA), is a progressive ophthalmological condition caused by degeneration of retinal ganglion cells (RGCs) that leads to visual loss (1). It is associated predominantly with mutations in the *OPA1* gene and has variable onset and severity. The pathophysiology of OPA1-related ADOA is believed to be mainly due to haploinsufficiency in OPA1, due to the preponderance of OPA1 mutations that lead to premature translation termination and null mutations (2). This leads to a ~50% reduction in OPA1 protein in most tissues tested (3). In addition, some mutations lead to unstable OPA1 transcripts, due to a premature stop codon, and these appear to be degraded by non-sense mediated mRNA decay, and also lead to haploinsufficiency (4). The second mechanism of disease is linked to missense mutations in the GTPase domain of OPA1, where a dominant-negative effect is postulated to lead to severe "plus" forms of the disease (5).

Affected individuals are usually identified early, as juveniles or adolescents. However, clinical symptoms may appear later in some individuals, such as loss of visual acuity and deficits in color vision (6). Currently, based on the fact that before the onset of symptoms individuals frequently have normal development and good health, supportive treatments are not instituted before the appearance of the clinical symptoms, and disease onset is thus considered age-dependent. As a part of the aging process, the amount of OPA1 protein is believed to decrease, potentially contributing to age-related deterioration of vision, muscle, and memory (7, 8). Moreover, the levels of proteins governing mitochondrial dynamics, which include OPA1, have been found to be significantly altered in Alzheimer Disease (AD) mice and patients (9). On the other hand, there

is a mounting body of evidence that suggests that on the cellular level *OPA1* mutations cause abnormalities demonstrable from birth, though many are successfully ameliorated (or compensated for) by cellular adaptive mechanisms. In turn, cellular adaptation, though beneficial as it allows normal development, exhausts the antioxidant system, reduces the control of inflammation, and the supply of adult stem cells, thus depleting natural defenses and therefore potentially accelerates the aging process.

Severe Developmental Pathologies Are Associated With Homozygous and Heterozygous Mutation of OPA1

OPA1 protein is part of the cellular control of cellular energy production and distribution and thus is essential for development, especially in neurons with long neurites (10). All fetuses carrying homozygous mutations in the *Opa1* gene in murine models die during embryonic development (11, 12). As a result, systematic evidence of homozygous pathology in mammals is rare (13). It has however been possible to investigate cellular changes using artificially created mosaics of homozygous cells in non-mammalian experimental models like *Drosophila* (14, 15), and stress adaptation and life-span changes using nematode, *C. elegans* (16). In humans, homozygous *OPA1* mutations are rarely seen due to presumed fetal loss and when they do occur are associated with very severe developmental conditions, such as encephalomyopathy, muscle weakness, cardiomyopathy, hypertonia, sensory deficits, and more general failure to thrive leading to early death (17). Severe developmental delays and early-onset optic atrophy are also typical for heterozygous mutations causing Behr syndrome, accompanied by spinocerebellar degeneration, ataxia, and sensory deficits (18–21).

Cellular Deficits With Impaired Mitochondrial Fusion

Cellular deficits caused by faulty mitochondrial fusion are well-documented. In budding yeast, the tubular mitochondrial network breaks into small spherical segments (22, 23). In *Drosophila*, a similar process affects the motility of the sperm cells and results in male sterility (17). Similar fragmentation is documented in primary cultures of various animal cells (24, 25) and patient-derived induced pluripotent stem (iPS) cells (26), as well as murine retinal ganglion cells from the B6;C3-$Opa1^{Q285STOP}$ mouse, $Opa1^{+/}$, (**Figure 1**) in which there is also accelerated mitochondrial movement (27). Defects in Opa1 primarily affect mitochondrial fusion and motility (28).

Recruitment of Antioxidant and Inflammatory Defenses

A reduction in mitochondrial quality control, and accelerated mitochondrial movement, are not the only compromises that allow survival. In *Drosophila*, mitochondrial fusion and fission imbalance is tolerable in young flies that mobilize natural antioxidant protection via Nrf2 and Foxo to up-regulate cytoprotective mechanisms (29). It nonetheless leads to accelerated aging and a much shorter life span (29).

Inflammation is another process that affects cell viability. Mitochondrial fusion and OPA1 protein are directly involved in this process via the TNFα-NF-kB–OPA1 regulatory pathway (29, 30). This pathway works via increasing mitochondrial fusion and improving respiratory chain efficiency in response to cellular stress. TNFα (Tumor Necrosis Factor alpha) is a protein (an inflammatory cytokine) produced by macrophages during acute inflammation. It is a signaling molecule that is passed on to other cells. NF-κB (nuclear factor kappa-light-chain-enhancer of activated B cells) is a cytosol-based protein complex that controls transcription of DNA and is involved in cellular responses to stress. While in an inactivated state, NF-κB is in complex with an inhibitory protein, but once activated, it is released from the complex and translocated into the nucleus, where it binds to response elements (specific sequences) of DNA, recruiting co-activators and RNA polymerase. The mRNAs are then translated into proteins changing cell function. Normally, inflammatory stress increases TNFα, which activates NF-kB, and ultimately increases the production of OPA1 protein. The latter part of the pathway NF-kB–OPA1 is also involved in synaptic development (30). The inflammatory response is usually regulated via complex multi-gene signaling adjusting the homeostatic balance of organelles in response to cellular stress (31).

Embryonic and Adult Stem Cell Recruitment and Depletion

Mitochondrial fusion is essential for normal embryonic development (32). Recently, it has been shown that in human stem cells OPA1 haploinsufficiency causes impairment in neural stem cell self-renewal, thus causing age-dependent depletion, leading to reduced adult neurogenesis and cognitive deficits (33). Similarly, depletion of Opa1 protein affects both stem cell identity and self-renewal, causing age-dependent depletion of adult stem cells and thus possible deficits in adult neurogenesis in a mouse model with a mutation in Dynamin-related Protein gene (DRP) (34). Several recent studies have looked into the molecular mechanisms of this depletion. Sênos Demarco et al. showed that in *Drosophila* stem cells, depletion of Opa1 leads to activation of Target of Rapamycin (TOR) and a marked accumulation of lipid droplets, thus reducing the capacity of stem cells for self-renewal (35). In *Drosophila*, Sandoval et al. showed that mitochondrial fusion regulates larval growth and synaptic development *via* steroid hormone production (36). Moreover, in genetically modified human embryonic and patient-derived induced pluripotent stem cells OPA1 haploinsufficiency leads to aberrant nuclear DNA methylation and thus alters DNA transcription in neural progenitor cells. For instance, the transcription factor needed for GABAergic neuronal development is suppressed, causing reduced generation of GABAergic interneurons, whereas the formation of glutamatergic neurons is not affected (33). The potential reduction in the generation of GABAergic interneurons requires further investigation and exploration, but theoretically, this could result in a more vulnerable neural network, which might require more repair or maintenance. A recent example of the effect of a poorly developed GABA-ergic network has recently
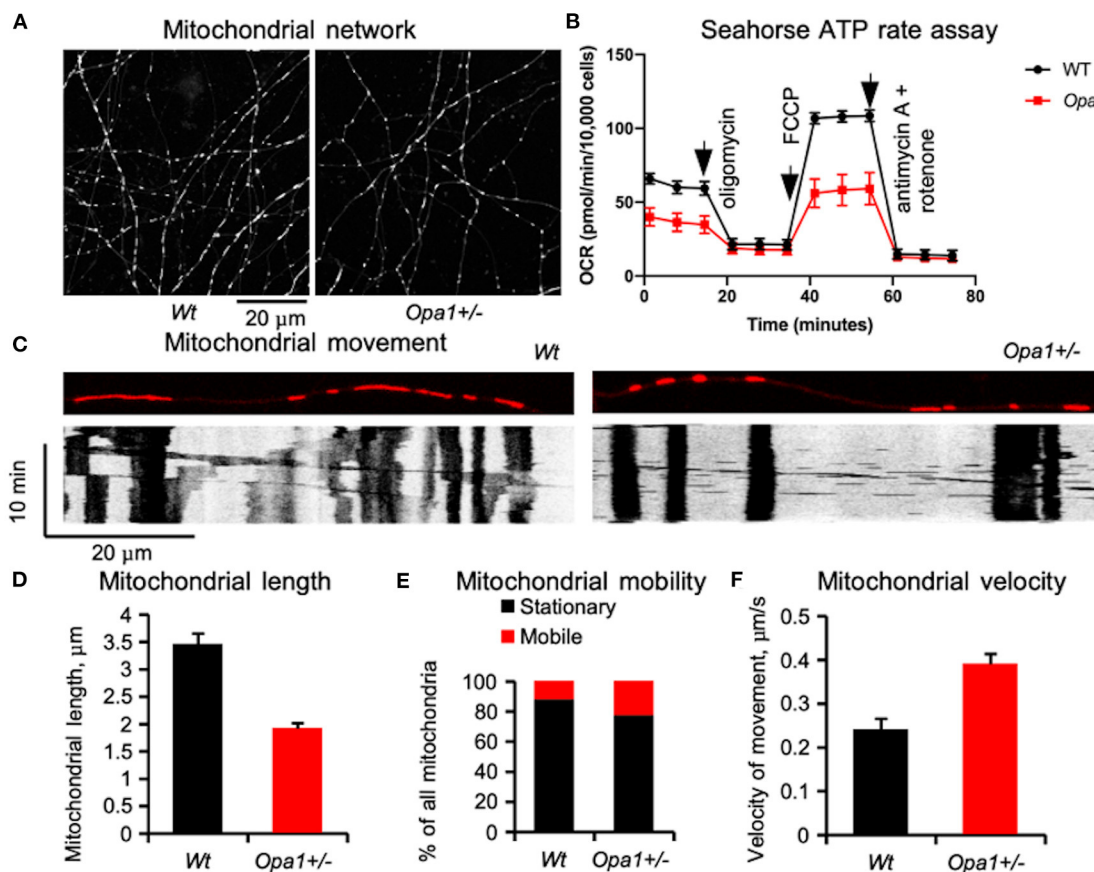
FIGURE 1 | Mitochondrial network in primary retinal ganglion cells (RGCs) in mutant mice (B6;C3-*Opa1*^{Q285STOP}, *Opa1*$^{+/-}$) [adapted from Sun et al. (27)]. **(A)** Tubular mitochondrial network in control and mutant mice labeled in live culture by MitoTracker®Red and recorded by time-lapse imaging on the 8th day *in vitro*. **(B)** Mitochondrial network functionality assessed by Seahorse assay. **(C)** Mitochondrial movement in RGC dendrites is illustrated by automatically generated kymographs using FIJI software. **(D)** Average length of a single mitochondrial segment. **(E)** Distribution of the mitochondrion population classified as stationary and motile. **(F)** Velocities of mitochondrial movement. The increased mitochondrial mobility and velocity may be a compensatory mechanism for a poor cellular distribution network. The data were obtained from 1280 mitochondria in 91 processes of wild-type RGCs and 1205 mitochondria in 92 processes of Opa1+/- RGCs.

been discussed in optic nerve hypoplasia and autism. Clinical observations and recent reports indicate a high frequency of autism spectrum disorders (ASD) in children with optic nerve hypoplasia (ONH) (37, 38). In children with ONH, there are additional characteristics of ASD beyond those attributable to visual impairment alone, such as echolalia and stereotypic motor movements.

Cellular Mechanisms of Accelerated Aging in Individuals With OPA1 Mutation

In *Drosophila*, experimental oxidative stress was seen in mitochondrial areas abnormally rich in myelin without cytochrome oxidase activity (39). Oxidative stress and up-regulated production of reactive oxygen species (ROS), mostly by mitochondria, are the main factors causing tissue damage. Though these processes are likely to occur independently of mutation, the early deployment of antioxidant defenses leaves limited capacity to cope with additional stress caused by mitochondrial aging. If tissue damage triggers an inflammatory response, then there is also a potentially limited ability to mobilize cellular resources or suppress inflammation. Reduced mitochondrial quality control, adopted early on to prevent degradation of functional, but fragmented mitochondria, also contribute to accelerated aging, by failing to identify and renew damaged mitochondrial fragments in a timely fashion. It is involved in the early loss of skeletal muscle mass and strength in OPA1 mutation carriers (40). Casuso and Huertas recently reviewed the topic in light of the support and protection offered by regular physical exercise (41). The down-regulation of mitochondrial fusion is linked with age-dependent axonal degeneration, with the visible accumulation of fragmented mitochondria in the axons without mitophagy (42).

Apart from the physical symptoms of aging associated with failing body strength and health, there is cognitive aging, characterized by increased anxiety and reduced working memory. On a cellular level, the symptoms are associated with synaptic loss in pyramidal cells and reduced numbers of inhibitory cells (especially somatostatin neurons) involved in
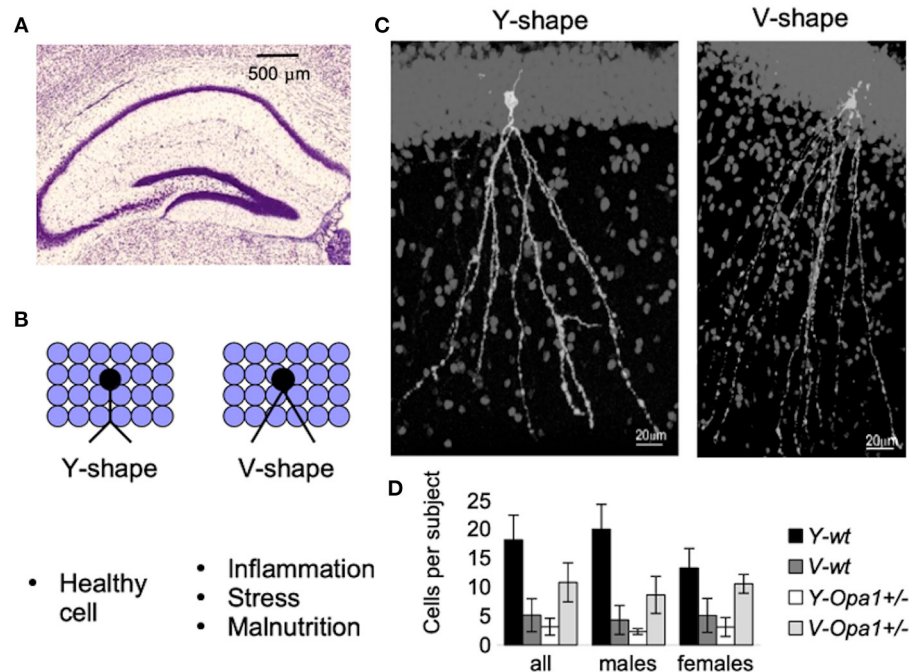
FIGURE 2 | New-born neurons are continuously being added to the hippocampal Dentate Gyrus (DG) throughout adulthood **(A)**. Detrimental factors (such as schizophrenia, stress, Alzheimer's disease, seizures, stroke, inflammation, dietary deficiencies, or the consumption of drugs of abuse or toxic substances) and neuroprotective factors (physical exercise and environmental enrichment) influence maturation and morphology of new-born granular cells [reviewed in Llorens-Martín et al. (45)]. For example, there is a striking difference in the shape of the apical dendrites **(B)**. These morphological alterations may have important consequences (such as change in the pattern of synaptic connections, or change in the pattern of dendritic summation, and ultimately, change in cell excitability and functionality). An example of granular cells with different dendritic shafts are represented in **(C)**. Though both wt and Opa1 +/- animals had both types of granular cell morphology, in aged mice, the Y-type was attributed to 80% of all Diolistically labeled DG granular cells in wt [see Bevan et al. (44) for the details]. By contrast, in age-matched Opa1 +/- animals more cells were of V-type **(D)**. These changes are likely to be induced by a combination of stress factors in conjunction with impaired adult hippocampal neurogenesis.

the signaling pathways (43). We recently characterized subtly reduced working memory in *Opa1* mutant mouse (B6;C3-*Opa1*^{Q285STOP}, *Opa1*$^{+/-}$) (44). We found that hippocampal CA1 cells showed age-related loss of synapses, developmental abnormalities such as the reduction in the number of GABA-ergic neurons, and defects in adult neurogenesis, which would contribute to the observed effect. **Figure 2** illustrates our additional finding in the Dentate Gyrus (DG) region of aged mutant mice. The changes were similar to those observed by Llorens-Martín et al. and are decremental (45).

DISCUSSION

Recent studies highlight the fact that fusion/fission mitochondrial dynamics and cellular metabolism are coupled: in cultured cell lines, elongated mitochondria are observed in conditions associated with increased ATP requirements (46, 47), whilst in nutrient-restricted conditions, mitochondria form large interconnected networks (48). When fusion is reduced secondary to nutrient excess or genetic abnormality (such as OPA1 deficiency) mitochondrial fragmentation promotes mitochondrial degradation through mitophagy (49). It appears that elongated shape and a fused mitochondrial network protect individual mitochondria from autophagosomal degradation

(50, 51). When the tubular network is fragmented not only does energy production decrease but mitochondria themselves are at risk of degradation. To protect mitochondria when the tubular network is compromised, the cellular mechanism responsible for "quality control" is adjusted (52), allowing a larger quantity of disconnected mitochondria to circulate in the cell. This adjustment helps to maintain a sufficient number of fragmented mitochondria to meet the immediate cellular demands in development when most mitochondria are healthy, but with time might lead to accumulation of damaged mitochondria. At present, it is not clear whether mitochondrial fragmentation itself causes any deficit in cellular function, although the mitochondrial network does influence cellular functioning. In cultured HeLa cells, for example, the mitochondrial network interacts with the endoplasmic reticulum (ER) and uses Ca^{2+} signals to rapidly tune ATP production to the demands of the cell (53). However, in the rat cardiac muscle, the developmentally fragmented mitochondrial network later assumes a tubular structure (54). In post-natal primary RGC culture from the B6;C3-*Opa1*^{Q285STOP}, *Opa1*$^{+/-}$, mouse the mitochondrial network forms tubular structures but remains, nonetheless, more fragmented compared to controls, and levels of ATP production are reduced (**Figure 1**). Another important function of the mitochondrial network is the rapid spatial distribution of

energy resources to distant cellular compartments. This function may be partially compensated via increased mitochondrial movement (27).

Moreover, a poorly controlled exuberant inflammatory response leads to tissue deterioration and accelerated aging. The chronic inflammatory response in cell lines and skeletal muscle caused by OPA1 deficiency is well-documented in patients and animal models (55–57). In addition, the adequate response to sepsis caused by pulmonary infection, whichoften complicates other chronic conditions, also requires rapid up-regulation of OPA1 (58). In post-mortem analyses of lung tissue obtained from areas with mild and severe emphysema, impaired fusion characterized by a low quantity of OPA1 protein is correlated with disease severity (59). Evidence from our lab suggests that levels of signaling protein NF-kB are already elevated in healthy Opa1 +/- mice compared to controls without changes in the levels of TNFα. This suggests that developmental adaptive mechanisms are likely to recruit a part of the inactive inflammatory pathway to alleviate cellular deficits in OPA1 during synaptic development (60–62). Unfortunately, this early recruitment of the regulatory pathway may compromise normal inflammatory responses, resulting in chronic inflammation or poor outcome in the case of severe acute inflammation (63, 64).

The aging process in mitochondrial networks at the microscopic level is very different from the tubular fragmentation described above. It characterized by mitochondrial swelling, reduced cristae, and damaged membranes (65, 66). Accelerated aging does not only manifest itself in sensory and cognitive deficits. There are numerous subtle changes that do not manifest themselves in everyday life. For example, recent studies showed that there is an elevated risk of cardiovascular conditions and reduced capacity for a successful recovery. By using C.elegans, Machiela et al. showed that disrupted mitochondrial fusion changed the normal pattern of responses to cellular stress. Cells became more resistant to both heat and oxidative stress, but more sensitive to osmotic variations and hypoxia. Sensitivity to hypoxia is critical in recovery from ischaemic stroke (67). Guo et al. showed that the increased risk of cerebral vascular injury in diabetic patients is partially due to chronically reduced levels of OPA1. They also reported more severe damage in this group of patients (68). Accordingly, Lai et al. demonstrated that rapid restoration of OPA1 levels after stroke reduces neuronal death and improved both survival and recovery of functions (69). Similarly, Xin and Lu showed in a murine model, that Opa1 expression was down-regulated in infarcted hearts, but Opa1 overexpression protected cardiomyocytes (70). Simulated ischaemia in the cardiac myogenic cell line H9c2 cells reduced OPA1 protein levels resulting in mitochondria fragmentation and apoptosis (71).

Thus, in this "Perspective" we summarize the evidence that OPA1 haploinsufficiency affects cellular functions from the molecular perspective of natural cellular resistance during development and adulthood. Deficits in OPA1 protein impact mitochondrial fusion, reduce cellular energy supply and thus impair cell survival. From the clinical perspective, this means that patients, identified as having a pathological mutation, may benefit from being monitoredbefore, or in the absence of, any clinical symptoms of disease. This could include careful multi-modal imaging of the retina and optic nerve and functional investigation with electrodiagnostic tests. Pre-symptomatic screening would contribute valuable clinical information allowing for the identification of markers of early disease and putative biomarkers that would be essential in the testing of novel therapeutic interventions. It also adds some weight to the idea that by supporting natural defenses, such as maintaining a healthy diet, avoiding smoking and alcohol consumption, and a regular exercise regime throughout the normal lifespan, it may be feasible to delay the onset of premature aging. Smoking is known to disturb mitochondrial function, and may thus be a factor that helps accelerate the onset and progression of visual loss in patients with mutations that impair mitochondrial function [as for example, in Leber Hereditary Optic Neuropathy and ADOA (72)].

There are many further potentially important research questions, such as why and how mitochondria in different tissues differ and whether this affects the apparent different rates of aging in different body tissues, which we would suggest may be worth addressing in future research.

DATA AVAILABILITY STATEMENT

The raw data supporting the conclusions of this article will be made available by the authors, without undue reservation.

ETHICS STATEMENT

The animal study was reviewed and approved by UK PPL Home Office PP7147250.

AUTHOR CONTRIBUTIONS

IE: conceptualization, methodology, investigation, writing-original draft preparation, and visualization. SS: investigation, visualization, writing-reviewing, and editing. MV: resources, writing-reviewing and editing, supervision, and funding acquisition. All authors: contributed to the article and approved the submitted version.

FUNDING

REFERENCES

1. El-Hattab AW, Suleiman J, Almannai M, Scaglia F. Mitochondrial dynamics: biological roles, molecular machinery, and related diseases. *Mol Genet Metab.* (2018) 125:315–21. doi: 10.1016/j.ymgme.2018.10.003

2. Amati-Bonneau P, Milea D, Bonneau D, Chevrollier A, Ferré M, Guillet V, et al. OPA1-associated disorders: phenotypes and pathophysiology. *Int J Biochem Cell Biol.* (2009) 41:1855–65. doi: 10.1016/j.biocel.2009.0401

3. Marchbank NJ, Craig JE, Leek JP, Toohey M, Churchill AJ, Markham AF, et al. Deletion of the OPA1 gene in a dominant optic atrophy family: evidence that haploinsufficiency is the cause of disease. *J Med Genet.* 2002 39:e47. doi: 10.1136/jmg.39.8e47

4. Schimpf S, Fuhrmann N, Schaich S, Wissinger B. Comprehensive cDNA study and quantitative transcript analysis of mutant OPA1 transcripts containing premature termination codons. *Hum Mutat.* 2008 29:106–12. doi: 10.1002/humu20607

5. Amati-Bonneau P, Valentino ML, Reynier P, Gallardo ME, Bornstein B, Boissière A, et al. OPA1 mutations induce mitochondrial DNA instability and optic atrophy "plus" phenotypes. *Brain.* 2008 131:338–51. doi: 10.1093/brain/awm298

6. Jurkute N, Leu C, Pogoda HM, Arno G, Robson AG, Nürnberg G, et al. SSBP1 mutations in dominant optic atrophy with variable retinal degeneration. *Ann. Neurol.* (2019) 86:368–83. doi: 10.1002/ana.25550

7. Shah SI, Paine JG, Perez C, Ullah G. Mitochondrial fragmentation and network architecture in degenerative diseases. *PLoS ONE.* (2019) 14:e0223014. doi: 10.1371/journal.pone.0223014

8. Zorov D, Vorobjev I, Popkov V, Babenko V, Zorova L, Pevzner I, et al. Lessons from the discovery of mitochondrial fragmentation (fission): a review and update. *Cells.* (2019) 8:175. doi: 10.3390/cells8020175

9. Murrell JR, Hake AM, Quaid KA, Farlow MR, Ghetti B. Early-onset Alzheimer disease caused by a new mutation (V717L) in the amyloid precursor protein gene. *Arch Neurol.* (2000) 57:885–7. doi: 10.1001/archneur.57.6.885

10. Gao J, Wang L, Liu J, Xie F, Su B, Wang X. Abnormalities of mitochondrial dynamics in neurodegenerative diseases. *Antioxidants.* (2017) 5:25. doi: 10.3390/antiox6020025

11. Baker C, Ebert S. Development of aerobic metabolism in utero: requirement for mitochondrial function during embryonic and fetal periods. *OA Biotechnol.* (2013) 2:16. doi: 10.13172/2052-0069-2-2-571

12. Davies VJ, Hollins AJ, Piechota MJ, Yip W, Davies JR, White KE, et al. Opa1 deficiency in a mouse model of autosomal dominant optic atrophy impairs mitochondrial morphology, optic nerve structure and visual function. *Hum Mol Genet.* (2007) 16:1307–18. doi: 10.1093/hmg/ddm079

13. Hartmann B, Wai T, Hu H, MacVicar T, Musante L, Fischer-Zirnsak B, et al. Homozygous YME1L1 mutation causes mitochondriopathy with optic atrophy and mitochondrial network fragmentation. *Elife.* (2016) 5:e16078. doi: 10.7554/eLife.16078

14. Lee T, Luo L. Mosaic analysis with a repressible cell marker (MARCM) for Drosophila neural development. *Trends Neurosci.* (2001) 24:351–254. doi: 10.1016/S0166-2236(00)01791-4

15. Smith GA, Lin TH, Sheehan AE, Van der Goes van Naters W, Neukomm LJ, Graves HK, et al. Glutathione S-transferase regulates mitochondrial populations in axons through increased glutathione oxidation. *Neuron.* (2019) 103:52–65.e6. doi: 10.1016/j.neuron.2019.04.017

16. Dancy BM, Sedensky MM, Morgan PG. Effects of the mitochondrial respiratory chain on longevity in C. elegans. *Exp Gerontol.* (2014) 56:245–55. doi: 10.1016/j.exger.2014.03.028

17. Spiegel R, Saada A, Flannery PJ, Burté F, Soiferman D, Khayat M, et al. Fatal infantile mitochondrial encephalomyopathy, hypertrophic cardiomyopathy and optic atrophy associated with a homozygous OPA1 mutation. *J Med Genet.* (2016) 53:127–31. doi: 10.1136/jmedgenet-2015-103361

18. Bonneau D, Colin E, Oca F, Ferré M, Chevrollier A, Guéguen N, et al. Early-onset Behr syndrome due to compound heterozygous mutations in OPA1. *Brain.* (2014) 137:e301. doi: 10.1093/brain/awu184

19. Carelli V, Sabatelli M, Carrozzo R, Rizza T, Schimpf S, Wissinger B, et al. "Behr syndrome" with OPA1 compound heterozygote mutations. *Brain.* (2015) 138:e321. doi: 10.1093/brain/awu234

20. Rahman S. Mitochondrial disease in children. *J Intern Med.* (2020) 287:609–33. doi: 10.1111/joim.13054

21. Schaaf CP, Blazo M, Lewis RA, Tonini RE, Takei H, Wang J, et al. Early-onset severe neuromuscular phenotype associated with compound heterozygosity for OPA1 mutations. *Mol Genet Metab.* (2011) 103:383–7. doi: 10.1016/j.ymgme.2011.04.018

22. Hermann GJ, Thatcher JW, Mills JP, Hales KG, Fuller MT, Nunnari J, et al. Mitochondrial fusion in yeast requires the transmembrane GTPase Fzo1p. *J Cell Biol.* (1998) 143:359–73. doi: 10.1083/jcb.143.2.359

23. Rapaport D, Brunner M, Neupert W, Westermann B. Fzo1p is a mitochondrial outer membrane protein essential for the biogenesis of functional mitochondria in Saccharomyces cerevisiae. *J Biol Chem.* (1998) 273:20150–5. doi: 10.1074/jbc.273.32.20150

24. Knott AB, Perkins G, Schwarzenbacher R, Bossy-Wetzel E. Mitochondrial fragmentation in neurodegeneration. *Nat Rev Neurosci.* (2008) 9:505–18. doi: 10.1038/nrn2417

25. Kushnareva Y, Seong Y, Andreyev AY, Kuwana T, Kiosses W, Votruba M, et al. Mitochondrial dysfunction in an Opa1Q285STOP mouse model of dominant optic atrophy results from Opa1 haploinsufficiency. *Cell Death Dis.* (2016) 7:e2309. doi: 10.1038/cddis.2016.160

26. Prieto J, León M, Ponsoda X, Sendra R, Bort R, Ferrer-Lorente R, et al. Early ERK1/2 activation promotes DRP1-dependent mitochondrial fission necessary for cell reprogramming. *Nat Commun.* (2016) 7:1–13. doi: 10.1038/ncomms11124

27. Sun S, Erchova I, Sengpiel F, Votruba M. Opa1 deficiency leads to diminished mitochondrial bioenergetics with compensatory increased mitochondrial motility. *Investig Ophthalmol Vis Sci.* (2020) 61:42. doi: 10.1167/IOVS.61.6.42

28. Chen H, Chan DC. Mitochondrial dynamics in mammals. *Curr Top Dev Biol.* (2004) 59:119–44. doi: 10.1016/S0070-2153(04)59005-1

29. Gumeni S, Evangelakou Z, Tsakiri EN, Scorrano L, Trougakos IP. Functional wiring of proteostatic and mitostatic modules ensures transient organismal survival during imbalanced mitochondrial dynamics. *Redox Biol.* (2019) 24:101219. doi: 10.1016/j.redox.2019.101219

30. Shen DN, Zhang LH, Wei EQ, Yang Y. Autophagy in synaptic development, function, and pathology. *Neurosci Bull.* (2015) 31:416–26. doi: 10.1007/s12264-015-1536-6

31. Müller-Rischart AK, Pilsl A, Beaudette P, Patra M, Hadian K, Funke M, et al. The E3 ligase parkin maintains mitochondrial integrity by increasing linear ubiquitination of NEMO. *Mol Cell.* (2013) 49:908–21. doi: 10.1016/j.molcel.2013.01036

32. Chen H, Detmer SA, Ewald AJ, Griffin EE, Fraser SE, Chan DC. Mitofusins Mfn1 and Mfn2 coordinately regulate mitochondrial fusion and are essential for embryonic development. *J Cell Biol.* (2003) 160:189–200. doi: 10.1083/jcb.200211046

33. Caglayan S, Hashim A, Cieslar-Pobuda A, Jensen V, Behringer S, Talug B, et al. Optic Atrophy 1 Controls human neuronal development by preventing aberrant nuclear DNA methylation. *iScience.* (2020) 23:101154. doi: 10.1016/j.isci.2020.101154

34. Khacho M, Clark A, Svoboda DS, Azzi J, MacLaurin JG, Meghaizel C, et al. Mitochondrial dynamics impacts stem cell identity and fate decisions by regulating a nuclear transcriptional program. *Cell Stem Cell.* (2016) 19:232–47. doi: 10.1016/j.stem.2016.04.015

35. Sênos Demarco R, Uyemura BS, D'Alterio C, Jones DL. Mitochondrial fusion regulates lipid homeostasis and stem cell maintenance in the Drosophila testis. *Nat Cell Biol.* (2019) 21:710–20. doi: 10.1038/s41556-019-0332-3

36. Sandoval H, Yao CK, Chen K, Jaiswal M, Donti T, Lin YQ, et al. Mitochondrial fusion but not fission regulates larval growth and synaptic development through steroid hormone production. *Elife.* (2014) 3:1–23. doi: 10.7554/eLife.0355

37. Ek U, Fernell E, Jacobson L. Cognitive and behavioural characteristics in blind children with bilateral optic nerve hypoplasia. *Acta Paediatr.* (2005) 94:1421–6. doi: 10.1111/j.1651-2227.2005.tb01814x

38. Parr JR, Dale NJ, Shaffer LM, Salt AT. Social communication difficulties and autism spectrum disorder in young children with optic nerve hypoplasia and/or septo-optic dysplasia. *Dev Med Child Neurol.* (2010) 52:917–21. doi: 10.1111/j.1469-8749.2010.03664x

39. Walker DW, Benzer S. Mitochondrial "swirls" induced by oxygen stress and in the Drosophila mutant hyperswirl. *Proc Natl Acad Sci USA.* (2004) 101:10290–5. doi: 10.1073/pnas.0403767101

40. Liu HW, Chang YC, Chan YC, Hu SH, Liu MY, et al. Dysregulations of mitochondrial quality control and autophagic flux at an early age lead to progression of sarcopenia in SAMP8 mice. *Biogerontology*. (2020) 21:367–80. doi: 10.1007/s10522-020-09867-x

41. Casuso RA, Huertas JR. The emerging role of skeletal muscle mitochondrial dynamics in exercise and ageing. *Ageing Res Rev*. (2020) 58:101025. doi: 10.1016/j.arr.2020.101025

42. Cao X, Wang H, Wang Z, Wang Q, Zhang S, Deng Y, et al. In vivo imaging reveals mitophagy independence in the maintenance of axonal mitochondria during normal aging. *Aging Cell*. (2017) 16:1180–90. doi: 10.1111/acel.12654

43. Shukla R, Prevot TD, French L, Isserlin R, Rocco BR, Banasr M, et al. The relative contributions of cell-dependent cortical microcircuit aging to cognition and anxiety. *Biol Psychiatry*. (2019) 85:257–67. doi: 10.1016/j.biopsych.2018.09.019

44. Bevan RJ, Williams PA, Waters CT, Thirgood R, Mui A, Seto S, et al. OPA1 deficiency accelerates hippocampal synaptic remodelling and age-related deficits in learning and memory. *Brain Commun*. (2020) 2:fcaa101. doi: 10.1093/braincomms/fcaa101

45. Llorens-Martín M, Rábano A, Ávila J. The ever-changing morphology of hippocampal granule neurons in physiology and pathology. *Front Neurosci*. (2016) 9:526. doi: 10.3389/fnins.2015.00526

46. Mitra K, Wunder C, Roysam B, Lin G, Lippincott-Schwartz JA hyperfused mitochondrial state achieved at G1-S regulates cyclin E buildup and entry into S phase. *Proc Natl Acad Sci USA*. (20098) 106:11960–5. doi: 10.1073/pnas.0904875106

47. Tondera D, Grandemange S, Jourdain A, Karbowski M, Mattenberger Y, Herzig S, et al. SlP-2 is required for stress-induced mitochondrial hyperfusion. *EMBO J*. (2009) 28:1589–600. doi: 10.1038/emboj.2009.89

48. Rambold AS, Cohen S, Lippincott-Schwartz J. Fatty acid trafficking in starved cells: regulation by lipid droplet lipolysis, autophagy, and mitochondrial fusion dynamics. *Dev Cell*. (2015) 32:678–92. doi: 10.1016/j.devcel.2015.01.029

49. Youle RJ, Van Der Bliek AM. Mitochondrial fission, fusion, and stress. *Science*. (2012) 337:1062–5. doi: 10.1126/science.1219855

50. Gomes LC, Benedetto G. Di, Scorrano L. During autophagy mitochondria elongate, are spared from degradation and sustain cell viability. *Nat Cell Biol*. (2011) 13:589–8. doi: 10.1038/ncb2220

51. Rambold AS, Kostelecky B, Elia N, Lippincott-Schwartz J. Tubular network formation protects mitochondria from autophagosomal deadation during nutrient starvation. *Proc Natl Acad Sci USA*. (2011) 108:10190–5. doi: 10.1073/pnas.1107402108

52. Alavi MV, Fuhrmann N. Dominant optic atrophy, OPA1, and mitochondrial quality control: understanding mitochondrial network dynamics. *Mol Neurodegener*. (2013) 8:1–12. doi: 10.1186/1750-1326-8-32

53. Rizzuto R, Pinton P, Carrington W, Fay FS, Fogarty KE, Lifshitz LM, et al. Close contacts with the endoplasmic reticulum as determinants of mitochondrial Ca2+ responses. *Science*. (1998) 280:1763–6. doi: 10.1126/science.280.5370.1763

54. Bakeeva LE, Chentsov YS, Skulachev VP. Intermitochondrial contacts in myocardiocytes. *J Mol Cell. Cardiol*. (1983) 15:413–20. doi: 10.1016/0022-2828(83)90261-4

55. Baltrusch S. Mitochondrial network regulation and its potential interference with inflammatory signals in pancreatic beta cells. *Diabetologia*. (2016) 59:683–7. doi: 10.1007/s00125-016-3891-x

56. Rodríguez-Nuevo A, Díaz-Ramos A, Noguera E, Díaz-Sáez F, Duran X, Muñoz JP, et al. Mitochondrial DNA and TLR9 drive muscle inflammation upon Opa1 deficiency. *EMBO J*. (2018) 37:e96553. doi: 10.15252/embj.201796553

57. Tezze C, Romanello V, Desbats MA, Fadini GP, Albiero M, Favaro G, et al. Age-Associated loss of OPA1 in muscle impacts muscle mass, metabolic homeostasis, systemic inflammation, and epithelial senescence. *Cell Metab*. (2017) 25: 374–89.e6. doi: 10.1016/j.cmet.2017.04.021

58. Shi J, Yu J, Zhang Y, Wu L, Dong S, Wu L, et al. PI3K/Akt pathway-mediated HO-1 induction regulates mitochondrial quality control and attenuates endotoxin-induced acute lung injury. *Lab Investig*. (2019) 99:1795–809. doi: 10.1038/s41374-019-0286-x

59. Kosmider B, Lin CR, Karim L, Tomar D, Vlasenko L, Marchetti N, et al. Mitochondrial dysfunction in human primary alveolar type II cells in emphysema. *E Bio Med*. (2019) 46:305–16. doi: 10.1016/j.ebiom.2019.07.063

60. Albensi BC, Mattson MP. Evidence for the involvement of TNF and NF-κB in hippocampal synaptic plasticity. *Synapse*. (2013) 35:151–9. doi: 10.1002/(SICI)1098-2396(200002)35:2<151::AID-SYN8>3.0.CO;2-P

61. Meffert MK, Chang JM, Wiltgen BJ, Fanselow MS, Baltimore D. NF-κB functions in synaptic signaling and behavior. *Nat Neurosci*. (2003) 6:1072–8. doi: 10.1038/nn1110

62. Perkins ND. Integrating cell-signalling pathways with NF-κB and IKK function. *Nat Rev Mol Cell Biol*. (2007) 8:49–62. doi: 10.1038/nrm2083

63. Bonizzi G, Karin M. The two NF-κB activation pathways and their role in innate and adaptive immunity. *Trends Immunol*. (2004) 25:280–8. doi: 10.1016/j.it.2004.03008

64. Perkins ND, Gilmore TD. Good cop, bad cop: the different faces of NF-κB. *Cell Death Differ*. (2006) 13:759–72. doi: 10.1038/sj.cdd4401838

65. Brunk UT, Terman A. The mitochondrial-lysosomal axis theory of aging: accumulation of damaged mitochondria as a result of imperfect autophagocytosis. *Eur J Biochem*. (2002) 269:1996–2002. doi: 10.1046/j.1432-1033.2002.02869.x

66. Feher J, Kovacs I, Artico M, Cavallotti C, Papale A, Balacco Gabrieli C. Mitochondrial alterations of retinal pigment epithelium in age-related macular degeneration. *Neurobiol Aging*. (2006) 27:983–93. doi: 10.1016/j.neurobiolaging.2005.05.012

67. Machiela E, Liontis T, Dues DJ, Rudich PD, Traa A, Wyman L, et al. Disruption of mitochondrial dynamics increases stress resistance through activation of multiple stress response pathways. *FASEB J*. (2020) 34:8475–92. doi: 10.1096/fj.201903235R

68. Guo Y, Wang S, Liu Y, Fan L, Booz GW, Roman RJ, et al. Accelerated cerebral vascular injury in diabetes is associated with vascular smooth muscle cell dysfunction. *Gero Sci*. (2020) 42:547–61. doi: 10.1007/s11357-020-00179-z

69. Lai Y, Lin P, Chen M, Zhang Y, Chen J, Zheng M, et al. Restoration of L-OPA1 alleviates acute ischemic stroke injury in rats via inhibiting neuronal apoptosis and preserving mitochondrial function. *Redox Biol*. (2020) 34:101503. doi: 10.1016/j.redox.2020.101503

70. Xin T, Lu C. Irisin activates Opa1-induced mitophagy to protect cardiomyocytes against apoptosis following myocardial infarction. *Aging*. (2020). 12:4474–88. doi: 10.18632/aging.102899

71. Chen L, Gong Q, Stice JP, Knowlton AA. Mitochondrial OPA1, apoptosis, and heart failure. *Cardiovasc Res*. (2009) 84:91–9. doi: 10.1093/cvr/cvp181

72. Tsao K, Aitken PA, Johns DR. Smoking as an aetiological factor in a pedigree with Leber's hereditary optic neuropathy. *Br J Ophthalmol*. (1999) 83:577–81. doi: 10.1136/bjo.83.5577

frontiers
in Neurology

Check for
updates

Retinal Ganglion Cells—Diversity of Cell Types and Clinical Relevance

Ungsoo Samuel Kim [1,2,3,4]*, Omar A. Mahroo [4,5,6], John D. Mollon [7] and
Patrick Yu-Wai-Man [2,3,4,5]

[1] Kim's Eye Hospital, Seoul, South Korea, [2] John van Geest Centre for Brain Repair and MRC Mitochondrial Biology Unit,
Department of Clinical Neurosciences, University of Cambridge, Cambridge, United Kingdom, [3] Cambridge Eye Unit,
Addenbrooke's Hospital, Cambridge University Hospitals, Cambridge, United Kingdom, [4] Moorfields Eye Hospital NHS
Foundation Trust, London, United Kingdom, [5] Institute of Ophthalmology, University College London, London,
United Kingdom, [6] Section of Ophthalmology, King's College London, St. Thomas' Hospital Campus, London,
United Kingdom, [7] Department of Psychology, University of Cambridge, Cambridge, United Kingdom

Retinal ganglion cells (RGCs) are the bridging neurons that connect the retinal input to the visual processing centres within the central nervous system. There is a remarkable diversity of RGCs and the various subtypes have unique morphological features, distinct functions, and characteristic pathways linking the inner retina to the relevant brain areas. A number of psychophysical and electrophysiological tests have been refined to investigate this large and varied population of RGCs. Technological advances, such as high-resolution optical coherence tomography imaging, have provided additional tools to define the pattern of RGC involvement and the chronological sequence of events in both inherited and acquired optic neuropathies. The mechanistic insights gained from these studies, in particular the selective vulnerability and relative resilience of particular RGC subtypes, are of fundamental importance as they are directly relevant to the development of targeted therapies for these invariably progressive blinding diseases. This review provides a comprehensive description of the various types of RGCs, the developments in proposed methods of classification, and the current gaps in our knowledge of how these RGCs are differentially affected depending on the underlying aetiology. The synthesis of the current body of knowledge on the diversity of RGCs and the pathways that are potentially amenable to therapeutic modulation will hopefully lead to much needed effective treatments for patients with optic neuropathies.

Keywords: retinal ganglion cell, optic neuropathies, hereditary optic neuropathies, acquired optic neuropathies, electrophysiological tests, neuro-ophthalmology

INTRODUCTION

It was a clinical ophthalmologist, and an unusually interesting one, who first proposed that different fibres in the optic nerve carry different attributes of the retinal image, such as colour and spatial detail. Born in Charleston in 1830, John Julian Chisolm graduated from the Medical College of South Carolina in 1850 and gained further training on two visits to Europe (1). After the bombardment of Fort Sumter, he was commissioned into the Confederate Army and within 4 months had published the first of three editions of his "Manual of Military Surgery." In the years after the Civil War, he specialised in ophthalmology and in 1869, he reported, in the Moorfields house journal, how form vision had recovered before colour vision in a case of neuritis, leading him

to ask "…whether there are special nerve fibres, for the recognition of special colours, independent of those used in the clear definition of objects." (2). As early as the eighteenth century, there had been suggestions that there are different retinal fibres for different colours [e.g., (3, 4)], but Chisolm's is likely to be one of the first suggestions that different *attributes* of the image—such as form and colour—are carried by different fibres.

Today, it is clear that the retina does not deliver to the brain a pixel-by-pixel representation of the pattern of light falling on the photoreceptors. There are about 120 million rods and 6 million cones, whilst the output of the retina is transmitted by around 1.2 million retinal ganglion cells. Thus, there exists significant "pre-processing" of the visual signal by the retinal neuronal layers. The retinal ganglion cells (RGCs) extract in parallel different attributes of the image—spatial contrast, colour, motion, flicker, fine and coarse textures, absolute light level—and deliver this information to different sites within the visual system (5, 6). At least 18 different types of ganglion cells are now thought to be present in the primate and human retina, all of them functionally and morphologically distinct (7, 8). The individual types gain their functional specificities in turn from dedicated circuits that lie between the photoreceptors and the ganglion cells (9). The primate retina is currently thought to include 2 types of horizontal cells, 12 types of bipolar cells and more than 25 types of amacrine cells (**Table 1**).

Our purpose in this review is to provide clinicians with a brief survey of the different types of ganglion cells to highlight the possibility of either selective impairment or selective survival of particular types of cells. Subsequently, we discuss both clinical and research methods for evaluating the structure and function of RGCs, and survey a number of relevant clinical conditions before briefly discussing future avenues of research. This review will focus on primate and human studies. Lower mammals appear to enjoy a richer range of ganglion cell types with 40 or more different types having been reported in the mouse (16, 17). It is certainly attractive to consider the extensive literature devoted to the mouse since a remarkable array of histological, physiological and genetic methods have become available to study murine ganglion cells over the past two decades—methods that cannot all be applied to primates. In many areas, there is wide conservation across mammalian phylogeny, not only of cell morphologies, but also of the physiological circuits that underlie the functional specialisation of particular types of cell. On the other hand, the retina of each species is well adapted to the visual theatre into which that species is born, having evolved to match the requirements of that animal's visual world and to serve the animal's survival and reproduction (18). Analogies between different species may, therefore, sometimes be misleading (19). Even between macaques and humans, there may be occasional differences in the genes expressed in otherwise corresponding types of ganglion cells (20).

"Midget" and "parasol" types comprise more than 80% of all ganglion cells in human and primate retinas (20). Given this predominance, it is tempting to neglect the many minority types, but functional importance should not be equated with relative numbers. Midget and parasol cells have relatively small dendritic fields and therefore, large numbers are needed to tessellate—to

tile—the retina. Typically, the rarer ganglion cells have larger, often much larger, dendritic fields (7), and thus many fewer are needed to tesselate the entire retina. Yet, these wide-field cells may have a critical functional role, perhaps in everyday life or perhaps in unusual, but life-threatening conditions. In the case of several wide-field ganglion cells, this function is still unknown, and it may fall to an alert clinician, in the tradition of Chisolm, to detect the selective impairment that provides important clues.

Classification of Ganglion Cells—Methods
The taxonomy and the nomenclature of ganglion cells, like taxonomies and nomenclatures in other branches of biology, have generated unexpectedly contentious debates, especially when different methods of classification give different solutions or when nomenclatures are translated from one species to another (21). We briefly survey the several techniques that have led to the current taxonomy of ganglion cells. The alternative methods can themselves be grouped into anatomical, molecular, and functional classification.

Anatomical Classification
The cell bodies of most ganglion cells, and the layer formed by their axons, lie close to the inner limiting membrane adjacent to the vitreous, although occasional "displaced" ganglion cells are seen among amacrine cells in the inner nuclear layer [(22, 23), p. 309]. In the central regions of the retina, there are up to eight layers of ganglion cells, whereas in the far periphery, near the *ora serrata*, there are only sparse clumps of two or three ganglion cells with gaps between them (23).

Morphology
A fundamental basis for classification—and the one mainly adopted in the present review—is the size and morphology of the cell body and dendrites, as well as the extent of the dendritic field (**Figure 1**). Already in 1893, using the silver staining method of Golgi, Cajal distinguished several types of ganglion cells by such features, but it was not until 1935 that the predominant ganglion cells of the central region of the primate retina, the midget cells, were described by Stephen Polyak (who had not yet anglicised his name) (24).

Upstream Connexions: The Input Circuits and the Stratification of Dendrites
The functional properties of a given ganglion cell must necessarily depend on the excitatory and inhibitory inputs it receives from bipolar cells and from amacrine cells. The many different types of amacrine cells allow the construction of specialised circuits that determine the responses of their associated ganglion cells. In principle, it would be possible for two ganglion cells of identical morphology to receive different inputs and thus differ in their functional properties.

A fundamental basis for classifying ganglion cells is therefore the stratum, or strata, of the inner plexiform layer (IPL) in which their dendrites extend. Some are "monostratified," their dendrites confined to one stratum; some are "bistratified," having two distinct layers of dendrites (**Figure 1**). The level or levels at which the dendrites of a given ganglion cell stratify are very

characteristic (6). One gross division is between the inner and outer layers of the inner plexiform layers. Bipolar cells of the OFF type predominantly make contact with ganglion cells in the outer part whereas bipolar cells of the ON-type predominantly synapse in the inner part.

Downstream Connexions: The Projections of Retinal Ganglion Cells

A further anatomical classification, and one of special interest to the neuro-ophthalmologist, can be based on the projection sites of each class of ganglion cell. Besides the lateral geniculate nucleus, there are several other brain areas that receive direct projections from the retina, including the superior colliculus, the pulvinar complex, the olivary pretectal nucleus, the supraoptic nucleus of the optic tract, the paraventricular nucleus, the suprachiasmatic nucleus, and the dorsal raphe nucleus (see **Figure 2**) (25–27).

Classically, the projections of the ganglion cell layer could be established by anterograde tracing, e.g., by intraocular injection of a radioactive agent or cholera toxin subunit B (28), but

anterograde tracing of this kind does not identify the type, or types, of ganglion cell in which the projection originates. Retrograde methods, e.g., injecting horseradish peroxidase into the central site, allow specific ganglion cells to be labelled in the retina. An example would be the study by Cowey et al. showing retrograde labelling of several types of primate ganglion cells—including parasol and midget—after injections to the pulvinar (29). One modification of the retrograde method was introduced by Rodieck and Watanabe, who used a fluorescent marker for retrograde tracing and then, in an *in vitro* preparation, injected rhodamine-conjugated horseradish peroxidase into individual cells that had been labelled by the retrograde marker—a procedure that gave better filling of dendrites than did simple retrograde tracing with horseradish peroxidase (30).

Molecular Classification

The Golgi method is "noted for its fickleness" (31): this is its strength, in that it exquisitely reveals isolated neurons against a pale background, but it is also its weakness, in that the random staining is unpredictable and not specific to a particular type of cell (32). What are obviously desirable, especially for quantitative purposes, are methods that label either a single class of ganglion cells or only a small number of classes. In the case of lower mammals, many molecular markers (e.g., using antibodies or gene expression) have been developed to identify individual classes (**Table 2**) [e.g., (46)].

There has been less work of this kind in primates, but of particularly note is the work by Peng et al. (19) and Yan et al. (20) who identified RNA expressed in individual cells from macaque and human retinas (**Table 3**). In macaque, they were able to group peripheral ganglion cells into 18 clusters and foveal ganglion cells into 16 clusters. Three of the peripheral clusters in macaque retina (and two in the case of human) expressed *OPN4*, the gene for melanopsin and thus a marker of intrinsically

---

TABLE 1 | The number of types of photoreceptors, bipolar cells, and retinal ganglion cells in different species.

	Mouse	**Cat**	**Rabbit**	**Primates**
Photoreceptors	3 (one rod and S- and M- cones) (10)	3 (one rod and S- and M- cones)	3 (one rod and S- and M-cones)	4 (one rod and three cones)
Bipolar cells	~15 (11)	~9 (12)	~13 (13)	~12 (14)
Retinal ganglion cells	~30 (5)	~23 (12)	~20? (15)	Up to 18
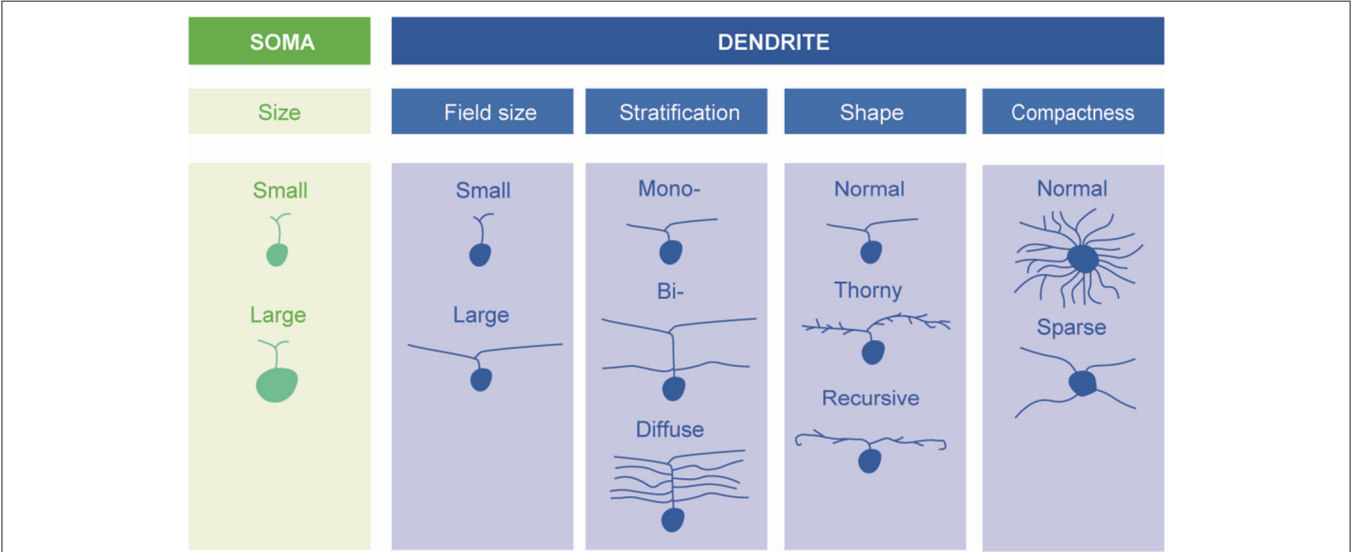
FIGURE 1 | Schematic description of retinal ganglion cells. Morphological types of RGCs are classified based on soma size and dendrite morphology (*by Ungsoo S. Kim*).

FIGURE 2 | Pathways of retinal ganglion cells. OPN, olivary pretectal nucleus; RGCs, retinal ganglion cells; SC, superior colliculus; SCN, suprachiasmatic nucleus (*by Ungsoo S. Kim*).
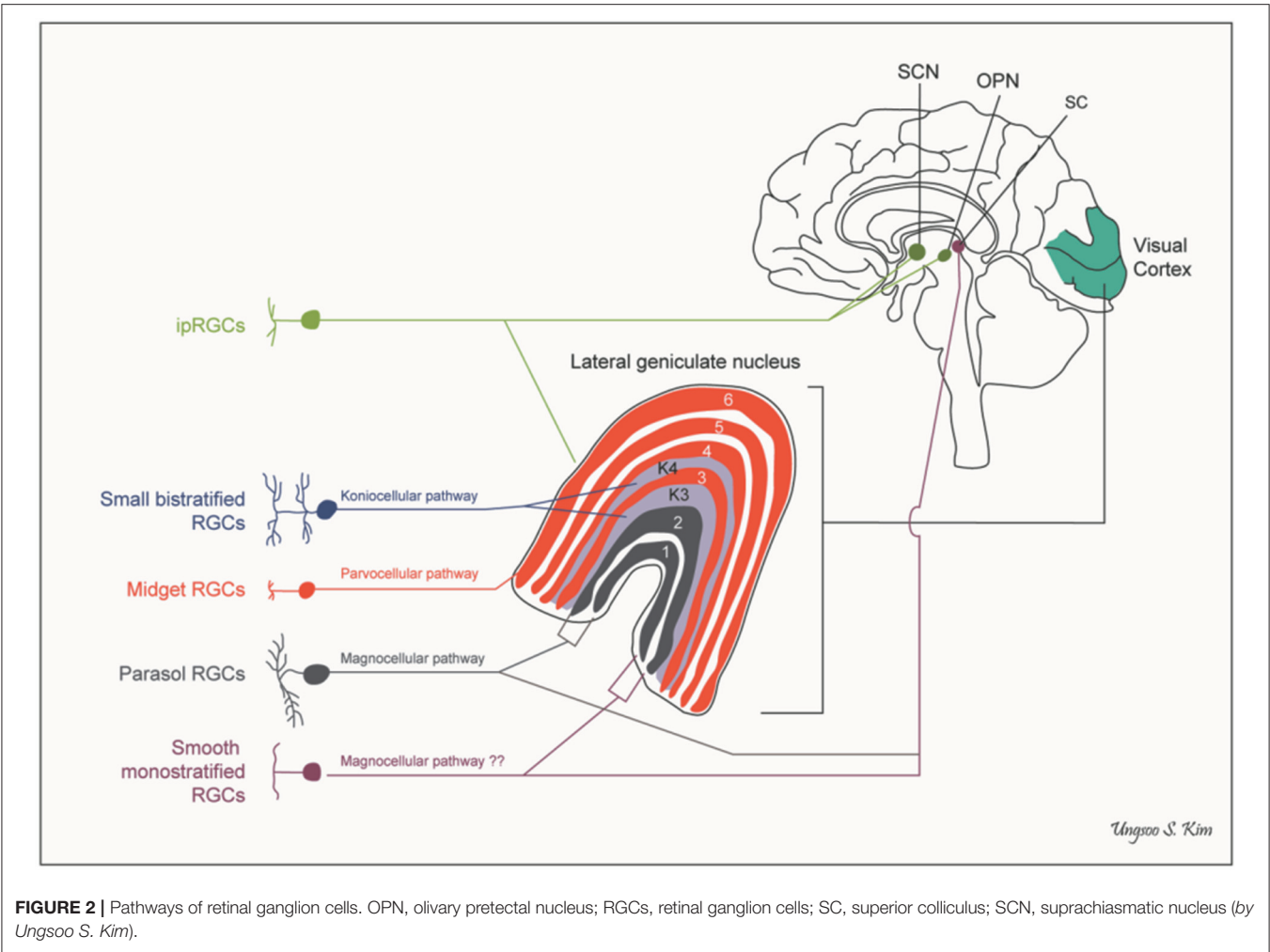
TABLE 2 | Antibodies used in immunohistochemistry for retinal ganglion cells.

Antigen	Host species	Specificity	References
βIII-tubulin	Mouse	Monoclonal	(33)
Islet-1	Mouse	Monoclonal	(34)
Syntaxin-1	Mouse	Monoclonal	(35)
GFAP	Mouse	Monoclonal	(36)
ED1	Rabbit	Monoclonal	(37)
Brn3a	Goat	Polyclonal	(38)
Thy1 (CD90)	Mouse	Monoclonal/Polyclonal	(39)
CaBP (DB3a)	Mouse	Monoclonal	(40)
CD15 (FMB, DB6)	Mouse	Monoclonal	(41, 42)
RBPMS	Rabbit, Mammalian	Polyclonal	(43–45)

TABLE 3 | Expression molecular markers of major retinal ganglion cells in primates.

Type of retinal ganglion cells	Expression molecular markers	References
ON-midget RGCs	*TPBG, GUCY1A3*	(47)
OFF-midget RGCs	*TBR1, GUCY1A3*	(19)
ON-parasol RGCs	*CHRNA2, SPP1, RBPMS2*	(19, 48)
OFF-parasol RGCs	*CA8, SPP1, RBPMS2*	(19, 48)
Large sparse RGCs	*SATB2*	(49)
ipRGCs*	*OPN4*	(50, 51)

ipRGCs, intrinsically photosensitive retinal ganglion cells.

photosensitive RGCs (ipRGCs). Fourteen of the foveal clusters corresponded to peripheral clusters. Although a similar set of transcription factors is used in mouse and primate ganglion cells, there was little correspondence in the detailed RNA expression patterns of individual cell types. In particular, there was no clear mouse equivalent of the midget ganglion cell of the primate. The patterns of RNA expression were very similar for human and macaque retinas, but occasional differences were seen. For example, the gene *RBPMS2* was expressed in human, but not macaque midget ganglion cells. In the present context, it is significant that genes known to be associated with glaucoma

were found to be predominantly expressed in ganglion cells, sometimes selectively—e.g., *SIX6* in midgets (19).

Functional Classification

In functional experiments, a physiological measure of a cell's response is recorded when the retina is stimulated with a specific stimulus. Psychophysical work has often guided the choice of stimulus. In the second half of the twentieth century, psychophysicists endeavoured to isolate "mechanisms" or "channels" within the visual system. These constructs were hypothetical, but the hope—not without foundation—was that they corresponded to independent neural channels. The isolation of a given channel was achieved by construction of a stimulus to which the channel might be maximally sensitive and by the use of selective adaptation stimuli to reduce the sensitivity of other channels [e.g., (52–54)]. The techniques that were honed by psychophysicists were often adopted by electrophysiologists and applied to individual ganglion cells. The same techniques often also inspired new clinical testing methods, such as frequency-doubling perimetry, designed to isolate channels with non-linear responses (55). Psychophysics has also inspired the instruments used to deliver the carefully crafted stimuli needed in electrophysiological work—Maxwellian-view optics in the 1960's, computer-controlled CRT displays in the 1980's, and digital light processors in this century.

The celebrated study of Kuffler initiated the extracellular recording of action potentials from individual ganglion cells in the mammalian retina by means of fine-tipped microelectrodes (56). Kuffler demonstrated the antagonistic centre-surround arrangement that characterises the receptive fields of many ganglion cells: stimulation of the centre of the receptive field evokes an ON response in some cells and an OFF response in others, whereas stimulation of a surrounding region evokes the opposite response (**Figure 3**).

A pioneer in the study of primate RGCs was Peter Gouras, who made microelectrode recordings *in vivo* from *Macaca mulatta* and made a basic distinction between cells with transient ("phasic") responses and those with sustained ("tonic") responses (57). Influenced by the psychophysical work of Stiles (58), Gouras presented small monochromatic flashes of varying wavelength on monochromatic adapting fields and showed that sustained cells typically drew inputs from one class of cone in the centre of their receptive field and inhibitory inputs from other types of cone in the surround. Given the specificity of the centre input and the predominance of sustained cells in the central field, he identified them with the midget cells of Polyak. The phasic cells were more common in the periphery and appeared to draw inputs of the same sign from long- and middle-wave cones, with little input from short-wave cones.

In the last two decades, it has become possible to record concurrently from several hundred ganglion cells in an eye-cup preparation. A segment of peripheral retina, with pigment epithelium intact, can be placed with ganglion cell layer downwards on a planar array of, say, 512 extracellular micro-electrodes. In the work of Field et al. for example, the macaque retina was stimulated with a lattice of square pixels that varied randomly and independently in chromaticity (59). The

responses of individual ganglion cells, identified later off-line, were correlated with the random pattern of stimulation to determine their preferred stimuli.

The introduction of adaptive-optics scanning-light ophthalmoscopy (AOSLO) combined with calcium imaging has been used to monitor the responses of individual ganglion cells in the eye of a living primate [e.g., (60)]. Action potentials cause rapid changes in intracellular free calcium and these can be revealed with a fluorescent protein calcium sensor. McGregor et al. used the sensor GCaMP6s for that purpose. While the retina was stimulated with orange (590 nm) drifting gratings, a 488-nm laser was focussed on the ganglion cell layer to excite the calcium sensor, and the fluorescence was detected in a band at 517–520 nm. A limitation of currently available calcium sensors, such as GCaMP6s, is that they have relatively large time constants (0.6 s) and so cannot follow high frequencies of modulation.

Combinations of Methods

A critical task has been to relate one method of classification to a second. An early success was achieved by intracellular recording with a micropipette electrode filled with a dye such as Procion yellow (61): after a basic characterisation of the cell's response, the passage of hyperpolarizing current could be used to inject the stain into the cell, for later histological examination. Nelson et al. used such a method in eye-cup preparations from cat to show the fundamental mammalian separation of the inner plexiform layer into ON and OFF sublaminae (62). Dacey and Lee used a refinement of this technique in which primate ganglion cells of specific morphology were targeted in a flat-mount preparation under visual inspection, recordings were made with an intracellular micropipette, and the cell was stained by intracellular injection of the fluorescent dye pyranine during recording (63). It was this work that first identified the small bistratified ganglion cell as carrying the excitatory signal of short-wave primate cones.

In 2003, Dacey et al. introduced a powerful technique that has been central to our modern understanding of the range of ganglion cell types (64). The method allows the morphology of the cell to be related not only to stratification level in the inner plexiform layer and to downstream projection sites, but also to the functional characteristics of the cell. Rhodamine dextran was injected *in vivo* into a central site (e.g., the lateral geniculate nucleus or the superior colliculus) and the dye travelled retrogradely to the retina over the course of 4 to 7 days. In a subsequent *in vitro* preparation of retina, including the retinal pigment epithelium (RPE) and choroid, the rhodamine dextran was seen to be sequestered within the cytoplasm of ganglion cell bodies, but if, under visual inspection, an individual cell was briefly exposed to light, then the tracer was liberated and spread throughout all the processes of the cell. The tracer did not appear to impair neuronal function, and the responses of the cell could be examined with an extracellular microelectrode, while visual stimuli were delivered via the microscope used for selecting cells and placing the electrode (64).

Peng et al. have linked their single-cell RNA analyses to morphology by combining fluorescent *in situ* hybridisation
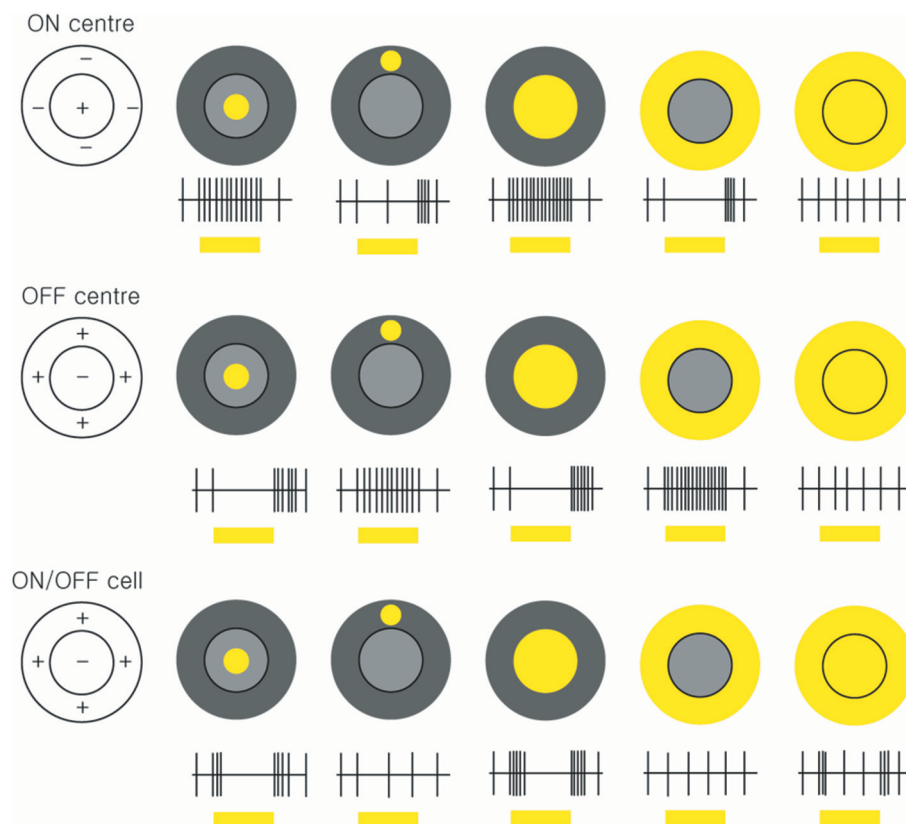
FIGURE 3 | Receptive fields and responses of ON-centre, OFF-centre, and ON/OFF retinal ganglion cells. ON-centre RGCs (upper panels) increase their rate of discharge when the light illuminates in the centre. However, when the surround field is illuminated, the ON-centre RGCs are suppressed. OFF-center RGCs respond when the light turns off (middle panels). ON/OFF cells are triggered briefly when the light turns on or off (lower panels) (*by Ungsoo S. Kim*).

("FISH") with sparse viral labelling (19). By this means, they were able to confirm—for ON- and OFF-midgets and ON- and OFF-parasols—the tentative identifications that had emerged from their analyses of RNA patterns.

Types of Retinal Ganglion Cells

Although there is some degree of consensus on major retinal ganglion cell types including midget RGCs, parasol RGCs and small bistratified RGCs, there has been some debate over classification of the remaining types. The functions of the remaining RGCs have been inferred from animal studies (**Table 4**).

Midget RGCs (P-Cell, mRGCs)

This major cell type accounts for 70% of RGCs. The midget RGCs have a small-sized body with small fields of dendrites (5–10 μm in diameter in the central retina and up to 225 μm in the periphery), which correspond to smaller receptive fields than those of other RGCs. These cells are located mainly in the central retina and project to the parvocellular pathway (66, 67). Midget RGCs have a one-to-one connectivity with midget bipolar cells, which draw their input from a single cone (68). There are two types of

midget RGCs: the outer stratified OFF-midget cells show smaller dendritic fields and higher cell densities than the inner ON-midget cells.

The parvocellular pathway is dominated by midget RGCs. Functional assessments of these cells demonstrate that their luminance contrast sensitivity is lower than that of parasol RGCs and most show clear chromatic opponency (69). In general, midget cells have red–green opponency, parasol RGCs are achromatic, and bistratified ganglion cells connect with S-cone ON and L-M cone OFF pathways. However, recent studies suggest that some OFF-midget cells receive signals from short wavelength (blue) sensitive cones (14, 70). Electron microscopy reconstructions of retinal circuits suggest the possibility that a small proportion of midget ganglion cells might have blue–OFF, yellow–ON receptive fields. In addition to colour discrimination, midget RGCs also subserve pattern, texture and stereoscopic depth perception (71).

Parasol RGCs (M-Cell, pRGCs)

Parasol RGCs project to the magnocellular layer of the LGN. As with midget cells, there are two types of parasol cells in primates: ON-parasol cells respond with an increase in firing rate at the

TABLE 4 | The classification of retinal ganglion cells in primates.

	Stratification	Dendritic field size (μm)	Function
Midget	Inner (above the axon terminals of DB6 bipolar cells) Outer (CD15-labeled OFF midget bipolar cells)	10–100 μm	Colour (red-green)
Parasol	Inner (above the DB6 cells) Outer (at the level of the calbindin-labelled DB3a cells)	30–300 μm	Movement
Small bistratified	Inner (above the level of DB6 axons) Outer (near or above the level of DB3a axons)		Colour (short-wave ON)
Large bistratified	Inner/Outer		
Smooth monostratified	Outer	Fewer, straight dendrites 250–340 μm	
Narrow thorny (outer/inner stratifying)	Outer (calbindin-labelled DB3a cells)/Inner (DB6 cells)	190–300 μm	
Broad thorny	In the middle of IPL (DB3a cells to CD15-labeled DB6 cells)	170–600 μm	Local edge detectors?
Recursive bistratified	DB6 cells		ON-OFF direction
Recursive monostratified			
Large sparse		240–333 μm	
Giant sparse	Bistratified (65) (Inner / Outer)	441–533 μm	

Nomenclature by Masri et al. (8).

onset of light in the centre of their receptive field whereas OFF-parasol cells react to off stimuli (63). In synaptic connexions between ON-centre parasol cells and other cells, ~20% of the input is from bipolar cells and the remainder of the signal is introduced from amacrine cells (72).

Parasol RGCs have larger receptive fields and cell bodies, have higher sensitivity to luminance contrast, and present little or no chromatic antagonism, in contrast to midget RGCs (73). Parasol RGCs play a role in motion perception, flicker perception and depth processing based on motion parallax (71). They largely comprise the magnocellular pathway.

Small Bistratified RGCs

This cell type accounts for ~5–8% of RGCs (8). The small bistratified RGCs (sbRGCs) project to the koniocellular layers of the LGN. Small bistratified cells have branches in both layers (inner ON- IPL and outer OFF-IPL): inner ON-IPL branches receive excitatory input from S-ON bipolar cells initiated by S-cones, while opposed (L+M)-OFF light responses arrive through outer OFF-IPL branches (63). This arrangement is thought to give good colour vision with low spatial resolution.

Large Bistratified RGCs

The inputs of large bistratified RGCs have not been elucidated. Large bistratified cells may receive not only S-cone ON-pathway input, but also (L+M) cone OFF-opponency (inhibitory) signals. However, the precise role of this cell type is not yet clear (74).

Smooth Monostratified RGCs

Smooth monostratified RGCs (smRGCs) have irregular receptive fields with multiple distinct hotspots of light sensitivity. These cells again can be divided into ON- and OFF-cells (75). They might contribute to signalling spatial information via a non-linear mechanism, whereby output is not linearly related to input (76).

Recursive Monostratified/Bistratified RGCs

The recursive RGCs have moderately densely branched dendritic trees in which many secondary branches tend to curve back towards the soma or close loops of apposing and recursive dendrites. In addition, many dendrites overlap those of neighbouring cells (77). These features resemble those of the directionally selective, motion-sensitive RGCs (dsRGCs) of the rabbit, in which seven types of dsRGCs have been described, namely, ON-types specific to three different directions and ON-OFF types, specific to four different directions. To date, only one population of a bistratified ON-OFF type has been described in the macaque retina (78–80).

Thorny RGCs

There are three types of thorny RGCs in the primate retina that account for ~1% of ganglion cells (77). Broad thorny RGCs are given various names such as thorny diffuse, T-group cells, S3 narrow thorny, and hedge cells (30, 49, 81). The dendrites of broad thorny RGCs span a whole layer of the inner plexiform layer. It is presumed that the cells may contribute to ON/OFF-centre light responses that are strongly suppressed by stimulation of the receptive field surround, such as local edge detector cells in rabbits (82). Additionally, two narrowly stratified cells, including outer and inner, are found in primates and their connectivity has not been clarified yet.

Large Sparse RGCs

These cell types are monostratified cells that receive input from amacrine and bipolar cells. The transcription factor Satb2 is expressed in large sparse RGCs in macaque and human retina (83).

Melanopsin-Containing Intrinsically Photosensitive RGCs (ipRGCs)

The ipRGCs constitute 1% of the total RGC population in humans (84). These cells have large, sparse dendritic fields. They are intrinsically photosensitive because of the expression of the melanopsin photopigment and capable of phototransduction independently of rods and cones (84). In mouse retinas, six subtypes (M1, M2, M3, M4, M5, and M6) of ipRGCs have been identified with distinctive anatomical and functional properties (**Figure 4**) (85). M1 and M2 ipRGCs account for the majority (74–90%) of ipRGCs. The main function of ipRGCs, in particular of the Brn3b-M1subtype, is to contribute to circadian photoentrainment through the projections to the suprachiasmatic nucleus (SCN) of the hypothalamus (86), but they are also relevant for other non-image forming functions of the eye, including the regulation of the pupillary light reflex through the projections to the OPN. M1 and M2 ipRGCs project to both the SCN and the olivary pretectal nucleus (OPN); however, M1 ipRGCs innervate the outer shell region of the OPN, where projection neurons that innervate the pre-autonomic Edinger-Westphal nucleus reside, whilst M2 ipRGCs innervate the OPN central core (87). The input dendrites of M2 and M4 ipRGCs are in the inner retina (ON-pathway), whereas those of M1 ipRGCs are located near the inner nuclear layer (OFF-pathway). The dendrites of M4 and M5 ipRGCs are located in the inner lamina of the inner plexiform layer. M4 ipRGCs have a larger cell body compared with M5 ipRGCs that have small, highly branched dendrites arrayed uniformly around the soma.

In humans, three ipRGC subtypes (M1, M2, and M4) have been defined (88). M1 ipRGCs have outer stratifying dendrites with a few smooth spines in the outer IPL, whereas M2 ipRGCs stratify in the inner part of the inner plexiform layer (IPL) close to the ganglion cell layer. M1 ipRGCs have been divided into two subtypes, gigantic M1 RGCs (GM1 cells) with round or oval large soma and displaced M1 RGCs (DM1 cells). Both ipRGC types receive inputs from DB6 bipolar cells and project to the dorsal LGN (89). M2 ipRGCs have larger soma and more branched dendrites than M1 ipRGCs. M1 ipRGCs are reported to receive an inhibitory input from short-wave cones via an S-cone amacrine cell (90), whereas M2 ipRGCs receive input from S-On bipolar cells and contribute to the blue cone pathway (91). M1 ipRGCs project to the SCN to synchronise the circadian clock and M2 ipRGCs project to the OPN in the thalamus to control pupillary response.

The ipRGCs are relatively preserved in the mitochondrial optic neuropathies, such as Leber hereditary optic neuropathy (LHON) and autosomal dominant optic atrophy (ADOA). However, ipRGCs are affected in other optic neuropathies, such as glaucoma, and late-onset neurodegenerative disorders, such as Alzheimer disease and Parkinson disease (92–95).

Miscellaneous RGCs

There are a small number of unclassified RGCs in primates that do not fit with any of the previously described RGCs (8). Further work is needed to elucidate the characteristics of this miscellaneous group of RGCs.

Clinical Aspects of RGC—Methods of Assessment and Clinical Entities

Clinical Structural and Functional Assessment of RGCs

Although RGCs have been extensively studied in primates, the clinical assessment of RGCs has proven more challenging as they cannot be evaluated directly.

Structural Quantification of RGCs

Optical Coherence Tomography

Optical coherence tomography (OCT) is a non-invasive imaging technique that uses low-coherence light waves to capture a cross-section of various tissues. Major advances have led to the development of spectral domain OCT, which can produce a segmentation of ten layers of retina, including the retinal nerve fibre layer (RNFL) and ganglion cell layer. OCT has become a standard tool to investigate changes with RGCs as it is non-invasive, rapid, highly reproducible (96–98).

The RNFL can be measured in both the peripapillary and the macular areas. Several studies suggest that changes can be detected earlier by assessing the thickness of the RNFL in the macula compared with the peripapillary RNFL, owing to the latter's thickness (99, 100). There is a good correlation between RNFL thickness and both visual acuity and visual field changes, offering an objective structural parameter for assessing glaucoma and other optic neuropathies (101–103). However, to avoid misinterpretation of OCT, several factors need to be considered: segmentation errors can occur particularly in the presence of a tilted optic disc (104); and RNFL thickness is also affected by age as well as by refractive error and axial length. In addition, there is lag time before any changes in the thickness of the RNFL can be detected after disease onset (105), and the thickness can be overestimated in the presence of optic disc or RNFL swelling.

In addition, RNFL thickness exhibits a floor effect that must be considered in advanced optic neuropathies. RNFL thinning reaches a trough at a certain level owing to residual tissues such as vessels and glial cells (106, 107). Furthermore, RNFL loss usually signifies irreversible damage and functional tests (as described below) might be needed to identify ganglion cell dysfunction at a potentially reversible stage. It is well-established that visual acuity and visual fields can recover despite extensive RGC layer thinning (108, 109).

Microcysts in the inner nuclear layer have been reported on macular OCT imaging in some patients with advanced loss of macular RGCs. These are thought to arise from retrograde transsynaptic degeneration and/or vitreous traction in the presence of RGC and RNFL loss (110, 111). They do not seem to be specific to a particular aetiology, having been reported in patients with inherited optic neuropathies, demyelinating optic neuritis, compressive and nutritional optic neuropathies, endemic optic neuropathy and advanced glaucoma (112–114). It is not clear why these microcysts develop in only a subgroup of patients. They are seen more often in younger patients who may have a more adherent vitreous surface and ILM tension has been implicated as part of the pathophysiology (110). However, microcysts have also been reported as a long-term consequence

FIGURE 4 | Melanopsin-containing intrinsically photosensitive RGCs in primates. Inner stratifying ipRGCs (M2 ipRGCs) have larger soma and more branched dendrites than outer stratifying ipRGCs. In addition, the dendrites of M1 ipRGCs are mainly located in the outer IPL layer, whereas M2 ipRGCs are in the outer IPL layer close to the ganglion cell layer. M1 ipRGCs project to the suprachiasmatic nucleus (SCN) to synchronize the circadian clock and M2 ipRGCs project to the olivary pretectal nucleus (OPN) in the thalamus to control pupillary response. A, amacrine cell; Off-B, Off-bipolar cell; On-B, On-bipolar cell (*by Ungsoo S. Kim*).

associated with RGC loss in patients with silicon oil-related visual loss (115). These patients have undergone prior removal of the vitreous suggesting that simple vitreous traction may not be sufficient to explain the development of these microcysts.

Detection of Apoptosing Retinal Cells

The detection of apoptosing retinal cells (DARC) is a new technique that enables visualisation of real-time RGC apoptosis using fluorescently-labelled annexin A5. This 36 kDa protein is expressed in humans and it is a well-established indicator of apoptosis (116)). DARC has the advantage of early detection of RGC loss before visual deterioration has occurred, and it being considered for the evaluation of optic neuropathies, including glaucoma disease progression (117).

Functional Evaluation of RGCs

A number of psychophysical measurements can be used to investigate changes in RGC function.

Visual Acuity Tests

Visual acuity has been defined as the "spatial resolving capacity" of the visual system and it is the most common primary outcome measure in clinical trials. Although Snellen charts are widely used, the LogMAR scale based on the Early Treatment Diabetic Retinopathy Study (ETDRS) chart is the gold standard for clinical trials, overcoming many of the limitations of Snellen charts.

However, as visual acuity tests central foveal function, patients can have widespread ganglion cell loss with preserved central visual acuity.

Spatial and Temporal Contrast Sensitivity Tests

Achromatic stimuli of low and high spatial frequencies can be used to differentiate responses from the magnocellular and parvocellular systems. The magnocellular pathway has lower spatial resolution and responds to higher temporal frequencies than the parvocellular pathway (118). However, this difference is relatively small and the two pathways have a degree of overlap.

Colour Vision Tests

Colour vision impairment is a frequent feature of ganglion cell pathology, but outer retinal dysfunction can also affect colour vision, such as anomalies of the cone photoreceptors. Congenital stationary red-green colour deficiencies commonly affect men, owing to loss or alteration of the long or medium wavelength opsin genes on the X-chromosome (119). Rarely, abnormalities in the same genetic region can give rise to S-cone monochromacy. Congenital tritan anomalies, arising from abnormalities in S-cones are also rare. Progressive or later onset cone or macular dystrophies, or congenital achromatopsia, will also affect colour vision, but in these conditions visual acuity is also usually impaired (120). In acquired ganglion cell pathology, however, visual acuity can be preserved with colour vision being

preferentially affected. Many optic neuropathies affect red-green discrimination, although glaucoma commonly affects the blue-yellow axis (120).

Colour vision tests are widely used to screen patients with congenital colour vision defects and to investigate acquired pathology. There are three broad types of colour vision tests in practice (121). Pseudoisochromatic tests, such as the Ishihara, the Hardy-Rand-Rittler (HRR), and the Standard Pseudoisochromatic Plates (SPP), the Colour Vision Testing Made Easy (CVTME), and the Cambridge Colour Test are widely used. In arrangement tests, such as the Farnsworth-Munsell (FM) Dichotomous D-15 tests and 100-hue test, the patient is required to arrange a set of colours in order. The FM 100-hue test is highly sensitive, but time-consuming. Lastly, anomaloscopes are based on colour-matching where the observer adjusts a mixture of red and green lights to match a monochromatic orange light.

As congenital anomalies of colour perception more commonly affect red-green discrimination, many standard tests such as the Ishihara plates and the Nagel anomaloscope do not probe for tritan disorders, which are common in acquired pathologies. Tritan defects can be identified readily by other tests, including the D-15 and FM 100-hue, the Cambridge Colour Test, and the HRR plates. In addition, more specialised psychophysical methods, including measurement of the three primary colour vision mechanisms, colour adaptometry, and colour perimetry can be applied (122). Among them, SWAP, a specialised type of perimetry, can also be considered a colour vision test, as the targets are short-wave and the field is of long wavelength and high intensity (in order to adapt the long- and middle-wave cones) (123).

Visual Field Tests

In addition to conventional visual field testing, short wavelength automated perimetry (SWAP) probes the small bistratified ganglion ceullar and the konioceullar pathway, and high-pass resolution (ring) perimetry tests the parvocellular pathway, whereas flicker perimetry, motion perimetry, and frequency doubling technology (FDT) target the magnocellular pathway (124). Among these tests, SWAP and FDT are available as commercial products.

(1) Frequency Doubling Technology (FDT)

FDT has the advantage of greater sensitivity, potentially detecting RGC damage earlier than standard automated perimetry (SAP) (125). Modern FDT uses targets of low spatial frequency that flicker at a high temporal frequency and that predominantly stimulate the magnocellular pathway, which corresponds to motion detection and flicker detection (126). FDT has been put forward for the early detection of glaucoma on the basis that the magnocellular pathway is more vulnerable in glaucoma (127, 128). However, there is evidence that both the parvocellular and magnocellular pathways are affected early in glaucoma with no significant differences between these two pathways in terms of their vulnerability (129). Furthermore, a recent study indicated that FDT is neither sensitive nor specific as a screening tool for glaucoma (130). Further studies are, therefore, needed to evaluate the role of FDT in the early detection of glaucoma.

(2) Short Wavelength Automated Perimetry (SWAP)

Unlike standard visual field testing, which uses a white stimulus on a white background, SWAP employs a blue stimulus on a yellow background. Several studies suggested that SWAP is more sensitive for the early detection of glaucomatous changes compared with standard visual field testing (131–133). There is, however, no definitive evidence that the small bistratified ganglion cells (short-wave response) are more vulnerable in glaucoma. SWAP was reported to be 10–20 times more sensitive than standard perimetry in patients with ADOA (134). As a result, SWAP was able to differentiate between normal tension glaucoma with or without *OPA1* polymorphism (135). However, SWAP has some limitations as it is time-consuming, it needs a higher level of cooperation, and it has lower reproducibility compared with standard perimetry (136).

Chromatic Pupillometry

The primate pupil responds to signals from ipRGCs, which additionally receive input derived from cone responses. Chromatic pupillometry uses selective wavelengths to quantify pupil size before, during, and after a light stimulus has been applied. Comparison of pupillary responses to short-wavelength and long-wavelength light can selectively probe the function of outer retinal photoreceptors or the intrinsic response of ipRGCs. The ipRGCs are blue light sensitive and maximally sensitive to wavelengths that lie between the peak sensitivities of the rods and S-cones. Several studies using chromatic pupillometry in experimental animal models have shown that the light sensitive ipRGCs were spared in retinitis pigmentosa characterised by marked photoreceptor loss (137). Generally, the ipRGCs are relatively preserved in mitochondrial optic neuropathies, such as LHON and ADOA (138, 139), but affected in other optic neuropathies such as glaucoma, non-arteritic anterior ischemic optic neuropathy and demyelinating optic neuritis (140). Bichromatic pupillometry has been used to differentiate between mitochondrial and non-mitochondrial optic neuropathies (94, 140).

Electrophysiological Tests

Electrophysiology allows direct objective assessment of electrical responses *in vivo*. The visual evoked potential (VEP), recorded over the visual cortex, has long been used as a means of assessing the function of the visual pathway, as well as demonstrating developmental abnormalities, such as the misrouting of ganglion cell axons in albinism (141). In addition, the electroretinogram (ERG), which represents the summed electrical response of the retina to light stimuli, can be recorded non-invasively. The pattern ERG (PERG), arising from stimulation of the macula, is largely derived from responses in the macular RGCs. In contrast, the full-field ERG, which is generated from the stimulation of the whole retina, is usually used to evaluate responses from photoreceptors and bipolar cells. However, a late component, the photopic negative response (PhNR) has been shown to arise in ganglion cells.

(1) Pattern Electroretinogram

The PERG is recorded in response to a patterned stimulus (typically a checkerboard pattern reversing 4 times per second),

which stimulates the central 15 degrees of the retina (142). The PERG comprises a cornea-positive wave at 50 ms (termed P50) and a negative wave at 95 ms (termed N95). The test is performed in photopic conditions with undilated pupils and it requires optimal refraction. The response is driven by the macular cone photoreceptors, but it appears to arise largely from the macular RGCs, whose signals appear to give rise to the N95 component and the majority of the P50 component (143, 144). Various optic neuropathies that affect the ganglion cells within the retina (either as the primary site of impairment or from retrograde degeneration from an optic nerve lesion), for example demyelinating optic neuritis, ischemic optic neuropathy, compressive optic neuropathy, toxic optic neuropathy, and inherited optic neuropathies can result in a reduction of the N95 and P50 amplitudes, with N95 being reduced more than P50, and a shortening of the P50 peak time (145–147). Whilst the PERG is sensitive to macular RGC dysfunction, precise correlation with RGC subtype is not known, and the test will not detect extramacular RGC impairment.

(2) Photopic Negative Response

The PhNR is a negative wave of long latency that follows the b-wave of the photopic cone-driven ERG and it arises in RGCs (148). Whilst it can be detected in standard white-on-white flash responses, specific chromatic protocols can be used to optimise the PhNR signal (149). As with the PERG, the amplitude of the PhNR decreases in optic nerve disorders (150, 151). Unlike in PERG recordings, optimal refraction is not needed, but the pupils need to be dilated. In addition, a hand-held mini-Ganzfeld stimulator is available to test PhNR (152). The flashes stimulate the retina as a whole so the PhNR can be indicative of global RGC function.

Focal PhNR recordings can be performed to assess RGCs over a particular region (typically the macula) (153). The PhNR can be used to examine the parvocellular pathway whereas the steady-state PERG is focused on the magnocellular pathway in glaucoma (154). Although the PERG and PhNR can detect glaucoma, there is no significant correlation between PhNR ratio and PERG ratio values (155).

Clinical Correlates—Structure and Function

Inherited and acquired optic neuropathies are important causes of registrable blindness. Treatment options remain limited, and when available, they mostly slow down or prevent further loss of RGCs. Visual loss is usually irreversible although in some cases, spontaneous visual recovery can occur owing to the functional recovery of RGCs that have not undergone apoptosis. To better inform future treatment strategies, it is essential to gain a better understanding of the pattern of RGC loss and whether different aetiological triggers result in global or more selective loss of RGCs, and how these relate to the visual deficits and eventual outcome. It remains a challenging task as patients are not always examined in the acute stage of the disease and serial measurements are needed to document progression over time. Nevertheless, we are gaining a better understanding of the structure-function relationship in different optic neuropathies

aided by the availability of high-resolution retinal imaging with OCT and more sophisticated visual electrophysiological and psychophysical tools (**Figure 5**).

Inherited Optic Neuropathies

The minimum prevalence of inherited optic neuropathies has been estimated at 1 in 10,000 (156). This group of disorders is genetically heterogeneous with disease-causing mutations occurring in both mitochondrial and nuclear DNA (157). Remarkably, all genes identified to date encode proteins that are either directly or indirectly involved in regulating mitochondrial function. The generation of ATP by the mitochondrial respiratory chain is central to cell survival and mitochondria also regulate other key pathways, including the level of reactive oxygen species and the tight control of apoptosis. An intriguing aspect of inherited optic neuropathies is the preferential vulnerability of RGCs compared with other neuronal populations despite the ubiquitous expression of the genes involved. There have been limited post mortem studies on the pattern of RGC loss in inherited optic neuropathies owing to the lack of access to diseased human tissues. Nevertheless, useful insight has been obtained with the application of high-resolution OCT imaging and psychophysical evaluation of patients at different stages of the disease process. The two best studied inherited optic neuropathies are LHON and ADOA.

(1) Leber Hereditary Optic Neuropathy

LHON is a primary mitochondrial DNA (mtDNA) disorder and ∼ 90% of cases are due to one of three mtDNA point mutations, namely, m.3460G>A (*MT-ND1*), m.11778G>A (*MT-ND4*), and m.14484T>C (*MT-ND6*) (158, 159). The peak age of onset is from 15 to 35 years old and the majority of patients are men (80–90%) (160). Although bilateral simultaneous onset can occur in some patients, sequential involvement of the second eye within a few months is more typical. LHON is characterised by severe visual loss with dyschromatopsia and a dense central or cecocentral scotoma on visual field testing. OCT initially shows swelling of the RNFL, follows by marked thinning of RNFL, especially in the temporal quadrant corresponding to the papillomacular bundle (161). Childhood-onset LHON and the m.14484T>C mutation are associated with a more favourable visual outcome (38, 162). Most patients with LHON are registered legally blind with <20% of patients carrying the m.11778G>A mutation experiencing some visual recovery (159, 163).

In LHON, RGCs with the smallest calibre axons, which have smaller mitochondrial reserve per energy requirement, are preferentially affected and these are predominantly located within the papillomacular bundle (164, 165). The peripapillary RNFL is swollen in the acute stage of LHON, as demonstrated by OCT, with subsequent thinning occurring as the disease progresses into the chronic stage. Measurement of ganglion cell and inner plexiform layer (GC-IPL) thickness in the macular area indicate that pathological thinning is already evident in the pre-symptomatic stage about 6 weeks before the onset of visual loss in the fellow eye (166). These findings suggest that midget RGCs, which are a major component of the papillomacular bundle, could be more vulnerable to the underlying mtDNA

FIGURE 5 | Pattern of RGC involvement in optic neuropathies. The types of RGCs affected in inherited optic neuropathies and acquired optic neuropathies are indicated by black and red lines, respectively. The dotted green line indicates the preservation of ipRGCs in inherited optic neuropathies. ADOA, autosomal dominant optic atrophy; FDT, frequency doubling technology; ipRGCs, intrinsically photosensitive retinal ganglion cells; LHON, Leber hereditary optic neuropathy; mRGCs, midget retinal ganglion cells; pRGCs, parasol retinal ganglion cells; sbRGCs, small bistratified retinal ganglion cells; smRGCs, smooth monostratified RGCs; SWAP, short wavelength automated perimetry (*by Ungsoo S. Kim*).

mutation. Selective attenuation of four of the six layers in the LGN that are connected to the parvocellular pathway have been reported, but this feature is controversial as the magnocellular pathway is known to be also affected in LHON (167, 168). Further investigations are needed to determine the primary defect.

The ipRGC subtype is relatively preserved in LHON, explaining why the pupillary light reflex is maintained even in severely affected patients (138). The mechanisms that account for this enhanced resilience of ipRGCs remain unclear, although several hypotheses have been proposed (140). From an anatomical perspective, ipRGCs are predominantly located in the parafoveal area and at the far end of the nasal hemiretina, rather than feeding into the papillomacular bundle (92). In a post mortem study of a patient carrying the m.3460G>A mtDNA mutation, the pupillary fibres in the pretectum were found to be preserved (169). It is possible that ipRGCs are protected because of their higher concentration of mitochondrial cytochrome *c* oxidase and a greater abundance of mitochondria (140). Several protective factors such as PI3K and pituitary adenylate cyclase-activating polypeptide (PACAP) may further reinforce the survival of ipRGCs under certain conditions (170, 171).

(2) Autosomal Dominant Optic Atrophy

ADOA is the most common inherited optic neuropathy with an estimated prevalence of 1 in 25,000 in the general population (172). Mutations in the nuclear gene *OPA1* (3q28-q29) account

for ~70% of all cases of ADOA (173). The classical clinical features of ADOA are progressive bilateral visual loss starting in early childhood, dyschromatopsia, a central or cecocentral scotoma, and optic disc pallor that is more prominent temporally due to the preferential involvement of the papillomacular bundle (174). There is a marked variability in disease severity with visual acuity ranging from 6/6 to light perception, and variable rates of disease progression even within the same family (175). OCT typically shows RNFL thinning, which is more marked temporally, with gradual loss of RGCs occurring over time (176). The disease process is thought to start *in utero* with *OPA1* carriers having a reduced number of RGCs at birth compared with normal healthy individuals (138).

In ADOA, midget RGCs, parasol RGCs and small bistratified RGCs are all affected, impairing sensitivity to high spatial frequencies, long- and middle-wave colour discrimination, sensitivity to high temporal frequencies, and short-wave sensitivity. The S-cone–related losses showed a significant deterioration with increasing patient age and could therefore prove useful biomarkers of disease progression in ADOA (177). The S-cone chromatic response and koniocellular pathway are impaired in the early stage of the disease, which suggest a vulnerability of small bistratified RGCs (173). Although tritanopia has been reported as the characteristic colour vision defect in ADOA, only 7.5% of patients with ADOA had exclusively tritanopia in one study, with the most common

colour defect in 81.2% of patients being of the mixed type (134).

As in LHON, the pupillary response in ADOA is relatively preserved, indicating that ipRGCs in mitochondrial optic neuropathies appear to be more resistant to the underlying mitochondrial dysfunction compared with other RGC subtypes. Studies using chromatic pupillometry also reported preservation of ipRGCs in ADOA patients with severe visual loss and optic atrophy (178, 179).

Acquired Optic Neuropathies

There is a long list of aetiological factors that can result in RGC injury and optic nerve degeneration. Compared with inherited optic neuropathies, fewer studies have focused specifically on RGC pathophysiology in acquired optic neuropathies. More work is, therefore, needed to elucidate subtype selectivity, if any, of RGC loss in ischemic, compressive, inflammatory, autoimmune and paraneoplastic optic neuropathies. However, we do know that most toxic optic neuropathies have an underlying mitochondrial aetiology (180). There is a growing body of evidence that mitochondrial dysfunction plays a prominent pathophysiological role in glaucoma, demyelinating optic neuritis and toxic optic neuropathies (181, 182). This aetiological link is relevant and comparing the pattern of RGC loss between these acquired optic neuropathies and classical monogenic optic neuropathies could reveal common pathways amenable to therapeutic intervention.

(1) Glaucoma

Glaucoma is a leading cause of irreversible blindness affecting 3–5% of the population over the age of 70 years (183). Extrafoveal RGCs usually deteriorate in the early stages resulting in arcuate scotomas in the visual field. Traditional anatomical studies reported greater loss of axons of large diameter, corresponding to the magnocellular pathway (parasol cells) (184), and the magnocellular LGN layers were more affected compared with the parvocellular LGN layers (185). However, there are rarer types of retinal ganglion cells with large axons and further investigations are needed to evaluate the changes of these cells in glaucoma. The relative vulnerability of large axons in glaucoma may simply reflect the anatomical location of the affected ganglion cells. Glaucoma patients have poor response to high temporal frequency light stimuli that correspond to the magnocellular pathway. In a primate study using immunohistochemistry, a decrease in large RGCs was observed after elevating IOP (186). This specific vulnerability was ascribed to calcium-permeable receptors, the relative proximity of RGCs and their dendrites to blood supply in the IPL layer, and the differing metabolic requirements of these particular large cell types (187). However, other studies suggested no predilection for a specific pathway (188, 189). Compared with inherited optic neuropathies, the ipRGCs are vulnerable in both patients with confirmed glaucoma and glaucoma suspects (190, 191). In contrast, ocular hypertension does not seem to result in significant loss of ipRGCs (192).

(2) Demyelinating Optic Neuritis

Inflammatory demyelination resulting in optic neuritis is a major manifestation of multiple sclerosis. Inflammation of the retinal vascular endothelium can precede demyelination and perivascular cuffing and oedema of the optic nerve sheath leads to breakdown of myelin (193). Idiopathic demyelinating optic neuritis leads to visual loss with minimal axonal loss.

Optic neuritis is associated with alteration of both the parvocellular and magnocellular pathways (194). Viret et al. suggested that the more heavily myelinated magnocellular axons are more vulnerable in patients with optic neuritis because low spatial frequencies, which are transmitted by the magnocellular pathway, are affected predominantly 1 month after the acute phase of the optic neuritis episode (195). Despite the recovery of visual acuity, the magnocellular pathway did not fully normalise (196). In contrast, a significant loss at high spatial frequencies has been reported in the affected eye and the parvocellular pathway was more impaired in patients with resolved optic neuritis who had 20/20 visual acuity after recovery (197). Fallowfield and Krauskopf suggested that chromatic discrimination is more severely impaired than luminance discrimination in the demyelinating diseases (198). This discrepancy might be due to differences in the timing and severity of optic neuritis. Consequently, it is still unclear which pathway is more vulnerable in the context of demyelinating optic neuritis (196). Both red-green and tritan defects have been reported in optic neuritis (199). Characteristics of colour deficiency may change over time as assessed with the FM 100-hue test, with blue-yellow defects being more common in the acute stage and red-green changes being predominant in the chronic stage (200). It is possible, of course, that the variability of symptoms in optic neuritis reflects immunologically distinct conditions that differentially affect different types of RGCs.

(3) Toxic Optic Neuropathy

Various substances such as ethambutol, isoniazid, linezolid, chloramphenicol and methanol can cause optic nerve dysfunction, probably through acquired mitochondrial dysfunction (180). As in inherited optic neuropathies, the papillomacular bundle is selectively vulnerable and this typical feature can be confirmed by optical coherence tomography, which shows a profound decrease in temporal RNFL thickness. The parvocellular pathway within the papillomacular bundle is affected extensively likely secondary to a number of factors, including smaller and more thinly myelinated nerve fibres and a faster firing response with higher average rates of action potentials (201). However, there is a lack of evidence on whether this is simply because the parvocellular neurons predominate in the papillomacular bundle, or whether the midget cells are the primary target of the triggering toxic substances.

Clinical Relevance and Future Work

The physiological features of the major RGC subtypes (mRGCs, pRGCs, and sbRGCs) are well-known, but the role and characteristics of other RGCs require further study. An in-depth characterisation of the chronological structural and functional changes occurring within the RGC layer in optic nerve disorders, including inherited and acquired optic neuropathies, are important to inform the future design of clinical trials. Understanding which RGC subtypes are selectively affected will help optimise outcome measures in natural history studies and

trials of experimental therapies. As mentioned earlier, the FDT test is used for the early detection of glaucoma because the magnocellular pathway is more vulnerable (127). Given that a common variant in the *SIX6* gene (rs33912345) is strongly associated with primary open-angle glaucoma (POAG) and the fact that this gene is highly expressed in midget RGCs, tests that evaluate this particular cell type could prove to be a useful sensitive biomarker of disease progression (19, 202).

The remarkable advances in gene delivery and editing technology have led to an increasing number of clinical trials for optic neuropathies, in particular gene replacement therapy for monogenic inherited optic neuropathies (203). Gene therapy using adeno-associated viral vectors is currently favoured and there is now cumulative evidence of its long-term safety and efficacy in delivering gene constructs to retinal cells (204, 205). Promising results have been obtained with allotopic expression of the *MT-DN4* gene in patients with LHON treated within 1 year of disease onset (206, 207). To enhance success of gene therapy, optimised tissue-specific promoters, which control expression of the therapeutic gene, are needed, and these could potentially. be optimised for the relevant RGC subtype (208). Genomic editing, such as the CRISPR-Cas system, and stem cell therapy is an exciting development that has the potential to revolutionise the treatment of ophthalmological disorders given the eye's relative ease of anatomical access and its relative immune privilege (209, 210). The intriguing preservation of ipRGCs in mitochondrial optic neuropathies needs to be investigated further as the factors that confer this resilience would be obvious therapeutic targets (211).

There is increasing interest in employing RGCs to restore visual function in the retinal dystrophies marked by widespread loss of rods and cones (212). Optogenetic therapies are being developed to confer light sensitivity to inner retinal neurons, which are spared in these forms of outer retinal degeneration. Another approach is the use of electronic implants to stimulate these inner retinal neurons so that visual signals can be transmitted to the brain. A better understanding of inner retinal connectivity, specifically that of RGCs, is essential to optimise these innovative sight restoring strategies. Elucidating the selective vulnerability of RGCs compared with other retinal and neuronal cell types in inherited optic neuropathies is key to developing targeted treatments for this group of disorders. The availability of high-throughput transcriptomic techniques that can be conducted at the single cell level is an exciting development, providing us with powerful tools to identify pathways that can be modulated for generalizable, mutation-independent neuroprotective strategies (213). Although appealing, regenerative medicine will require not only the replacement of the missing RGCs, but also the establishment of the sophisticated circuitry that allows the integration of signals from various pathways to achieve a reasonable degree of visual perception (214).

CONCLUSION

Ganglion cells constitute the output pathway of the retina, transmitting highly processed and integrated signals to the visual processing areas in the brain. Up to 18 types of RGCs have been reported, constituting a sophisticated repertoire of cell types each with specific attributes contributing to visual perception. Future studies will further dissect the selectivity and timing of impairment of RGC subtypes in various optic neuropathies and how these could be modulated in the context of experimental therapies. The refinement of tests to assess RGC structure and function is relevant not only for clinical practise, but also for deep phenotyping as part of natural history studies and to define relevant outcome measures for clinical trials. We are now entering an exciting translational phase for optic neuropathies with the confluence of genetic breakthroughs and targeted therapies giving hope that we will soon be able to slow or prevent the irreversible loss of RGCs in these blinding diseases.

AUTHOR CONTRIBUTIONS

UK, PY-W-M, and JM contributed to the conception and design of the study. UK wrote the first draft of the manuscript. UK, PY-W-M, JM, and OM wrote sections of the manuscript. All authors contributed to manuscript revision, read, and approved the submitted version.

FUNDING

REFERENCES

1. Carroll JJ. *In Honor of Julian John Chisolm MD*. Baltimore, MD: University of Maryland (1930).

2. Chisholm JJ. Colour blindness, an effect of neuritis. *Ophthal Hosp Rep.* (1869) 6:214–15.

3. Bonnet C. *Essai de Psychologie; ou Considérations sur les Opérations de l'Âme, sur l'Habitude et sur l'Éducation*. London (1755).

4. Palmer G. *Théorie de la Lumière, Applicable Aux Arts, et Principalement à la Peinture*. Paris: Hardouin et Gattey (1786).

5. Sanes JR, Masland RH. The types of retinal ganglion cells: current status and implications for neuronal classification. *Annu Rev Neurosci.* (2015) 38:221–46. doi: 10.1146/annurev-neuro-071714-034120

6. Dacey DM. Origins of perception: retinal ganglion cell diversity and the creation of parallel visual pathways. In: Gazzaniga MS, editor. *The Cognitive Neurosciences*. Cambridge, MA: MIT (2004). pp. 281–301.

7. Yamada ES, Bordt AS, Marshak DW. Wide-field ganglion cells in macaque retinas. *Visual Neurosci.* (2005) 22:383–93. doi: 10.1017/S095252380522401X

8. Masri RA, Percival KA, Koizumi A, Martin PR, Grunert U. Survey of retinal ganglion cell morphology in marmoset. *J Comp Neurol.* (2019) 527:236–58. doi: 10.1002/cne.24157

9. Diamond JS. Inhibitory interneurons in the retina: types, circuitry, and function. *Annu Rev Vis Sci.* (2017) 3:1–24. doi: 10.1146/annurev-vision-102016-061345

10. Fu Y, Yau KW. Phototransduction in mouse rods and cones. *Pflugers Arch.* (2007) 454:805–19. doi: 10.1007/s00424-006-0194-y

11. Tsukamoto Y, Omi N. Classification of mouse retinal bipolar cells: type-specific connectivity with special reference to rod-driven AII amacrine pathways. *Front Neuroanat.* (2017) 11:92. doi: 10.3389/fnana.2017.00092

12. Kolb H, Nelson R, Mariani A. Amacrine cells, bipolar cells and ganglion cells of the cat retina: a Golgi study. *Vision Res.* (1981) 21:1081–114. doi: 10.1016/0042-6989(81)90013-4

13. MacNeil MA, Heussy JK, Dacheux RF, Raviola E, Masland RH. The population of bipolar cells in the rabbit retina. *J Comp Neurol.* (2004) 472:73–86. doi: 10.1002/cne.20063

14. Tsukamoto Y, Omi N. OFF bipolar cells in macaque retina: type-specific connectivity in the outer and inner synaptic layers. *Front Neuroanat.* (2015) 9:122. doi: 10.3389/fnana.2015.00122

15. Rockhill RL, Daly FJ, MacNeil MA, Brown SP, Masland RH. The diversity of ganglion cells in a mammalian retina. *J Neurosci.* (2002) 22:3831–43. doi: 10.1523/JNEUROSCI.22-09-03831.2002

16. Tran NM, Shekhar K, Whitney IE, Jacobi A, Benhar I, Hong G, et al. Single-cell profiles of retinal ganglion cells differing in resilience to injury reveal neuroprotective genes. *Neuron.* (2019) 104:1039–55 e12. doi: 10.1016/j.neuron.2019.11.006

17. Rheaume BA, Jereen A, Bolisetty M, Sajid MS, Yang Y, Renna K, et al. Single cell transcriptome profiling of retinal ganglion cells identifies cellular subtypes. *Nat Commun.* (2018) 9:2759. doi: 10.1038/s41467-018-05792-3

18. Baden T, Euler T, Berens P. Understanding the retinal basis of vision across species. *Nat Rev.* (2020) 21:5–20. doi: 10.1038/s41583-019-0242-1

19. Peng YR, Shekhar K, Yan W, Herrmann D, Sappington A, Bryman GS, et al. Molecular classification and comparative taxonomics of foveal and peripheral cells in primate retina. *Cell.* (2019) 176:1222–37 e22. doi: 10.1016/j.cell.2019.01.004

20. Yan W, Peng YR, van Zyl T, Regev A, Shekhar K, Juric D, et al. Cell atlas of the human fovea and peripheral retina. *Sci Rep.* (2020) 10:9802. doi: 10.1038/s41598-020-66092-9

21. Vlasits AL, Euler T, Franke K. Function first: classifying cell types and circuits of the retina. *Curr Opin Neurobiol.* (2019) 56:8–15. doi: 10.1016/j.conb.2018.10.011

22. Vrabec F. "Displaced nerve cells" in the human retina. *Graefes Arch Clin Exp Ophthalmol.* (1986) 224:143–6. doi: 10.1007/BF02141487

23. Polyak SL. *The Retina.* Chicago, IL: University of Chicago Press (1941).

24. Poljak S. Structure of the retina in primates. *Acta Ophthalmol.* (1935) 13:52–60. doi: 10.1111/j.1755-3768.1935.tb04189.x

25. Sadun AA, Schaechter JD, Smith LE. A retinohypothalamic pathway in man: light mediation of circadian rhythms. *Brain Res.* (1984) 302:371–7. doi: 10.1016/0006-8993(84)90252-X

26. Schaechter JD, Sadun AA. A second hypothalamic nucleus receiving retinal input in man: the paraventricular nucleus. *Brain Res.* (1985) 340:243–50. doi: 10.1016/0006-8993(85)90920-5

27. Sadun AA. Vision: a multimodal sense. *Bull Clin Neurosci.* (1985) 50:61–8.

28. Frazao R, Pinato L, da Silva AV, Britto LR, Oliveira JA, Nogueira MI. Evidence of reciprocal connections between the dorsal raphe nucleus and the retina in the monkey *Cebus apella. Neurosci Lett.* (2008) 430:119–23. doi: 10.1016/j.neulet.2007.10.032

29. Cowey A, Stoerig P, Bannister M. Retinal ganglion cells labelled from the pulvinar nucleus in macaque monkeys. *Neuroscience.* (1994) 61:691–705. doi: 10.1016/0306-4522(94)90445-6

30. Rodieck RW, Watanabe M. Survey of the morphology of macaque retinal ganglion cells that project to the pretectum, superior colliculus, and parvicellular laminae of the lateral geniculate nucleus. *J Comp Neuol.* (1993) 338:289–303. doi: 10.1002/cne.903380211

31. Polyak S. Retinal structure and colour vision. *Documenta Ophthalmol.* (1949) 3:24–46. doi: 10.1007/BF00162597

32. Kang HW, Kim HK, Moon BH, Lee SJ, Lee SJ, Rhyu IJ. Comprehensive review of Golgi staining methods for nervous tissue. *Appl Microsc.* (2017) 47:63–9. doi: 10.9729/AM.2017.47.2.63

33. Sharma RK, Netland PA. Early born lineage of retinal neurons express class III beta-tubulin isotype. *Brain Res.* (2007) 1176:11–7. doi: 10.1016/j.brainres.2007.07.090

34. Johnson TV, DeKorver NW, Levasseur VA, Osborne A, Tassoni A, Lorber B, et al. Identification of retinal ganglion cell neuroprotection conferred by platelet-derived growth factor through analysis of the mesenchymal stem cell secretome. *Brain.* (2014) 137:503–19. doi: 10.1093/brain/awt292

35. Sherry DM, Mitchell R, Standifer KM, B. du Plessis, Distribution of plasma membrane-associated syntaxins 1 through 4 indicates distinct trafficking functions in the synaptic layers of the mouse retina. *BMC Neurosci.* (2006) 7:54. doi: 10.1186/1471-2202-7-54

36. Sarthy PV, Fu M, Huang J. Developmental expression of the glial fibrillary acidic protein (GFAP) gene in the mouse retina. *Cell Mol Neurobiol.* (1991) 11:623–37. doi: 10.1007/BF00741450

37. Noristani R, Kuehn S, Stute G, Reinehr S, Stellbogen M, Dick HB, et al. Retinal and optic nerve damage is associated with early glial responses in an experimental autoimmune glaucoma model. *J Mol Neurosci.* (2016) 58:470–82. doi: 10.1007/s12031-015-0707-2

38. Majander A, Bowman R, Poulton J, Antcliff RJ, Reddy MA, Michaelides M, et al. Childhood-onset Leber hereditary optic neuropathy. *Br J Ophthalmol.* (2017) 101:1505–9. doi: 10.1136/bjophthalmol-2016-310072

39. Huang W, Fileta J, Guo Y, Grosskreutz CL. Downregulation of Thy1 in retinal ganglion cells in experimental glaucoma. *Curr Eye Res.* (2006) 31:265–71. doi: 10.1080/02713680500545671

40. Kovacs-Oller T, Szarka G, Tengolics AJ, Ganczer A, Balogh B, Szabo-Meleg E, et al. Spatial expression pattern of the major Ca(2+)-buffer proteins in mouse retinal ganglion cells. *Cells.* (2020) 9. doi: 10.20944/preprints202002.0145.v1

41. Jakobs TC, Ben Y, Masland RH. CD15 immunoreactive amacrine cells in the mouse retina. *J Comp Neurol.* (2003) 465:361–71. doi: 10.1002/cne.10845

42. Lee EJ, Shon WH, Kim IB, Kwon SO, Oh SJ, Chun MH. Localization of CD15 immunoreactivity in the rat retina. *Cell Tissue Res.* (2002) 310:131–6. doi: 10.1007/s00441-002-0620-1

43. Pereiro X, Ruzafa N, Urcola JH, Sharma SC, Vecino E. Differential distribution of RBPMS in pig, rat, and human retina after damage. *Int J Mol Sci.* (2020) 21:9330. doi: 10.3390/ijms21239330

44. Rodriguez AR, de Sevilla Muller LP, Brecha NC. The RNA binding protein RBPMS is a selective marker of ganglion cells in the mammalian retina. *J Comp Neurol.* (2014) 522:1411–43. doi: 10.1002/cne.23521

45. Masri RA, Grunert U, Martin PR. Analysis of parvocellular and magnocellular visual pathways in human retina. *J Neurosci.* (2020) 40:8132–48. doi: 10.1523/JNEUROSCI.1671-20.2020

46. Mead B, Thompson A, Scheven BA, Logan A, Berry M, Leadbeater W. Comparative evaluation of methods for estimating retinal ganglion cell loss in retinal sections and wholemounts. *PLoS ONE.* (2014) 9:e110612. doi: 10.1371/journal.pone.0110612

47. Soto F, Hsiang JC, Rajagopal R, Piggott K, Harocopos GJ, Couch SM, et al. Efficient coding by midget and parasol ganglion cells in the human retina. *Neuron.* (2020) 107:656–66 e5. doi: 10.1016/j.neuron.2020.05.030

48. Langer KB, Ohlemacher SK, Phillips MJ, Fligor CM, Jiang P, Gamm DM, et al. Retinal ganglion cell diversity and subtype specification from human pluripotent stem cells. *Stem Cell Rep.* (2018) 10:1282–93. doi: 10.1016/j.stemcr.2018.02.010

49. Ghosh KK, Goodchild AK, Sefton AE, Martin PR. Morphology of retinal ganglion cells in a new world monkey, the marmoset *Callithrix jacchus. J Comp Neurol.* (1996) 366:76–92.

50. Mao CA, Li H, Zhang Z, Kiyama T, Panda S, Hattar S, et al. T-box transcription regulator Tbr2 is essential for the formation and maintenance of Opn4/melanopsin-expressing intrinsically photosensitive retinal ganglion cells. *J Neurosci.* (2014) 34:13083–95. doi: 10.1523/JNEUROSCI.1027-14.2014

51. Hughes S, Jagannath A, Rodgers J, Hankins MW, Peirson SN, Foster RG. Signalling by melanopsin (OPN4) expressing photosensitive retinal ganglion cells. *Eye.* (2016) 30:247–54. doi: 10.1038/eye.2015.264

52. Stiles WS. Mechanism concepts in colour theory. *J Colour Group.* (1967) 1:106–23.

53. Graham N, Robson JG, Nachmias J. Grating summation in fovea and periphery. *Vis Res.* (1978) 18:815–25. doi: 10.1016/0042-6989(78)90122-0

54. Pokorny J. Review: steady and pulsed pedestals, the how and why of post-receptoral pathway separation. *J Vis.* (2011) 11:1–23. doi: 10.1167/11.5.7

55. Johnson CA, Samuels SJ. Screening for glaucomatous visual field loss with frequency-doubling perimetry. *Invest Ophthalmol Vis Sci.* (1997) 38:413–25.

56. Kuffler SW. Discharge patterns and functional organization of mammalian retina. *J Neurophysiol.* (1953) 16:37–68. doi: 10.1152/jn.1953.16.1.37

57. Gouras P. Identification of cone mechanisms in monkey ganglion cells. *J Physiol.* (1968) 199:533–47. doi: 10.1113/jphysiol.1968.sp008667

58. Stiles WS. Color vision: the approach through increment threshold sensitivity. *Proc Natl Acad Sci USA.* (1959) 45:100–114. doi: 10.1073/pnas.45.1.100

59. Field GD, Gauthier JL, Sher A, Greschner M, Machado TA, Jepson LH, et al. Functional connectivity in the retina at the resolution of photoreceptors. *Nature.* (2010) 467:673–7. doi: 10.1038/nature09424

60. McGregor JE, Godat T, Dhakal KR, Parkins K, Strazzeri JM, Bateman BA, et al. Optogenetic restoration of retinal ganglion cell activity in the living primate. *Nat Commun.* (2020) 11:1703. doi: 10.1038/s41467-020-15317-6

61. Houchin J. Procion Yellow electrodes for intracellular recording and staining of neurones in the somatosensory cortex of the rat. *J Physiol.* (1973) 232:67–9P.

62. Nelson R, Famiglietti EV Jr, Kolb H. Intracellular staining reveals different levels of stratification for on- and off-center ganglion cells in cat retina. *J Neurophysiol.* (1978) 41:472–83. doi: 10.1152/jn.1978.41.2.472

63. Dacey DM, Lee BB. The 'blue-on' opponent pathway in primate retina originates from a distinct bistratified ganglion cell type. *Nature.* (1994) 367:731–5. doi: 10.1038/367731a0

64. Dacey DM, Peterson BB, Robinson FR, Gamlin PD. Fireworks in the primate retina: *in vitro* photodynamics reveals diverse LGN-projecting ganglion cell types. *Neuron.* (2003) 37:15–27. doi: 10.1016/S0896-6273(02)01143-1

65. Moritoh S, Komatsu Y, Yamamori T, Koizumi A. Diversity of retinal ganglion cells identified by transient GFP transfection in organotypic tissue culture of adult marmoset monkey retina. *PLoS ONE.* (2013) 8:e54667. doi: 10.1371/journal.pone.0054667

66. Dacey DM. The mosaic of midget ganglion cells in the human retina. *J Neurosci.* (1993) 13:5334–55. doi: 10.1523/JNEUROSCI.13-12-05334.1993

67. Yamada ES, Silveira LC, Perry VH. Morphology, dendritic field size, somal size, density, and coverage of M and P retinal ganglion cells of dichromatic Cebus monkeys. *Vis Neurosci.* (1996) 13:1011–29. doi: 10.1017/S0952523800007677

68. Kling A, Field GD, Brainard DH, Chichilnisky EJ. Probing computation in the primate visual system at single-cone resolution. *Annu Rev Neurosci.* (2019) 42:169–86. doi: 10.1146/annurev-neuro-070918-050233

69. Wiesel TN, Hubel DH. Spatial and chromatic interactions in the lateral geniculate body of the rhesus monkey. *J Neurophysiol.* (1966) 29:1115–56. doi: 10.1152/jn.1966.29.6.1115

70. Wool LE, Packer OS, Zaidi Q, Dacey DM. Connectomic identification and three-dimensional color tuning of S-OFF midget ganglion cells in the primate retina. *J Neurosci.* (2019) 39:7893–909. doi: 10.1523/JNEUROSCI.0778-19.2019

71. Schiller PH. Parallel information processing channels created in the retina. *Proc Natl Acad Sci USA.* (2010) 107:17087–94. doi: 10.1073/pnas.1011782107

72. Jacoby R, Stafford D, Kouyama N, Marshak D. Synaptic inputs to ON parasol ganglion cells in the primate retina. *J Neurosci.* (1996) 16:8041–56. doi: 10.1523/JNEUROSCI.16-24-08041.1996

73. Kaplan E, Shapley RM. The primate retina contains two types of ganglion cells, with high and low contrast sensitivity. *Proc Natl Acad Sci USA.* (1986) 83:2755–7. doi: 10.1073/pnas.83.8.2755

74. Dacey DM, Packer OS. Colour coding in the primate retina: diverse cell types and cone-specific circuitry. *Curr Opin Neurobiol.* (2003) 13:421–7. doi: 10.1016/S0959-4388(03)00103-X

75. Crook JD, Peterson BB, Packer OS, Robinson FR, Gamlin PD, Troy JB, et al. The smooth monostratified ganglion cell: evidence for spatial diversity in the Y-cell pathway to the lateral geniculate nucleus and

76. Rhoades CE, Shah NP, Manookin MB, Brackbill N, Kling A, Goetz G, et al. Unusual physiological properties of smooth monostratified ganglion cell types in primate retina. *Neuron.* (2019) 103:658–72 e6. doi: 10.1016/j.neuron.2019.05.036

77. Grunert U, Martin PR. Cell types and cell circuits in human and non-human primate retina. *Prog Retin Eye Res.* (2020) 78:100844. doi: 10.1016/j.preteyeres.2020.100844

78. Detwiler PB, Crook JD, Robinson F, Dacey DM. The recursive bistratified ganglion cell type of the macaque monkey retina is ON-OFF direction selective [ARVO Annual Meeting Abstract]. *Invest Ophth Vis Sci.* (2019) 60:3884.

79. Dacey DM, Kim YJ, Packer OS, Detwiler PB. ON-OFF direction selective ganglion cells in macaque monkey retina are tracer-coupled to an ON-OFF direction selective amacrine cell type. *Invest Ophth Vis Sci.* (2019) 60:5280.

80. Dacey D, Kim Y, Packer O, Detwiler, PB. ON-OFF direction selective ganglion cells in macaque monkey retina are tracer-coupled to an ON-OFF direction selective amacrine cell type. In: *ARVO Annual Meeting IOVS.* Vancouver, BC (2019).

81. Peterson BB, Dacey DM. Morphology of wide-field bistratified and diffuse human retinal ganglion cells. *Vis Neurosci.* (2000) 17:567–78. doi: 10.1017/S0952523800174073

82. Puller C, Manookin MB, Neitz J, Rieke F, Neitz M. Broad thorny ganglion cells: a candidate for visual pursuit error signaling in the primate retina. *J Neurosci.* (2015) 35:5397–408. doi: 10.1523/JNEUROSCI.4369-14.2015

83. Nasir-Ahmad S, Lee SCS, Martin PR, Grunert U. Identification of retinal ganglion cell types expressing the transcription factor Satb2 in three primate species. *J Comp Neurol.* (2021). doi: 10.1002/cne.25120. [Epub ahead of print].

84. Munch M, Kawasaki A. Intrinsically photosensitive retinal ganglion cells: classification, function and clinical implications. *Curr Opin Neurol.* (2013) 26:45–51. doi: 10.1097/WCO.0b013e32835c5e78

85. Schmidt TM, Chen SK, Hattar S. Intrinsically photosensitive retinal ganglion cells: many subtypes, diverse functions. *Trends Neurosci.* (2011) 34:572–80. doi: 10.1016/j.tins.2011.07.001

86. Chen SK, Badea TC, Hattar S. Photoentrainment and pupillary light reflex are mediated by distinct populations of ipRGCs. *Nature.* (2011) 476:92–5. doi: 10.1038/nature10206

87. Baver SB, Pickard GE, Sollars PJ, Pickard GE. Two types of melanopsin retinal ganglion cell differentially innervate the hypothalamic suprachiasmatic nucleus and the olivary pretectal nucleus. *Eur J Neurosci.* (2008) 27:1763–70. doi: 10.1111/j.1460-9568.2008.06149.x

88. Hannibal J, Christiansen AT, Heegaard S, Fahrenkrug J, Kiilgaard JF. Melanopsin expressing human retinal ganglion cells: subtypes, distribution, intraretinal connectivity. *J Comp Neurol.* (2017) 525:1934–61. doi: 10.1002/cne.24181

89. Liao HW, Ren X, Peterson BB, Marshak DW, Yau KW, Gamlin PD, et al. Melanopsin-expressing ganglion cells on macaque and human retinas form two morphologically distinct populations. *J Comp Neurol.* (2016) 524:2845–72. doi: 10.1002/cne.23995

90. Patterson SS, Kuchenbecker JA, Anderson JR, Neitz M, Neitz J. A color vision circuit for non-image-forming vision in the primate retina. *Curr Biol.* (2020) 30:1269–74 e2. doi: 10.1016/j.cub.2020.01.040

91. Patterson SS, Mazzaferri MA, Bordt AS, Chang J, Neitz M, Neitz J. Another blue-ON ganglion cell in the primate retina. *Curr Biol.* (2020) 30:R1409–10. doi: 10.1016/j.cub.2020.10.010

92. La Morgia C, Ross-Cisneros FN, Sadun AA, Hannibal J, Munarini A, Mantovani V, et al. Melanopsin retinal ganglion cells are resistant to neurodegeneration in mitochondrial optic neuropathies. *Brain.* (2010) 133:2426–38. doi: 10.1093/brain/awq155

93. Georg B, Ghelli A, Giordano C, Ross-Cisneros FN, Sadun AA, Carelli V, et al. Melanopsin-expressing retinal ganglion cells are resistant to cell injury, but not always. *Mitochondrion.* (2017) 36:77–84. doi: 10.1016/j.mito.2017.04.003

94. Moura AL, Nagy BV, La Morgia C, Barboni P, Oliveira AG, Salomao SR, et al. The pupil light reflex in Leber's hereditary optic neuropathy: evidence for preservation of melanopsin-expressing retinal ganglion cells. *Invest Ophthalmol Vis Sci.* (2013) 54:4471–7. doi: 10.1167/iovs.12-11137

95. Joyce DS, Feigl B, Kerr G, Roeder L, Zele AJ. Melanopsin-mediated pupil function is impaired in Parkinson's disease. *Sci Rep.* (2018) 8:7796. doi: 10.1038/s41598-018-26078-0

96. Garcia-Martin E, Satue M, Fuertes I, Otin S, Alarcia R, Herrero R, et al. Ability and reproducibility of Fourier-domain optical coherence tomography to detect retinal nerve fiber layer atrophy in Parkinson's disease. *Ophthalmology.* (2012) 119:2161–7. doi: 10.1016/j.ophtha.2012.05.003

97. Hong S, Kim CY, Lee WS, Seong GJ. Reproducibility of peripapillary retinal nerve fiber layer thickness with spectral domain cirrus high-definition optical coherence tomography in normal eyes. *Jpn J Ophthalmol.* (2010) 54:43–7. doi: 10.1007/s10384-009-0762-8

98. Sabour S, Naderi M, Jalalvandi F. Precision of optic nerve head and retinal nerve fiber layer parameter measurements by spectral-domain optical coherence tomography: methodological issues on reproducibility. *J Glaucoma.* (2018) 27:e95. doi: 10.1097/IJG.0000000000000926

99. Jeoung JW, Choi YJ, Park KH, Kim DM. Macular ganglion cell imaging study: glaucoma diagnostic accuracy of spectral-domain optical coherence tomography. *Invest Ophthalmol Vis Sci.* (2013) 54:4422–9. doi: 10.1167/iovs.12-11273

100. Jeong JH, Choi YJ, Park KH, Kim DM, Jeoung JW. Macular ganglion cell imaging study: covariate effects on the spectral domain optical coherence tomography for glaucoma diagnosis. *PLoS ONE.* (2016) 11:e0160448. doi: 10.1371/journal.pone.0160448

101. Mwanza JC, Warren JL, Budenz DL, G. Ganglion Cell Analysis Study, Combining spectral domain optical coherence tomography structural parameters for the diagnosis of glaucoma with early visual field loss. *Invest Ophthalmol Vis Sci.* (2013) 54:8393–400. doi: 10.1167/iovs.13-12749

102. Penteado RC, Zangwill LM, Daga FB, Saunders LJ, Manalastas PIC, Shoji T, et al. Optical coherence tomography angiography macular vascular density measurements and the central 10-2 visual field in glaucoma. *J Glaucoma.* (2018) 27:481–9. doi: 10.1097/IJG.0000000000000964

103. Parrozzani R, Miglionico G, Leonardi F, Pulze S, Trevisson E, Clementi M, et al. Correlation of peripapillary retinal nerve fibre layer thickness with visual acuity in paediatric patients affected by optic pathway glioma. *Acta Ophthalmol.* (2018) 96:e1004–9. doi: 10.1111/aos.13803

104. Chen JJ, Kardon RH. Avoiding clinical misinterpretation and artifacts of optical coherence tomography analysis of the optic nerve, retinal nerve fiber layer, and ganglion cell layer. *J Neuroophthalmol.* (2016) 36:417–38. doi: 10.1097/WNO.0000000000000422

105. Kanamori A, Nakamura M, Yamada Y, Negi A. Longitudinal study of retinal nerve fiber layer thickness and ganglion cell complex in traumatic optic neuropathy. *Arch Ophthalmol.* (2012) 130:1067–9. doi: 10.1001/archophthalmol.2012.470

106. Mwanza JC, Budenz DL, Warren JL, Webel AD, Reynolds CE, Barbosa DT, et al. Retinal nerve fibre layer thickness floor and corresponding functional loss in glaucoma. *Br J Ophthalmol.* (2015) 99:732–7. doi: 10.1136/bjophthalmol-2014-305745

107. Bowd C, Zangwill LM, Weinreb RN, Medeiros FA, Belghith A. Estimating optical coherence tomography structural measurement floors to improve detection of progression in advanced glaucoma. *Am J Ophthalmol.* (2017) 175:37–44. doi: 10.1016/j.ajo.2016.11.010

108. Vuong LN. Hedges TR III, ganglion cell layer complex measurements in compressive optic neuropathy. *Curr Opin Ophthalmol.* (2017) 28:573–8. doi: 10.1097/ICU.0000000000000428

109. Higashiyama T, Nishida Y, Ohji M. Optical coherence tomography angiography in eyes with good visual acuity recovery after treatment for optic neuritis. *PLoS ONE.* (2017) 12:e0172168. doi: 10.1371/journal.pone.0172168

110. Lujan BJ, Horton JC. Microcysts in the inner nuclear layer from optic atrophy are caused by retrograde trans-synaptic degeneration combined with vitreous traction on the retinal surface. *Brain.* (2013) 136:e260. doi: 10.1093/brain/awt154

111. Abegg M, Dysli M, Wolf S, Kowal J, Dufour P, Zinkernagel M. Microcystic macular edema: retrograde maculopathy caused by optic neuropathy. *Ophthalmology.* (2014) 121:142–9. doi: 10.1016/j.ophtha.2013.08.045

112. Barboni P, Carelli V, Savini G, Carbonelli M, La Morgia C, Sadun AA. Microcystic macular degeneration from optic neuropathy: not inflammatory, not trans-synaptic degeneration. *Brain.* (2013) 136:e239. doi: 10.1093/brain/awt014

113. Carbonelli M, La Morgia C, Savini G, Cascavilla ML, Borrelli E, Chicani F, et al. Macular microcysts in mitochondrial optic neuropathies: prevalence and retinal layer thickness measurements. *PLoS ONE.* (2015) 10:e0127906. doi: 10.1371/journal.pone.0127906

114. Kisimbi J, Shalchi Z, Mahroo OA, Mhina C, Sanyiwa AJ, Mabey D, et al. Macular spectral domain optical coherence tomography findings in Tanzanian endemic optic neuropathy. *Brain.* (2013) 136:3418–26. doi: 10.1093/brain/awt221

115. Shalchi Z, Mahroo OA, Shunmugam M, Mohamed M, Sullivan PM, Williamson TH. Spectral domain optical coherence tomography findings in long-term silicone oil-related visual loss. *Retina.* (2015) 35:555–63. doi: 10.1097/IAE.0000000000000325

116. Yap TE, Davis BM, Guo L, Normando EM, Cordeiro MF. Annexins in glaucoma. *Int J Mol Sci.* (2018) 19:1218. doi: 10.3390/ijms19041218

117. Normando EM, Turner LA, Cordeiro MF. The potential of annexin-labelling for the diagnosis and follow-up of glaucoma. *Cell Tissue Res.* (2013) 353:279–85. doi: 10.1007/s00441-013-1554-5

118. Skottun BC. On the use of spatial frequency to isolate contributions from the magnocellular and parvocellular systems and the dorsal and ventral cortical streams. *Neurosci Biobehav Rev.* (2015) 56:266–75. doi: 10.1016/j.neubiorev.2015.07.002

119. Baraas RC, Pedersen HR, Hagen LA. Single-cone imaging in inherited and acquired colour vision deficiencies. *Curr Opin Behav Sci.* (2019) 30:55–59. doi: 10.1016/j.cobeha.2019.05.006

120. Simunovic MP. Acquired color vision deficiency. *Surv Ophthalmol.* (2016) 61:132–55. doi: 10.1016/j.survophthal.2015.11.004

121. Dain SJ. Clinical colour vision tests. *Clin Exp Optom.* (2004) 87:276–93. doi: 10.1111/j.1444-0938.2004.tb05057.x

122. Pokorny J, Smith VC, Verriest G, Pinckers JLG. *Congenital and Acquired Color Vision Defects.* New York, NY: Grune & Stratton (1979).

123. Mok KH, Lee VW. Nerve fiber analyzer and short-wavelength automated perimetry in glaucoma suspects: a pilot study. *Ophthalmology.* (2000) 107:2101–4. doi: 10.1016/S0161-6420(00)00378-X

124. Riordan-Eva P. Clinical assessment of optic nerve disorders. *Eye.* (2004) 18:1161–8. doi: 10.1038/sj.eye.6701575

125. Fan X, Wu LL, Ma ZZ, Xiao GG, Liu F Jr. Usefulness of frequency-doubling technology for perimetrically normal eyes of open-angle glaucoma patients with unilateral field loss. *Ophthalmology.* (2010) 117:1530–7 e1–2. doi: 10.1016/j.ophtha.2009.12.034

126. Kelly DH. Nonlinear visual responses to flickering sinusoidal gratings. *J Opt Soc Am.* (1981) 71:1051–5. doi: 10.1364/JOSA.71.001051

127. Brusini P, Busatto P. Frequency doubling perimetry in glaucoma early diagnosis. *Acta Ophthalmol Scand Suppl.* (1998) 76:23–4.

128. Chaturvedi N, Hedley-Whyte ET, Dreyer EB. Lateral geniculate nucleus in glaucoma. *Am J Ophthalmol.* (1993) 116:182–8. doi: 10.1016/S0002-9394(14)71283-8

129. Yucel YH, Zhang Q, Gupta N, Kaufman PL, Weinreb RN. Loss of neurons in magnocellular and parvocellular layers of the lateral geniculate nucleus in glaucoma. *Arch Ophthalmol.* (2000) 118:378–84. doi: 10.1001/archopht.118.3.378

130. Boland MV, Gupta P, Ko F, Zhao D, Guallar E, Friedman DS. Evaluation of frequency-doubling technology perimetry as a means of screening for glaucoma and other eye diseases using the national health and nutrition examination survey. *JAMA Ophthalmol.* (2016) 134:57–62. doi: 10.1001/jamaophthalmol.2015.4459

131. Johnson CA, Adams AJ, Casson EJ, Brandt JD. Progression of early glaucomatous visual field loss as detected by blue-on-yellow and standard white-on-white automated perimetry. *Arch Ophthalmol.* (1993) 111:651–6. doi: 10.1001/archopht.1993.01090050085035

132. Polo V, Larrosa JM, Pinilla I, Perez S, Gonzalvo F, Honrubia FM. Predictive value of short-wavelength automated perimetry: a 3-year follow-up study. *Ophthalmology.* (2002) 109:761–5. doi: 10.1016/S0161-6420(01)01014-4

133. Bayer AU, Maag KP, Erb C. Detection of optic neuropathy in glaucomatous eyes with normal standard visual fields using a test battery of short-wavelength automated perimetry and pattern electroretinography. *Ophthalmology.* (2002) 109:1350–61. doi: 10.1016/S0161-6420(02)01100-4

134. Votruba M, Fitzke FW, Holder GE, Carter A, Bhattacharya SS, Moore AT. Clinical features in affected individuals from 21 pedigrees

with dominant optic atrophy. *Arch Ophthalmol.* (1998) 116:351–8. doi: 10.1001/archopht.116.3.351

135. Walters JW, Gaume A, Pate L. Short wavelength-automated perimetry compared with standard achromatic perimetry in autosomal dominant optic atrophy. *Br J Ophthalmol.* (2006) 90:1267–70. doi: 10.1136/bjo.2006.097196

136. Demirel S, Johnson CA. Short wavelength automated perimetry (SWAP) in ophthalmic practice. *J Am Optom Assoc.* (1996) 67:451–6.

137. Kardon R, Anderson SC, Damarjian TG, Grace EM, Stone E, Kawasaki A. Chromatic pupillometry in patients with retinitis pigmentosa. *Ophthalmology.* (2011) 118:376–81. doi: 10.1016/j.ophtha.2010.06.033

138. Kawasaki A, Herbst K, Sander B, Milea D. Selective wavelength pupillometry in Leber hereditary optic neuropathy. *Clin Exp Ophthalmol.* (2010) 38:322–4. doi: 10.1111/j.1442-9071.2010.02212.x

139. Perganta G, Barnard AR, Katti C, Vachtsevanos A, Douglas RH, MacLaren RE, et al. Non-image-forming light driven functions are preserved in a mouse model of autosomal dominant optic atrophy. *PLoS ONE.* (2013) 8:e56350. doi: 10.1371/journal.pone.0056350

140. Ba-Ali S, Lund-Andersen H. Pupillometric evaluation of the melanopsin containing retinal ganglion cells in mitochondrial and non-mitochondrial optic neuropathies. *Mitochondrion.* (2017) 36:124–9. doi: 10.1016/j.mito.2017.07.003

141. Odom JV, Bach M, Brigell M, Holder GE, McCulloch DL, Mizota A, et al. International Society for Clinical Electrophysiology of, ISCEV standard for clinical visual evoked potentials: (2016 update). *Doc Ophthalmol.* (2016) 133:1–9. doi: 10.1007/s10633-016-9553-y

142. Bach M, Brigell MG, Hawlina M, Holder GE, Johnson MA, McCulloch DL, et al. ISCEV standard for clinical pattern electroretinography (PERG): 2012 update. *Doc Ophthalmol.* (2013) 126:1–7. doi: 10.1007/s10633-012-9353-y

143. Ostrin LA, Choh V, Wildsoet CF. The pattern ERG in chicks - stimulus dependence and optic nerve section. *Vis Res.* (2016) 128:45–52. doi: 10.1016/j.visres.2016.09.009

144. Viswanathan S, Frishman LJ, Robson JG. The uniform field and pattern ERG in macaques with experimental glaucoma: removal of spiking activity. *Invest Ophthalmol Vis Sci.* (2000) 41:2797–810.

145. Holder GE. Electrophysiological assessment of optic nerve disease. *Eye.* (2004) 18:1133–43. doi: 10.1038/sj.eye.6701573

146. Kakisu Y, Adachi-Usami E, Mizota A. Pattern electroretinogram and visual evoked cortical potential in ethambutol optic neuropathy. *Doc Ophthalmol.* (1987) 67:327–34. doi: 10.1007/BF00143950

147. Majander A, Robson AG, Joao C, Holder GE, Chinnery PF, Moore AT, et al. The pattern of retinal ganglion cell dysfunction in Leber hereditary optic neuropathy. *Mitochondrion.* (2017) 36:138–49. doi: 10.1016/j.mito.2017.07.006

148. Viswanathan S, Frishman LJ, Robson JG, Harwerth RS, Smith EL III. The photopic negative response of the macaque electroretinogram: reduction by experimental glaucoma. *Invest Ophthalmol Vis Sci.* (1999) 40:1124–36.

149. Frishman L, Sustar M, Kremers J, McAnany JJ, Sarossy M, Tzekov R, et al. ISCEV extended protocol for the photopic negative response (PhNR) of the full-field electroretinogram. *Doc Ophthalmol.* (2018) 136:207–11. doi: 10.1007/s10633-018-9638-x

150. Machida S. Clinical applications of the photopic negative response to optic nerve and retinal diseases. *J Ophthalmol.* (2012) 2012:397178. doi: 10.1155/2012/397178

151. Karanjia R, Berezovsky A, Sacai PY, Cavascan NN, Liu HY, Nazarali S, et al. The photopic negative response: an objective measure of retinal ganglion cell function in patients with Leber's hereditary optic neuropathy. *Investig Ophthalmol Visual Sci.* (2017) 58:BIO300–6. doi: 10.1167/iovs.17-21773

152. Berezovsky A, Karanjia R, Fernandes AG, Botelho GIS, Bueno TLN, Ferraz NN, et al. Photopic negative response using a handheld mini-ganzfeld stimulator in healthy adults: normative values, intra- and inter-session variability. *Doc Ophthalmol.* (2020) 142:153–63. doi: 10.1007/s10633-020-09784-x

153. Machida S, Toba Y, Ohtaki A, Gotoh Y, Kaneko M, Kurosaka D. Photopic negative response of focal electoretinograms in glaucomatous eyes. *Invest Ophthalmol Vis Sci.* (2008) 49:5636–44. doi: 10.1167/iovs.08-1946

154. Prencipe M, Perossini T, Brancoli G, Perossini M. The photopic negative response (PhNR): measurement approaches and utility in glaucoma. *Int Ophthalmol.* (2020) 40:3565–76. doi: 10.1007/s10792-020-01515-0

155. Preiser D, Lagreze WA, Bach M, Poloschek CM. Photopic negative response versus pattern electroretinogram in early glaucoma. *Invest Ophthalmol Vis Sci.* (2013) 54:1182–91. doi: 10.1167/iovs.12-11201

156. Bargiela D, Yu-Wai-Man P, Keogh M, Horvath R, Chinnery PF. Prevalence of neurogenetic disorders in the North of England. *Neurology.* (2015) 85:1195–201. doi: 10.1212/WNL.0000000000001995

157. Jurkute N, Majander A, Bowman R, Votruba M, Abbs S, Acheson J, et al. Clinical utility gene card for: inherited optic neuropathies including next-generation sequencing-based approaches. *Eur J Hum Genet.* (2019) 27:494–502. doi: 10.1038/s41431-018-0235-y

158. Yu-Wai-Man P, Griffiths PG, Brown DT, Howell N, Turnbull DM, Chinnery PF. The epidemiology of Leber hereditary optic neuropathy in the North East of England. *Am J Hum Genet.* (2003) 72:333–9. doi: 10.1086/346066

159. Yu-Wai-Man P, Griffiths PG, Howell N, Turnbull DM, Chinnery PF. The epidemiology of Leber hereditary optic neuropathy in the North East of England. *Am J Hum Genet.* (2016) 98:1271. doi: 10.1016/j.ajhg.2016.05.015

160. Kim US, Jurkute N, Yu-Wai-Man P. Leber hereditary optic neuropathy-light at the end of the tunnel? *Asia Pac J Ophthalmol.* (2018) 7:242–5. doi: 10.22608/APO.2018293

161. Jurkute N, Yu-Wai-Man P. Leber hereditary optic neuropathy: bridging the translational gap. *Curr Opin Ophthalmol.* (2017) 28:403–9. doi: 10.1097/ICU.0000000000000410

162. Oostra RJ, Bolhuis PA, Wijburg FA, Zorn-Ende G, Bleeker-Wagemakers EM. Leber's hereditary optic neuropathy: correlations between mitochondrial genotype and visual outcome. *J Med Genet.* (1994) 31:280–6. doi: 10.1136/jmg.31.4.280

163. Newman NJ, Carelli V, Taiel M, Yu-Wai-Man P. Visual outcomes in Leber hereditary optic neuropathy patients with the m.11778G>A (MTND4) mitochondrial DNA mutation. *J Neuroophthalmol.* (2020) 40:547–57. doi: 10.1097/WNO.0000000000001045

164. Sadun AA, Win PH, Ross-Cisneros FN, Walker SO, Carelli V. Leber's hereditary optic neuropathy differentially affects smaller axons in the optic nerve. *Trans Am Ophthalmol Soc.* (2000) 98:223–32; discussion 232–5.

165. Pan BX, Ross-Cisneros FN, Carelli V, Rue KS, Salomao SR, Moraes-Filho MN, et al. Mathematically modeling the involvement of axons in Leber's hereditary optic neuropathy. *Invest Ophthalmol Vis Sci.* (2012) 53:7608–17. doi: 10.1167/iovs.12-10452

166. Carelli V, Carbonelli M, de Coo IF, Kawasaki A, Klopstock T, Lagreze WA, et al. International consensus statement on the clinical and therapeutic management of Leber hereditary optic neuropathy. *J Neuroophthalmol.* (2017) 37:371–81. doi: 10.1097/WNO.0000000000000570

167. Kerrison JB, Howell N, Miller NR, Hirst L, Green WR. Leber hereditary optic neuropathy. Electron microscopy and molecular genetic analysis of a case. *Ophthalmology.* (1995) 102:1509–16. doi: 10.1016/S0161-6420(95)30838-X

168. Gualtieri M, Bandeira M, Hamer RD, Costa MF, Oliveira AG, Moura AL, et al. Psychophysical analysis of contrast processing segregated into magnocellular and parvocellular systems in asymptomatic carriers of 11778 Leber's hereditary optic neuropathy. *Vis Neurosci.* (2008) 25:469–74. doi: 10.1017/S0952523808080462

169. Bose S, Dhillon N, Ross-Cisneros FN, Carelli V. Relative post-mortem sparing of afferent pupil fibers in a patient with 3460 Leber's hereditary optic neuropathy. *Graefes Arch Clin Exp Ophthalmol.* (2005) 243:1175–9. doi: 10.1007/s00417-005-0023-6

170. Hannibal J. Roles of PACAP-containing retinal ganglion cells in circadian timing. *Int Rev Cytol.* (2006) 251:1–39. doi: 10.1016/S0074-7696(06)51001-0

171. Li SY, Yau SY, Chen BY, Tay DK, Lee VW, Pu ML, et al. Enhanced survival of melanopsin-expressing retinal ganglion cells after injury is associated with the PI3 K/Akt pathway. *Cell Mol Neurobiol.* (2008) 28:1095–107. doi: 10.1007/s10571-008-9286-x

172. Yu-Wai-Man P, Chinnery PF. Dominant optic atrophy: novel OPA1 mutations and revised prevalence estimates. *Ophthalmology.* (2013) 120:1712 e1. doi: 10.1016/j.ophtha.2013.04.022

173. Lenaers G, Hamel C, Delettre C, Amati-Bonneau P, Procaccio V, Bonneau D, et al. Dominant optic atrophy. *Orphanet J Rare Dis.* (2012) 7:46. doi: 10.1186/1750-1172-7-46

174. Chun BY, Rizzo JF III. Dominant optic atrophy and Leber's hereditary optic neuropathy: update on clinical features and current therapeutic approaches. *Semin Pediatr Neurol.* (2017) 24:129–34. doi: 10.1016/j.spen.2017.06.001

175. Yu-Wai-Man P, Griffiths PG, Burke A, Sellar PW, Clarke MP, Gnanaraj L, et al. The prevalence and natural history of dominant optic atrophy due to OPA1 mutations. *Ophthalmology.* (2010) 117:1538–46 e1. doi: 10.1016/j.ophtha.2009.12.038

176. Barboni P, Savini G, Parisi V, Carbonelli M, La Morgia C, Maresca A, et al. Retinal nerve fiber layer thickness in dominant optic atrophy measurements by optical coherence tomography and correlation with age. *Ophthalmology.* (2011) 118:2076–80. doi: 10.1016/j.ophtha.2011.02.027

177. Majander A, Joao C, Rider AT, Henning GB, Votruba M, Moore AT, et al. The pattern of retinal ganglion cell loss in OPA1-related autosomal dominant optic atrophy inferred from temporal, spatial, and chromatic sensitivity losses. *Invest Ophthalmol Vis Sci.* (2017) 58:502–16. doi: 10.1167/iovs.16-20309

178. Kawasaki A, Collomb S, Leon L, Munch M. Pupil responses derived from outer and inner retinal photoreception are normal in patients with hereditary optic neuropathy. *Exp Eye Res.* (2014) 120:161–6. doi: 10.1016/j.exer.2013.11.005

179. Nissen C, Ronnback C, Sander B, Herbst K, Milea D, Larsen M, et al. Dissociation of pupillary post-illumination responses from visual function in confirmed OPA1 c.983A > G and c.2708_2711delTTAG autosomal dominant optic atrophy. *Front Neurol.* (2015) 6:5. doi: 10.3389/fneur.2015.00005

180. Wang MY, Sadun AA. Drug-related mitochondrial optic neuropathies. *J Neuroophthalmol.* (2013) 33:172–8. doi: 10.1097/WNO.0b013e31829 01969

181. Osborne NN, Nunez-Alvarez C, Joglar B, Del Olmo-Aguado S. Glaucoma: Focus on mitochondria in relation to pathogenesis and neuroprotection. *Eur J Pharmacol.* (2016) 787:127–33. doi: 10.1016/j.ejphar.2016.04.032

182. Guy J. Optic nerve degeneration in experimental autoimmune encephalomyelitis. *Ophthalmic Res.* (2008) 40:212–6. doi: 10.1159/000119879

183. Jonas JB, Aung T, Bourne RR, Bron AM, Ritch R, Panda-Jonas S. Glaucoma. *Lancet.* (2017) 390:2183–93. doi: 10.1016/S0140-6736(17) 31469-1

184. Quigley HA, Dunkelberger GR, Green WR. Chronic human glaucoma causing selectively greater loss of large optic nerve fibers. *Ophthalmology.* (1988) 95:357–63. doi: 10.1016/S0161-6420(88) 33176-3

185. Dandona L, Hendrickson A, Quigley HA. Selective effects of experimental glaucoma on axonal transport by retinal ganglion cells to the dorsal lateral geniculate nucleus. *Invest Ophthalmol Vis Sci.* (1991) 32:1593–9.

186. Vickers JC, Schumer RA, Podos SM, Wang RF, Riederer BM, Morrison JH. Differential vulnerability of neurochemically identified subpopulations of retinal neurons in a monkey model of glaucoma. *Brain Res.* (1995) 680:23–35. doi: 10.1016/0006-8993(95)00211-8

187. Wang AY, Lee PY, Bui BV, Jobling AI, Greferath U, Brandli A, et al. Potential mechanisms of retinal ganglion cell type-specific vulnerability in glaucoma. *Clin Exp Optom.* (2020) 103:562–71. doi: 10.1111/cxo.13031

188. Morgan JE, Uchida H, Caprioli J. Retinal ganglion cell death in experimental glaucoma. *Br J Ophthalmol.* (2000) 84:303–10. doi: 10.1136/bjo.84.3.303

189. McKendrick AM, Sampson GP, Walland MJ, Badcock DR. Contrast sensitivity changes due to glaucoma and normal aging: low-spatial-frequency losses in both magnocellular and parvocellular pathways. *Invest Ophthalmol Vis Sci.* (2007) 48:2115–22. doi: 10.1167/iovs.06-1208

190. Feigl B, Mattes D, Thomas R, Zele AJ. Intrinsically photosensitive (melanopsin) retinal ganglion cell function in glaucoma. *Invest Ophthalmol Vis Sci.* (2011) 52:4362–7. doi: 10.1167/iovs.10-7069

191. Adhikari P, Zele AJ, Thomas R, Feigl B. Quadrant field pupillometry detects melanopsin dysfunction in glaucoma suspects and early glaucoma. *Sci Rep.* (2016) 6:33373. doi: 10.1038/srep 33373

192. Kelbsch C, Maeda F, Strasser T, Blumenstock G, Wilhelm B, Wilhelm H, et al. Pupillary responses driven by ipRGCs and classical photoreceptors are impaired in glaucoma. *Graefes Arch Clin Exp Ophthalmol.* (2016) 254:1361–70. doi: 10.1007/s00417-016-3351-9

193. Lightman S, McDonald WI, Bird AC, Francis DA, Hoskins A, Batchelor JR, et al. Retinal venous sheathing in optic neuritis. Its significance for the pathogenesis of multiple sclerosis. *Brain.* (1987) 110(Pt. 2):405–14. doi: 10.1093/brain/110.2.405

194. Cao D, Zele AJ, Pokorny J, Lee DY, Messner LV, Diehl C, et al. Functional loss in the magnocellular and parvocellular pathways in patients with optic neuritis. *Invest Ophthalmol Vis Sci.* (2011) 52:8900–7. doi: 10.1167/iovs.11-7644

195. Viret AC, Cavezian C, Coubard O, Vasseur V, Raz N, Levin N, et al. Optic neuritis: from magnocellular to cognitive residual dysfunction. *Behav Neurol.* (2013) 27:277–83. doi: 10.1155/2013/142680

196. Regan D, Kothe AC, Sharpe JA. Recognition of motion-defined shapes in patients with multiple sclerosis and optic neuritis. *Brain.* (1991) 114(Pt. 3):1129–55. doi: 10.1093/brain/114.3.1129

197. Wall M. Loss of P retinal ganglion cell function in resolved optic neuritis. *Neurology.* (1990) 40:649–53. doi: 10.1212/WNL.40.4.649

198. Fallowfield L, Krauskopf J. Selective loss of chromatic sensitivity in demyelinating disease. *Invest Ophthalmol Vis Sci.* (1984) 25:771–3.

199. Schneck ME, Haegerstrom-Portnoy G. Color vision defect type and spatial vision in the optic neuritis treatment trial. *Invest Ophthalmol Vis Sci.* (1997) 38:2278–89.

200. Katz B. The dyschromatopsia of optic neuritis: a descriptive analysis of data from the optic neuritis treatment trial. *Trans Am Ophthalmol Soc.* (1995) 93:685–708.

201. Zoumalan CI, Agarwal M, Sadun AA. Optical coherence tomography can measure axonal loss in patients with ethambutol-induced optic neuropathy. *Graefes Arch Clin Exp Ophthalmol.* (2005) 243:410–6. doi: 10.1007/s00417-004-1053-1

202. Khawaja AP, Chan MPY, Yip JLY, Broadway DC, Garway-Heath DF, Viswanathan AC, et al. A common glaucoma-risk variant of SIX6 alters retinal nerve fiber layer and optic disc measures in a European population: the EPIC-Norfolk Eye Study. *J Glaucoma.* (2018) 27:743–9. doi: 10.1097/IJG.0000000000001026

203. Yu-Wai-Man P. Harnessing the power of genetic engineering for patients with mitochondrial eye diseases. *J Neuroophthalmol.* (2017) 37:56–64. doi: 10.1097/WNO.0000000000000476

204. Vignal C, Uretsky S, Fitoussi S, Galy A, Blouin L, Girmens JF, et al. Safety of rAAV2/2-ND4 gene therapy for Leber hereditary optic neuropathy. *Ophthalmology.* (2018) 125:945–7. doi: 10.1016/j.ophtha.2017.12.036

205. Feuer WJ, Schiffman JC, Davis JL, Porciatti V, Gonzalez P, Koilkonda RD, et al. Gene therapy for Leber hereditary optic neuropathy: initial results. *Ophthalmology.* (2016) 123:558–70. doi: 10.1016/j.ophtha.2015.10.025

206. Yu-Wai-Man P, Newman NJ, Carelli V, Moster ML, Biousse V, Sadun AA, et al. Bilateral visual improvement with unilateral gene therapy injection for Leber hereditary optic neuropathy. *Sci Transl Med.* (2020) 12:eaaz7423. doi: 10.1126/scitranslmed.aaz7423

207. Newman NJ, Yu-Wai-Man P, Carelli V, Moster ML, Biousse V, Vignal-Clermont C, et al. Efficacy and safety of intravitreal gene therapy for Leber hereditary optic neuropathy treated within 6 months of disease onset. *Ophthalmology.* (2021) doi: 10.1016/j.ophtha.2020.12.012. [Epub ahead of print].

208. Hanlon KS, Chadderton N, Palfi A, Blanco Fernandez A, Humphries P, Kenna PF, et al. A novel retinal ganglion cell promoter for utility in AAV vectors. *Front Neurosci.* (2017) 11:521. doi: 10.3389/fnins.2017.00521

209. DiCarlo JE, Mahajan VB, Tsang SH. Gene therapy and genome surgery in the retina. *J Clin Invest.* (2018) 128:2177–88. doi: 10.1172/JCI120429

210. Khan S, Hung SS-C, Wong RC-B. The use of induced pluripotent stem cells for studying and treating optic neuropathies. *Curr Opin Organ Transplant.* (2016) 21:484–9. doi: 10.1097/MOT.00000000000 00348

211. La Morgia C, Carelli V, Carbonelli M. Melanopsin retinal ganglion cells and pupil: clinical implications for neuro-ophthalmology. *Front Neurol.* (2018) 9:1047. doi: 10.3389/fneur.2018.01047

212. Mazzoni F, Novelli E, Strettoi E. Retinal ganglion cells survive and maintain normal dendritic morphology in a mouse model of inherited photoreceptor degeneration. *J Neurosci.* (2008) 28:14282–92. doi: 10.1523/JNEUROSCI.4968-08.2008

213. Gilhooley MJ, Owen N, Moosajee M, Wai Man PY. From transcriptomics to treatment in inherited optic neuropathies. *Genes.* (2021) 12:147. doi: 10.3390/genes12020147

214. Shah NP, Chichilnisky EJ. Computational challenges and opportunities for a bi-directional artificial retina. *J Neural Eng.* (2020) 17:055002. doi: 10.1088/1741-2552/aba8b1

Intravitreal Gene Therapy vs. Natural History in Patients With Leber Hereditary Optic Neuropathy Carrying the m.11778G>A *ND4* Mutation: Systematic Review and Indirect Comparison

Nancy J. Newman[1]*, Patrick Yu-Wai-Man[2,3,4,5], Valerio Carelli[6,7], Valerie Biousse[1],
Mark L. Moster[8], Catherine Vignal-Clermont[9,10], Robert C. Sergott[8],
Thomas Klopstock[11,12,13], Alfredo A. Sadun[14], Jean-François Girmens[10],
Chiara La Morgia[6], Adam A. DeBusk[8], Neringa Jurkute[4,5], Claudia Priglinger[15],
Rustum Karanjia[14,16], Constant Josse[17], Julie Salzmann[18], François Montestruc[17],
Michel Roux[19], Magali Taiel[19] and José-Alain Sahel[20,21,22,23] for the LHON Study Group

[1] Departments of Ophthalmology, Neurology and Neurological Surgery, Emory University School of Medicine, Atlanta, GA, United States, [2] Cambridge Centre for Brain Repair and MRC Mitochondrial Biology Unit, Department of Clinical Neurosciences, University of Cambridge, Cambridge, United Kingdom, [3] Cambridge Eye Unit, Addenbrooke's Hospital, Cambridge University Hospitals, Cambridge, United Kingdom, [4] Moorfields Eye Hospital National Health Service Foundation Trust, London, United Kingdom, [5] UCL Institute of Ophthalmology, University College London, London, United Kingdom, [6] Istituto di Ricovero e Cura a Carattere Scientifico Istituto delle Scienze Neurologiche di Bologna, Unitá Operativa Compless Clinica Neurologica, Bologna, Italy, [7] Unit of Neurology, Department of Biomedical and Neuromotor Sciences, University of Bologna, Bologna, Italy, [8] Departments of Neurology and Ophthalmology, Wills Eye Hospital and Thomas Jefferson University, Philadelphia, PA, United States, [9] Department of Neuro Ophthalmology and Emergencies, A. de Rothschild Foundation Hospital, Paris, France, [10] Centre d'investigation Clinique, Centre Hospitalier National d'Ophtalmologie des Quinze Vingts, Paris, France, [11] Department of Neurology, Friedrich-Baur-Institute, University Hospital, Ludwig-Maximilians-University Munich, Munich, Germany, [12] German Center for Neurodegenerative Diseases, Munich, Germany, [13] Munich Cluster for Systems Neurology, Munich, Germany, [14] Doheny Eye Institute, School of Medicine, University of California, Los Angeles, Los Angeles, CA, United States, [15] Department of Ophthalmology, University Hospital, Ludwig-Maximilians-University Munich, Munich, Germany, [16] Department of Ophthalmology, University of Ottawa Eye, Ottawa, ON, Canada, [17] eXYSTAT, Data Management and Statistic, Malakoff, France, [18] Medical and Regulatory Consulting, Paris, France, [19] GenSight Biologics, Paris, France, [20] Sorbonne Université, INSERM, CNRS, Institut de la Vision, Paris, France, [21] A. de Rothschild Foundation Hospital, Paris, France, [22] Department of Ophthalmology, The University of Pittsburgh School of Medicine, Pittsburgh, PA, United States, [23] CHNO des Quinze-Vingts, Institut Hospitalo-Universitaire FOReSIGHT, INSERM-DGOS CIC 1423, Paris, France

Objective: This work aimed to compare the evolution of visual outcomes in Leber hereditary optic neuropathy (LHON) patients treated with intravitreal gene therapy to the spontaneous evolution in prior natural history (NH) studies.

Design: A combined analysis of two phase three randomized, double-masked, sham-controlled studies (REVERSE and RESCUE) and their joint long-term extension trial (CLIN06) evaluated the efficacy of rAAV2/2-*ND4* vs. 11 pooled NH studies used as an external control.

Subjects: The LHON subjects carried the m.11778G>A *ND4* mutation and were aged ≥15 years at onset of vision loss.

Methods: A total of 76 subjects received a single intravitreal rAAV2/2-*ND4* injection in one eye and sham injection in the fellow eye within 1 year after vision loss in REVERSE

Newman et al.

Efficacy of rAAV2/2-ND4 in LHON vs. Natural History

and RESCUE. Both eyes were considered as treated due to the rAAV2/2-*ND4* treatment efficacy observed in the contralateral eyes. Best corrected visual acuity (BCVA) from REVERSE, RESCUE, and CLIN06 up to 4.3 years after vision loss was compared to the visual acuity of 208 NH subjects matched for age and *ND4* genotype. The NH subjects were from a LHON registry (REALITY) and from 10 NH studies. A locally estimated scatterplot smoothing (LOESS), non-parametric, local regression model was used to modelize visual acuity curves over time, and linear mixed model was used for statistical inferences.

Main Outcome Measures: The main outcome measure was evolution of visual acuity from 12 months after vision loss, when REVERSE and RESCUE patients had been treated with rAAV2/2-*ND4*.

Results: The LOESS curves showed that the BCVA of the treated patients progressively improved from month 12 to 52 after vision loss. At month 48, there was a statistically and clinically relevant difference in visual acuity of -0.33 logarithm of the minimal angle of resolution (LogMAR) (16.5 ETDRS letters equivalent) in favor of treated eyes vs. NH eyes ($p < 0.01$). Most treated eyes (88.7%) were on-chart at month 48 as compared to 48.1% of the NH eyes ($p < 0.01$). The treatment effect at last observation remained statistically and clinically significant when adjusted for age and duration of follow-up (-0.32 LogMAR, $p < 0.0001$).

Conclusions: The m.11778G>A LHON patients treated with rAAV2/2-*ND4* exhibited an improvement of visual acuity over more than 4 years after vision loss to a degree not demonstrated in NH studies.

Clinical Trial Registration: NCT02652767, NCT02652780, NCT03406104, and NCT03295071.

INTRODUCTION

Leber hereditary optic neuropathy (LHON) is a rare genetic disease caused by mutations of mitochondrial genes of the respiratory chain complex I, leading to selective degeneration of retinal ganglion cells and optic nerve atrophy (1). The disease typically manifests as severe central visual loss in one eye, followed by second eye involvement with a median interval of 8 weeks (2–4). The decline in visual acuity is subacute to rapidly progressive, with visual acuity usually deteriorating to values worse than 20/200 over a few months after onset (2, 5). Such sudden and profound vision loss occurring in well-sighted individuals, usually young adults, has a dramatic impact on their quality of life (5). Thus, targeted drug discovery and new therapeutic approaches are crucial to improve the visual prognosis of patients with LHON. While the oral drug idebenone has shown some benefit (6–8), leading to its approval for the treatment of LHON in Europe, there is still a pressing medical need for further therapies with a significant therapeutic benefit in LHON (7).

Among the three most common point mutations found in LHON, the m.11778G>A mutation in the mitochondrial *ND4* gene is the most prevalent, accounting for ~70% of LHON patients worldwide (9). Moreover, it is associated with a poor prognosis, with spontaneous visual recovery limited to <15% of patients, as shown by a recent meta-analysis of 695 patients with the m.11778G>A mutation (10).

rAAV2/2-*ND4* (also called lenadogene nolparvovec) is a replication-defective, recombinant adeno-associated virus vector serotype 2 (rAAV2) containing a codon-modified complementary DNA (cDNA) encoding the human wild-type mitochondrial ND4 protein. It is believed to restore the functional ND4 protein, thereby preventing the neuronal degeneration of retinal ganglion cells, as demonstrated in a rat model of LHON (11). In a phase 1/2 study conducted in 15 LHON patients harboring the m.11778G>A *ND4* mutation (hereafter named *MT-ND4* patients), a single intravitreal injection (IVT) of lenadogene nolparvovec was well-tolerated and associated with a clinically significant improvement in visual function outcomes (12, 13). A visual benefit induced by lenadogene nolparvovec was recently suggested by two randomized, double-masked, sham-controlled phase three studies REVERSE [patients with a vision loss between 6 and 12 months; NCT02652780 (14)] and RESCUE [patients with a vision loss below 6 months; NCT02652767 (15)]. In both studies, lenadogene nolparvovec was injected in one eye, while

Newman et al.

Efficacy of rAAV2/2-ND4 in LHON vs. Natural History

the fellow eye received a sham injection, with the unexpected result of sustained visual improvement in both eyes. At 96 weeks post-injection, the mean gain from nadir (worst vision point) in REVERSE and RESCUE studies was, respectively, +28 and +26 in treated eyes and +24 and +23 ETDRS letters in sham eyes (14, 15). The REVERSE and RESCUE patients are currently followed in an extension study for up to 5 years after injection (CLIN06, NCT03406104). This bilateral improvement after the unilateral injection of a gene therapy product has also been observed in other clinical studies of LHON (16, 17). A mechanistic explanation could be transfer of the viral vector from the injected eye to the contralateral eye through the optic chiasm, as suggested by a non-human primate biodistribution study using unilaterally injected lenadogene nolparvovec (14).

In order to better characterize the efficacy of gene therapy in *MT-ND4* LHON patients, we indirectly compared the evolution of visual outcomes of treated patients in the REVERSE, RESCUE, and CLIN06 studies to the spontaneous evolution of natural history patients from a LHON registry study and previously published reports of LHON patients with visual outcome data used as an external control.

METHODS

Patients Treated With Gene Therapy—Efficacy Pool

We analyzed the evolution of best corrected visual acuity (BCVA) from a pooled dataset of 76 LHON patients treated with a single IVT injection of lenadogene nolparvovec. The BCVA data were collected from study inclusion to week 96 after treatment in REVERSE (NCT02652780) (14) and RESCUE (NCT02652767) (15) and from week 96 after treatment to the last available observation in the ongoing long-term follow-up CLIN06 study of REVERSE and RESCUE (NCT03406104) (see **Supplementary Table 1**).

The study design and results of REVERSE and RESCUE have been previously reported (14, 15). Briefly, REVERSE and RESCUE were randomized, double-masked, sham-controlled, multi-center phase 3 clinical trials with a similar design, aiming at evaluating the efficacy and safety of lenadogene nolparvovec in LHON patients. The right eye of each subject was randomly allocated to receive either lenadogene nolparvovec or sham treatment in a 1:1 allocation ratio. The fellow (left) eye received the treatment not allocated to the right eye. Lenadogene nolparvovec at 9×10^{10} viral genomes (vg)/eye was administered once *via* a single IVT. Sham IVT injection was performed once by applying pressure to the eye at the location of a typical procedure using the blunt end of a syringe without a needle. Both studies enrolled symptomatic LHON patients aged 15 years or older and harboring the m.11778G>A *ND4* mutation. The only difference between the two studies was the timing of the onset of vision loss: from 181 to 365 days in both eyes in REVERSE and ≤180 days in the first-affected eye in RESCUE. A total of 37 patients (REVERSE) and 39 patients (RESCUE) were enrolled and treated.

All REVERSE and RESCUE patients who completed the study up to week 96 after injection were offered to participate in the extension CLIN06 study, for a total of 5 years of follow-up after injection. A total of 62 patients (31 from REVERSE and 31 from RESCUE) were enrolled in the extension study which is ongoing. For our analysis, we used all available BCVA data at the time of this report, including assessments up to 4 years after injection. Based on clinical results and non-human primate data (14), both treated and sham eyes were considered exposed to the study drug and pooled in the treated patient group.

The protocols of all three studies (RESCUE, REVERSE, and CLIN06) were approved by local independent ethics committees, and informed consent was obtained from all participants. All studies were performed in compliance with Good Clinical Practice and adhered to the ethical principles outlined in the Declaration of Helsinki.

Natural History Patients—External Control Group—Natural History Pool

Natural history patients (those not treated with lenadogene nolparvovec, although they could have been treated with idebenone), with age and LHON genotype adjusted to those of treated patients, were used as an external control for the analysis. To this end, we created a large database containing visual outcome data from 11 studies originating from two main sources: (i) the REALITY LHON registry (NCT03295071) (18) sponsored by GenSight Biologics and (ii) 10 published studies on LHON identified after a systematic review of the literature (3, 19–27). Studies were included in the database only if they reported individual (patient- and eye-level) visual acuity values along with documentation of the time after vision loss in cohorts of at least five *MT-ND4* patients. For relevant comparison with treated patients, we included only patients from the pooled database who matched the inclusion criteria of REVERSE and RESCUE as regards age and LHON genotype (i.e., symptomatic LHON patients carrying the m.11778G>A *ND4* mutation who were 15 years or older at the onset of vision loss). Further details on REALITY and on the systematic literature review are provided in the **Supplementary Methods** and **Supplementary Table 1**.

Handling of Data

For the analyses, all visual acuity values (from treated and natural history patients) were converted to logarithm of the minimal angle of resolution (LogMAR) using standard formula for on-chart eyes (28) and the following conventions for off-chart eyes: patients only able to count fingers or detect hand motion were assigned LogMAR values of +2.0 and +2.3, respectively, according to the Lange scale (29); light perception and no light perception visual acuities were assigned LogMAR values of +4.0 and +4.5, respectively, to align with the equivalence used in the lenadogene nolparvovec studies and the REALITY registry (14, 15, 18). All eyes were assigned a LogMAR value of 0 at 1 month before the onset of vision loss, in line with the normal visual acuity of LHON mutation carriers before expression of the disease as described in the literature (30, 31) and pre-symptomatic data of lenadogene nolparvovec studies and REALITY registry. All extracted data and conversions of

	Treated (N = 76)	Natural history (N = 208)	Total (N = 284)	*P*-value
Number of eyes with visual acuity values	152	408[a]	560	
Gender				
Male (%)	61 (80.3%)	142 (82.6%)	203 (81.9%)	0.67 (C)
Missing data	0	36[b]	36	
Age at onset of vision loss (years)				
Median	32.5	23.5	25.0	<0.01 (KW)
Range	15.0–69.0	15.0–71.0	15.0–71.0	
Number of visual acuity assessments per patient				
Median	26.0	2.0	2.0	<0.01 (KW)
Mean (SD)	26.8 (5.2)	4.1 (4.0)	10.2 (11.0)	
Patient follow-up since vision loss (months)[c]				
Median	39.8	25.3	34.6	0.01 (KW)
Range	8.1–51.5	0.0–768.0	0.0–768.0	
Q1–Q3	32.1–44.1	4.0–108.4	7.6–49.5	
Patients with follow-up >36 months	64.5%	38.0%	45.1%	<0.01 (C)
Time from vision loss to treatment (months)				
Median	6.5	NA	NA	NA
Range	2.3–12.8	NA	NA	

C, chi-square test; KW, Kruskal–Wallis test; NA, not applicable; SD, standard deviation.
[a]*Eight natural history patient had visual acuity values in one eye only, leading to a sample size of 408 eyes.*
[b]*All gender missing data were from the natural history study of Lam in 2014 (20).*
[c]*Defined as the time from vision loss to the last available visual acuity value, regardless of the eye.*

visual acuity values to LogMAR underwent a thorough quality control process for ensuring the accuracy of all LogMAR reported values.

Statistical Methods

All data from treated and natural history patients were imported in a pooled database for the analyses. All analyses were performed at the patient level and at the eye level.

In a first step, we explored graphically the evolution of visual acuity in treated and natural history eyes more than 12 months after vision loss, when all REVERSE and RESCUE patients would have been treated with rAAV2/2-*ND4*, using a locally estimated scatterplot smoothing (LOESS), non-parametric, local regression model in which each patient's eyes were considered independently. Smoothing parameters were based on the corrected Akaike Information Criterion (SAS default method with values from 0.3 to 0.6). LOESS curves with 95% confidence interval (CI) were presented from 12 months up to 52 months after vision loss, corresponding to the maximal duration of follow-up for treated eyes in the extension study. All subsequent visual acuity values of natural history eyes were assigned to the 52-month timepoint using the next observation carried backward method. Using this method, all visual acuity values from the efficacy and natural history pools could be plotted on the same figure.

In a second step, we compared the visual outcomes between treated eyes and natural history eyes at 12, 18, 24, 36, and 48 months after vision loss (when all treated eyes were on treatment) and at the last available visual acuity value. For the 12- to 48-month analysis, only the closest value to the

nominal timepoint was selected for each eye based on pre-specified time windows (month 12: [9;15] months; Month 18: [15;21] months; Month 24: [21;30] months; Month 36: [30;42] months; Month 48: [42;54] months). Conversely, for the analysis at the last available visual acuity value, final visual acuity values from all eyes were considered in the analysis, maximizing the sample size. The following visual outcomes were analyzed: visual acuity values in LogMAR, eye response rates at a threshold of LogMAR $\leq$ 1.6 (on-chart values on the ETDRS scale) and LogMAR $\leq$ 1.3 (cutoff for blindness according to WHO), and eye response rates with an improvement from nadir $\geq$ 0.3. For improvement from nadir, only eyes with at least two visual acuity assessments were selected for the analyses. Comparisons of visual outcomes were performed by a non-parametric test (Kruskal–Wallis for visual acuity values and chi-square test for eye response rates). In addition, a parametric model with repeated measures on patients was also used for the analyses on both eyes in order to take into account the inter-eye correlation of each patient (mixed-model analysis of covariance for visual acuity values and generalized linear mixed model for eye response rate).

In order to control the potential confounding covariates in the comparative analysis, the treatment effect at last available visual acuity value was also estimated by a multivariate analysis with repeated measures on patients. Age at onset of vision loss, gender, and duration of follow-up were explored as covariates in the multivariate analysis.

Additional analyses were also performed separately considering only the better eye and worse eye of each patient. Better eye and worse eye were selected based on their visual

Newman et al.

Efficacy of rAAV2/2-ND4 in LHON vs. Natural History

acuity value at last available evaluation or at their nadir in cases of identical values at last available evaluation or on their mean value in cases of identical nadir values. For patients who had visual acuity data in one eye only, the eye was included in both better-eye and worse-eye analyses.

All statistical analyses were carried out with SAS® software version 9.4. Statistical significance was set at $P < 0.05$.

RESULTS

Characteristics of the Analyzed Population

Among the 44 patients enrolled in the REALITY study, 23 were *MT-ND4* LHON aged 15 years or older. Among the 304 *MT-ND4* patients in the natural history studies, 185 met the inclusion criteria of age at onset $\geq$ 15 years and at least one available visual acuity value with time from onset of vision loss. Thus, a total of 208 eligible natural history patients (408 eyes) were used as the external control cohort for comparison with the 76 treated patients (152 eyes) from the REVERSE and RESCUE studies (see **Supplementary Table 1** and **Table 1** for details).

The characteristics of the patients at onset of vision loss are described in **Table 1**. Overall, both treated and natural history patients were typical of the *MT-ND4* LHON population with a high proportion of males (81.9%) and a young age at onset of vision loss (median, 25 years). Natural history patients had a younger age of onset (median, 23.5 years) compared to treated patients (median, 32.5 years).

The mean number of visual acuity assessments per patient was larger in the treated group (26.8) as compared with the natural history group (4.1). Treated patients had a longer median follow-up duration after vision loss (39.8 months) than natural history patients (25.3 months). Conversely, the follow-up values of treated patients were distributed over a narrow range (25% of patients have been followed for more than 44.1 months; maximal follow-up, 51.5 months) as opposed to a wider distribution for natural history patients (25% of patients were followed for more than 108.4 months; maximal follow-up, 768 months).

The treated patients received lenadogene nolparvovec injection between 2.3 and 12.8 months after vision loss (median, 6.5 months). Half of the eyes (54%) had received treatment at month 6 ([3, 9] months) after vision loss, nearly all eyes (93%) at month 12 ([9, 15] months) after vision loss, and all patients (100%) at month 18 ([15, 21] months) after vision loss. We started the indirect comparison at month 12, which coincided with the time when nearly all eyes had received treatment.

Global Evolution of Visual Acuity Over Time

The LOESS regression curve for treated patients (in red in **Figure 1**; see **Supplementary Figure 1** for the scatterplot) showed a progressive and sustained improvement of BCVA from month 12 up to month 52. Notably, the lowest point of the curve (corresponding to the worst visual acuities) remained on-chart, with BCVA values not exceeding 1.6 LogMAR.

The natural history patients showed a clear distinctive pattern from treated patients as illustrated by the LOESS regression
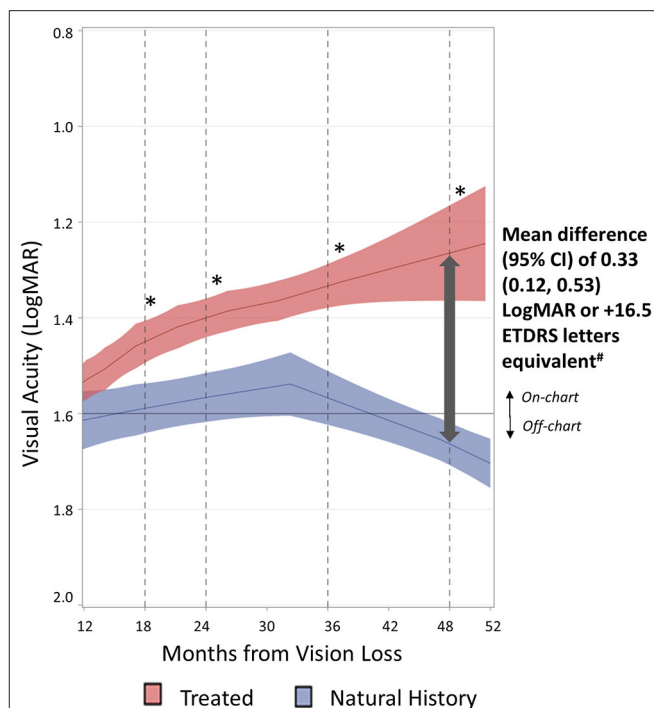
FIGURE 1 | Evolution of visual acuities of treated eyes vs. natural history eyes. The evolution of visual acuities over time for treated eyes ($n = 152$) and natural history eyes ($n = 408$) was estimated by LOESS regression (solid line) with 95% confidence interval around the fitted curve (shaded area). Smoothing parameter: 0.332 for treated eyes and 0.408 for natural history eyes. *A statistically significant difference between treated and natural history eyes is illustrated by the non-overlapping confidence intervals (CI) of LOESS curves. #Mean differences and 95% CI at month 48 were computed based on a separate analysis described in **Table 2**.

curves shown in blue in **Figure 1** (see **Supplementary Figure 1** for the scatterplot). In natural history patients, visual acuities plateaued around 1.6 LogMAR, with no recovery over 2 years (up to month 36 after vision loss). A progressive and continuous decline to off-chart values was then noted from month 36 up to month 52. The 52-month timepoint shown in **Figure 1** also takes into account all subsequent visual acuity values of natural history patients.

The divergence observed between the two curves from month 12 after vision loss is further evidenced by the absence of overlap in 95% CI at all later timepoints. Indeed the natural history patients showed an absence of visual recovery over the entire period from month 12 to 52, whereas the treated patients showed a gradual and consistent improvement over the same time period.

The treatment effect was also observed when REVERSE and RESCUE studies were analyzed separately, showing a similar improvement in the visual acuity LOESS curve of the treated patients vs. the external control group (see **Supplementary Figures 2**, **3**).

Additionally, the treatment effect for both eyes was also observed when the better eye and worse eye of patients were analyzed separately.

Newman et al.

Efficacy of rAAV2/2-*ND4* in LHON vs. Natural History

Time from vision loss	Treated (N = 152 eyes)	Natural history (N = 408 eyes)
Month 12—[9, 15] months		
Number of eyes	150	76
Visual acuity (LogMAR)		
Median	1.55	1.70
Mean (SD)	1.57 (0.55)	1.69 (0.67)
95% CI (mean)	(1.48, 1.66)	(1.54, 1.84)
Mean difference (95% CI)	0.118# (−0.047, 0.282)	
Month 18—[15, 21] months		
Number of eyes	149	57
Visual acuity (LogMAR)		
Median	1.40	1.60
Mean (SD)	1.46 (0.51)	1.60 (0.54)
95% CI (mean)	(1.38, 1.54)	(1.46, 1.75)
Mean difference (95% CI)	0.144# (−0.017, 0.304)	
Month 24—[21, 30] months		
Number of eyes	146	80
Visual acuity (LogMAR)		
Median	1.40	1.52
Mean (SD)	1.40 (0.59)	1.54 (0.52)
95% CI (mean)	(1.30, 1.50)	(1.42, 1.65)
Mean difference (95% CI)	0.139## (−0.016, 0.293)	
Month 36—[30, 42] months		
Number of eyes	128	66
Visual acuity (LogMAR)		
Median	1.30	1.55
Mean (SD)	1.33 (0.59)	1.52 (0.47)
95% CI (mean)	(1.23, 1.44)	(1.40, 1.63)
Mean difference (95% CI)	0.183##, * (0.018, 0.348)	
Month 48—[42, 54] months		
Number of eyes	62	27
Visual acuity (LogMAR)		
Median	1.30	1.62
Mean (SD)	1.26 (0.45)	1.59 (0.44)
95% CI (mean)	(1.14, 1.37)	(1.41, 1.76)
Mean difference (95% CI)	0.329##, ** (0.125, 0.534)	

CI, confidence interval; LogMAR, logarithm of the minimal angle of resolution; SD, standard deviation.

The time from vison loss was calculated for each eye of each patient. For each eye, only the closest value to the nominal timepoint was selected based on the time windows indicated in brackets.

#P < 0.05, ##P < 0.01: statistically significant differences vs. natural history eyes using Kruskal–Wallis test.

*P < 0.05, **P < 0.01: statistically significant difference vs. natural history eyes using mixed ANCOVA with repeated measures on a patient.

Comparison of Visual Acuities at Each Timepoint

Table 2 presents the results from month 12 to 48 after vision loss when treated eyes had been injected with lenadogene nolparvovec. In agreement with LOESS regression curves, quantitative analyses showed better visual acuity of treated eyes when compared with natural history eyes at all evaluated timepoints from month 12 to 48. The difference in mean visual acuity between treated and natural history eyes was statistically significant at all time points based on a non-parametric Kruskal–Wallis test and at month 36 and 48 based on a mixed ANCOVA model, taking into account the inter-eye correlation for each patient. The mean visual acuities with 95% CI for treated eyes and natural history eyes were, respectively, 1.26 (1.14, 1.37) and 1.59 (1.41, 1.76) LogMAR at month 48 ($p < 0.01$ for both Kruskal–Wallis and mixed ANCOVA), with a mean difference of 0.33 (0.12, 0.53) LogMAR in favor of treated eyes (**Table 2**). The median visual acuities for treated eyes and natural history eyes were, respectively, 1.30 vs. 1.62 LogMAR at month 48.

The treatment effect was also observed when REVERSE and RESCUE studies were analyzed separately vs. the external control group. The mean visual acuity difference with 95% CI between treated eyes and natural history eyes at month 48 was 0.31 (0.10, 0.52) LogMAR for REVERSE ($p < 0.01$ for both statistical tests) and 0.49 (0.08, 0.89) LogMAR for RESCUE ($p = 0.03$ for both statistical tests) in favor of treated eyes (see **Supplementary Table 2**).

Similar results were obtained when better eyes and worse eyes were analyzed separately, although a statistical significance was not reached at all timepoints (see **Supplementary Table 3**).

Comparison of Visual Acuities at Last Available Observation

Table 3 presents the analyses at last available visual acuities comparing treated eyes vs. natural history eyes, with separate analyses performed for each study (REVERSE and RESCUE) and for better and worse eyes.

The mean visual acuities with 95% CI for treated and natural history eyes were, respectively, 1.36 (1.27, 1.46) and 1.68 (1.62, 1.74) LogMAR at the last observation ($p < 0.01$ for both Kruskal–Wallis and mixed ANCOVA), with a mean difference of 0.31 (0.20, 0.43) LogMAR in favor of treated eyes. The median visual acuities for treated eyes and natural history eyes were, respectively, 1.40 and 1.70 LogMAR.

For REVERSE and RESCUE studies, the mean BCVAs with 95% CI for treated eyes were 1.29 (1.18, 1.40) and 1.43 (1.27, 1.59) LogMAR, respectively, while the mean visual acuity for natural history eyes was 1.68 (1.62, 1.74) LogMAR. The mean difference with 95% CI between REVERSE treated eyes and natural history eyes was 0.38 (0.24, 0.53) LogMAR in favor of treated eyes ($p < 0.01$ for both statistical tests). The mean difference between RESCUE treated eyes and natural history eyes was 0.25 (0.10, 0.40) LogMAR in favor of treated eyes ($p < 0.01$ for both statistical tests). The median visual acuity was 1.30 for REVERSE and 1.40 for RESCUE, vs. a median LogMAR of 1.70 for natural history eyes.

For analyses performed on better eyes, the mean visual acuities with 95% CI for treated and natural history eyes were, respectively, 1.24 (1.12, 1.37) and 1.57 (1.49, 1.65) LogMAR at the last observation ($p < 0.01$ for Kruskal–Wallis test), with a mean difference of 0.32 (0.17, 0.48) LogMAR in favor of treated eyes. For analyses performed on worse eyes, the mean visual acuities with 95% CI for treated eyes and natural history eyes were, respectively, 1.48 (1.33, 1.63) and 1.79 (1.71, 1.86) LogMAR at the

Newman et al.

Efficacy of rAAV2/2-*ND4* in LHON vs. Natural History

last observation ($p < 0.01$ for Kruskal–Wallis test), with a mean difference of 0.31 (0.15, 0.46) LogMAR in favor of treated eyes.

Multivariate Analysis of Visual Acuities

We performed a multivariate analysis to explore the potential impact of age at onset, gender, and duration of follow-up on the treatment effect at last visual acuity observation. Both age at onset ($p = 0.0050$) and follow-up duration ($p = 0.0108$) showed a statistically significant effect on visual acuity: younger patients and those with a shorter follow-up had better visual acuity independent of treatment. In contrast, gender had no effect on visual acuity outcome ($p = 0.9236$).

When considering the significant covariates in the analysis (age at onset and duration of follow-up), the treatment effect was confirmed in favor of treated eyes, with a statistically significant least squares mean difference in visual acuity of 0.32 (0.20, 0.44) LogMAR as compared with natural history eyes ($p < 0.0001$) (**Table 4**).

Eye Response Rates

At month 48 after vision loss, most (55/62) treated eyes [88.7%; 95% CI (78.1, 95.3)] were on-chart (LogMAR $\leq$ 1.6) as compared to less than half of the eyes (13/27) in the natural history group [48.1%, 95% CI (28.7, 68.1)] (**Figure 2**, left panel). The difference was statistically significant at $p < 0.01$ with both statistical tests (with or without considering the inter-eye correlation of each patient). Comparable results were observed for the response rates using the 1.3-LogMAR threshold (cutoff for blindness according to WHO criteria) (**Figure 2**, right panel). At month 48, 34/62 treated eyes [54.8%; 95% CI (41.7, 67.5%)] were responders as compared to 8/27 [29.6%, 95% CI (13.8, 50.2)] in the natural history group ($p = 0.03$ with chi-square test).

At last observation, 122/152 treated eyes [80.3%; 95% CI (73.0, 86.3)] were on-chart (LogMAR $\leq$ 1.6), as compared to 181/408 natural history eyes [44.4%; 95% CI (39.5, 49.3%)], with a statistically significant difference with both statistical tests ($p < 0.01$) (**Figure 2**, left panel). Similar results were observed when evaluating the REVERSE and RESCUE studies separately, with 85.1% [95% CI (75.0, 92.3)] and 75.6% [95% CI (64.6, 84.7)] of treated eyes being on-chart at last observation, respectively ($p < 0.01$ with both statistical tests vs. natural history eyes).

When using the 1.3-LogMAR response threshold at last observation, 71/152 treated eyes [46.7%; 95% CI (38.6, 55.0)] were responders as compared to 111/408 natural history eyes [27.2%; 95% CI (22.9, 31.8)] ($p < 0.01$ with both statistical tests) (**Figure 2**, right panel).

The proportion of eyes showing a meaningful improvement from nadir of at least 0.3 LogMAR was greater in the treated group as compared to the natural history group: 35/62 [56.5%; 95% CI (43.3, 69.0)] of treated eyes vs. 4/25 [16.0%; 95% CI (4.5, 36.1)] of natural history eyes at month 48 [$p < 0.01$ (chi-square) and $p = 0.02$ (repeated measures)] and 75/152 [49.3%, 95% CI (41.1, 57.6)] of treated eyes vs. 36/127 [28.3%; 95% CI (20.7, 37.0)] of natural history eyes at last observation ($p < 0.01$ with both statistical tests).

TABLE 3 | Visual acuity of treated eyes vs. natural history (NH) eyes at last observation.

	Both eyes				Better eye		Worse eye	
	All treated	REVERSE	RESCUE	NH	All treated	NH	All treated	NH
Number of eyes	152	74	78	408	76	208	76	208
Visual acuity (LogMAR)								
Median	1.40	1.30	1.40	1.70	1.30	1.60	1.45	2.00
Mean (SD)	1.36 (0.60)	1.29 (0.47)	1.43 (0.71)	1.68 (0.61)	1.24 (0.54)	1.57 (0.62)	1.48 (0.64)	1.79 (0.57)
95% CI (mean)	(1.27, 1.46)	(1.18, 1.40)	(1.27, 1.59)	(1.62, 1.74)	(1.12, 1.37)	(1.49, 1.65)	(1.33, 1.63)	(1.71, 1.86)
Mean difference vs. NH (95% CI)	0.31##, ** (0.20, 0.43)	0.38##, ** (0.24, 0.53)	0.25##, ** (0.10, 0.40)	-	0.32## (0.17, 0.48)	-	0.31## (0.15, 0.46)	-

CI, confidence interval; NH, natural history; LogMAR, logarithm of the minimal angle of resolution; SD, standard deviation.
##P < 0.01: statistically significant differences vs. NH eyes using Kruskal–Wallis test.
**P < 0.01: statistically significant difference vs. NH eyes using mixed ANCOVA with repeated measures on a patient.

Newman et al.

Efficacy of rAAV2/2-ND4 in LHON vs. Natural History

	Treated (N = 152 eyes)	Natural history (N = 408 eyes)
Number of eyes	152	408
Time from vision loss to last observation (months)		
Median (range)	39.9 (8.1–51.5)	28.4 (0.0–768.0)
Visual acuity (LogMAR)		
LS means (95% CI)	1.36 (1.26, 1.46)	1.68 (1.62, 1.74)
Effect estimate with 95% CI	0.32 (0.20, 0.44)***	

CI, confidence interval; LogMAR, logarithm of the minimal angle of resolution; LS, least squares.

***P < 0.0001: statistically significant treatment effect using multivariate analysis, with age and duration of follow-up as covariates (repeated measures on a patient).

The treatment effect on responder rates observed for both eyes was similar to that seen when considering better eyes or worse eyes.

DISCUSSION

In this pooled analysis, we demonstrated a sustained and clinically relevant improvement in the visual acuities of *MT-ND4* LHON patients treated with lenadogene nolparvovec when compared to the spontaneous evolution of vision in an external control group comprised of natural history genetically and age-matched LHON patients.

The RESCUE and REVERSE studies demonstrated bilateral visual improvement after unilateral injection with lenadogene nolparvovec in *MT-ND4* LHON patients (14, 15). As the visual improvement was observed in both treated and sham eyes, the primary endpoint, which was based on the difference from baseline between sham and treated eyes, was not met in both studies. RESCUE included subjects at an earlier stage of LHON who had not yet reached their nadir at the time of treatment, so it is perhaps not unexpected that visual outcomes at week 96 had not recovered to the baseline values along the early curve of anticipated visual decline despite clear improvement from nadir. Indeed, from a clinical standpoint, the level of visual improvement achieved from nadir was substantial in both studies, with a mean gain in ETDRS letters at week 96 after treatment of +28 and +24 in REVERSE and of +26 and +23 in RESCUE for treated eyes and sham eyes, respectively. Surprisingly, the earlier treatment (within 6 months after vision loss) in RESCUE did not provide better outcomes than in REVERSE (between 6 and 12 months after vision loss). However, these results are still striking considering that a clinically relevant improvement of visual acuity remains an uncommon feature in *MT-ND4* LHON subjects.
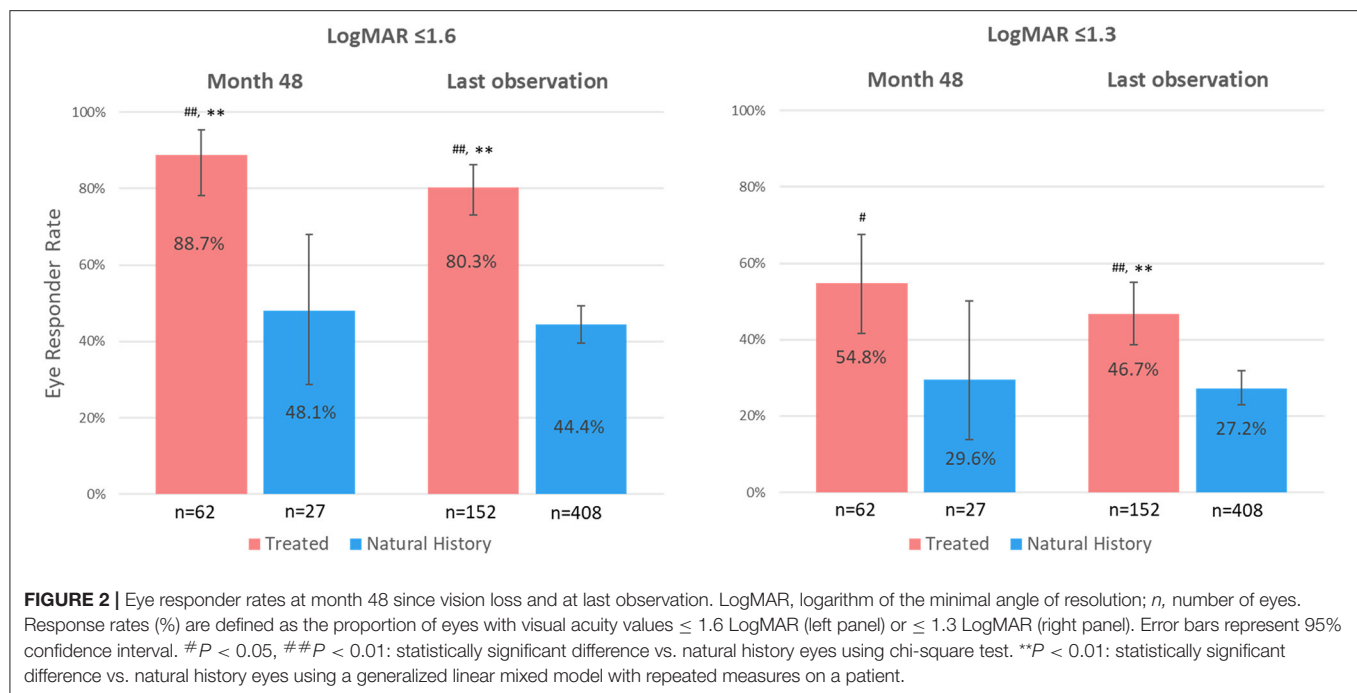
In a recent meta-analysis of untreated *MT-ND4* LHON patients aged at least 15 years at onset of vision loss reported in the world literature, only 11.3% of patients showed some spontaneous visual recovery, although the definitions used for

recovery varied among studies (10). In contrast, the great majority of treated patients (81% for REVERSE and 71% for RESCUE) had a clinically relevant recovery in BCVA from nadir at week 96 after treatment when using a valid recovery endpoint endorsed by an international group of experts (7, 15). While these results are strongly supportive of a treatment-related effect in REVERSE and RESCUE, the absence of an adequate placebo group of untreated subjects in both studies precludes drawing definitive conclusions regarding treatment benefit.

Here we try to address this issue by comparing the visual outcomes of treated patients to an external control group of individual natural history *MT-ND4* LHON patients. The use of an external control in supporting treatment efficacy is acknowledged by many regulatory agencies, and this approach has been increasingly used in rare diseases and in oncology trials where the use of a placebo group is not ethically feasible (32, 33). In this regard, a number of groups, including ours, have conducted LHON registry studies for use as external comparators in drug trials (20, 26, 34). However, these registries are usually limited in size owing to the rarity of the disease, thereby limiting the statistical power of such comparisons. In our own LHON registry study, REALITY, we included a total of 44 LHON patients, of whom only 23 met the inclusion criteria of REVERSE and RESCUE trials (18). In order to reach a sufficient sample size to enable a statistically meaningful comparison with treated patients, we complemented our natural history dataset with patient-level data identified through a systematic review of the literature. This allowed us to build a large database of 208 natural history LHON patients who shared the same characteristics as those included in REVERSE and RESCUE.

This work is the first to thoroughly describe the spontaneous evolution of visual acuity after vision loss in such a large cohort of natural history *MT-ND4* LHON patients. We showed that, in natural history eyes, after the initial acute phase of visual acuity decline to nadir, visual acuity plateaued with no recovery over 2 years (from month 12 to 36 after vision loss). These data are consistent with the known temporal course of clinical and pathophysiological changes in LHON described in the literature (2, 5, 35). Interestingly, in our study, the stable phase of natural history patients was followed by a trend for a later decline in visual acuity from 3 years after onset, suggesting that visual outcomes may continue to deteriorate.

The first thorough investigation of the natural history of visual function of LHON patients dates back to 1963 when van Senus provided a detailed individual description of a Dutch cohort of 27 LHON pedigrees, of whom 12 were later molecularly confirmed as carrying the *MT-ND4* mutation (36, 37). While we could not include these patients in our analyses due to the imprecision of reported visual acuity values (available only as ranges) and uncertainty regarding the timing of measurements after vision loss, these natural history data are overall coherent with those described in our analyses. Indeed the majority of MT-*ND4* patients aged 15 years or older from the van Senus cohort had a poor visual acuity at the time of investigation, with 110/121 (91%) eyes having visual acuity worse than 6/60 (20/200; LogMAR +1.0), 100/121 (83%) eyes worse than 3/60 (20/400; LogMAR +1.3), and 69/121 (57%) eyes worse than 6/300

FIGURE 2 | Eye responder rates at month 48 since vision loss and at last observation. LogMAR, logarithm of the minimal angle of resolution; *n*, number of eyes. Response rates (%) are defined as the proportion of eyes with visual acuity values ≤ 1.6 LogMAR (left panel) or ≤ 1.3 LogMAR (right panel). Error bars represent 95% confidence interval. #$P < 0.05$, ##$P < 0.01$: statistically significant difference vs. natural history eyes using chi-square test. **$P < 0.01$: statistically significant difference vs. natural history eyes using a generalized linear mixed model with repeated measures on a patient.

(20/1,000; LogMAR +1.7). Among those *MT-ND4* patients for whom two visual acuity points in time were reported, only 5/54 (9%) eyes in four patients had documented improvement in visual acuity of at least −0.2 LogMAR between onset of vision loss and time of investigation (36).

In our analysis, a young age at onset was an independent predictor of better visual outcomes. A better prognosis is known to be driven by onset in children of 12 years old or younger (10, 38–40). Here we report that better visual outcomes at younger ages may hold true for patients aged 15 years or older at onset.

In contrast to the evolution seen in natural history eyes, treated eyes followed a clearly distinct pattern, with a sustained, continuous, and progressive improvement in visual acuity from 12 to 52 months after the onset of vision loss. At month 48, there was a statistically significant and clinically relevant difference in the mean visual acuity of 0.33 LogMAR (+16.5 ETDRS letters equivalent) in favor of treated eyes as compared to natural history eyes ($p < 0.01$). This level of improvement translated into a better quality of life for patients in both the REVERSE and RESCUE studies, especially for mental health, dependency, and role difficulty dimensions as measured by the National Eye Institute Visual Function Questionnaire-25 (14, 15). It is noteworthy that the improvement exceeded +15 ETDRS letters, a response level recognized as clinically relevant by regulators (41). Moreover, the magnitude of the treatment effect was not impacted when known confounding variables (onset age and duration of follow-up) were accounted for in multivariate analyses, with a statistically significant and clinically relevant mean difference of 0.32 LogMAR (+16 ETDRS letters) at the last visual acuity measurement in favor of treated eyes. As regards responder rates, most treated eyes (89%) were on-chart at

month 48, compared to less than half (48%) of the natural history eyes (cutoff for response: LogMAR ≤ 1.6). When using the 1.3-LogMAR cutoff for blindness, the responder rates at month 48 (LogMAR ≤ 1.3) were 55% for treated eyes vs. 30% for natural history eyes. Similarly, a higher proportion of treated eyes had a gain from nadir of at least 0.3 LogMAR when compared with natural history eyes (57 vs. 16% at month 48). However, the nadir of natural history studies is not as well-documented as the nadir from RESCUE and REVERSE trials, hence limiting the interpretation of these findings.

Importantly, we included all treated and sham eyes of unilaterally injected patients in our analyses based on the assumption that sham eyes were exposed to lenadogene nolparvovec, presumably by transfer of the viral vector through the optic chiasm (14). Interestingly, the significant treatment effect vs. natural history eyes observed when considering all eyes was maintained in the analyses performed separately on better eyes and on worse eyes, as seen in **Table 3**. A study investigating the effect of unilateral vs. bilateral injection of lenadogene nolparvovec in *MT-ND4* LHON patients is underway and should provide more information on the potential additional benefit provided by bilateral treatment with lenadogene nolparvovec (NCT03293524).

We previously reported that lenadogene nolparvovec improved visual outcomes up to 96 weeks after treatment in REVERSE and RESCUE, which corresponds to ~2.5 years after vision loss (14, 15). Here we extend these findings by showing the persistence of visual benefit in the long term, with continuous improvement in BCVA up to the last available observation [i.e., 51.5 months (4.3 years) from vision loss]. Moreover, the long-term trend depicted in the regression analyses suggests that

Newman et al.

Efficacy of rAAV2/2-*ND4* in LHON vs. Natural History

visual improvement in treated patients may continue to progress with time, in line with the improvement noted up to 7 years after treatment in a small cohort of *MT-ND4* LHON patients treated with another gene therapy product, although the majority of patients in that study were younger than 15 years in age (16). Further results of the ongoing CLIN06 study with follow-up planned for 5 years after treatment (~6 years after vision loss) should provide similar information for patients treated with lenadogene nolparvovec.

To enable a fair comparison in a non-randomized setting and even more so when using an external comparator, it is essential that treated and control groups share comparable characteristics. To ensure the comparability of groups, we carefully selected natural history patients who would have been eligible for our gene therapy trials as regards the age of onset and genotype, two criteria that have been shown to be major determinants of spontaneous recovery in LHON (10). In this report, both treated and natural history groups were typical of the general *MT-ND4* LHON population described in the literature, with a predominance of male patients (around 80%) and a median age at onset in the 20-30 s (5). It should be noted, however, that when compared with treated patients, natural history patients were relatively younger (median age of 23 years vs. 32 years at onset) and were followed for a shorter period of time (median follow-up of 25 vs. 40 months). However, because both a younger age at onset and a shorter follow-up (when visual acuity may not have yet reached its worst level) are associated with a better visual outcome, this imbalance between groups was more likely to disadvantage treated eyes, thus reinforcing the significance of the observed difference between groups. Indeed when these two confounding variables were considered in the multivariate analyses, the difference in visual acuities between treated and natural history eyes was statistically significant (0.32 LogMAR difference in favor of treated eyes, $p < 0.0001$). Furthermore, it should be emphasized that we also retained natural history patients who may have been treated with idebenone, further potentially disfavoring the treated patients who, by study exclusion criteria, were not taking this medication.

Our study has several limitations. Although we used a systematic approach in selecting natural history data from the literature, we excluded studies containing only aggregated patient visual acuity data, which could have led to a potential bias in the inclusion of certain patients. Despite this reduction of the natural history database related to methodological concerns to enable rigorous indirect comparison analyses, the external control group ultimately included a substantial number of patients representative of the *MT-ND4* LHON population. The LOESS method used for describing the evolution of visual acuity is a non-parametric approach which does not take into account the intra-patient correlation, leading to a possible under-estimation of the confidence interval around the fitted curves. As such, the LOESS analysis should be regarded as descriptive in nature rather than inferential. However, we also performed formal statistical tests that took into account the intra-patient correlation, hence supporting the generalizability of

the treatment effect. Furthermore, the treatment effect observed for both eyes was similar to that seen for better and worse eyes, indicating that the impact of inter-eye correlation is minimal on treatment effect. While the time from vision loss to treatment for all 152 treated eyes was 12.8 months, we chose to present our results from month 12. Indeed this does not have any impact on the interpretations of findings, as nearly all eyes (93%) had received the treatment by month 12.

Another concern relates to the heterogeneity of the collected visual acuities in our natural history cohort. Crucially, very few of the natural history studies specified that the visual acuities obtained were BCVAs, and there was no standardized assessment of vision as in rigorously performed clinical trial studies where LogMAR vision is measured using the ETDRS chart using a set protocol. Furthermore, most of the natural history studies were retrospective reviews of their patient cohorts, with most natural history data being cross-sectional (recorded at individual points in time) as opposed to longitudinal for treated eyes (several measurements over time). This difference in the frequency and number of visual acuity assessments per patient may have had an impact on the precision of the visual acuity LOESS model curves for the natural history patients, more so if visual acuity was not always determined with the optimal refraction. However, we believe this had a limited impact on the modelized curves because of the observed stability of the visual acuities over time across the different natural history studies. Furthermore, the most important outcome for the patient is the final visual outcome (last available visual acuity) which was largely reported many months after visual loss onset in the natural history studies that we included in our analyses.

Ultimately, a randomized trial vs. a true parallel placebo group would be the ideal next step to enhance the efficacy of gene therapy with lenadogene nolparvovec. However, there are many barriers to this approach, both operationally and ethically. Among the former include the potentially confounding concurrent, but non-uniform, use of idebenone and the challenges of recruitment for this rare disease. Ethical concerns would include the safety of intravitreal injection of placebo and the absence or delay of treatment in this neurodegenerative disease that is rapidly non-reversible.

In summary, we demonstrate that gene therapy with lenadogene nolparvovec induced a progressive, sustained, and statistically significant improvement of visual acuity up to more than 4 years after vision loss in LHON patients carrying the m.11778G>A mutation when compared to the spontaneous evolution of a large group of matched natural history patients used as an external comparator. Similarly, the same analyses applied to better and worse eyes and to the REVERSE and RESCUE study populations, considered independently, show similar results. The sensitivity analyses controlling for potential confounding factors confirm the robustness of the indirect comparison results. Finally, the strong temporal relationship between the start of improvement and administration of treatment and the size of the treatment effect observed further support the validity of our findings.

Newman et al.

Efficacy of rAAV2/2-*ND4* in LHON vs. Natural History

DATA AVAILABILITY STATEMENT

The raw data supporting the conclusions of this article will be made available by the authors, without undue reservation.

ETHICS STATEMENT

The studies involving human participants were reviewed and approved by For REALITY: Western Copernicus Group IRB (for all US sites); Wills Eye Hospital IRB; Emory University IRB; UCLA Office of Human Research Protection Program; Baylor IRB; Massachusetts Eye and Ear IRB; CPP Sud-Ouest & Outre-Mer 4 (for all French sites); Comitato Etico Area Vasta Emilia Centro; Comitato Etico IRCCS Ospedale San Raffaele di Milano; Agencia Española del Medicamento y Productos Sanitarios (for all Spanish sites); CEICm idcsalud a Catalunya; Health Research Authority (for all UK sites); NRES Committee London Bloomsbury (for all UK sites); Moorfields Eye Hospital NHS Foundation Trust For RESCUE/REVERSE: West London & GTAC Research Ethics Committee; Ethics Committee of the LMU Munich; Comitato Etico Interaziendale Bologna-Imola (CE-BI); CPP Ile-de-France V; Emory IRB; UCLA IRB; Wills Eye Hospital IRB For CLIN06: Wills Eye Hospital IRB; CPP Sud-Est III; LMU Ethikkommission bei der LMU Munchen; NHS South Central - Oxford A Research Ethics Committee; UCLA Institutional Biosafety Committee; Emory University IRB; Comitato Etico di Area Vasta Emilia.

AUTHOR CONTRIBUTIONS

NN, PY-W-M, VC, VB, CV-C, RS, CJ, JS, FM, MR, MT, and J-AS contributed to the conception and design of the studies. NN, PY-W-M, VC, VB, MM, CV-C, RS, TK, AS, J-FG, CL, AD, NJ, CP, and RK contributed to data collection. CJ and FM contributed to statistical analyses. NN, PY-W-M, VC, VB, MM, CV-C, RS, TK, AS, J-FG, CL, AD, NJ, CP, RK, CJ, JS, FM, MR, MT, and J-AS contributed to analysis and interpretation. JS, NN, PY-W-M, and MT contributed to writing and are major contributors in the revisions. All the authors contributed to manuscript revision and read and approved the submitted version.

FUNDING

ACKNOWLEDGMENTS

SUPPLEMENTARY MATERIAL

The Supplementary Material for this article can be found online at: https://www.frontiersin.org/articles/10.3389/fneur.2021.662838/full#supplementary-material

REFERENCES

1. Yu-Wai-Man P, Votruba M, Burté F, La Morgia C, Barboni P, Carelli V. A neurodegenerative perspective on mitochondrial optic neuropathies. *Acta Neuropathol.* (2016) 132:789–806. doi: 10.1007/s00401-016-1625-2

2. Riordan-Eva P, Sanders MD, Govan GG, Sweeney MG, Da Costa J, Harding AE. The clinical features of Leber's hereditary optic neuropathy defined by the presence of a pathogenic mitochondrial DNA mutation. *Brain.* (1995) 118 (Pt 2):319–37. doi: 10.1093/brain/118.2.319

3. Newman NJ, Lott MT, Wallace DC. The clinical characteristics of pedigrees of Leber's hereditary optic neuropathy with the 11778 mutation. *Am J Ophthalmol.* (1991) 111:750–62. doi: 10.1016/S0002-9394(14)76784-4

4. Yu-Wai-Man P, Turnbull DM, Chinnery PF. Leber hereditary optic neuropathy. *J Med Genet.* (2002) 39:162–9. doi: 10.1136/jmg.39.3.162

5. Newman NJ. Hereditary optic neuropathies: from the mitochondria to the optic nerve. *Am J Ophthalmol.* (2005) 140:517–23. doi: 10.1016/j.ajo.2005.03.017

6. Klopstock T, Yu-Wai-Man P, Dimitriadis K, Rouleau J, Heck S, Bailie M, et al. A randomized placebo-controlled trial of idebenone in Leber's hereditary optic neuropathy. *Brain.* (2011) 134:2677–86. doi: 10.1093/brain/awr170

7. Carelli V, Carbonelli M, de Coo IF, Kawasaki A, Klopstock T, Lagrèze WA, et al. International consensus statement on the clinical and therapeutic management of Leber hereditary optic neuropathy. *J Neuroophthalmol.* (2017) 37:371–81. doi: 10.1097/WNO.0000000000000570

8. Catarino CB, von Livonius B, Priglinger C, Banik R, Matloob S, Tamhankar MA, et al. Real-world clinical experience with idebenone in the treatment of Leber hereditary optic neuropathy. *J Neuro-Ophthalmol.* (2020) 40:558–65. doi: 10.1097/WNO.0000000000001023

9. Poincenot L, Pearson AL, Karanjia R. Demographics of a large international population of patients affected by Leber's hereditary optic neuropathy. *Ophthalmology.* (2020) 127:679–88. doi: 10.1016/j.ophtha.2019.11.014

10. Newman NJ, Carelli V, Taiel M, Yu-Wai-Man P. Visual outcomes in Leber hereditary optic neuropathy patients with the m.11778G>A (MTND4) mitochondrial dna mutation. *J Neuroophthalmol.* (2020) 40:547–57. doi: 10.1097/WNO.0000000000001045

11. Cwerman-Thibault H, Augustin S, Lechauve C, Ayache J, Ellouze S, Sahel J-A, et al. Nuclear expression of mitochondrial ND4 leads to the protein assembling in complex I and prevents optic atrophy and visual loss. *Mol Ther Methods Clin Dev.* (2015) 2:15003. doi: 10.1038/mtm.2015.3

12. Vignal C, Uretsky S, Fitoussi S, Galy A, Blouin L, Girmens J-F, et al. Safety of rAAV2/2-ND4 gene therapy for Leber hereditary optic neuropathy. *Ophthalmology.* (2018) 125:945–7. doi: 10.1016/j.ophtha.2017.12.036

13. Vignal-Clermont C, Girmens J-F, Audo I, Said SM, Errera M-H, Plaine L, et al. Safety of intravitreal gene therapy for treatment of subjects with Leber hereditary optic neuropathy due to mutations in the mitochondrial ND4 gene: the REVEAL study. *BioDrugs.* (2021) 35:201-14. doi: 10.1007/s40259-021-00468-9

14. Yu-Wai-Man P, Newman NJ, Carelli V, Moster ML, Biousse V, Sadun AA, et al. Bilateral visual improvement with unilateral gene therapy injection for Leber hereditary optic neuropathy. *Sci Transl Med.* (2020) 12:eaaz7423. doi: 10.1126/scitranslmed.aaz7423

15. Newman NJ, Yu-Wai-Man P, Carelli V, Moster ML, Biousse V, Vignal-Clermont C, et al. Efficacy and safety of intravitreal gene therapy for leber hereditary optic neuropathy treated within 6 months of disease onset. *Ophthalmology.* (2021) 128:649–60. doi: 10.1016/j.ophtha.2020.12.012

16. Yuan J, Zhang Y, Liu H, Wang D, Du Y, Tian Z, et al. Seven-year follow-up of gene therapy for Leber's hereditary optic neuropathy. *Ophthalmology.* (2020) 127:1125–7. doi: 10.1016/j.ophtha.2020.02.023

17. Guy J, Feuer WJ, Davis JL, Porciatti V, Gonzalez PJ, Koilkonda RD, et al. Gene therapy for Leber hereditary optic neuropathy: low- and medium-dose visual results. *Ophthalmology.* (2017) 124:1621–34. doi: 10.1016/j.ophtha.2017.05.016

18. Yu-Wai-Man P, Newman NJ, Carelli V, La Morgia C, Biousse V, Bandello FM, et al. Natural history of patients with Leber hereditary optic neuropathy-results from the REALITY study. *Eye.* (2021). doi: 10.1038/s41433-021-01535-9

19. Hotta Y, Fujiki K, Hayakawa M, Nakajima A, Kanai A, Mashima Y, et al. Clinical features of Japanese Leber's hereditary optic neuropathy with 11778 mutation of mitochondrial DNA. *Jpn J Ophthalmol.* (1995) 39:96–108.

20. Lam BL, Feuer WJ, Schiffman JC, Porciatti V, Vandenbroucke R, Rosa PR, et al. Trial end points and natural history in patients with G11778A leber hereditary optic neuropathy: preparation for gene therapy clinical trial. *JAMA Ophthalmol.* (2014) 132:428–36. doi: 10.1001/jamaophthalmol.2013.7971

21. Nakamura M, Fujiwara Y, Yamamoto M. Homoplasmic and exclusive ND4 gene mutation in Japanese pedigrees with Leber's disease. *Investig Ophthalmol Vis Sci.* (1993) 34:488–495.

22. Qu J, Li R, Zhou X, Tong Y, Yang L, Chen J, et al. Cosegregation of the ND4 G11696A mutation with the LHON-associated ND4 G11778A mutation in a four generation Chinese family. *Mitochondrion.* (2007) 7:140–6. doi: 10.1016/j.mito.2006.11.015

23. Qu J, Zhou X, Zhang J, Zhao F, Sun Y-H, Tong Y, et al. Extremely low penetrance of Leber's hereditary optic neuropathy in 8 Han Chinese families carrying the ND4 G11778A mutation. *Ophthalmology.* (2009) 116:558-64.e3. doi: 10.1016/j.ophtha.2008.10.022

24. Romero P, Fernández V, Slabaugh M, Seleme N, Reyes N, Gallardo P, et al. Pan-American mDNA haplogroups in Chilean patients with Leber's hereditary optic neuropathy. *Mol Vis.* (2014) 20:334–40. Available online at: http://www.molvis.org/molvis/v20/334/

25. Sadun F, De Negri AM, Carelli V, Salomao SR, Berezovsky A, Andrade R, et al. Ophthalmologic findings in a large pedigree of 11778/Haplogroup J Leber hereditary optic neuropathy. *Am J Ophthalmol.* (2004) 137:271–7. doi: 10.1016/j.ajo.2003.08.010

26. Yang S, Yang H, Ma S, Wang S, He H, Zhao M, et al. Evaluation of Leber's hereditary optic neuropathy patients prior to a gene therapy clinical trial. *Medicine (Baltimore).* (2016) 95:e5110. doi: 10.1097/MD.0000000000005110

27. Zhou X, Zhang H, Zhao F, Ji Y, Tong Y, Zhang J, et al. Very high penetrance and occurrence of Leber's hereditary optic neuropathy in a large Han Chinese pedigree carrying the ND4 G11778A mutation. *Mol Genet Metab.* (2010) 100:379–84. doi: 10.1016/j.ymgme.2010.04.013

28. Holladay JT. Proper method for calculating average visual acuity. *J Refract Surg.* (1997) 13:388–91. doi: 10.3928/1081-597X-19970701-16

29. Lange C, Feltgen N, Junker B, Schulze-Bonsel K, Bach M. Resolving the clinical acuity categories "hand motion" and "counting fingers" using the Freiburg Visual Acuity Test (FrACT). *Graefes Arch Clin Exp Ophthalmol.* (2009) 247:137–42. doi: 10.1007/s00417-008-0926-0

30. Guy J, Feuer WJ, Porciatti V, Schiffman J, Abukhalil F, Vandenbroucke R, et al. Retinal ganglion cell dysfunction in asymptomatic G11778A: Leber hereditary optic neuropathy. *Invest Ophthalmol Vis Sci.* (2014) 55:841–8. doi: 10.1167/iovs.13-13365

31. Hwang TJ, Karanjia R, Moraes-Filho MN, Gale J, Tran JS, Chu ER, et al. Natural history of conversion of Leber's hereditary optic neuropathy: a prospective case series. *Ophthalmology.* (2017) 124:843–50. doi: 10.1016/j.ophtha.2017.01.002

32. Augustine EF, Adams HR, Mink JW. Clinical trials in rare disease: challenges and opportunities. *J Child Neurol.* (2013) 28:1142–50. doi: 10.1177/0883073813495959

33. Goring S, Taylor A, Müller K, Li TJJ, Korol EE, Levy AR, et al. Characteristics of non-randomised studies using comparisons with external controls submitted for regulatory approval in the USA and Europe: a systematic review. *BMJ Open.* (2019) 9:e024895. doi: 10.1136/bmjopen-2018-024895

34. Balducci N, Cascavilla ML, Ciardella A, La Morgia C, Triolo G, Parisi V, et al. Peripapillary vessel density changes in Leber's hereditary optic neuropathy: a new biomarker. *Clin Experiment Ophthalmol.* (2018) 46:1055–62. doi: 10.1111/ceo.13326

35. Liu H-L, Yuan J-J, Tian Z, Li X, Song L, Li B. What are the characteristics and progression of visual field defects in patients with Leber hereditary optic neuropathy: a prospective single-centre study in China. *BMJ Open.* (2019) 9:e025307. doi: 10.1136/bmjopen-2018-025307

36. van Senus AH. Leber's disease in the Netherlands. *Doc Ophthalmol.* (1963) 17:1–162. doi: 10.1007/BF00573524

37. Howell N, Oostra R-J, Bolhuis PA, Spruijt L, Clarke LA, Mackey DA, et al. Sequence analysis of the mitochondrial genomes from dutch pedigrees with Leber hereditary optic neuropathy. *Am J Hum Genet.* (2003) 72:1460–9. doi: 10.1086/375537

38. Barboni P, Savini G, Valentino ML, La Morgia C, Bellusci C, De Negri AM, et al. Leber's hereditary optic neuropathy with childhood onset. *Invest Ophthalmol Vis Sci.* (2006) 47:5303–9. doi: 10.1167/iovs.06-0520

39. Majander A, Bowman R, Poulton J, Antcliff RJ, Reddy MA, Michaelides M, et al. Childhood-onset Leber hereditary optic neuropathy. *Br J Ophthalmol.* (2017) 101:1505–9. doi: 10.1136/bjophthalmol-2016-310072

40. Moon Y, Kim US, Han J, Ahn H, Lim HT. Clinical and optic disc characteristics of patients showing visual recovery in Leber hereditary optic neuropathy. *J Neuro-Ophthalmol.* (2020) 40:15–21. doi: 10.1097/WNO.0000000000000830

41. Csaky K, Ferris F, Chew EY, Nair P, Cheetham JK, Duncan JL. Report from the nei/fda endpoints workshop on age-related macular degeneration and inherited retinal diseases. *Invest Ophthalmol Vis Sci.* (2017) 58:3456–63. doi: 10.1167/iovs.17-22339

Conflict of Interest: NN is a consultant for GenSight, Santhera Pharmaceuticals, and Stealth BioTherapeutics, has received research support from GenSight and Santhera Pharmaceuticals, has served on the Data Safety Monitoring Board for the Quark NAION study, and is a medical–legal consultant. PY-W-M is a consultant for GenSight and Stealth BioTherapeutics and has received research support from GenSight and Santhera Pharmaceuticals. VC is a consultant for Santhera Pharmaceuticals, GenSight, and Stealth BioTherapeutics and has received research support from Santhera Pharmaceuticals and Stealth BioTherapeutics. VB is a consultant for GenSight, Santhera Pharmaceuticals, and Stealth BioTherapeutics and has received research support from GenSight and Santhera Pharmaceuticals. MM is a consultant for GenSight Biologics and has received research support from GenSight. CV-C is a consultant for GenSight Biologics and Santhera Pharmaceuticals. RS is a consultant for GenSight Biologics. TK is a consultant for Santhera Pharmaceuticals, Chiesi, and GenSight Biologics and has received research support from Santhera Pharmaceuticals, GenSight Biologics, and Stealth BioTherapeutics. AS is a consultant for Stealth BioTherapeutics. CJ is an employee of eXYSTAT and a consultant for GenSight Biologics. FM is a co-founder of eXYSTAT and a consultant for GenSight Biologics. JS is a consultant for GenSight Biologics. MR and MT are GenSight Biologics employees. J-AS is a co-founder and shareholder of GenSight Biologics and a patent co-author on allotopic transport.

The remaining authors declare that the research was conducted in the absence of any commercial or financial relationships that could be construed as a potential conflict of interest.

The reviewer GS declared a past co-authorship with two of the authors NN, VB the handling editor.

Check for
updates

Leber Hereditary Optic Neuropathy: Review of Treatment and Management

Rabih Hage* and Catherine Vignal-Clermont

Neuro-ophthalmology Department, Hôpital Fondation Rothschild, Paris, France

Leber hereditary optic neuropathy (LHON) is a maternally inherited mitochondrial disease that specifically targets the retinal ganglion cells by reducing their ability to produce enough energy to sustain. The mutations of the mitochondrial DNA that cause LHON are silent until an unknown trigger causes bilateral central visual scotoma. After the onset of loss of vision, most patients experience progressive worsening within the following months. Few of them regain some vision after a period of ~1 year. Management of LHON patients has been focused on understanding the triggers of the disease and its pathophysiology to prevent the onset of visual loss in a carrier. Medical treatment is recommended once visual loss has started in at least one eye. Research evaluated drugs that are thought to be able to restore the mitochondrial electron transport chain of the retinal ganglion cells. Significant advances were made in evaluating free radical cell scavengers and gene therapy as potential treatments for LHON. Although encouraging the results of clinical trial have been mixed in stopping the worsening of visual loss. In patients with chronic disease of over 1 year, efficient treatment that restores vision is yet to be discovered. In this review, we summarize the management strategies for patients with LHON before, during, and after the loss of vision, explain the rationale and effectiveness of previous and current treatments, and report findings about emerging treatments.

Keywords: Leber's optic neuropathy, idebenone, gene therapy, mitochondrial disease, visual loss

INTRODUCTION

Inherited mitochondrial diseases (IMDs) are maternally transmitted genetic disorders involving defective cellular energy production. Management and treatment of IMDs remain major challenges for modern medicine due to their rare and heterogeneous nature. Dramatic progress has been achieved in understanding their pathogenesis, but, to date, this has not led to the discovery of a cure.

Leber hereditary optic neuropathy (LHON) is one of the most common IMDs. In 90% of cases, it is caused by one of three primary point mitochondrial mutations. These mutations are clinically silent until some yet unknown trigger induces a respiratory chain dysfunction in the retinal ganglion cells, leading to decreased vision in both eyes (in most cases sequentially, from a few weeks to a few months apart). The loss of vision usually consists in bilateral central scotoma, but the entire visual field can be lost in the most severe cases. Because it involves a specific cell type and permits the administration of treatment during the window of time between the onset of vision loss in the first and second eyes, LHON is a good candidate for clinical trials.

In the last few years, clinical trials for gene therapy as well as idebenone, a synthetic analog of coenzyme Q_{10}, have sought to reduce the impact and progression of LHON after its onset. So far, these trials have received most attention. Though encouraging however, the results have been mixed.

In this review, we summarize the management strategies for patients with LHON before, during, and after the loss of vision, explain the rationale and effectiveness of previous and current treatments, and report findings about emerging treatments.

PATHOPHYSIOLOGY AND ANIMAL MODEL

Retinal ganglion cells (RGCs) are neurons located in the inner part of the retina. Their axons bundle around the optic disc and, as they pass through the lamina cribrosa, form the optic nerve. These axons are divided into a myelinated postlaminar part and a non-myelinated prelaminar segment that has higher energy needs and concentration of mitochondria than most, if not all other, neurons. RGCs find their energy in the oxidative phosphorylation (OXPHOS) of nutrients that happens in the mitochondria and produces adenosine triphosphate (ATP). OXPHOS involves several enzymes, including the nicotinamide adenine dinucleotide (NADH):ubiquinone oxidoreductase, also known as NADH dehydrogenase or complex I, which is compounded of several subunits. Three primary point mitochondrial DNA (mtDNA) mutations are found in 90% of LHON patients. These mutations affect different subunits of NADH dehydrogenase, causing dysfunction of the electron transport chain (ETC), decrease in ATP production, and excessive generation of reactive oxidative species (ROS), leading to energy production failure and, eventually, cell death. The result is visual loss in symptomatic patients (1). Beginning with the most frequent, the primary three point mutations are: G11778A, T14484, and G3460A. Since they affect, respectively, subunits 4, 6, and 1 of the NADH dehydrogenase, they are referred to as ND4, ND6, and ND1 mutations. It is virtually impossible to differentiate these mutations clinically at the acute phase of the disease, but the most common one, ND4, has the worst prognosis, with only 4% chance of visual recovery (2). A recent meta-analysis by Newman et al. gathered information about visual outcome in patients with the ND4 mutation from 15 studies (12 retrospective and 3 prospective) (3). They showed that visual recovery, whose definition varied across the studies covered, occurred in 23 out of 204 patients.

Other mutations might be dominant in selected population groups with fewer available genetic data. Non-primary mutations have heterogeneous prognosis, and a limited number of case reports have been published, which prohibit drawing broad conclusions about the severity of each mutation (4).

Visual loss in LHON is directly related to RGC injury and death and, therefore, to the impaired energy production of RGC mitochondria. Research has focused on restoring ATP production in a complex I-deficient mitochondria as well as on identifying the cascade of events that triggers complex I dysfunction. An animal model of complex I deficiency was developed by Zhang et al. (5) in order to test candidate drug treatments. This model consisted in intravitreous injection of a complex I inhibitor (rotenone) in mice's eyes. The effect was consistent with the degeneration of RGC in LHON (5). This animal model has been used to test the neuroprotective strategies discussed in Section Prevention below (6).

PREVENTION

Clinicians face two possible scenarios when it comes to a LHON patient. First, the patient has developed recent visual loss and all the medical efforts are focused on reducing its severity. Second, the patient is asymptomatic but knows that he has inherited the mutation from their mother. Here, the clinician's primary concern is to identify the risk factors that can trigger the disease.

However, not all LHON mutation carriers experience loss of vision. Most reports have given penetrances as high as 50–60% in males and 10–20% in females (7–10), although lower penetrances (of 20–27% in males and 4–8% in females) have also been reported in larger cohorts (11). Age is a confounding factor since some late-onset cases have been reported and since younger asymptomatic individuals could have developed symptoms later in their life (12). Why some carriers never develop any symptoms is currently unknown. It is believed that a combination of genetic and environmental influences play a significant role.

Risk Factors for Visual Loss in LHON
Genetic Risk Factors
Penetrance seems not to be related to the type of mutation (11). In the large majority of LHON patients, the mutations are homoplasmic mutants, but the disease has also been reported in heteroplasmic individuals. However, these genetic results should be interpreted with caution since mtDNA in peripheral blood might not reflect the heteroplasmic load in the RGC (13). Finally, it has been shown that the high sequence variability of the mitochondrial genome, which characterizes the different mtDNA haplogroups, modulates the penetrance of IMDs in general, and LHON in particular. Haplotype J is believed to be associated with higher susceptibility to LHON mutations because of a lower amount of mtDNA and mtDNA-encoded polypeptides (14). This might be useful for studying large cohorts but is of little value when it comes to evaluating risk for LHON in individual carriers. At the level of the individual, it has been shown that increased mitochondrial mass protects against the adverse effects of LHON mutation. Giordano et al. (15) have shown in 2014 that mitochondrial mass might explain the variability in penetrance of LHON mutations.

Environmental Risk Factors
LHON is characterized by rapidly progressive, though painless, loss of vision with central visual scotoma. This presentation is shared with toxic and nutritional optic neuropathies (TNONs), with the exception that, in the latter, visual loss is experienced simultaneously in both eyes. Because of these common clinical features, toxic substances such as tobacco and alcohol are pointed out as possible triggers for LHON. Discontinuation of intoxication can bring about some visual improvement in TNON.

This has led some authors to try tobacco smoke antagonists as a possible treatment for LHON. In 1968, Foulds et al. (16) realized that hydroxocobalamine (vitamin B12) had shown efficiency at treating what was then called "tobacco amblyopia" and decided to treat LHON patients with it. They suspected that the cyanogenic substances contained in tobacco smoke might trigger LHON. Twenty years later, Berninger studied rhodanese activity in LHON patients (17). Berninger thought this mitochondrial enzyme could play a role in the pathophysiology of LHON since it was known to detoxify cyanide by converting it to thiocyanate. Thirteen LHON patients where tested for rhodanese activity, including one at the acute phase of the disease, but none showed abnormal results. Cyanide levels in the blood were also within normal limits.

Preventive Measures

In 2009, Kirkman et al. conducted a large, multicenter epidemiological study of 196 affected and 206 unaffected carriers of one of the three primary mtDNA mutations. They identified a strong and consistent association between visual loss and smoking, independent of gender and alcohol intake, with a clinical penetrance of 93% in men who smoked (18). The authors concluded that patients should be advised to stop smoking and to reduce their consumption of alcohol.

There is indisputable evidence that tobacco and alcohol play a role in triggering LHON. Other, currently unknown, environmental factors must be implicated since the disease also affects children as well as adults with no history of smoking or drinking. However, childhood-onset LHON has a better prognosis for visual acuity (19).

MEDICAL TREATMENT

Antioxidants

Oxidative stress modulation has been at the center of IMD treatment strategies. The theoretical goal is to increase mitochondrial respiration and reduce ROS that are produced by IMDs. Various molecules have been tried, with different combinations of vitamins (B2, B3, B12, C, E, and folic acid), ubiquinone, and other supplements (e.g., alpha-lipoic acid, carnitine, creatine, L-arginine, glutathion, and dichloroacetate) (20–22). Unfortunately, there is not enough scientific evidence to support their use in LHON.

The ubiquinone family was the most promising treatment. It includes coenzyme Q_{10}, an electron shuttle between complex I and complex II of the ETC in the mitochondrial membrane. Coenzyme Q_{10} has been beneficial in other IMDs in which its deficiency causes encephalomyelopathy, but it has not shown improvement in LHON, although a few case reports suggested otherwise (23, 24). A major limitation of coenzyme Q_{10} is its inability to cross the blood–brain barrier when taken orally. To address this issue, idebenone, a synthetic hydrosoluble analog of coenzyme Q_{10}, was developed. Idebenone showed a protective effect against complex I-deficient retinal ganglion cell death *in vitro*. It also allowed recovery of vision in rotenone mice (25). The first report of a LHON patient treated with it was

FIGURE 1 | Algorithm for management of patients with Leber optic neuropathy mutation.
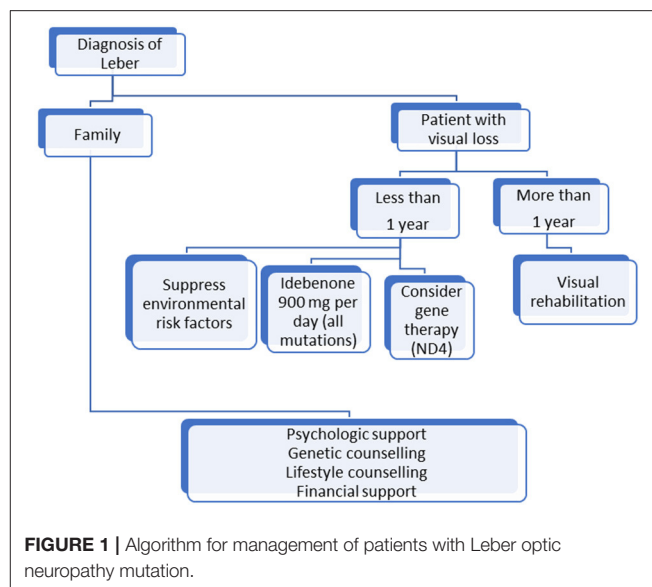
published in the Lancet in 1992. A 10-year-old boy with the ND4 mutation was started with 90 mg of idebenone daily, and his vision improved from 6/90 OU to 6/6 in the right eye after 4 months and in the left eye after 7 months (26). Other isolated case reports and small retrospective open-labeled studies have further supported the claim that idebenone might be an effective treatment for improving vision or shortening time to visual recovery in LHON (27–29). In 2011, the "Rescue of Hereditary Optic Disease Outpatient Study" (RHODOS) prospectively randomized 85 patients with LHON with <5 years of visual loss to either a group that received idebenone 900 mg/day or to a group that received a placebo in a double-blinded fashion (30). Treatment lasted 24 weeks; it was found safe and well-tolerated. Primary end point was the best recovery in visual acuity. The study failed to show any significant differences in this regard between the active drug and the placebo. However, a trend was noticed in favor of idebenone when the authors analyzed changes in best visual acuity and excluded patients with the 14488 mutation, known for a higher rate of spontaneous recovery. Two years later, the same team reported persistence of the treatment effect in 60 out of the 85 patients included in the first study (31). The lack of significance of RHODOS might have been linked to the inclusion criteria. Patients with a disease onset as old as 5 years were included. For some of them, optic atrophy had already reached its peak. The likelihood of a positive response was higher among patients with more recent disease onset. In the light of these results, idebenone (Raxone®) was approved by the European Medicine Agency to treat LHON in 2015 in adolescents and adult patients at 900 mg/day divided into three doses. As of 2021, a non-interventional study is ongoing, the "Post-Authorisation Safety Study with Raxone® in LHON Patients" (PAROS) study (NCT02771379). It aims to evaluate the long-term safety effectiveness profiles of idebenone when used under conditions of routine clinical care.

Gene Therapy

Bases for Gene Therapy in LHON

In genetic diseases, symptoms are linked to the absence of a protein produced by a gene that is missing or mutated. The goal of gene therapy (GT) is to allow the production of a functional protein by delivering, into a target cell, a copy of a gene that does not include the deleterious mutation. GT uses viral vectors to deliver the desired gene to the nucleus of the target cell. In IMDs, the defective gene is in the mitochondria so the ideal scenario would be to deliver the copy of the gene there. However, this has been impossible, given that mitochondria have a double-membrane structure that constitutes a physical barrier for gene therapy. Furthermore, a higher amount of gene would have to be delivered to a sufficient number of mitochondria in each cell in order to achieve efficacy. Because of these restrictions, a technique called "allotopic expression" has been developed. It consists in functional relocation of mitochondrial genes into the nucleus, followed by import of the gene-encoded polypeptide from the cytoplasm into the mitochondria (32–34).

In LHON, GT consists in delivering a gene to the nucleus of the RGC. This leads to the production, in the cytoplasm or the ribosomes of the RGCs, of a protein that is then redirected into the mitochondria. The goal, more specifically, is to introduce an unmutated MT-ND4 gene into the patient's RGC mitochondria. In 2002, Guy et al. were the first team to use an adeno-associated viral vector (AAVV) to transfect a synthetic ND4 subunit into the mitochondria of cybrids with the ND4 mutation (35). The transfected cells produced three times as much ATP than the mock-transfected cybrids, which the authors interpreted as a successful restoration of complex I-dependent respiration. A series of animal experiments followed, in which rabbit, rat, and murine models received AAVV-mediated gene delivery of human ND4 intravitreously. The different teams showed that injection technique was safe and that there was no ocular complication related to the treatment itself. They also showed mitochondrial internalization of the AAVV, expression of its genetic content, and complementation of the pathogenic phenotype (36–42). Because the ND4 mutation is the most common cause of LHON, GT efforts tend to focus on it. Patients with ND1, ND6, or other LHON mutations are not candidates for gene therapy as of 2021.

Clinical Trials

In 2016, Feuer et al. reported the first case series of five legally blind patients with ND4 mutation who were treated with gene therapy in one eye as part of a wider clinical trial meant to evaluate the efficacy of this treatment in LHON. Four out of five participants had visual loss for over 1 year. Three-month follow-up was reported. No patient experienced serious safety events. Two of them showed significant increase in visual acuity (hand motion to seven letters in one and to 15 letters in the second). Interestingly, the patient who had the most dramatic improvement in his visual acuity also showed visual improvement in the contralateral non-injected eye (43). Low and medium doses were used to treat these patients as well as another nine patients whose cases were reported subsequently in 2017 (44). The authors found that the difference in visual acuity between the treated and untreated eye was significantly higher

than what they found in their previous natural history study (45). From an anatomical standpoint, there were no significant differences in the thickness of the retinal fiber layers.

GT took a step forward in 2017 with two phase III clinical trials called *rescue* and *reverse* that only differed in the duration of vision loss (≤6 months for rescue, and >6 months to 1 year for reverse). These studies were randomized, double masked, sham controlled, and multicentric. Included patients had one eye injected with GS010, a recombinant, adeno-associated virus containing a modified cDNA encoding the human wild-type mitochondrial ND4 protein and supporting allotopic expression. The other eye received a sham injection. On average, patients experienced an improvement in their visual acuity of about three lines (15 letters). Surprisingly, a similar improvement of about 13 letters was reported in the other, sham-treated eye. This raised suspicion of transfer of viral vector DNA from the injected eye to the fellow eye, through the optic pathways. A recent non-human primate study demonstrated that this type of transfer is possible (46).

These results are encouraging, but the visual improvement remains limited and variable. GT needs more assessment before it is deemed efficient and is used as a routine care option in LHON. A new clinical trial using GS010 called *reflect* is currently ongoing. In it, patients have both eyes injected with the active drug. Enrollment is over now, and the first results are expected in the next few months.

Other Medical Treatments

Other treatments than idebenone continue to be used to improve visual acuity in LHON. Reports exist for each modality, and they mostly represent therapeutic interventions that are supported by very few medical teams, if not just one.

EPI-743

Alpha-tocotrienol quinone (EPI-743) is a para-benzoquinone that replenishes glutathione stores and has proved to be 1,000 times more efficient than idebenone at reducing oxidative stress *in vitro* (47, 48). This neuroprotective and antioxidant drug demonstrated visual improvement in four out of five LHON patients in whom it was started <4 months after the onset of visual loss (49). EPI-743 has been used in other IMDs, but further investigations are needed to validate its usefulness in LHON (50).

Cyclosporine

Cyclosporine A inhibits the opening of the mitochondrial permeability transition pore that plays a crucial role in damage-induced cell death, thereby blocking the apoptosis. Its therapeutic potential in LHON has been evaluated prospectively in five patients with confirmed primary mitochondrial DNA mutations and strictly unilateral optic neuropathy that occurred within 6 months prior to enrollment. Despite treatment with oral cyclosporine A, all patients eventually experienced bilateral eye involvement within 11–65 weeks after the initiation of treatment. Over the study time period, the average best-corrected visual acuity worsened in the first affected eye. By the end of the study, both eyes were equally affected (51).

Brimonidine

Brimonidine is an α-2 agonist that is routinely used, as a topical agent, to lower the intraocular pressure in open-angle glaucoma (52). Experimental studies on rats have shown that brimonidine can have a neuroprotective effect on injured optic nerves by reducing apoptosis in cases of elevated intraocular pressure or retinal ischemia (53). In an open-labeled trial, brimonidine was used in nine LHON patients who had recently developed visual loss in one eye. The drug failed to prevent the involvement of the second eye. The authors hypothesized that apoptosis might not be a significant mechanism in RGC death in LHON or that RGC already presented asymptomatic irreversible injury when treatment was started (54).

Perspective

New treatment strategies are being considered, but some have never been tested clinically.

- Nutritional interventions are thought to have the potential to enhance mitochondrial bioenergetic capacity. Ketogenic diet (high in fat and low in carbohydrates) mimics the state of ketosis induced by starvation and is thought to have a neuroprotective effect by increasing antioxidant capacity (55, 56).
- The Stem Cell Ophthalmology Treatment Study (SCOTS) included five LHON patients who were given autologous stem cell concentrate through a combination of different modalities (retrobulbar injection, intravitreous injection, vitrectomy with subretinal injection, and intravenously). Three of them had improvement of their vision from hand motion or count finger to a measurable acuity in one eye. However, these three patients did not have the ND4 mutation and were treated at an early stage of their disease. Another study of bone marrow-derived mesenchymal stem cell therapy, SCOTS2, is ongoing. Further evaluation are needed to draw a conclusion on the efficacy of stem cell therapy in LHON (57).
- Mitochondrial biogenesis is a physiological process in which cells increase the mass and number of their mitochondria, allowing greater energy production. Increased mitochondrial biogenesis happens in LHON carriers and is thought to have a protective effect (15). Theoretically, pharmaceutical activation of mitochondrial biogenesis could be used as prevention in carriers, but this complex process is not yet fully understood.
- The gender bias in LHON has led some authors to consider the potential protective value of estrogens and their interactions with RGCs. Pisano et al. have shown that estrogens that bind specifically to receptors located in RGCs can reduce apoptosis in LHON cybrid cells carrying the ND4 mutation (58). The authors concluded that estrogens should be considered a potential preventive measure in carriers and called for a trial in the LHON genetic mouse model.
- Regenerative medicine aims to replace damaged cells. It encompasses several modalities, including induced pluripotent stem cells (iPSCs). In the case of LHON, and most chronic optic neuropathies, the target cells would be the RGCs. Regenerative medicine would be considered when a significant number of RGCs has been lost after the onset of the optic neuropathy. Multiple iPSC lines have been generated from fibroblasts of LHON patients. These lines offer unique opportunities to investigate LHON phenotypes and regulatory mechanisms at the cellular level (59–61). Unfortunately, the generated cells are not organized as they would be in the retina, which prevents their use in cell therapy. 3D approaches that rely on retinal cells other than RGCs are currently under development. Their goal is to allow the iPSC-derived RGCs to be integrated into an environment where they can interact with other constituents of the retinal tissue (62). The greatest challenge of regenerative medicine is ultimately to allow regeneration of the optic nerve itself. To do this, the cells obtained would have to first reach their target location in the retina and then send their axons all the way to the lateral geniculate body, with half of them crossing the optic chiasm along the way (63).
- Mitochondrial replacement therapy (MRT) is a technology that uncouples the inheritance of mtDNA from nuclear DNA. There are several techniques for MRT that differ in the biological form of the nuclear genome when it is transferred within the karyoplast, all of which combine the mother's nuclear DNA with unaffected mtDNA. Hyslop et al. reported the first preclinical study on the pronuclear transfer technique in 2016. This technique consists in transferring the pronuclei from a zygote to another enucleated one. It was shown to restore mitochondrial function even though it only led to a reduction, rather than a complete replacement, of the mutant load (64). In LHON, a technique using iPSC-derived RGCs allowed significant reduction in the level of apoptosis in cybrid-corrected RGCs (65). MRT has never been used to prevent the transmission of a LHON mutation. The first human born from MRT was reported in 2017 by Zhang et al. In that case, MRT was administered to prevent a mitochondrial disease that would have resulted in the *in utero* death of the embryo (66). Because it entails the manipulation of human gametes in a similar way to cloning techniques, MRT raises ethical concerns that still need to be addressed as the technology evolves.

SUPPORTIVE TREATMENT

In LHON, visual impairment can be sudden and dramatic. Few patients recover enough vision to resume a normal life. Thus, LHON is often experienced as an earthquake in the life of an otherwise healthy individual. The lack of efficient treatment leads to situations where patients seek medical advice from multiple specialists, and the main complaints are low vision and inability to cope with simple, everyday tasks. Patients can feel or become dependent as they are unable to mourn the loss of normal vision, as they have experienced it until then. The disease often comes with devastating social cost that caregivers must not overlook.

Psychological Complications

Reactive depression is common, and a patient's social network can be of great help. However, psychological support must always be offered to all patients after a diagnosis of LHON, whether they are symptomatic or not. In a study about psychological

morbidity of LHON, half of the 103 included patients met the depression criteria after vision loss. The authors found that older age was correlated with higher depression prevalence than younger age (67).

Genetic Counseling

Genetic counseling allows patients to adapt to the psychological and familial implications of LHON. However, the only certainty it gives them is that men will not transmit the mutation to their offspring while women will transmit it to all of theirs. Other variables, such as the risk that siblings of affected individuals will also develop visual loss, are impossible to predict.

Low Vision Rehabilitation

LHON patients are good candidates for low vision rehabilitation (LVR) when they have a central scotoma and residual peripheral visual field. Patients are taught skills to adapt to their vision and optimize their use of the residual visual field. Reading aids, such as magnifiers or filters, are of great help for improving vision-related quality of life in these patients (68).

INTERNATIONAL CONSENSUS STATEMENT

At a conference held in Milan in 2016, a panel of experts from Europe and North America provided consensus statements about therapeutic management of LHON. These statements sought to address the concerns of clinicians and to help in the decision-making process for patient clinical management. There was

strong consensus that positive prognostic factors, such as young age or ND6 mutation, do not affect management. The panel concluded that the first-line treatment for non-chronic patients (<1 year since the onset of the disease) should include idebenone at a dose of 900 mg/day for at least 1 year, but that there was no evidence that recommended treatment in the case of chronic ones (over 1 year after the onset in the second eye). For relatives, they recommended lifestyle counseling without treatment (69). At the time, GT was not included in the panel's therapeutic recommendations.

Based on these recommendations, we propose a simple algorithm in **Figure 1** for LHON patients' management. Research has made great progress but, until an efficient treatment that restores vision is discovered, LHON management must be multidisciplinary and life-long and include prevention and rehabilitation, which remain the only ways to improve patients' quality of life.

AUTHOR CONTRIBUTIONS

RH and CV-C contributed equally in the writing of this manuscript. Both authors contributed to the article and approved the submitted version.

ACKNOWLEDGMENTS

REFERENCES

1. Bahr T, Welburn K, Donnelly J, Bai Y. Emerging model systems and treatment approaches for Leber's hereditary optic neuropathy: challenges and opportunities. *Biochim Biophys Acta Mol Basis Dis.* (2020) 1866:165743. doi: 10.1016/j.bbadis.2020.165743

2. Oostra RJ, Bolhuis PA, Wijburg FA, Zorn-Ende G, Bleeker-Wagemakers EM. Leber's hereditary optic neuropathy: correlations between mitochondrial genotype and visual outcome. *J Med Genet.* (1994) 31:280–86. doi: 10.1136/jmg.31.4.280

3. Newman NJ, Carelli V, Taiel M, Yu-Wai-Man P. Visual outcomes in Leber hereditary optic neuropathy patients with the m.11778G>A (MTND4) mitochondrial DNA mutation. *J Neuroophthalmol.* (2020) 40:547–57. doi: 10.1097/WNO.0000000000001045

4. Achilli A, Iommarini L, Olivieri A, Pala M, Hooshiar Kashani B, Reynier P, et al. Rare primary mitochondrial DNA mutations probable synergistic variants in Leber's hereditary optic neuropathy. *PLoS ONE.* (2012) 7:e42242. doi: 10.1371/journal.pone.0042242

5. Zhang X, Jones D, Gonzalez-Lima F. A potential model for Leber's hereditary optic neuropathy: rotenone effects on retinal ganglion cells. *Invest Ophthalmol Vis Sci.* (2002) 43:235–235.

6. Rojas JC, Gonzalez-Lima F. Mitochondrial optic neuropathy: *in vivo* model of neurodegeneration and neuroprotective strategies. *Eye Brain.* (2010) 2:21–37. doi: 10.2147/EB.S9363

7. Seedorff T. The inheritance of Leber's disease. *Acta Ophthalmologica.* (1985) 63:135–145. doi: 10.1111/j.1755-3768.1985.tb01526.x

8. Harding AE, Sweeney MG, Govan GG, Riordan-Eva P. Pedigree analysis in Leber hereditary optic neuropathy families with a pathogenic mtDNA mutation. *Am J Hum Genet.* (1995) 57:77–86.

9. Man PYW, Turnbull DM, Chinnery PF. Leber hereditary optic neuropathy. *J Med Genet.* (2002) 39:162–9. doi: 10.1136/jmg.39.3.162

10. Nikoskelainen EK, Savontaus M-L, Wanne OP, Katila MJ, Nummelin KU. Leber's hereditary optic neuroretinopathy, a maternally inherited disease: a genealogic study in four pedigrees. *Arch Ophthalmol.* (1987) 105:665–71. doi: 10.1001/archopht.1987.01060050083043

11. Puomila A, Hämäläinen P, Kivioja S, Savontaus M-L, Koivumäki S, Huoponen K, et al. Epidemiology and penetrance of Leber hereditary optic neuropathy in Finland. *Eur J Hum Genet.* (2007) 15:1079–89. doi: 10.1038/sj.ejhg.5201828

12. Ajax ET, Kardon R. Late-onset Leber's hereditary optic neuropathy. *J Neuroophthalmol.* (1998) 18:30–1. doi: 10.1097/00041327-199803000-00007

13. Caporali L, Maresca A, Capristo M, Del Dotto V, Tagliavini F, Valentino ML, et al. Incomplete penetrance in mitochondrial optic neuropathies. *Mitochondrion.* (2017) 36:130–7. doi: 10.1016/j.mito.2017.07.004

14. Gómez-Durán A, Pacheu-Grau D, Martínez-Romero Í, López-Gallardo E, López-Pérez MJ, Montoya J, et al. Oxidative phosphorylation differences between mitochondrial DNA haplogroups modify the risk of Leber's hereditary optic neuropathy. *Biochim Biophys Acta.* (2012) 1822:1216–22. doi: 10.1016/j.bbadis.2012.04.014

15. Giordano C, Iommarini L, Giordano L, Maresca A, Pisano A, Valentino ML, et al. Efficient mitochondrial biogenesis drives incomplete penetrance in Leber's hereditary optic neuropathy. *Brain.* (2014) 137:335–53. doi: 10.1093/brain/awt343

16. Foulds WS, Cant JS, Chisholm IA, Bronte-Stewart J, Wilson J. Hydroxocobalamin in the treatment of Leber's hereditary optic atrophy. *Lancet.* (1968) 1:896–7. doi: 10.1016/S0140-6736(68)90243-2

17. Berninger TA, von Meyer L, Siess E, Schon O, Goebel FD. Leber's hereditary optic atrophy: further evidence for a defect of cyanide metabolism? *Br J Ophthalmol.* (1989) 73:314–6. doi: 10.1136/bjo.73.4.314

18. Kirkman MA, Yu-Wai-Man P, Korsten A, Leonhardt M, Dimitriadis K, De Coo IF, et al. Gene–environment interactions in Leber hereditary optic neuropathy. *Brain.* (2009) 132:2317–26. doi: 10.1093/brain/awp158

19. Majander A, Bowman R, Poulton J, Antcliff RJ, Reddy MA, Michaelides M, et al. Childhood-onset Leber hereditary optic neuropathy. *Br J Ophthalmol.* (2017) 101:1505–9. doi: 10.1136/bjophthalmol-2016-310072

20. Pfeffer G, Majamaa K, Turnbull DM, Thorburn D, Chinnery PF. Treatment for mitochondrial disorders. *Cochrane Database Syst Rev.* (2012) 2012:CD004426. doi: 10.1002/14651858.CD004426.pub3

21. Newman NJ. Treatment of Leber hereditary optic neuropathy. *Brain.* (2011) 134:2447–50. doi: 10.1093/brain/awr192

22. Ghelli A, Porcelli AM, Zanna C, Martinuzzi A, Carelli V, Rugolo M. Protection against oxidant-induced apoptosis by exogenous glutathione in Leber hereditary optic neuropathy cybrids. *Invest Ophthalmol Vis Sci.* (2008) 49:671–6. doi: 10.1167/iovs.07-0880

23. Hargreaves IP. Coenzyme Q10 as a therapy for mitochondrial disease. *Int J Biochem Cell Biol.* (2014) 49:105–11. doi: 10.1016/j.biocel.2014.01.020

24. Huang C-C, Kuo H-C, Chu C-C, Kao L-Y. Rapid visual recovery after coenzyme q10 treatment of leber hereditary optic neuropathy. *J Neuroophthalmol.* (2002) 22:66. doi: 10.1097/00041327-200203000-00036

25. Heitz FD, Erb M, Anklin C, Robay D, Pernet V, Gueven N. Idebenone protects against retinal damage and loss of vision in a mouse model of Leber's hereditary optic neuropathy. *PLoS ONE.* (2012) 7:e45182. doi: 10.1371/journal.pone.0045182

26. Mashima Y, Hiida Y, Oguchi Y. Remission of Leber's hereditary optic neuropathy with idebenone. *Lancet.* (1992) 340:368–9. doi: 10.1016/0140-6736(92)91442-B

27. Mashima Y, Hiida Y, Oguchi Y. Lack of differences among mitochondrial DNA in family members with Leber's hereditary optic neuropathy and differing visual outcomes. *J Neuroophthalmol.* (1995) 15:15–9. doi: 10.1097/00041327-199503000-00004

28. Cortelli P, Montagna P, Pierangeli G, Lodi R, Barboni P, Liguori R, et al. Clinical and brain bioenergetics improvement with idebenone in a patient with Leber's hereditary optic neuropathy: a clinical and 31P-MRS study. *J Neurol Sci.* (1997) 148:25–31. doi: 10.1016/S0022-510X(96)00311-5

29. Mashima Y, Kigasawa K, Wakakura M, Oguchi Y. Do idebenone and vitamin therapy shorten the time to achieve visual recovery in Leber hereditary optic neuropathy? *J Neuroophthalmol.* (2000) 20:166–70. doi: 10.1097/00041327-200020030-00006

30. Klopstock T, Yu-Wai-Man P, Dimitriadis K, Rouleau J, Heck S, Bailie M, et al. A randomized placebo-controlled trial of idebenone in Leber's hereditary optic neuropathy. *Brain.* (2011) 134:2677–86. doi: 10.1093/brain/awr170

31. Klopstock T, Metz G, Yu-Wai-Man P, Büchner B, Gallenmüller C, Bailie M, et al. Persistence of the treatment effect of idebenone in Leber's hereditary optic neuropathy. *Brain.* (2013) 136:e230. doi: 10.1093/brain/aws279

32. de Grey AD. Mitochondrial gene therapy: an arena for the biomedical use of inteins. *Trends Biotechnol.* (2000) 18:394–9. doi: 10.1016/S0167-7799(00)01476-1

33. Nagley P, Farrell LB, Gearing DP, Nero D, Meltzer S, Devenish RJ. Assembly of functional proton-translocating ATPase complex in yeast mitochondria with cytoplasmically synthesized subunit 8, a polypeptide normally encoded within the organelle. *Proc Natl Acad Sci U S A.* (1988) 85:2091–5. doi: 10.1073/pnas.85.7.2091

34. Artika IM. Allotopic expression of mitochondrial genes: basic strategy and progress. *Genes Dis.* (2020) 7:578–84. doi: 10.1016/j.gendis.2019.08.001

35. Guy J, Qi X, Pallotti F, Schon EA, Manfredi G, Carelli V, et al. Rescue of a mitochondrial deficiency causing Leber hereditary optic neuropathy. *Ann Neurol.* (2002) 52:534–42. doi: 10.1002/ana.10354

36. Ellouze S, Augustin S, Bouaita A, Bonnet C, Simonutti M, Forster V, et al. Optimized allotopic expression of the human mitochondrial ND4 prevents blindness in a rat model of mitochondrial dysfunction. *Am J Hum Genet.* (2008) 83:373–87. doi: 10.1016/j.ajhg.2008.08.013

37. Marella M, Seo BB, Thomas BB, Matsuno-Yagi A, Yagi T. Successful amelioration of mitochondrial optic neuropathy using the yeast NDI1 gene in a rat animal model. *PLoS ONE.* (2010) 5:e11472. doi: 10.1371/journal.pone.0011472

38. Shi H, Gao J, Pei H, Liu R, Hu W, Wan X, et al. Adeno-associated virus-mediated gene delivery of the human ND4 complex I subunit in rabbit eyes. *Clin Exp Ophthalmol.* (2012) 40:888–94. doi: 10.1111/j.1442-9071.2012.02815.x

39. Yu H, Koilkonda RD, Chou T-H, Porciatti V, Ozdemir SS, Chiodo V, et al. Gene delivery to mitochondria by targeting modified adenoassociated virus suppresses Leber's hereditary optic neuropathy in a mouse model. *Proc Natl Acad Sci U S A.* (2012) 109:E1238–47. doi: 10.1073/pnas.1119577109

40. Chadderton N, Palfi A, Millington-Ward S, Gobbo O, Overlack N, Carrigan M, et al. Intravitreal delivery of AAV-NDI1 provides functional benefit in a murine model of Leber hereditary optic neuropathy. *Eur J Hum Genet.* (2013) 21:62–8. doi: 10.1038/ejhg.2012.112

41. Koilkonda RD, Yu H, Chou T-H, Feuer WJ, Ruggeri M, Porciatti V, et al. Safety and effects of the vector for the Leber hereditary optic neuropathy gene therapy clinical trial. *JAMA Ophthalmol.* (2014) 132:409–20. doi: 10.1001/jamaophthalmol.2013.7630

42. Koilkonda R, Yu H, Talla V, Porciatti V, Feuer WJ, Hauswirth WW, et al. LHON gene therapy vector prevents visual loss and optic neuropathy induced by G11778A mutant mitochondrial DNA: biodistribution and toxicology profile. *Invest Ophthalmol Vis Sci.* (2014) 55:7739–53. doi: 10.1167/iovs.14-15388

43. Feuer WJ, Schiffman JC, Davis JL, Porciatti V, Gonzalez P, Koilkonda RD, et al. Gene Therapy for Leber Hereditary Optic Neuropathy. *Ophthalmology.* (2016) 123:558–570. doi: 10.1016/j.ophtha.2015.10.025

44. Guy J, Feuer WJ, Davis JL, Porciatti V, Gonzalez PJ, Koilkonda RD, et al. Gene therapy for Leber hereditary optic neuropathy: low- and medium-dose visual results. *Ophthalmology.* (2017) 124:1621–34. doi: 10.1016/j.ophtha.2017.05.016

45. Lam BL, Feuer WJ, Schiffman JC, Porciatti V, Vandenbroucke R, Rosa PR, et al. Trial end points and natural history in patients with G11778A Leber hereditary optic neuropathy : preparation for gene therapy clinical trial. *JAMA Ophthalmol.* (2014) 132:428–36. doi: 10.1001/jamaophthalmol.2013.7971

46. Yu-Wai-Man P, Newman NJ, Carelli V, Moster ML, Biousse V, Sadun AA, et al. Bilateral visual improvement with unilateral gene therapy injection for Leber hereditary optic neuropathy. *Sci Transl Med.* (2020) 12:eaaz7423. doi: 10.1126/scitranslmed.aaz7423

47. Enns GM, Kinsman SL, Perlman SL, Spicer KM, Abdenur JE, Cohen BH, et al. Initial experience in the treatment of inherited mitochondrial disease with EPI-743. *Mol Genet Metab.* (2012) 105:91–102. doi: 10.1016/j.ymgme.2011.10.009

48. Shrader WD, Amagata A, Barnes A, Enns GM, Hinman A, Jankowski O, et al. α-Tocotrienol quinone modulates oxidative stress response and the biochemistry of aging. *Bioorg Med Chem Lett.* (2011) 21:3693–8. doi: 10.1016/j.bmcl.2011.04.085

49. Sadun AA. Effect of EPI-743 on the clinical course of the mitochondrial disease Leber hereditary optic neuropathy. *Arch Neurol.* (2012) 69:331. doi: 10.1001/archneurol.2011.2972

50. Martinelli D, Catteruccia M, Piemonte F, Pastore A, Tozzi G, Dionisi-Vici C, et al. EPI-743 reverses the progression of the pediatric mitochondrial disease–genetically defined Leigh Syndrome. *Mol Genet Metab.* (2012) 107:383–8. doi: 10.1016/j.ymgme.2012.09.007

51. Leruez S, Verny C, Bonneau D, Procaccio V, Lenaers G, Amati-Bonneau P, et al. Cyclosporine A does not prevent second-eye involvement in Leber's hereditary optic neuropathy. *Orphanet J Rare Dis.* (2018) 13:33. doi: 10.1186/s13023-018-0773-y

52. Wilensky JT. The role of brimonidine in the treatment of open-angle glaucoma. *Surv Ophthalmol.* (1996) 41 (Suppl. 1):S3–7. doi: 10.1016/S0039-6257(96)82026-1

53. Wheeler L, WoldeMussie E, Lai R. Role of alpha-2 agonists in neuroprotection. *Surv Ophthalmol.* (2003) 48 (Suppl. 1):S47–51. doi: 10.1016/S0039-6257(03)00004-3

54. Newman NJ, Biousse V, David R, Bhatti MT, Hamilton SR, Farris BK, et al. Prophylaxis for second eye involvement in leber hereditary optic neuropathy: an open-labeled, nonrandomized multicenter trial of topical brimonidine purite. *Am J Ophthalmol.* (2005) 140:407–15. doi: 10.1016/j.ajo.2005.03.058

55. Storoni M, Robert MP, Plant GT. The therapeutic potential of a calorie-restricted ketogenic diet for the management of Leber hereditary optic neuropathy. *Nutr Neurosci.* (2019) 22:156–64. doi: 10.1080/1028415X.2017.1368170

56. Emperador S, López-Gallardo E, Hernández-Ainsa C, Habbane M, Montoya J, Bayona-Bafaluy MP, et al. Ketogenic treatment reduces the percentage of a LHON heteroplasmic mutation and increases mtDNA amount of a LHON homoplasmic mutation. *Orphanet J Rare Dis.* (2019) 14:150. doi: 10.1186/s13023-019-1128-z

57. Weiss JN, Levy S, Benes SC. Stem cell ophthalmology treatment study (SCOTS): bone marrow-derived stem cells in the treatment of Leber's hereditary optic neuropathy. *Neural Regen Res.* (2016) 11:1685–94. doi: 10.4103/1673-5374.193251

58. Giordano C, Montopoli M, Perli E, Orlandi M, Fantin M, Ross-Cisneros FN, et al. Oestrogens ameliorate mitochondrial dysfunction in Leber's hereditary optic neuropathy. *Brain.* (2011) 134:220–34. doi: 10.1093/brain/awq276

59. Peron C, Mauceri R, Cabassi T, Segnali A, Maresca A, Iannielli A, et al. Generation of a human iPSC line, FINCBi001-A, carrying a homoplasmic m.G3460A mutation in MT-ND1 associated with Leber's Hereditary optic Neuropathy (LHON). *Stem Cell Res.* (2020) 48:101939. doi: 10.1016/j.scr.2020.1 01939

60. García-López M, Arenas J, Gallardo ME. Hereditary optic neuropathies: induced pluripotent stem cell-based 2D/3D approaches. *Genes.* (2021) 12:112. doi: 10.3390/genes12010112

61. Lu H-E, Yang Y-P, Chen Y-T, Wu Y-R, Wang C-L, Tsai F-T, et al. Generation of patient-specific induced pluripotent stem cells from Leber's hereditary optic neuropathy. *Stem Cell Res.* (2018) 28:56–60. doi: 10.1016/j.scr.2018.01.029

62. Kundu J, Michaelson A, Baranov P, Young MJ, Carrier RL. Approaches to cell delivery: substrates and scaffolds for cell therapy. *Dev Ophthalmol.* (2014) 53:143–54. doi: 10.1159/000357369

63. Crair MC, Mason CA. Reconnecting eye to brain. *J Neurosci.* (2016) 36:10707–22. doi: 10.1523/JNEUROSCI.1711-16.2016

64. Hyslop LA, Blakeley P, Craven L, Richardson J, Fogarty NME, Fragouli E, et al. Towards clinical application of pronuclear transfer to prevent mitochondrial DNA disease. *Nature.* (2016) 534:383–6. doi: 10.1038/nature18303

65. Wong RCB, Lim SY, Hung SSC, Jackson S, Khan S, Van Bergen NJ, et al. Mitochondrial replacement in an iPSC model of Leber's hereditary optic neuropathy. *Aging.* (2017) 9:1341–50. doi: 10.18632/aging.101231

66. Zhang J, Liu H, Luo S, Lu Z, Chávez-Badiola A, Liu Z, et al. Live birth derived from oocyte spindle transfer to prevent mitochondrial disease. *Reprod Biomed Online.* (2017) 34:361–8. doi: 10.1016/j.rbmo.2017.01.013

67. Garcia GA, Khoshnevis M, Gale J, Frousiakis SE, Hwang TJ, Poincenot L, et al. Profound vision loss impairs psychological well-being in young and middle-aged individuals. *Clin Ophthalmol.* (2017) 11:417–27. doi: 10.2147/OPTH.S1 13414

68. van Nispen RM, Virgili G, Hoeben M, Langelaan M, Klevering J, Keunen JE, et al. Low vision rehabilitation for better quality of life in visually impaired adults. *Cochrane Database Syst Rev.* (2020) 1:CD006543. doi: 10.1002/14651858.CD006543.pub2

69. Carelli V, Carbonelli M, de Coo IF, Kawasaki A, Klopstock T, Lagrèze WA, et al. International consensus statement on the clinical and therapeutic management of Leber hereditary optic neuropathy. *J Neuroophthalmol.* (2017) 37:371–81. doi: 10.1097/WNO.00000000000 00570

Exploiting hiPSCs in Leber's Hereditary Optic Neuropathy (LHON): Present Achievements and Future Perspectives

Camille Peron[1], Alessandra Maresca[2], Andrea Cavaliere[1], Angelo Iannielli[3,4], Vania Broccoli[3,4], Valerio Carelli[2,5], Ivano Di Meo[1] and Valeria Tiranti[1]*

[1] Unit of Medical Genetics and Neurogenetics, Fondazione IRCCS Istituto Neurologico Carlo Besta, Milan, Italy, [2] IRCCS Istituto delle Scienze Neurologiche di Bologna, Programma di Neurogenetica, Bologna, Italy, [3] San Raffaele Scientific Institute, Milan, Italy, [4] National Research Council (CNR), Institute of Neuroscience, Milan, Italy, [5] Department of Biomedical and Neuromotor Sciences-DIBINEM, University of Bologna, Bologna, Italy

More than 30 years after discovering Leber's hereditary optic neuropathy (LHON) as the first maternally inherited disease associated with homoplasmic mtDNA mutations, we still struggle to achieve effective therapies. LHON is characterized by selective degeneration of retinal ganglion cells (RGCs) and is the most frequent mitochondrial disease, which leads young people to blindness, in particular males. Despite that causative mutations are present in all tissues, only a specific cell type is affected. Our deep understanding of the pathogenic mechanisms in LHON is hampered by the lack of appropriate models since investigations have been traditionally performed in non-neuronal cells. Effective in-vitro models of LHON are now emerging, casting promise to speed our understanding of pathophysiology and test therapeutic strategies to accelerate translation into clinic. We here review the potentials of these new models and their impact on the future of LHON patients.

Keywords: Leber's hereditary optic neuropathy, human induced pluripotent stem cells, mitochondrial disorders, organoids, retinal ganglion cells (RGC)

INTRODUCTION

Leber's hereditary optic neuropathy (LHON) is caused by maternally inherited missense point mutations of mitochondrial DNA (mtDNA) (1) and is estimated as the most-frequent mitochondrial disease (2). This blinding disorder is characterized by selective degeneration of retinal ganglion cells (RGCs), the retinal neurons projecting their axons, which form the optic nerve to the brain. Thus, the extended loss of RGCs and their axons leads to optic nerve atrophy, with a severe defect of central vision, in most cases leaving the patient legally blind (3, 4). Almost all LHON maternal lineages present with homoplasmic mutation (100% mtDNA copies are mutant in all tissues), having one of three frequent mtDNA mutations found in over 90% of patients worldwide (m.11778G>A/MT-ND4, m.3460G>A/MT-ND1, m.14484T>C/MT-ND6), but only some individuals develop the disease. Also, despite that the homoplasmic mtDNA mutation is present in all tissues, only a cellular type, that is, RGCs, undergoes degeneration. The pathogenic mechanism leading to cell death is thus extremely tissue and cell specific (3, 4). The phenotype of these mutations characterized by defective ATP synthesis when driven by complex I substrates (5),

increased oxidative stress (6, 7), and increased propensity to undergo apoptosis (8, 9) has been thoroughly investigated in cybrids, lymphocytes, and fibroblasts but not in RGCs, the disease's target, which are not easily accessible and cannot be maintained *in vitro* (10).

Moreover, given the difficulties in manipulating mtDNA, very few animal models with mtDNA pathogenic mutations are available (11), preventing the possibility to study the affected tissues and organs and test therapeutic options.

To overcome these issues, we and other investigators exploited innovative approaches, based on the use of human-induced pluripotent stem cells (hiPSCs) as a faithful source of human neuronal cells and RGCs.

The use of hiPSCs to obtain terminally differentiated cells of a variety of tissues is a revolutionary approach to understanding disease mechanisms, performing drug screening, and testing gene or cell therapy (12–15).

Several studies have demonstrated the possibility to generate neurons and RGCs from plated hiPSC-derived embryoid bodies (16–19). In addition, different groups developed 3D culture systems recapitulating key steps of retinal development and allowing the generation of self-organizing retinal organoids containing RGCs (15, 20–25). These models provide a bridge between traditional 2D cell culture and mouse models, representing a paraphysiologic system with pros and cons (26), but of paramount importance for modeling mtDNA-related disorders.

Modeling LHON mutations in differentiated neurons and organoids will provide not only insights into the tissue-specific disease pathogenic mechanisms, but it will offer the unique opportunity to test *in-vitro* pharmacological approaches in a model system much more relevant than traditional non-neuronal cell cultures, such as fibroblasts, lymphoblasts, or cybrids. Moreover, patient-specific hiPSCs allow studying the effect of the mtDNA mutation in the context of patient-specific nuclear background, which, in LHON particularly, plays a pivotal role in the modulation of disease's presentation (27).

We here discuss our experience with the generation of hiPSCs from LHON-affected patients integrated with the data present in the literature. We particularly emphasize the translational potential for patients in exploiting LHON neuronal cells and RGCs to advance our knowledge of pathogenic mechanisms and test therapies.

REPROGRAMMING FIBROBLASTS OR PERIPHERAL BLOOD MONONUCLEAR CELLS PBMCS FROM LHON PATIENTS

Since the epochal discovery of induced pluripotent stem cells by the Yamanaka group in 2006 (28), many researchers generated hiPSC by reprogramming differentiated cells obtained from mitochondrial disease patients [MELAS syndrome (29), MERRF syndrome (30), Pearson syndrome (31); reviewed by Liang (32)]. Unexpectedly, even if LHON is the most-frequent mitochondrial disease, to date only a few groups, including ours (33), had generated LHON hiPSCs by reprogramming fibroblasts or

peripheral blood mononuclear cells (PBMCs) derived from patients (34–38).

One group from Taiwan reprogrammed PBMCs from two LHON m.11778G>A patients and one LHON m.11778G>A unaffected carrier using the Sendai virus (37). The authors reported a slightly increased complex I (CI) activity, failing statistical significance, in the LHON hiPSCs, both affected and carrier, as compared to control. The authors reported a slightly increased of complex I (CI) activity in both affected and carrier LHON hiPSCs as compared to control, that failed to reach statistical significance.

Another group reprogrammed fibroblasts from two LHON m.11778G>A patients as well as one LHON proband carrying two mutations m.4160T>C and m.14484T>C, using episomal vectors expressing six reprogramming factors OCT4, SOX2, KLF4, L-MYC, LIN28, and shRNA for p53 (34). They investigated hypothetical difficulties in reprogramming cell lines with OXPHOS defects since Yokota et al. reported reduced reprogramming efficiency in mitochondrial encephalomyopathy with lactic acidosis and stroke-like episodes syndrome (MELAS) fibroblasts carrying more than 90% of the m.3243A>G mtDNA mutation (39). Hung and collaborators reprogrammed fibroblasts carrying the homoplasmic LHON mutations and found no significant differences in the number of hiPSC colonies between controls and LHON patients (21 colonies on average for the controls, and 13 colonies on average for the LHON patients). Differently, our own experience with LHON was more similar to what observed by Yokota, since we noticed that LHON fibroblasts or PMBCs are refractory to be reprogrammed to hiPSC.

Specifically, we attempted to reprogram different LHON cell lines: two m.3460G>A patients, four m.11778G>A patients, and two unaffected m.11778G>A carriers (**Table 1**). As shown in **Table 1** and **Figure 1A**, the number of clones obtained was in general very low, even if numerous attempts were performed also in different laboratories. Conversely, using fibroblasts derived from healthy controls or disease's patients affected by mitochondrial disorders, including dominant optic atrophy (*OPA1* mutation), Pearson (40), and MPAN (41), we obtained on average from 10 to 20 clones of hiPSC (**Table 1** and **Figure 1B**) per reprogramming experiment. To overcome this issue, we tested the reprogramming efficiency of LHON cells under hypoxia laboratory conditions (5% pO$_2$, more similar to physiological oxygen tension *in vivo*), a condition previously used to enhance the generation of hiPSC (42), and recently demonstrated to be specifically beneficial in several OXPHOS defects, by improving disease phenotype in mice and cells (43). In fact, under traditional culturing conditions cellular models of mitochondrial respiratory-chain disease and Friedreich's ataxia showed proliferative defects, which could be reversed by lowering oxygen tension (44). In addition, hypoxia was able to prevent and even reverse the neurological phenotype in a Leigh syndrome mouse model characterized by CI deficiency due to *Ndufs4* gene ablation (45). Based on this evidence and since LHON mutations were associated with reduced CI-driven ATP synthesis and increased ROS production (46), we hypothesized that hypoxic cell culture conditions during reprogramming
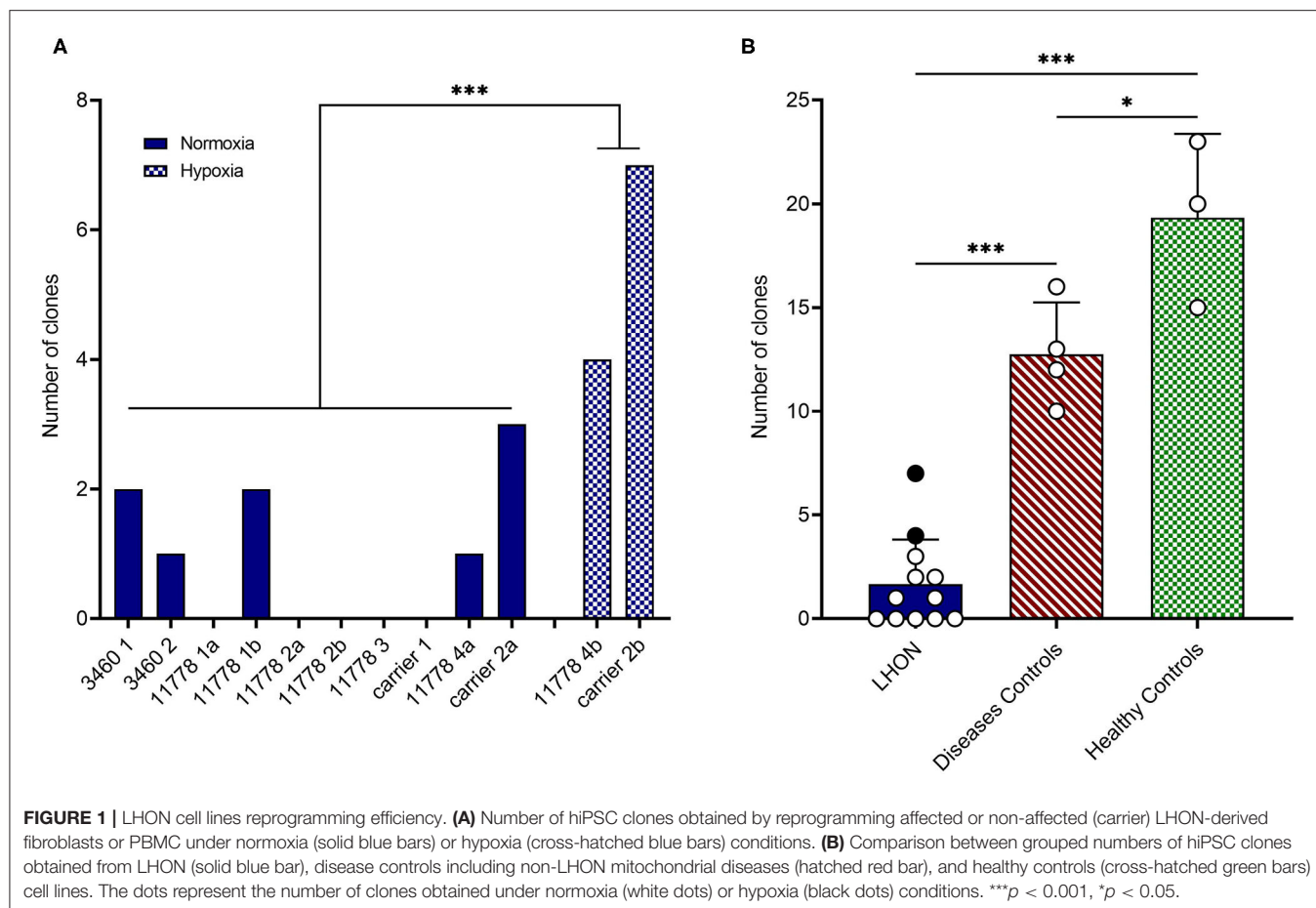
TABLE 1 | Characteristics of cell lines subjected to reprogramming.

Individuals	Cell line name	Gene mutated	Nucleotide change	Cell type reprogrammed	Reprogramming conditions	Clones obtained
LHON patients	3460 1	MT-ND1	m.3460G>A	FB	Normoxia	2
	3460 2	MT-ND1	m.3460G>A	FB	Normoxia	1
	11778 1a	MT-ND4	m.11778G>A	FB	Normoxia	0
	11778 1b	MT-ND4	m.11778G>A	FB	Normoxia	2
	11778 2a	MT-ND4	m.11778G>A	FB	Normoxia	0
	11778 2b	MT-ND4	m.11778G>A	FB	Normoxia	0
	11778 3	MT-ND4	m.11778G>A	FB	Normoxia	0
	11778 4a	MT-ND4	m.11778G>A	PBMC	Normoxia	1
	11778 4b	MT-ND4	m.11778G>A	PBMC	Hypoxia	4
	carrier 1	MT-ND4	carrier m.11778G>A	FB	Normoxia	0
	Carrier 2a	MT-ND4	carrier 90% m.11778G>A	PBMC	Normoxia	3
	Carrier 2b	MT-ND4	carrier 90% m.11778G>A	PBMC	Hypoxia	7
Disease controls	DOA	OPA1	c.1334 G>A	FB	Normoxia	13
	MPAN	C19orf12	c.172G>A	FB	Normoxia	12
	Pearson 1	mtDNA macrodeletion	m.9449_14550 del	FB	Normoxia	10
	Pearson 2	mtDNA macrodeletion	m.8469_13460 del	FB	Normoxia	16
Healthy controls	Control 1	None	none	FB	Normoxia	23
	Control 2	None	none	FB	Normoxia	20
	Control 3	None	none	PBMC	Normoxia	15

could increase the number of hiPSC clones generated. Thus, we recently reprogrammed PBMCs derived from one LHON m.11778G>A patient and one carrier, in parallel under normoxic (11778 4a and Carrier 2a) and hypoxic (11778 4b and Carrier 2b) conditions (5% oxygen), following published procedures (42). We found that this hypoxic condition significantly increased the number of hiPSC clones generated (**Table 1** and **Figure 1A**). In fact, while under normoxic conditions, we obtained around nine LHON hiPSCs clones in 10 different reprogramming experiments (0.9 clones/reprogramming cycle), and this number increased, under hypoxic conditions, to 11 clones in two reprogramming experiments (5.5 clones/reprogramming cycle). Although these last results derived from only two experiments and need to be further consolidated, they indicated a statistically significant improvement of the reprogramming efficiency (**Figure 1A**), which remains largely below that observed for the disease control group (12.7 clones/reprogramming cycle) and for the healthy control group (19.3 clones/reprogramming cycle) (**Figure 1B**). This amelioration of the reprogramming efficiency is relevant not only to obtain enough biological material for further investigations but could also unravel an insight into pathogenic mechanisms, relevant for the disease, and for the development of targeted effective therapy. Remarkably, the subacute phase of LHON is hallmarked by well-known vascular changes, and ongoing discussions revolve around the issue of pseudo-hypoxic signaling that RGCs may produce as their metabolic unbalance reaches the threshold for triggering the disease, possibly underlying the microangiopathy in LHON (3, 4, 47, 48).

GENERATION OF RGCs FROM LHON PATIENTS

In the last years, a few protocols have been developed with the purpose to differentiate RGCs directly from patients-derived hiPSCs. However, very few of these RGCs models have been produced for LHON. The first model was reported in 2017 by the Wong group, who generated RGCs from one healthy control and one patient carrying in combination the two homoplasmic mtDNA mutations m.4160T>C and m.14484T>C. Interestingly, they used cybrid technology to also generate patients' fibroblasts homoplasmic for the wild-type mtDNA, thus creating an isogenic control hiPSCs and derived RGCs (35). They found an increased level of apoptosis in LHON RGCs not observed in the healthy and isogenic corrected RGCs, demonstrating that this phenotype was a direct consequence of the LHON mutations. Another group generated hiPSCs-derived RGCs from a m.11778G>A LHON-affected and unaffected carrier, belonging both to the same family (37). They observed enhanced mitochondrial biogenesis, decreased basal respiration, and increased oxidative stress in both affected and unaffected RGCs. However, defective neurite outgrowth was only found in the affected RGCs, while carrier cells exhibited a prominently higher expression of the gene encoding γ-synuclein. Interestingly, increased CI activity was observed in RGCs derived from the asymptomatic carrier but not from the affected patient. Differences in affected and unaffected RGCs carrying homoplasmic m.11778G>A mutation were also found by Yang et al. (49). Both lines showed increased ROS production, but only the affected cells were characterized by

FIGURE 1 | LHON cell lines reprogramming efficiency. **(A)** Number of hiPSC clones obtained by reprogramming affected or non-affected (carrier) LHON-derived fibroblasts or PBMC under normoxia (solid blue bars) or hypoxia (cross-hatched blue bars) conditions. **(B)** Comparison between grouped numbers of hiPSC clones obtained from LHON (solid blue bar), disease controls including non-LHON mitochondrial diseases (hatched red bar), and healthy controls (cross-hatched green bars) cell lines. The dots represent the number of clones obtained under normoxia (white dots) or hypoxia (black dots) conditions. ***$p < 0.001$, *$p < 0.05$.

increased apoptosis and altered mitochondrial transport pattern along the axons, with an increase in retrograde and a decrease in stationary mitochondria. Furthermore, affected RGCs displayed a significant increase of KIF5A, a member of the kinesin-1 family KIF5, involved in the transport of mitochondria along the axons. Another study carried out on hiPSC-derived RGCs by Yang et al. (50) highlighted the possible role played by AMPA receptors and excitotoxicity in m.11778G>A LHON patients. They used a modified protocol of differentiation of hiPSCs to RGCs to obtain a highly homogeneous RGCs population. They showed how the *MT-ND4*-mutated LHON-RGC cells exhibited significantly reduced GluR1/R2 (subunits of AMPA receptors) and their associated scaffold proteins and the resulting different pattern of response to glutamate stimulation compared to control.

Lastly, Edo et al. (51) demonstrated that hiPSC-derived RGCs can suppress the immune activity of T-cells via TGF-β, have a poor expression of HLA class I, and no expression of HLA class II (CD80 and CD86 co-stimulatory molecules), opening the possibility of using these cells in transplant without the risk of rejection.

GENERATION OF NEURONS FROM LHON PATIENTS

Almost two decades ago, the Cortopassi group generated cybrids using the neuronal precursor cell line NT2, containing mitochondria from patients with m.11778G>A and m.3460G>A mutations (52). Differentiation of LHON-NT2 cells resulted in a decreased number of cells, reduction of mtDNA amount, and increased ROS production, compared to the parental line. To our knowledge, no hiPSCs-derived neuronal model different from RGCs has been generated to date. Although it is clear that RGCs represent the best model to unravel LHON pathomechanisms, hiPSCs differentiation in non-RGCs neurons could be informative as well to study the selective degeneration of RGCs in patients. To maintain the transparency of the retina to light, the retinal segment of the RGCs axon is unmyelinated, increasing the energetic demand for action potential firing along this portion and making these cells particularly susceptible to energetic deficit (53). The generation of *in-vitro* myelinated neurons through co-cultures of Schwann cells and hiPSCs-derived neurons (54) might be informative to establish the involvement of myelin in the pathogenesis of the disease.

STATE OF THE ART ON ORGANOIDS IMPLEMENTATION

The use of 3D organoids generated *in vitro* from patient-derived cells may represent an important interface between *in-vitro* and *in-vivo* modeling of LHON, being more accessible and easier to obtain than mouse models and overcoming the anatomical interspecies differences between humans and rodents.

The first human brain and retinal organoids have been generated about 10 years ago from different groups (55, 56). Lancaster and colleagues successfully modeled genetic microcephaly using hiPSCs derived from patients' fibroblasts to generate brain organoids.

Only a year before, the Sasai group had generated a 3D optic structure by self-organization of cultured human embryonic stem cells (ESCs). The optic cup consisted of the retinal pigmented epithelium, and an inner neural retina correctly organized into multilayered tissue containing photoreceptors (rods and cones), interneuron precursors, and RGCs (57). Both these protocols exploited the capacity of embryoid bodies (EBs) (ESCs or hiPSCs-derived) to proceed spontaneously toward ectodermal commitment without extrinsic signaling factors, which instead are necessary for mesodermal and endodermal specifications (26, 58).

Several modifications and adjustments to the pivotal approaches of Lancaster (55, 59) and Sasai group (57, 60), have been done in the following years, essentially identifying distinct extrinsic factors to obtaining specific regions in the organoids (60, 61), or by-passing the EBs formation step (62). Moreover, improvements toward standardization are constantly evolving, such as the use of completely xeno-free culture methods (62) or the introduction of technologies allowing large-scale controlled organoids production, such as bioreactors or microfluidics chips (26). Importantly, also protocols for cryopreservation at intermediate steps of differentiation have been established, allowing the biobanking of the *in-vitro*-generated organoids, an additional advantage compared to animal models (26, 57, 62).

THERAPEUTIC APPROACHES

Despite the numerous clinical and pre-clinical investigations carried out to date, effective therapies for LHON are still limited. Effective means that therapy should be able to tangibly modify the disease natural history either by aborting or reverting the catastrophic wave of cell death, or at least limiting the progression so that the visual function is substantially preserved based on anatomical RGCs measurable sparing. Multiple clinical trials have been conducted in recent years, essentially targeting the main pathways involved in the pathogenic mechanism (63). Several antioxidants molecules, some of which with direct effects on mitochondrial respiration, have been tested in patients: idebenone, Coenzyme Q10 (CoQ10), EPI-743, Elamipretide, curcumin (63).

To date, idebenone (Raxone®) is the only drug approved by the European Medicines Agency for LHON. It has been documented that idebenone can increase the rate of visual recovery in LHON patients after reaching a nadir of visual loss (64–66); however, its efficacy remains incomplete and variable amongst treated subjects.

The only treatment explored in LHON hiPSCs-derived RGCs was the antioxidant N-acetyl-L-cysteine, which was shown to reduce the ROS production and apoptosis, also rescuing the defective mitochondrial transport observed in the LHON cells (49).

Additional compounds targeting other pathways involved in the LHON pathogenesis (mitobiogenesis, mitophagy, mitoinflammation) have been evaluated only in patient-derived primary cells or in cybrids, such as phytoestrogens (67), rapamycin (68), papaverine, and zolpidem (69). Moreover, other potential strategies are emerging, for example, the inhibition of the miRNA181a/b, acting on both mitobiogenesis and mitophagy (70). All these pharmacological approaches should be reevaluated also in RGC to understand if they are efficacious and rapidly translatable into a therapy.

Besides pharmacological clinical trials, encouraging results are nowadays being reported by clinical trials with gene therapy for patients carrying the m.11778G>A/*MT-ND4* mutation [reviewed in Amore et al. (63)], using the Adeno-Associated Virus (AAV)-mediated allotopic expression of a wild-type recoded version of the mtDNA-encoded ND4 subunit of complex I (71, 72). To better refine the efficiency of allotropic expression strategy in the context of RGCs, detailing the mitochondrial import of wild-type ND4 protein, its competition with the endogenously expressed mutant ND4, and finally the dynamics of complex I assembly of either one or the other ND4 subunits, may greatly benefit of 3D organoid modeling of LHON. This might resolve some of the criticisms previously raised by the preclinical studies (73–75). The same approach could be developed for the other LHON-related mutations, and different approaches based on gene therapy might be proposed in the future, for example, modulating the expression of modifying genes or miRNAs (70) or applying possible gene-editing strategies, as recently proposed for mtDNA (76). Similarly, the feasibility of mitochondrial import of nucleic acids, claimed by some studies (77, 78), may benefit the use of eye/brain organoids carrying LHON mutations, reproducing those experiments and possibly paving the road for further gene therapy strategies.

DISCUSSION

In-vitro modeling of LHON through 2D cell cultures, including patient-derived hiPSCs and neurons, allowed important steps forward in the understanding of the pathogenic mechanism of this complex and fascinating disease. We here presented evidence that LHON hiPSCs are difficult to obtain as compared to other apparently more severe mitochondrial disorders, but this reduced efficiency could be improved by performing the reprogramming experiment under hypoxic conditions. This observation would deserve further investigation since obtaining a large number of hiPSCs clones is instrumental to further develop differentiated 2D cell cultures. Although 2D cell cultures show several advantages such as easy manipulation and analysis (good

accessibility of nutrients and/or drugs, excellent visualization and tracking of cells at microscopy by live-cell imaging), the complex 3D architecture of *in-vivo* tissues is not reproduced by this method, nor are the interactions between different co-resident populations of specialized cells (79). This is particularly important for LHON, in which RGCs are the only cells affected in the retina. The application of the innovative single-cell omics on hiPSCs-derived 3D organoids can provide useful insight on the cell specificity of LHON disease. A recent study has already paved the way for this approach, performing single-cell transcriptomics on *in-vitro*-generated human retinal organoids and *ex-vivo* adult human retinas, allowing mapping of disease-associated genes to particular cell types (25). This work highlights the importance of investigating mechanisms of disease in RGCs since they could be differently regulated in the traditional cell models so far exploited. Many of the findings so far achieved in LHON should be revalidated in RGC models to assure that the right pathogenic mechanism was effectively targeted by therapies.

Modeling mitochondrial diseases caused by mtDNA mutations in animals is still challenging due to the difficulties in manipulating the mitochondrial genome (80, 81), although a new promising method has been recently described Mok et al. (76). In 2012, the group of Doug Wallace, a pioneer in the field of mitochondrial medicine, successfully generated a mouse model carrying a mutation in the *MT-ND6* gene, which developed a pathology closely resembling LHON at 2 years of age, although the mouse did not show reduced visual responses (82). This model was instrumental to reproduce some of the hallmark features observed in human post-mortem LHON retina (83, 84); however, mice, because they lack the macular region, ultimately fail to reproduce the natural history that clinically characterizes humans with the characteristic catastrophic evolution of RGC neurodegeneration (3, 4).

Thus, it will be fundamental to investigate pathogenic mechanism of LHON disease in hiPSCs-derived cell/tissue-specific models and retinal organoids might be instrumental to assess efficacy/toxicity in the pre-clinical phases. The issue of maintaining organoids in a spinning bioreactor under hypoxic conditions, with the intent of reproducing the brain endogenous developmental program, could be crucial, especially for LHON in light of our observation, but also in general for other diseases. To date, only a few brain organoids models of mitochondrial diseases have been reported, specifically for MELAS syndrome, mitochondrial neurogastrointestinal encephalomyopathy, Friedrich ataxia, and Leigh syndrome (85–88). We think that modeling LHON with retinal organoids would provide substantial progress in the understanding of the

pathogenic mechanisms and in identifying the correct targets for therapy development. To this end, testing pharmacological and gene therapy approaches with human transgenes packaged in the appropriate AAV vector constructs, currently performed in animal models with obvious problematic issues (89, 90), may benefit human-patient-derived eye/brain organoids, certainly allowing to speed translation from pre-clinical science to approval for human clinical trials of regulatory agencies such as the Food and Drug Administration (FDA) and European Medicines Agency (EMA).

DATA AVAILABILITY STATEMENT

The raw data supporting the conclusions of this article will be made available by the authors, without undue reservation.

ETHICS STATEMENT

The studies involving human participants were reviewed and approved by Fondazione IRCCS Istituto Neurologico Carlo Besta. The patients/participants provided their written informed consent to participate in this study.

AUTHOR CONTRIBUTIONS

CP, AC, AI, and ID perform experiments, analyzed data, generated the table and figure, and analyzed the literature. AM, VB, and VC analyzed the literature. VT concept the manuscript architecture, supervised the analysis of the data, and of the literature. VT performed the final revision of the manuscript. All the authors draft the manuscript.

FUNDING

ACKNOWLEDGMENTS

REFERENCES

1. Wallace DC, Singh G, Lott MT, Hodge JA, Schurr TG, Lezza AM, et al. Mitochondrial DNA mutation associated with Leber's hereditary optic neuropathy. *Science.* (1988) 242:1427–30. doi: 10.1126/science.3201231
2. Chinnery PF, Turnbull DM. Mitochondrial DNA mutations in the pathogenesis of human disease. *Mol Med Today.* (2000) 6:425–32. doi: 10.1016/S1357-4310(00)01805-0

3. Carelli V, Ross-Cisneros FN, Sadun AA. Mitochondrial dysfunction as a cause of optic neuropathies. *Progr Retinal Eye Res.* (2004) 23:53–89. doi: 10.1016/j.preteyeres.2003.10.003
4. Yu-Wai-Man P, Griffiths PG, Chinnery PF. Mitochondrial optic neuropathies - disease mechanisms and therapeutic strategies. *Prog Retin Eye Res.* (2011) 30:81–114. doi: 10.1016/j.preteyeres.2010.11.002
5. Baracca A, Solaini G, Sgarbi G, Lenaz G, Baruzzi A, Schapira AHV, et al. Severe impairment of complex I-driven adenosine triphosphate synthesis in

leber hereditary optic neuropathy cybrids. *Arch Neurol.* (2005) 62:730–6. doi: 10.1001/archneur.62.5.730

6. Beretta S, Mattavelli L, Sala G, Tremolizzo L, Schapira AHV, Martinuzzi A, et al. Leber hereditary optic neuropathy mtDNA mutations disrupt glutamate transport in cybrid cell lines. *Brain.* (2004) 127:2183–92. doi: 10.1093/brain/awh258

7. Floreani M, Napoli E, Martinuzzi A, Pantano G, De Riva V, Trevisan R, et al. Antioxidant defences in cybrids harboring mtDNA mutations associated with Leber's hereditary optic neuropathy. *FEBS J.* (2005) 272:1124–35. doi: 10.1111/j.1742-4658.2004.04542.x

8. Ghelli A, Zanna C, Porcelli AM, Schapira AHV, Martinuzzi A, Carelli V, et al. Leber's hereditary optic neuropathy (LHON) pathogenic mutations induce mitochondrial-dependent apoptotic death in transmitochondrial cells incubated with galactose medium. *J Biol Chem.* (2003) 278:4145–50. doi: 10.1074/jbc.M210285200

9. Zanna C, Ghelli A, Porcelli AM, Martinuzzi A, Carelli V, Rugolo M. Caspase-independent death of Leber's hereditary optic neuropathy cybrids is driven by energetic failure and mediated by AIF and Endonuclease G. *Apoptosis.* (2005) 10:997–1007. doi: 10.1007/s10495-005-0742-5

10. Zhang X-M, Liu DT, Chiang SW-Y, Choy K-W, Pang C-P, Lam DS-C, et al. Immunopanning purification and long-term culture of human retinal ganglion cells. *Mol Vis.* (2010) 16:2867–72. Available online at: http://www.molvis.org/molvis/v16/a307/

11. Stewart JB. Current progress with mammalian models of mitochondrial DNA disease. *J Inherited Metabolic Dis.* (2021) 44:325–42. doi: 10.1002/jimd.12324

12. Llonch S, Carido M, Ader M. Organoid technology for retinal repair. *Dev Biol.* (2018) 433:132–43. doi: 10.1016/j.ydbio.2017.09.028

13. Ahmad R, Sportelli V, Ziller M, Spengler D, Hoffmann A. Tracing early neurodevelopment in schizophrenia with induced pluripotent stem cells. *Cells.* (2018) 7:140. doi: 10.3390/cells7090140

14. Miltner AM, La Torre A. Retinal ganglion cell replacement: current status and challenges ahead: retinal ganglion cell replacement. *Dev Dyn.* (2019) 248:118–28. doi: 10.1002/dvdy.24672

15. Rabesandratana O, Chaffiol A, Mialot A, Slembrouck-Brec A, Joffrois C, Nanteau C, et al. Generation of a transplantable population of human iPSC-derived retinal ganglion cells. *Front Cell Dev Biol.* (2020) 8:585675. doi: 10.3389/fcell.2020.585675

16. Riazifar H, Jia Y, Chen J, Lynch G, Huang T. Chemically induced specification of retinal ganglion cells from human embryonic and induced pluripotent stem cells. *Stem Cells Transl Med.* (2014) 3:424–32. doi: 10.5966/sctm.2013-0147

17. Sluch VM, Davis CO, Ranganathan V, Kerr JM, Krick K, Martin R, et al. Differentiation of human ESCs to retinal ganglion cells using a CRISPR engineered reporter cell line. *Sci Rep.* (2015) 5:16595. doi: 10.1038/srep16595

18. Gill KP, Hung SSC, Sharov A, Lo CY, Needham K, Lidgerwood GE, et al. Enriched retinal ganglion cells derived from human embryonic stem cells. *Sci Rep.* (2016) 6:30552. doi: 10.1038/srep30552

19. Teotia P, Chopra DA, Dravid SM, Van Hook MJ, Qiu F, Morrison J, et al. Generation of functional human retinal ganglion cells with target specificity from pluripotent stem cells by chemically defined recapitulation of developmental mechanism. *Stem Cells.* (2017) 35:572–85. doi: 10.1002/stem.2513

20. Reichman S, Terray A, Slembrouck A, Nanteau C, Orieux G, Habeler W, et al. From confluent human iPS cells to self-forming neural retina and retinal pigmented epithelium. *Proc Natl Acad Sci USA.* (2014) 111:8518–23. doi: 10.1073/pnas.1324212111

21. Zhong X, Gutierrez C, Xue T, Hampton C, Vergara MN, Cao L-H, et al. Generation of three-dimensional retinal tissue with functional photoreceptors from human iPSCs. *Nat Commun.* (2014) 5:4047. doi: 10.1038/ncomms5047

22. Maekawa Y, Onishi A, Matsushita K, Koide N, Mandai M, Suzuma K, et al. Optimized culture system to induce neurite outgrowth from retinal ganglion cells in three-dimensional retinal aggregates differentiated from mouse and human embryonic stem cells. *Curr Eye Res.* (2016) 41:558–68. doi: 10.3109/02713683.2015.1038359

23. Ohlemacher SK, Sridhar A, Xiao Y, Hochstetler AE, Sarfarazi M, Cummins TR, et al. Stepwise differentiation of retinal ganglion cells from human pluripotent stem cells enables analysis of glaucomatous neurodegeneration. *Stem Cells.* (2016) 34:1553–62. doi: 10.1002/stem.2356

24. Fligor CM, Langer KB, Sridhar A, Ren Y, Shields PK, Edler MC, et al. Three-Dimensional retinal organoids facilitate the investigation of retinal ganglion cell development, organization and neurite outgrowth from human pluripotent stem cells. *Sci Rep.* (2018) 8:14520. doi: 10.1038/s41598-018-32871-8

25. Cowan CS, Renner M, De Gennaro M, Gross-Scherf B, Goldblum D, Hou Y, et al. Cell types of the human retina and its organoids at single-cell resolution. *Cell.* (2020) 182:1623–40.e34. doi: 10.1016/j.cell.2020.08.013

26. Li M, Izpisua Belmonte JC. Organoids - preclinical models of human disease. *N Engl J Med.* (2019) 380:569–79. doi: 10.1056/NEJMra1806175

27. Caporali L, Maresca A, Capristo M, Del Dotto V, Tagliavini F, Valentino ML, et al. Incomplete penetrance in mitochondrial optic neuropathies. *Mitochondrion.* (2017) 36:130–37. doi: 10.1016/j.mito.2017.07.004

28. Takahashi K, Yamanaka S. Induction of pluripotent stem cells from mouse embryonic and adult fibroblast cultures by defined factors. *Cell.* (2006) 126:663–76. doi: 10.1016/j.cell.2006.07.024

29. Hämäläinen RH, Manninen T, Koivumäki H, Kislin M, Otonkoski T, Suomalainen A. Tissue- and cell-type-specific manifestations of heteroplasmic mtDNA 3243A>G mutation in human induced pluripotent stem cell-derived disease model. *Proc Natl Acad Sci USA.* (2013) 110:E3622–30. doi: 10.1073/pnas.1311660110

30. Chou S-J, Ko Y-L, Yang Y-H, Yarmishyn AA, Wu Y-T, Chen C-T, et al. Generation of two isogenic human induced pluripotent stem cell lines from a 15 year-old female patient with MERRF syndrome and A8344G mutation of mitochondrial DNA. *Stem Cell Res.* (2018) 30:201–5. doi: 10.1016/j.scr.2018.05.011

31. Cherry ABC, Gagne KE, Mcloughlin EM, Baccei A, Gorman B, Hartung O, et al. Induced pluripotent stem cells with a mitochondrial DNA deletion. *Stem Cells.* (2013) 31:1287–97. doi: 10.1002/stem.1354

32. Liang X, Kristiansen CK, Vatne GH, Hong Y, Bindoff LA. Patient-specific neural progenitor cells derived from induced pluripotent stem cells offer a promise of good models for mitochondrial disease. *Cell Tissue Res.* (2020) 380:15–30. doi: 10.1007/s00441-019-03164-x

33. Peron C, Mauceri R, Cabassi T, Segnali A, Maresca A, Iannielli A, et al. Generation of a human iPSC line, FINCBi001-A, carrying a homoplasmic m.G3460A mutation in MT-ND1 associated with Leber's Hereditary optic Neuropathy (LHON). *Stem Cell Res.* (2020) 48:101939. doi: 10.1016/j.scr.2020.101939

34. Hung SSC, Van Bergen NJ, Jackson S, Liang H, Mackey DA, Hernández D, et al. Study of mitochondrial respiratory defects on reprogramming to human induced pluripotent stem cells. *Aging.* (2016) 8:945–57. doi: 10.18632/aging.100950

35. Wong RCB, Lim SY, Hung SSC, Jackson S, Khan S, Van Bergen NJ, et al. Mitochondrial replacement in an iPSC model of Leber's hereditary optic neuropathy. *Aging.* (2017) 9:1341–50. doi: 10.18632/aging.101231

36. Lu H-E, Yang Y-P, Chen Y-T, Wu Y-R, Wang C-L, Tsai F-T, et al. Generation of patient-specific induced pluripotent stem cells from Leber's hereditary optic neuropathy. *Stem Cell Res.* (2018) 28:56–60. doi: 10.1016/j.scr.2018.01.029

37. Wu Y-R, Wang A-G, Chen Y-T, Yarmishyn AA, Buddhakosai W, Yang T-C, et al. Bioactivity and gene expression profiles of hiPSC-generated retinal ganglion cells in MT-ND4 mutated Leber's hereditary optic neuropathy. *Exp Cell Res.* (2018) 363:299–309. doi: 10.1016/j.yexcr.2018.01.020

38. Bahr T, Welburn K, Donnelly J, Bai Y. Emerging model systems and treatment approaches for Leber's hereditary optic neuropathy: challenges and opportunities. *Biochimica et Biophysica Acta.* (2020) 1866:165743. doi: 10.1016/j.bbadis.2020.165743

39. Yokota M, Hatakeyama H, Okabe S, Ono Y, Goto Y. Mitochondrial respiratory dysfunction caused by a heteroplasmic mitochondrial DNA mutation blocks cellular reprogramming. *Hum Mol Genet.* (2015) 24:4698–709. doi: 10.1093/hmg/ddv201

40. Peron C, Mauceri R, Iannielli A, Cavaliere A, Legati A, Rizzo A, et al. Generation of two human iPSC lines, FINCBi002-A and FINCBi003-A, carrying heteroplasmic macrodeletion of mitochondrial DNA causing Pearson's syndrome. *Stem Cell Res.* (2021) 50:102151. doi: 10.1016/j.scr.2020.102151

41. Panteghini C, Zorzi G, Venco P, Dusi S, Reale C, Brunetti D, et al. C19orf12 and FA2H mutations are rare in Italian patients with neurodegeneration

with brain iron accumulation. *Semin Pediatr Neurol.* (2012) 19:75–81. doi: 10.1016/j.spen.2012.03.006

42. Yoshida Y, Takahashi K, Okita K, Ichisaka T, Yamanaka S. Hypoxia enhances the generation of induced pluripotent stem cells. *Cell Stem Cell.* (2009) 5:237–41. doi: 10.1016/j.stem.2009.08.001

43. Ferrari M, Jain IH, Goldberger O, Rezoagli E, Thoonen R, Cheng K-H, et al. Hypoxia treatment reverses neurodegenerative disease in a mouse model of Leigh syndrome. *PNAS.* (2017) 114:E4241–50. doi: 10.1073/pnas.1621511114

44. Ast T, Meisel JD, Patra S, Wang H, Grange RMH, Kim SH, et al. Hypoxia rescues frataxin loss by restoring iron sulfur cluster biogenesis. *Cell.* (2019) 177:1507–21.e16. doi: 10.1016/j.cell.2019.03.045

45. Jain IH, Zazzeron L, Goli R, Alexa K, Schatzman-Bone S, Dhillon H, et al. Hypoxia as a therapy for mitochondrial disease. *Science.* (2016) 352:54–61. doi: 10.1126/science.aad9642

46. Kirches E. LHON: mitochondrial mutations and more. *Curr Genomics.* (2011) 12:44–54. doi: 10.2174/138920211794520150

47. Balducci N, Cascavilla ML, Ciardella A, Morgia CL, Triolo G, Parisi V, et al. Peripapillary vessel density changes in Leber's hereditary optic neuropathy: a new biomarker. *Clin Exp Ophthalmol.* (2018) 46:1055–62. doi: 10.1111/ceo.13326

48. Kousal B, Kolarova H, Meliska M, Bydzovsky J, Diblik P, Kulhanek J, et al. Peripapillary microcirculation in Leber hereditary optic neuropathy. *Acta Ophthalmol.* (2019) 97:e71–6. doi: 10.1111/aos.13817

49. Yang T-C, Yarmishyn AA, Yang Y-P, Lu P-C, Chou S-J, Wang M-L, et al. Mitochondrial transport mediates survival of retinal ganglion cells in affected LHON patients. *Human Mol Genet.* (2020) 29:1454–64. doi: 10.1093/hmg/ddaa063

50. Yang Y-P, Nguyen PNN, Lin T-C, Yarmishyn AA, Chen W-S, Hwang D-K, et al. Glutamate stimulation dysregulates AMPA receptors-induced signal transduction pathway in leber's inherited optic neuropathy patient-specific hiPSC-derived retinal ganglion cells. *Cells.* (2019) 8:625. doi: 10.3390/cells8060625

51. Edo A, Sugita S, Futatsugi Y, Sho J, Onishi A, Kiuchi Y, et al. Capacity of retinal ganglion cells derived from human induced pluripotent stem cells to suppress T-Cells. *Int J Mol Sci.* (2020) 21:7831. doi: 10.3390/ijms21217831

52. Wong A, Cavelier L, Collins-Schramm HE, Seldin MF, McGrogan M, Savontaus M-L, et al. Differentiation-specific effects of LHON mutations introduced into neuronal NT2 cells. *Hum Mol Genet.* (2002) 11:431–8. doi: 10.1093/hmg/11.4.431

53. Carelli V, La Morgia C, Ross-Cisneros FN, Sadun AA. Optic neuropathies: the tip of the neurodegeneration iceberg. *Hum Mol Genet.* (2017) 26:R139–50. doi: 10.1093/hmg/ddx273

54. Clark AJ, Kaller MS, Galino J, Willison HJ, Rinaldi S, Bennett DLH. Co-cultures with stem cell-derived human sensory neurons reveal regulators of peripheral myelination. *Brain.* (2017) 140:898–913. doi: 10.1093/brain/awx012

55. Lancaster MA, Renner M, Martin C-A, Wenzel D, Bicknell LS, Hurles ME, et al. Cerebral organoids model human brain development and microcephaly. *Nature.* (2013) 501:373–9 doi: 10.1038/nature12517

56. Meyer JS, Shearer RL, Capowski EE, Wright LS, Wallace KA, McMillan EL, et al. Modeling early retinal development with human embryonic and induced pluripotent stem cells. *Proc Natl Acad Sci USA.* (2009) 106:16698–703. doi: 10.1073/pnas.0905245106

57. Nakano T, Ando S, Takata N, Kawada M, Muguruma K, Sekiguchi K, et al. Self-formation of optic cups and storable stratified neural retina from human ESCs. *Cell Stem Cell.* (2012) 10:771–85. doi: 10.1016/j.stem.2012.05.009

58. Nam KH, Yi SA, Jang HJ, Han J-W, Lee J. *In vitro* modeling for inherited neurological diseases using induced pluripotent stem cells: from 2D to organoid. *Arch Pharm Res.* (2020) 43:877–89. doi: 10.1007/s12272-020-01260-z

59. Lancaster MA, Knoblich JA. Generation of cerebral organoids from human pluripotent stem cells. *Nature Protocols.* (2014) 9:2329–40. doi: 10.1038/nprot.2014.158

60. Artero Castro A, Rodríguez Jimenez FJ, Jendelova P, Erceg S. Deciphering retinal diseases through the generation of three dimensional stem cell-derived organoids: concise review. *Stem Cells.* (2019) 37:1496–504. doi: 10.1002/stem.3089

61. Clevers H. Modeling development and disease with organoids. *Cell.* (2016) 165:1586–97. doi: 10.1016/j.cell.2016.05.082

62. Reichman S, Slembrouck A, Gagliardi G, Chaffiol A, Terray A, Nanteau C, et al. Generation of storable retinal organoids and retinal pigmented epithelium from adherent human iPS cells in xeno-free and feeder-free conditions. *Stem Cells.* (2017) 35:1176–88. doi: 10.1002/stem.2586

63. Amore G, Romagnoli M, Carbonelli M, Barboni P, Carelli V, La Morgia C. Therapeutic options in hereditary optic neuropathies. *Drugs.* (2020) 81:57–86. doi: 10.1007/s40265-020-01428-3

64. Carelli V, La Morgia C, Valentino ML, Rizzo G, Carbonelli M, De Negri AM, et al. Idebenone treatment in Leber's hereditary optic neuropathy. *Brain.* (2011) 134:e188. doi: 10.1093/brain/awr180

65. Klopstock T, Yu-Wai-Man P, Dimitriadis K, Rouleau J, Heck S, Bailie M, et al. A randomized placebo-controlled trial of idebenone in Leber's hereditary optic neuropathy. *Brain.* (2011) 134:2677–86. doi: 10.1093/brain/awr170

66. Catarino CB, von Livonius B, Priglinger C, Banik R, Matloob S, Tamhankar MA, et al. Real-World clinical experience with idebenone in the treatment of Leber hereditary optic neuropathy. *J Neuroophthalmol.* (2020) 40:558–65. doi: 10.1097/WNO.0000000000001023

67. Pisano A, Preziuso C, Iommarini L, Perli E, Grazioli P, Campese AF, et al. Targeting estrogen receptor β as preventive therapeutic strategy for Leber's hereditary optic neuropathy. *Hum Mol Genet.* (2015) 24:6921–31. doi: 10.1093/hmg/ddv396

68. Dai Y, Zheng K, Clark J, Swerdlow RH, Pulst SM, Sutton JP, et al. Rapamycin drives selection against a pathogenic heteroplasmic mitochondrial DNA mutation. *Hum Mol Genet.* (2014) 23:637–47. doi: 10.1093/hmg/ddt450

69. Datta S, Tomilov A, Cortopassi G. Identification of small molecules that improve ATP synthesis defects conferred by Leber's hereditary optic neuropathy mutations. *Mitochondrion.* (2016) 30:177–86. doi: 10.1016/j.mito.2016.08.002

70. Indrieri A, Carrella S, Romano A, Spaziano A, Marrocco E, Fernandez-Vizarra E, et al. miR-181a/b downregulation exerts a protective action on mitochondrial disease models. *EMBO Mol Med.* (2019) 11:e8734. doi: 10.15252/emmm.201708734

71. Yu-Wai-Man P, Newman NJ, Carelli V, Moster ML, Biousse V, Sadun AA, et al. Bilateral visual improvement with unilateral gene therapy injection for Leber hereditary optic neuropathy. *Sci Transl Med.* (2020) 12:eaaz7423. doi: 10.1126/scitranslmed.aaz7423

72. Newman NJ, Yu-Wai-Man P, Carelli V, Moster ML, Biousse V, Vignal-Clermont C, et al. Efficacy and safety of intravitreal gene therapy for leber hereditary optic neuropathy treated within 6 months of disease onset. *Ophthalmology.* (2021) 128:649–60. doi: 10.1016/j.ophtha.2020.12.012

73. Guy J, Qi X, Pallotti F, Schon EA, Manfredi G, Carelli V, et al. Rescue of a mitochondrial deficiency causing Leber hereditary optic neuropathy. *Ann Neurol.* (2002) 52:534–42. doi: 10.1002/ana.10354

74. Oca-Cossio J, Kenyon L, Hao H, Moraes CT. Limitations of allotopic expression of mitochondrial genes in mammalian cells. *Genetics.* (2003) 165:707–20. doi: 10.1093/genetics/165.2.707

75. Perales-Clemente E, Fernández-Silva P, Acín-Pérez R, Pérez-Martos A, Enríquez JA. Allotopic expression of mitochondrial-encoded genes in mammals: achieved goal, undemonstrated mechanism or impossible task? *Nucleic Acids Res.* (2011) 39:225–34. doi: 10.1093/nar/gkq769

76. Mok BY, de Moraes MH, Zeng J, Bosch DE, Kotrys AV, Raguram A, et al. A bacterial cytidine deaminase toxin enables CRISPR-free mitochondrial base editing. *Nature.* (2020) 583:631–7. doi: 10.1038/s41586-020-2477-4

77. Wang G, Chen H, Oktay Y, Zhang J, Allen E, Smith G, et al. PNPASE regulates RNA import into mitochondria. *Cell.* (2010) 142:456–67. doi: 10.1016/j.cell.2010.06.035

78. Yu H, Koilkonda RD, Chou T-H, Porciatti V, Ozdemir SS, Chiodo V, et al. Gene delivery to mitochondria by targeting modified adenoassociated virus suppresses Leber's hereditary optic neuropathy in a mouse model. *Proc Natl Acad Sci USA.* (2012) 109:E1238–47. doi: 10.1073/pnas.1119577109

79. Mason JO, Price DJ. Building brains in a dish: Prospects for growing cerebral organoids from stem cells. *Neuroscience.* (2016) 334:105–18. doi: 10.1016/j.neuroscience.2016.07.048

80. Tyynismaa H, Suomalainen A. Mouse models of mitochondrial DNA defects and their relevance for human disease. *EMBO Rep.* (2009) 10:137–43. doi: 10.1038/embor.2008.242

81. Menacho C, Prigione A. Tackling mitochondrial diversity in brain function: from animal models to human brain organoids. *Int J Biochem Cell Biol.* (2020) 123:105760. doi: 10.1016/j.biocel.2020.105760

82. Lin CS, Sharpley MS, Fan W, Waymire KG, Sadun AA, Carelli V, et al. Mouse mtDNA mutant model of Leber hereditary optic neuropathy. *Proc Natl Acad Sci USA.* (2012) 109:20065–70. doi: 10.1073/pnas.1217113109

83. Sadun AA, Win PH, Ross-Cisneros FN, Walker SO, Carelli V. Leber's hereditary optic neuropathy differentially affects smaller axons in the optic nerve. *Trans Am Ophthalmol Soc.* (2000) 98:223–32; discussion 232-235.

84. Pan BX, Ross-Cisneros FN, Carelli V, Rue KS, Salomao SR, Moraes-Filho MN, et al. Mathematically modeling the involvement of axons in Leber's hereditary optic neuropathy. *Invest Ophthalmol Vis Sci.* (2012) 53:7608–17. doi: 10.1167/iovs.12-10452

85. Winanto null, Khong ZJ, Soh B-S, Fan Y, Ng S-Y. Organoid cultures of MELAS neural cells reveal hyperactive Notch signaling that impacts neurodevelopment. *Cell Death Dis.* (2020) 11:182. doi: 10.1038/s41419-020-2383-6

86. Pacitti D, Bax BE. The development of an *in vitro* cerebral organoid model for investigating the pathomolecular mechanisms associated with the central nervous system involvement in Mitochondrial Neurogastrointestinal Encephalomyopathy (MNGIE). *Nucleosides Nucleotides Nucleic Acids.* (2018) 37:603–17. doi: 10.1080/15257770.2018.1492139

87. Mazzara PG, Muggeo S, Luoni M, Massimino L, Zaghi M, Valverde PT-T, et al. Frataxin gene editing rescues Friedreich's ataxia pathology in dorsal root ganglia organoid-derived sensory neurons. *Nat Commun.* (2020) 11:4178. doi: 10.1038/s41467-020-17954-3

88. Inak G, Rybak-Wolf A, Lisowski P, Jüttner R, Zink A, Mlody B, et al. SURF1 mutations causative of Leigh syndrome impair human neurogenesis. *bioRxiv.* (2019) 2019:551390. doi: 10.1101/551390

89. Feuer WJ, Schiffman JC, Davis JL, Porciatti V, Gonzalez P, Koilkonda RD, et al. Gene therapy for leber hereditary optic neuropathy. *Ophthalmology.* (2016) 123:558–70. doi: 10.1016/j.ophtha.2015.10.025

90. Cwerman-Thibault H, Sahel J-A, Corral-Debrinski M. Mitochondrial medicine: to a new era of gene therapy for mitochondrial DNA mutations. *J Inherit Metab Dis.* (2011) 34:327–44. doi: 10.1007/s10545-010-9131-5

Conflict of Interest: The authors declare that the research was conducted in the absence of any commercial or financial relationships that could be construed as a potential conflict of interest.

The handling editor is currently organizing a Research Topic with one of the author VC.

Check for
updates

Dominant Optic Atrophy (DOA): Modeling the Kaleidoscopic Roles of OPA1 in Mitochondrial Homeostasis

Valentina Del Dotto[1]* and Valerio Carelli[1,2]

[1] *Department of Biomedical and Neuromotor Sciences, University of Bologna, Bologna, Italy, [2] Istituto di Ricovero e Cura a Carattere Scientifico Istituto delle Scienze Neurologiche di Bologna, Programma di Neurogenetica, Bologna, Italy*

In the year 2000, the discovery of *OPA1* mutations as causative for dominant optic atrophy (DOA) was pivotal to rapidly expand the field of mitochondrial dynamics and describe the complex machinery governing this pathway, with a multitude of other genes and encoded proteins involved in neurodegenerative disorders of the optic nerve. OPA1 turned out to be a much more complex protein than initially envisaged, connecting multiple pathways beyond its strict role in mitochondrial fusion, such as sensing of OXPHOS needs and mitochondrial DNA maintenance. As a consequence, an increasing need to investigate OPA1 functions at multiple levels has imposed the development of multiple tools and models that are here reviewed. Translational mitochondrial medicine, with the ultimate objective of translating basic science necessary to understand pathogenic mechanisms into therapeutic strategies, requires disease modeling at multiple levels: from the simplest, like in yeast, to cell models, including the increasing use of reprogrammed stem cells (iPSCs) from patients, to animal models. In the present review, we thoroughly examine and provide the state of the art of all these approaches.

Keywords: OPA1 mutations, dominant optic atrophy, OPA1, mitochondria, cell models, mouse models, iPSCs, retinal ganglion cells

INTRODUCTION

In the year 2000, the human *OPA1* gene came to attention, as heterozygous mutations were associated with dominant optic atrophy (DOA) (1, 2), a blinding disorder originally described by the Danish ophthalmologist Paul Kjer in 1959, which usually leads to optic atrophy in the first decade of life (3). This gene encodes a protein for which the role as one of the mitochondrial factors involved in the machinery regulating mitochondrial dynamics, promoting fusion of the inner membrane of mitochondria and being key to mitochondrial DNA (mtDNA) maintenance, was clear by analogy with the orthologous genes *MGM1/MSP1* in yeast (4–6). OPA1 was rapidly revealed to have a very complex expression regulation, coming in multiple isoforms due to alternative splicing (7, 8). Only recently have we begun to understand the need for this complexity, revealing how sophisticated and possibly flexible the function of this protein is (9). In fact, besides the role of OPA1 in mitochondrial fusion, by studying OPA1 dysfunction in DOA patients and cell models, its implication in regulating bioenergetics has rapidly emerged (10, 11), contributing to mitochondrial cristae shaping and regulating apoptosis (12, 13), maintaining mtDNA integrity and copy number (14–17), contributing to mitochondrial quality control (18, 19), and ultimately representing a key cross-road for mitochondrial homeostasis, which is central to cell survival and function (20–22).

The identification of *OPA1* mutations as causative for selective neurodegeneration of retinal ganglion cells (RGCs) leading to optic atrophy was thus instrumental in opening a very active field of investigation for neurology and neuro-ophthalmology as well as in understanding new mechanistic pathways regulating mitochondria homeostasis and primarily mitochondrial dynamics (23). Congruently, the expanding spectrum of dominant and recessive mutations affecting the OPA1 protein has been reflected into a progressively larger landscape of clinical phenotypes linked to OPA1 dysfunction, including the vast catalog of the so-called DOA *plus* syndromes (14, 15) dominated by neurodegeneration and multisystem involvement (24), including multiple sclerosis (25, 26), Parkinsonism and dementia (18, 27), infantile Leigh syndrome (28), and cardiomyopathy (17).

Given the constantly growing interest in OPA1 function and dysfunction in relation to human diseases, their modeling is essential to rapidly progress our understanding and possibly provide therapeutic options. Thus, we review the currently available tools for the study of this protein, looking at the future of this rapidly evolving field.

OPA1 CELL MODELS

Yeast Models

Yeast, as a simple, easy-to-manipulate eukaryotic organism, is an extremely helpful model with which to understand mitochondrial function, providing insight into mitochondrial pathways and their regulation. Indeed, yeast has been instrumental in identifying key functions of *MGM1* and *MSP1*, the orthologous of *OPA1* in *Saccharomyces cerevisiae* and *Schizosaccharomyces pombe*, respectively (**Figure 1**). Mgm1 was first identified for its role in mtDNA maintenance (4, 29) and its relative effect on respiratory competence (4, 6). Subsequent reports highlighted the fusion capacity (30–32) and its role for *cristae* structure stability (32, 33). Similarly, Msp1 has been characterized as a protein involved in mtDNA maintenance (5), in mitochondrial network stability and respiratory function (34), and in the fusion of mitochondria (35). Mgm1 is proteolytically processed in two forms, long and short, by the rhomboid-type protease Pcp1, the homolog of the mammalian PARL (36, 37), whereas Msp1 is cleaved by both rhomboid and m-AAA proteases (38). The presence of both short and long forms of Mgm1 is required to maintain a tubular mitochondrial morphology and proper mtDNA amount (36, 39). The increased ratio of long to short form exerts a dominant negative effect on mitochondrial fusion, and a functional GTPase in the short form, but not in the long form, is necessary to tune fusion (39). Furthermore, one of the transmembrane segments of the dynamin Msp1 is required for mtDNA maintenance but not for the fusion activity (40).

Yeast may be used as a model of mitochondrial diseases to investigate the effect of pathogenic mutations on mitochondrial function. Due to the weak conservation of amino acid sequences between Mgm1 and OPA1 and the inefficiency of the human GTPase in complementing *MGM1* depletion, a chimeric protein composed of the N-terminal region of Mgm1 and the catalytic region of OPA1 (41) has been generated. Our group and other investigators used this chimeric model to dissect the effect of several mutations found in DOA patients, showing that pathogenic mutations caused mtDNA loss and mitochondrial fragmentation, reduced the processing of long to short forms, and impaired the respiratory capacity and oxidative growth in yeast (41–43). In addition to the validation of the pathogenicity, the possibility to compare haploid and diploid strains, expressing the mutant only or in combination with the wild-type chimeric protein, allowed for discrimination between hypomorphic, null, or dominant alleles (42).

Yeast is also a valuable system to screen for compounds with therapeutic potential to treat mitochondrial diseases as a "repurposing" strategy. Two research teams applied this approach in the context of *OPA1* mutations (44, 45). In the first screening, a collection of 1,600 repurposed drugs has been used and five compounds were able to suppress the lethality in restrictive conditions caused by a GTPase mutation of *MSP1* in *S. pombe*. Two drugs were able to rescue mtDNA depletion, and one of them recovered also mitochondrial network morphology (44). In the second screening, our group used the yeast strains with mutations on *MGM1* or on the chimeric Mgm1-OPA1 to evaluate the effect of more than 2,500 drugs from two chemical libraries (45). In this case, out of the 26 drugs able to rescue the oxidative growth phenotype, six of them reduced the mitochondrial DNA instability in yeast and were analyzed also in mammalian cell models (45). Therefore, although some differences are present between Mgm1/Msp1 and OPA1, yeast has proven to be a simple and very useful first-line tool for large-scale OPA1 drug screenings, and, coupled with more physiological models to cross-validate the outcomes, it might speed up the discovery of effective therapies for DOA.

Mouse and Rat Cell Models

The study of OPA1 in mammalian models, such as mouse and rat cells, in particular the mouse embryonic fibroblasts (MEFs), has been instrumental in deepening our understanding of the complex role played by OPA1 in multiple mitochondrial pathways (**Figure 1**).

Studies in MEFs led to the identification of the OPA1 cleavage sites S1 and S2, encoded by exon 5 and 5b and cleaved by OMA1 and YME1L, respectively, to generate a balanced mixture of long and short forms (46, 47). Recently, a previously suggested third site (48) has been identified, named S3, located in exon 4b, and cleaved by YME1L (49).

Overexpression or silencing of OPA1 in MEFs highlighted its fundamental role in maintaining a filamentous mitochondrial network and sustaining fusion (50, 51), supporting respiratory efficiency (51), and controlling *cristae* integrity and apoptosis (13). However, *Opa1* knockout (ko) mouse fibroblasts have also been extremely helpful in understanding the DOA pathogenic mechanism given the clear-cut phenotype due to the complete lack of the protein. Indeed, *Opa1* null cells have no fusion activity (9, 46, 52, 53), decreased the number of mtDNA and nucleoids (9, 53, 54), and caused profound alterations of *cristae* structure integrity (9, 53, 55). Furthermore, Opa1 ablation and OPA1 overexpression in mouse fibroblasts clarified the interplay between *cristae* and OPA1 in respiratory chain
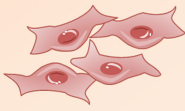
FIGURE 1 | Schematic figure of the five categories of cell models used to study OPA1 functions. The pathways reported in the literature to be regulated by OPA1 or altered by its kd/ko/mutations in the different models are identified by a checkmark.

supercomplexe (RCS) assembly (56) and identified the ATP synthase as the effector of the OPA1-mediated protection of mitochondrial functions (57). This model also provided details on the relationship between OPA1 and other interactors to sustain *cristae* architecture, such as the MICOS protein MIC60 (58, 59) and the SLC25A solute carriers family members, which activate the OPA1-mediated *cristae* remodeling in response to different energetic conditions (60).

Moreover, the complete absence of the protein was also instrumental in dissecting two fundamental and debated questions key to OPA1 complexity: the role of the isoforms and of the long and short forms. Expression of each of the eight isoforms in *Opa1* null MEFs disclosed that they are all able to rescue mtDNA content, *cristae* organization, and energetics (9), whereas the short forms are more efficient in restoring energetic efficiency (9, 53) and enhancing cell survival under oxidative stress (61). Importantly, it has been shown that long forms support mitochondrial fusion (9), whereas both long and short forms are necessary to preserve an interconnected mitochondrial

network (9, 46, 53). More recently, it has been reported that the presence of multiple isoforms generating different short forms is necessary to achieve a more filamentous mitochondrial network (49), confirming our seminal study (9).

The model of *Opa1* null MEFs has been also employed to study the pathogenic effect of *OPA1* missense mutations associated with DOA in an isogenic genetic background, evaluating the capability to restore mitochondrial defects (42, 62). We substantiated the more severe effect of mutations affecting the GTPase domain when compared to those in the dynamin domain or compared to hypomorphic mutations. This was true for all the mitochondrial readouts analyzed, faithfully mirroring the severity of clinical phenotypes (42). Additionally, these cell models underwent metabolomic and lipidomic studies (63–65). *Opa1* ko MEFs showed bioenergetic changes with altered metabolism of aspartate, glutamate, nucleotides, and NAD (63), and variations in triglycerides and lipids involved in membrane remodeling and in cell signaling pathways (64), similarly to what has been observed in primary *Opa1*-depleted cortical neurons

(66). An analysis of OPA1 mutated MEFs ranked the allele severity with the metabolic and lipid alterations, highlighting an increased spermine/spermidine ratio and a reduction in hydroxyproline, amino acid pool, and several phospholipids (65). Interestingly, the increase in glutathione in *Opa1* null MEFs (63) has been recently confirmed in a second study (67) and reported, together with the increased dependency on cysteine transport, as a metabolic adaptive mechanism to afford protection against oxidative stress in these cells (67). Finally, this cell model has been also used for drug screening on amelioration of mitochondrial readouts with different missense mutations, proving to be a valuable tool in testing new DOA therapeutic interventions (45).

Immortalized and Tumor Human Cell Models

After the discovery that mutations in the *OPA1* gene are the prevailing cause of DOA, several studies have been carried out using immortalized or human tumor-derived cells (**Figure 1**). These models have been instrumental in elucidating the manifold roles of this GTPase in mitochondrial homeostasis, avoiding the individual variations intrinsic to patient-derived primary cells.

Subcellular localization experiments were instrumental in identifying OPA1 as an inner-membrane protein, exposing the C-terminal portion in the IMS (68–71), which is present as a mixture of long and short forms (71, 72), the latter generated by the activity of the proteases YME1L (72, 73) and OMA1 (48). As the major pathogenic mechanism in OPA1-related DOA is haploinsufficiency, OPA1 downregulation has highlighted mitochondrial network fragmentation (12, 70, 73–75) and complete inhibition of mitochondria fusion (74, 76), confirming its pro-fusion role in mitochondrial dynamics. In addition, several studies found dissipation of the mitochondrial membrane potential (12, 76), drastic disorganization of the *cristae* structure (12, 70, 74, 75, 77), alteration of MICOS assembly (77) and increased sensitivity to apoptosis with the release of cytochrome c (12, 74, 76, 78). The link between OPA1, *cristae* integrity and apoptosis was confirmed in Hek293 cells by expressing a mutant OPA1 resistant to disassembly of its oligomers, which blocked cytochrome c release and apoptosis (79). Downregulation of OPA1 protein also induced mtDNA depletion (16, 75), bioenergetic defect (75, 80), altered Ca^{2+} homeostasis (75, 81) and mitophagy (82). Specific silencing of the three alternative splicing exons has been used in the attempt to unravel a precise mitochondrial function of the individual OPA1 isoforms (16, 83).

The pro-fusion role of long forms has been reported in several studies, where overexpression of long OPA1 was more efficient compared with the long/short combination in ameliorating the mitochondrial network morphology in knockdown (Kd)-*OPA1* cells (71) and in SH-SY5Y cells after hypoxia and re-oxygenation injury (84). Furthermore, it has been reported that SIRT4 overexpression increased OPA1 long-form promoting fusion, counteracting fission and mitophagy (85).

Human cells have been used also to confirm the new function identified in adipose-like mouse fibroblasts (86), where OPA1 localized in lipid droplets serves as an A-kinase anchoring protein (AKAP) and allows PKA to phosphorylate perilipin 1 to favor lipolytic stimulation (87).

Patients' Derived Fibroblasts and Lymphoblasts

Fibroblasts and lymphoblasts derived from patients are a model extensively used to study the pathophysiology of OPA1 mutations. The majority of the alterations identified in the previous models have been reconfirmed in patients' cells (**Figure 1**). Numerous studies of fibroblasts and lymphoblasts reported defective mitochondrial network dynamics (11, 18, 27, 42, 78, 88–95), energetic metabolism (11, 42, 88, 91, 93, 94, 96), *cristae* structure maintenance (11, 27, 93), and increased sensitivity to apoptosis stimuli (11, 96). Depletion of mtDNA copy number in fibroblasts has been reported in a few cases in the presence of missense (42, 96) or compound heterozygous mutations (19, 43).

Recently, increased ROS production (94, 96), low levels of antioxidant enzymes (97), and alteration of calcium uptake (98) have been also reported. Furthermore, direct involvement of OPA1 in quality control has been revealed in fibroblasts (18, 19, 95), where missense mutations induced an increase in both autophagy and mitophagy processes. Interestingly, basal mitophagy was increased in fibroblasts bearing dominant-negative *OPA1* mutations, whereas OPA1 haploinsufficiency seems to correlate with a reduction in mitochondrial turnover and autophagy (95).

Although these cells have been very useful when studying mitochondrial alterations, the presence of the wild-type allele often hides the effect of the mutated one, prompting the need to use galactose media to force oxidative metabolism and reveal the mitochondrial dysfunctions. Also, nuclear and mitochondrial genomes may variably contribute to the great heterogeneity observed in clinical and cellular phenotypes due to the same *OPA1* mutation. For example, analysis of mtDNA copy number revealed a depletion only in one of two fibroblasts with the same R445H mutations derived by patients belonging to the same family (42), suggesting that other genetic or environmental factors may contribute. Concordantly, mitochondrial OMI/HTRA2 has been recently reported as a new gene modifier of phenotype variability (99).

Although with these limitations, fibroblasts, if combined with other models, may be functional in identifying new pathways, confirming pathogenic mechanisms, or validating the efficacy of therapeutic molecules, as we recently reported (45).

iPSCs, NPCs, Neuron, and RGCs

In the last decade, the establishment of induced pluripotent stem cell (iPSC) technology has provided the opportunity to generate *in vitro* human models of neurological disorders. The iPSCs are stem cells-like reprogrammed *in vitro* from patient-derived primary cells, which can be then differentiated into specific somatic cell types (100). The iPSCs and terminally differentiated cells, therefore, allow us to study the exact cell type affected in the human disease to identify the pathological mechanism and to conduct drug screening on a human genetic background (**Figure 1**).

Human iPSCs lines have been generated from patients' fibroblasts carrying different *OPA1* mutations, such as the p.Gln621Ter (101) and the p.Ser545Arg (102) heterozygous mutations, and the compound heterozygous mutations causing Behr syndrome (103). All these iPSCs could differentiate into the three germ layers (endoderm, mesoderm, and ectoderm) (101–103).

Increased apoptosis and inefficient capability to differentiate into a neural rosette and RGCs were reported for the iPSCs derived from two other fibroblasts of patients carrying the intronic mutation c.2496+1G>T, suggesting the impact of apoptosis on RGCs possibly leading to early or congenital optic atrophy (104), as previously proposed by optical coherence tomography clinical studies (105). The addition of the neural induction medium, the secreted signaling molecule noggin, or the estrogen hormone promoted the differentiation into RGCs of the *OPA1*$^{+/-}$ iPSCs, possibly by inhibiting apoptosis (104).

Dopaminergic neurons carrying an *OPA1* mutation causing haploinsufficiency were generated via iPSCs from two patients belonging to the same family that, interestingly, developed different clinical phenotypes: isolated DOA or DOA with syndromic Parkinsonism (106). Both the cell lines showed a reduction in oxygen consumption rate (OCR), complex I levels, and activity, whereas only neurons derived from the patient with Parkinsonism presented mitochondrial fragmentation and an increase of the OPA1 short forms. In this study possible genetic modifiers of the different clinical phenotypes in the two patients, presenting the same OPA1 mutation, were not identified (106).

Neural progenitor cells (NPCs) from two *OPA1* missense mutations causing Parkinsonism and dementia (18) presented bioenergetic defect, mitochondrial network fragmentation, increased ROS levels, and alteration in the lysosome pathway (107). Even in this case, the *OPA1*-mutated NPCs showed a survival deficit, which was rescued by selective inhibition of necroptosis (107). The iPSC-derived neurons bearing these two *OPA1* mutations have been further studied in a microfluidic system where different neuronal subtypes were cultured together with a patterned organization of their projections and synaptic terminals (108). Analysis of neuronal projections revealed altered content, distribution, and movement of mitochondria along the axons of the neurons. Moreover, the impairment in synapse formation was followed by a progressive loss of synaptic contacts over time in the mutant neurons, suggesting a depletion of mitochondria in neuronal projections as a cause of loss of neuronal connectivity and neurodegeneration (108).

Recently, human embryonic stem cells (hESCs) with OPA1 haploinsufficiency induced by the CRISPR-Cas9 technology have been characterized and differentiated into NPCs. Interestingly, several genes involved in NPCs differentiation, GABAergic interneuron formation, and retinal development were downregulated in *OPA1*$^{+/-}$ NPCs due to increased CpG methylation (109). The increased ROS levels and downregulated FOXG1 expression, a factor crucial for GABAergic neuronal formation and retinal development, were confirmed also in NPCs derived from two other patients bearing the common c.2873_2876delTTAG mutation, suggesting that OPA1 haploinsufficiency may result in aberrant nuclear DNA methylation and an altered transcriptional program (109).

Although studying the cells targeted by the disease accelerates our understanding of OPA1-derived dysfunctions, these two-dimensional methods to studying neuronal dysfunction do not completely recapitulate the complexity of a human brain (110). The recently optimized protocols for modeling *in vitro* brain and retina organogenesis (111) represent a further fundamental step instrumental in disease modeling.

OPA1 ANIMAL MODELS

Drosophila melanogaster Models

Modeling of DOA has also been carried out in *Drosophila melanogaster* (**Figure 2**) and these studies emphasized the role of increased ROS production in leading to the pathologic phenotype, showing how this could be partially counterbalanced by antioxidant therapy (112). This supports the proposal of therapeutic approaches with antioxidants in human patients with DOA. The heterozygous mutant flies showed an age-dependent perturbation of visual functions, heart alterations (113), lifespan reduction, elevated ROS level, and the presence of irregular and dysmorphic mitochondria in the skeletal muscle (114). In summary, these two studies on the *Opa1* mutant *Drosophila* model showed an age-dependent multisystemic disorder, resembling the syndromic forms of DOA "plus" (113, 114).

Caenorhabditis elegans Models

The tight interconnection between OPA1 mutations and ROS alteration has been further confirmed in *Caenorhabditis elegans* (*C. elegans*) models. Indeed, the mutations in the *eat-3* gene, the *OPA1* worm orthologous gene, increased susceptibility to damage from free radicals, as shown by increased sensitivity to paraquat and to the loss of the mitochondrial superoxide dismutase sod-2 (115). Transgenic worms carrying loss of function *eat-3* mutations presented fragmented mitochondria (115–117) and aberrant *cristae* architecture (115, 117). The *eat-3* mutation caused an age-dependent and progressive deficit in movement, as well as in muscle and neuronal function (117), somehow mirroring the DOA "plus" clinical phenotypes. Interestingly, increased levels of elongated mitochondria have been linked to longevity, as mitochondrial fusion allows the survival of older animals (118), a finding supported by a second study showing that *eat-3* mutation reduced median animal lifespan (117), as already reported in the *Drosophila* model (114).

The increased autophagy/mitophagy as a key pathogenic mechanism in DOA has been confirmed also in *C. elegans,* where the expression of mutated OPA1 in GABAergic axons reduced mitochondrial content in axons, a phenotype that was counteracted by depletion of the *ATG8* homolog *lgg-2* (119).

Danio rerio (Zebrafish) Models

The effect of Opa1 depletion in the early development has been studied in a *Danio rerio* model using the antisense morpholino (120). The Opa1 morphants showed developmental delay, decreased blood circulation velocity, reduction of the eye size

ANIMAL MODELS	MITO DYNAMICS AND MORPHOLOGY	MITO ENERGETICS	mtDNA MAINTENANCE	ROS	APOPTOSIS/ REDUCED LIFESTAN	AUTOPHAGY/ MITOPHAGY	METABOLOMIC ANALYSIS	ER-STRESS, UPR, INFLAMMATION	DRUG SCREENING/ GENE THERAPY
DROSOPHILA MODELS	✓	✓		✓	✓				
C. ELEGANS MODELS	✓	✓		✓	✓	✓			
DANIO RERIO MODELS	✓								
MOUSE MODELS	✓	✓	✓	✓	✓	✓	✓	✓	✓

FIGURE 2 | Schematic figure of the four animal models used to study OPA1. The pathways reported in the literature to be regulated by OPA1 or altered by its kd/ko/mutations in the animal models are identified by a checkmark.

and heart rate, defects associated with increased mitochondrial fragmentation in muscle cells, and impaired bioenergetics (120).

The alteration of mitochondrial networks in Opa1 morphants has been reported more recently (121), confirming the main role of OPA1 in mitochondrial morphology.

Mouse Models

Three mouse models carrying a heterozygous germline mutant *Opa1* allele have been reported to date and have been instrumental in studying the pathogenic mechanisms of DOA (**Figure 2**) (122–124). Screening an ENU-mutagenized DNA library of mouse DNA led to generating two of the murine models, both recapitulating the human genetic defects that induce haploinsufficiency. The first, B6;C3-*Opa1*$^{329-355del}$ mutant mouse, leads to a splice error with the skipping of exon10, which ultimately causes an in-frame deletion of 27 amino acid residues in the dynamin GTPase domain (122). The second, B6;C3-*Opa1*^{Q285STOP} mutant mouse, results in a truncated protein (123). Both models have about a 50% reduction in OPA1 expression and the homozygous condition is embryonically lethal, pointing to the crucial role played by OPA1 during fetal development. The third model is a knock-in mouse carrying the common *OPA1 c.2708_2711delTTAG* mutation in humans in a C57Bl6/J mouse background (124). In these mice, a 25% reduction in OPA1 protein was recognized in the brain, retina, optic nerve, and glycolytic fibers, whereas the reduction

reached 50% in oxidative fibers and heart. Also, in this model, the homozygous condition was embryonically lethal.

In all three models, the heterozygous animals displayed a mild, age-dependent ocular phenotype with well-documented RGCs dysfunction and loss (122, 124–126). At histopathology, degenerative features were observed in the optic nerves including demyelination, various degrees of axonal degeneration, and abnormalities of mitochondria at the ultrastructure level (123–126).

Increased autophagy was reported in the RGCs of the B6;C3-*Opa1*^{Q285STOP} mutant mouse (127) and in the glycolytic fibers, RGCs, and peripheral neurons of the *Opa1*^{delTTAG} mutant mouse (124), highlighting the autophagic elimination of mitochondria with impaired fusion. More recently, increased mitophagy has been reported in the B6;C3-*Opa1*^{Q285STOP} mice (128) and confirmed in mouse RGCs overexpressing a mutated OPA1, showing also that reduced axonal mitochondrial density was linked to increased autophagic mitochondrial degradation in the RGCs soma, in close proximity to axonal hillocks (119). The B6;C3-*Opa1*$^{329-355del}$ mice were also reported to present an imbalance of redox state possibly increasing mitochondrial ROS, as suggested by the decrease in aconitase activity and induction of antioxidant defenses (97). Metabolic analysis of the optic nerve in female *Opa1*^{delTTAG} mice identified changes in the concentrations of metabolites involved in neuroprotection and of phospholipids, some of them suggestive of myelin sheath alteration (129). All

these dysfunctions may lead most RGCs to death but not the melanopsin-expressing RGCs, which are reported to survive in two DOA mice models (130, 131) according to evidence that also in humans this cell type is relatively resistant to cell death in mitochondrial optic neuropathies (132).

In summary, the phenotype in these mouse models resembles sufficiently the human disease, characterized by loss of RGCs and optic nerve atrophy. In humans, the disease may vary in clinical severity, from severe congenital cases to very mild, subclinical disease disclosed only by accurate ophthalmological investigations (133, 134). Interestingly, systemic examination of these animals revealed mild neuromuscular impairment, including decreased locomotor activity, abnormal clutching reflex, and tremor, in analogy to the continuum clinical spectrum in humans, ranging from DOA to DOA "plus" (134).

Remarkably, interesting results were obtained by a closer investigation of the RGCs synaptic connectivity in the B6;C3-$Opa1^{Q285STOP}$ mutant animals, looking at their dendrites instead of focusing only on axons (135, 136). Counterintuitively, the earliest pathological changes occurred in RGCs dendrites, showing pruning and marked reduction in their synaptic connectivity (135, 136). This dendropathy is, however, congruent with the crucial role played by OPA1 and mitochondrial fusion in maintaining dendrites and their synapses (137).

Furthermore, with aging impaired cardiac function has been reported in all three mice models. Indeed, at onset of blindness, the aged B6;C3-$OPA1^{Q285STOP}$ mice also showed cardiomyopathy, characterized by disruption of mitochondrial organization, mtDNA depletion, bioenergetic defect, and defective cardiac mitochondria (138). Reduction in cardiac adaptation to pressure overload and heart hypertrophy were observed also in the B6;C3-$Opa1^{329-355del}$ mice (139). Similar alterations in mitochondrial calcium handling affected these $Opa1$ mutant mice (139), observed also in the third $Opa1^{delTTAG}$ mice, together with increased sensitivity to cardiac ischemia/reperfusion injuries (140). Interestingly, cardiac involvement in patients carrying $OPA1$ mutation has been reported for the first time in two patients harboring a homozygous recessive $OPA1$ mutation leading to a fatal encephalopathy with progressive hypertrophic cardiomyopathy (17).

A further mouse model with deleted $Opa1$ in pancreatic beta cells showed glucose intolerance and impaired insulin secretion. It also presented a reduced glucose-stimulated ATP production and developed hyperglycemia. Focusing on mitochondrial function, the beta cells presented a severe alteration of mitochondrial structure and a reduction of subunits' level and activity of Complex IV (141).

Recently, muscle-specific $Opa1$ ablation mice models have been generated to investigate the tissue-specific role of $Opa1$ in muscle, highlighting its metabolic role (142–144). Pereira et al. showed that in mutant mice the progressive mitochondrial dysfunction led to an increased metabolic rate, muscle atrophy, and insulin resistance induced by a mechanism involving ER stress and secretion of fibroblast growth factor 21 (FGF21) (142). Increased FGF21 has been observed also in another muscle-specific $Opa1$-deletion mouse model, where, together

with ER stress and activation of the unfolded protein response (UPR), a catabolic program with muscle loss was activated, leading to systemic aging and premature death (143). In a third study, the enhanced FGF21 level and premature death elicited by $Opa1$ ablation were associated with muscle inflammation characterized by NF-kB activation and increased expression of pro-inflammatory genes; these features were blocked by mtDNA depletion and repression of TLR9 (144). All these features are of great interest, as plasma cytokines, including FGF21, have been recently validated as biomarkers for mitochondrial diseases, especially those with prominent muscle involvement (145, 146).

From a therapeutic point of view, all these mice models are instrumental in testing drugs or therapies. Indeed, the $Opa1^{delTTAG}$ mouse has been already tested for OPA1 isoform 1 gene therapy, proving to mitigate the OPA1-induced RGCs degeneration, encouraging a possible clinical translation in DOA patients (147). Furthermore, the most recent mouse model with RGC-specific overexpression of mutant OPA1 was instrumental in showing that contrasting the excess autophagy by various strategies was effective to avoid RGCs degeneration and restore vision (119).

IN VITRO MODELS

Over the last decade, to elucidate the OPA1 role in the fusion of the inner mitochondrial membrane, various *in vitro* assays with purified OPA1 have been developed. Initially, the simpler yeast mgm1 has been studied by purifying short Mgm1 (s-Mgm1), revealing that the protein exhibits GTP activity, self-assembles into low order oligomer, and interacts specifically with negatively charged phospholipids present in the mitochondrial membranes (148). Furthermore, it has been reported that s-Mgm1 oligomerization and its binding to mitochondrial phospholipids strongly stimulates its GTPase activity, and it assembles onto liposomes and boosts liposome interaction, indicating that s-Mgm1 can tether opposing membranes mediating their fusion (149). This hypothesis was supported by cryo-electron microscopy studies and liposome fusion assays, showing that s-Mgm1 self-associates to tether opposing membranes with a gap of 15 nm and the oligomers undergo GTP-dependent structural changes that may induce fusion (150). Together with the ability to cause phospholipid clustering, s-Mgm1 was also reported to trigger local membrane bending and the formation of tubular structures (151). The investigations of both long and short Mgm1 forms in fusion highlighted that both forms are preferentially inserted into liposomes containing the lipid cardiolipin acting together in trans to form a functional unit required for mitochondrial fusion (152).

Similar results have been obtained by studying the molecular mechanisms of OPA1-mediated fusion. Indeed, the association with liposomes containing negative phospholipids, such as cardiolipin, enhanced the GTPase activity of short forms of OPA1, promoted their assembly into oligomers, and led to membrane tubulation, activities that were selectively impaired by DOA mutations (62). Using an *in vitro* purified mitochondria system, it has been shown that mitochondrial fusion is dependent

on proteolytic processing of long forms (153). To disentangle the debated issue of the fusogenic capability of OPA1 forms, Ban et al. purified and analyzed short and long forms (154). The *in vitro* membrane fusion assays revealed that long forms and cardiolipin on opposite sides cooperate in mitochondrial inner membrane fusion, a process that is efficiently accelerated by a defined amount of short form and lowered by its excess level. On the other hand, a cardiolipin-independent interaction of long forms located on opposite membranes was reported to promote membrane tethering, thus sustaining the *cristae* structure (154). Concordantly, an *in vitro* reconstitution system, able to distinguish the sequential steps in membrane fusion, disclosed that the short form mediates membrane tethering, the long form is sufficient for membrane docking, hemifusion and low levels of content release, and the short form cooperates with the long form to mediate efficient and fast membrane pore opening (155). Importantly, as seen in other studies, the excess levels of short form inhibited fusion activity (155). Cryo-electron microscopic structures revealed that the short form presents the classic dynamin-like structure, can bind to membranes, induces membrane tubulation by forming a helical array, and GTPgS binding promotes changes in S-OPA1 assembly from a "closed" to an "open" conformation (156).

New mechanistic insight into how OPA1/Mgm1 mediates the membrane fusion has been provided by the recently solved crystal structures of short Mgm1 from *Chaetomium thermophilum* (157) and *Saccharomyces cerevisiae* (158). The fungus short Mgm1 was reported to form stalk-mediated tetramers and assemble on positively or negatively curved membranes (157), whereas the yeast short Mgm1 forms a concave membrane-associated head-to-tail trimeric structure built by intermolecular interactions (158). The crystal structure of the minimal GTPase domain (MGD) of OPA1 and biochemical analysis, instead, revealed that it can form nucleotide-dependent and -independent dimers, which may combine to form higher-order oligomers (159).

All these *in vitro* findings resolve some conflicting results obtained with cellular studies and helped to highlight the complexity of OPA1 activities, fundamental to maintain and support the inner membrane structure and fusion.

CONCLUSIONS

The investigation of OPA1 function has witnessed a tremendous deal of progress in the last decade thanks to a multitude of new models and approaches that we here reviewed. This progress was instrumental in refining the role of mitochondria in RGCs survival and to deepen our understanding of DOA pathogenesis to possibly establish effective therapies for these patients, currently an unmet need that urges a research effort. A few *proof of principle* studies already provided interesting results, such as by pharmacologically or genetically limiting the overactive autophagy in RGCs (119), or refining strategies based on gene therapy approaches (147). The multifaceted role of OPA1 in mitochondrial function and, more generally, in cell metabolism continues to surprise, and the possible therapeutic role of slight OPA1 overexpression has also been explored to counteract an array of different conditions (160–162), which is well-beyond the specific field of inherited optic neuropathies.

AUTHOR CONTRIBUTIONS

VD and VC contributed to the writing of the manuscript. Both authors contributed to the article and approved the submitted version.

FUNDING

REFERENCES

1. Delettre C, Lenaers G, Griffoin JM, Gigarel N, Lorenzo C, Belenguer P, et al. Nuclear gene OPA1, encoding a mitochondrial dynamin-related protein, is mutated in dominant optic atrophy. *Nat Genet.* (2000) 26:207–10. doi: 10.1038/79936

2. Alexander C, Votruba M, Pesch UE, Thiselton DL, Mayer S, Moore A, et al. OPA1, encoding a dynamin-related GTPase, is mutated in autosomal dominant optic atrophy linked to chromosome 3q28. *Nat Genet.* (2000) 26:211–5. doi: 10.1038/79944

3. Kjer P. Infantile optic atrophy with dominant mode of inheritance: a clinical and genetic study of 19 Danish families. *Acta Ophthalmol Suppl.* (1959) 164:1–147.

4. Guan K, Farh L, Marshall TK, Deschenes RJ. Normal mitochondrial structure and genome maintenance in yeast requires the dynamin-like product of the MGM1 gene. *Curr Genet.* (1993) 24:141–8. doi: 10.1007/BF00324678

5. Pelloquin L, Belenguer P, Menon Y, Ducommun B. Identification of a fission yeast dynamin-related protein involved in mitochondrial DNA maintenance. *Biochem Biophys Res Commun.* (1998) 251:720–6. doi: 10.1006/bbrc.1998.9539

6. Wong ED, Wagner JA, Gorsich SW, McCaffery JM, Shaw JM, Nunnari J. The dynamin-related GTPase, Mgm1p, is an intermembrane space protein required for maintenance of fusion competent mitochondria. *J Cell Biol.* (2000) 151:341–52. doi: 10.1083/jcb.151.2.341

7. Delettre C, Griffoin JM, Kaplan J, Dollfus H, Lorenz B, Faivre L, et al. Mutation spectrum and splicing variants in the OPA1 gene. *Hum Genet.* (2001) 109:584–91. doi: 10.1007/s00439-001-0633-y

8. Del Dotto V, Fogazza M, Carelli V, Rugolo M, Zanna C. Eight human OPA1 isoforms, long and short: what are they for? *Biochim Biophys Acta Bioenerg.* (2018) 1859:263–9. doi: 10.1016/j.bbabio.2018.01.005

9. Del Dotto V, Mishra P, Vidoni S, Fogazza M, Maresca A, Caporali L, et al. OPA1 Isoforms in the hierarchical organization of mitochondrial functions. *Cell Rep.* (2017) 19:2557–71. doi: 10.1016/j.celrep.2017.05.073

10. Lodi R, Tonon C, Valentino ML, Iotti S, Clementi V, Malucelli E, et al. Deficit of *in vivo* mitochondrial ATP production in OPA1-related dominant optic atrophy. *Ann Neurol.* (2004) 56:719–23. doi: 10.1002/ana.20278

11. Zanna C, Ghelli A, Porcelli AM, Karbowski M, Youle RJ, Schimpf S, et al. OPA1 mutations associated with dominant optic atrophy impair oxidative phosphorylation and mitochondrial fusion. *Brain*. (2008) 131:352–67. doi: 10.1093/brain/awm335

12. Olichon A, Baricault L, Gas N, Guillou E, Valette A, Belenguer P, et al. Loss of OPA1 perturbates the mitochondrial inner membrane structure and integrity, leading to cytochrome c release and apoptosis. *J Biol Chem*. (2003) 278:7743–6. doi: 10.1074/jbc.C200677200

13. Frezza C, Cipolat S, Martins de Brito O, Micaroni M, Beznoussenko GV, Rudka T, et al. OPA1 controls apoptotic cristae remodeling independently from mitochondrial fusion. *Cell*. (2006) 126:177–89. doi: 10.1016/j.cell.2006.06.025

14. Amati-Bonneau P, Valentino ML, Reynier P, Gallardo ME, Bornstein B, Boissière A, et al. OPA1 mutations induce mitochondrial DNA instability and optic atrophy "plus" phenotypes. *Brain*. (2008) 131:338–51. doi: 10.1093/brain/awm298

15. Hudson G, Amati-Bonneau P, Blakely EL, Stewart JD, He L, Schaefer AM, et al. Mutation of OPA1 causes dominant optic atrophy with external ophthalmoplegia, ataxia, deafness and multiple mitochondrial DNA deletions: a novel disorder of mtDNA maintenance. *Brain*. (2008) 131:329–37. doi: 10.1093/brain/awm272

16. Elachouri G, Vidoni S, Zanna C, Pattyn A, Boukhaddaoui H, Gaget K, et al. OPA1 links human mitochondrial genome maintenance to mtDNA replication and distribution. *Genome Res*. (2011) 21:12–20. doi: 10.1101/gr.108696.110

17. Spiegel R, Saada A, Flannery PJ, Burté F, Soiferman D, Khayat M, et al. Fatal infantile mitochondrial encephalomyopathy, hypertrophic cardiomyopathy and optic atrophy associated with a homozygous OPA1 mutation. *J Med Genet*. (2016) 53:127–31. doi: 10.1136/jmedgenet-2015-103361

18. Carelli V, Musumeci O, Caporali L, Zanna C, La Morgia C, Del Dotto V, et al. Syndromic parkinsonism and dementia associated with OPA1 missense mutations. *Ann Neurol*. (2015) 78:21–38. doi: 10.1002/ana.24410

19. Liao C, Ashley N, Diot A, Morten K, Phadwal K, Williams A, et al. Dysregulated mitophagy and mitochondrial organization in optic atrophy due to OPA1 mutations. *Neurology*. (2017) 88:131–42. doi: 10.1212/WNL.0000000000003491

20. Del Dotto V, Fogazza M, Lenaers G, Rugolo M, Carelli V, Zanna C. OPA1: how much do we know to approach therapy? *Pharmacol Res*. (2018) 131:199–210. doi: 10.1016/j.phrs.2018.02.018

21. Chan DC. Mitochondrial dynamics and its involvement in disease. *Annu Rev Pathol*. (2020) 15:235–59. doi: 10.1146/annurev-pathmechdis-012419-032711

22. Giacomello M, Pyakurel A, Glytsou C, Scorrano L. The cell biology of mitochondrial membrane dynamics. *Nat Rev Mol Cell Biol*. (2020) 21:204–24. doi: 10.1038/s41580-020-0210-7

23. Burté F, Carelli V, Chinnery PF, Yu-Wai-Man P. Disturbed mitochondrial dynamics and neurodegenerative disorders. *Nat Rev Neurol*. (2015) 11:11–24. doi: 10.1038/nrneurol.2014.228

24. Yu-Wai-Man P, Griffiths PG, Gorman GS, Lourenco CM, Wright AF, Auer-Grumbach M, et al. Multi-system neurological disease is common in patients with OPA1 mutations. *Brain*. (2010) 133:771–86. doi: 10.1093/brain/awq007

25. Verny C, Loiseau D, Scherer C, Lejeune P, Chevrollier A, Gueguen N, et al. Multiple sclerosis-like disorder in OPA1-related autosomal dominant optic atrophy. *Neurology*. (2008) 70:1152–3. doi: 10.1212/01.wnl.0000289194.89359.a1

26. Yu-Wai-Man P, Spyropoulos A, Duncan HJ, Guadagno JV, Chinnery PF. A multiple sclerosis-like disorder in patients with OPA1 mutations. *Ann Clin Transl Neurol*. (2016) 3:723–9. doi: 10.1002/acn3.323

27. Lynch DS, Loh SHY, Harley J, Noyce AJ, Martins LM, Wood NW, et al. Nonsyndromic Parkinson disease in a family with autosomal dominant optic atrophy due to OPA1 mutations. *Neurol Genet*. (2017) 3:e188. doi: 10.1212/NXG.0000000000000188

28. Rubegni A, Pisano T, Bacci G, Tessa A, Battini R, Procopio E, et al. Leigh-like neuroimaging features associated with new biallelic mutations in OPA1. *Eur J Paediatr Neurol*. (2017) 21:671–7. doi: 10.1016/j.ejpn.2017.04.004

29. Jones BA, Fangman WL. Mitochondrial DNA maintenance in yeast requires a protein containing a region related to the GTP-binding domain of dynamin. *Genes Dev*. (1992) 6:380–9. doi: 10.1101/gad.6.3.380

30. Wong ED, Wagner JA, Scott SV, Okreglak V, Holewinske TJ, Cassidy-Stone A, et al. The intramitochondrial dynamin-related GTPase, Mgm1p, is a component of a protein complex that mediates mitochondrial fusion. *J Cell Biol*. (2003) 160:303–11. doi: 10.1083/jcb.200209015

31. Sesaki H, Southard SM, Yaffe MP, Jensen RE. Mgm1p, a dynamin-related GTPase, is essential for fusion of the mitochondrial outer membrane. *Mol Biol Cell*. (2003) 14:2342–56. doi: 10.1091/mbc.e02-12-0788

32. Meeusen S, DeVay R, Block J, Cassidy-Stone A, Wayson S, McCaffery JM, et al. Mitochondrial inner-membrane fusion and crista maintenance requires the dynamin-related GTPase Mgm1. *Cell*. (2006) 127:383–95. doi: 10.1016/j.cell.2006.09.021

33. Amutha B, Gordon DM, Gu Y, Pain D. A novel role of Mgm1p, a dynamin-related GTPase, in ATP synthase assembly and cristae formation/maintenance. *Biochem J*. (2004) 381:19–23. doi: 10.1042/BJ20040566

34. Pelloquin L, Belenguer P, Menon Y, Gas N, Ducommun B. Fission yeast Msp1 is a mitochondrial dynamin-related protein. *J Cell Sci*. (1999) 112:4151–61.

35. Guillou E, Bousquet C, Daloyau M, Emorine LJ, Belenguer P. Msp1p is an intermembrane space dynamin-related protein that mediates mitochondrial fusion in a Dnm1p-dependent manner in *S. pombe*. *FEBS Lett*. (2005) 579:1109–16. doi: 10.1016/j.febslet.2004.12.083

36. Herlan M, Vogel F, Bornhovd C, Neupert W, Reichert AS. Processing of Mgm1 by the rhomboid-type protease Pcp1 is required for maintenance of mitochondrial morphology and of mitochondrial DNA. *J Biol Chem*. (2003) 278:27781–8. doi: 10.1074/jbc.M211311200

37. McQuibban GA, Saurya S, Freeman M. Mitochondrial membrane remodelling regulated by a conserved rhomboid protease. *Nature*. (2003) 423:537–41. doi: 10.1038/nature01633

38. Leroy I, Khosrobakhsh F, Diot A, Daloyau M, Arnauné-Pelloquin L, Cavelier C, et al. Processing of the dynamin Msp1p in *S. pombe* reveals an evolutionary switch between its orthologs Mgm1p in *S. cerevisiae* and OPA1 in mammals. *FEBS Lett*. (2010) 584:3153–7. doi: 10.1016/j.febslet.2010.05.060

39. Zick M, Duvezin-Caubet S, Schäfer A, Vogel F, Neupert W, Reichert AS. Distinct roles of the two isoforms of the dynamin-like GTPase Mgm1 in mitochondrial fusion. *FEBS Lett*. (2009) 583:2237–43. doi: 10.1016/j.febslet.2009.05.053

40. Diot A, Guillou E, Daloyau M, Arnauné-Pelloquin L, Emorine LJ, Belenguer P. Transmembrane segments of the dynamin Msp1p uncouple its functions in the control of mitochondrial morphology and genome maintenance. *J Cell Sci*. (2009) 122:2632–9. doi: 10.1242/jcs.040139

41. Nolli C, Goffrini P, Lazzaretti M, Zanna C, Vitale R, Lodi T, et al. Validation of a MGM1/OPA1 chimeric gene for functional analysis in yeast of mutations associated with dominant optic atrophy. *Mitochondrion*. (2015) 25:38–48. doi: 10.1016/j.mito.2015.10.002

42. Del Dotto V, Fogazza M, Musiani F, Maresca A, Aleo SJ, Caporali L, et al. Deciphering OPA1 mutations pathogenicity by combined analysis of human, mouse and yeast cell models. *Biochim Biophys Acta Mol Basis Dis*. (2018) 1864:3496–514. doi: 10.1016/j.bbadis.2018.08.004

43. Nasca A, Rizza T, Doimo M, Legati A, Ciolfi A, Diodato D, et al. Not only dominant, not only optic atrophy: expanding the clinical spectrum associated with OPA1 mutations. *Orphanet J Rare Dis*. (2017) 12:89. doi: 10.1186/s13023-017-0641-1

44. Delerue T, Tribouillard-Tanvier D, Daloyau M, Khosrobakhsh F, Emorine LJ, Friocourt G, et al. A yeast-based screening assay identifies repurposed drugs that suppress mitochondrial fusion and mtDNA maintenance defects. *Dis Model Mech*. (2019) 12:dmm036558. doi: 10.1242/dmm.036558

45. Aleo SJ, Del Dotto V, Fogazza M, Maresca A, Lodi T, Goffrini P, et al. Drug repositioning as a therapeutic strategy for neurodegenerations associated with OPA1 mutations. *Hum Mol Genet*. (2021) 29:3631–45. doi: 10.1093/hmg/ddaa244

46. Song Z, Chen H, Fiket M, Alexander C, Chan DC. OPA1 processing controls mitochondrial fusion and is regulated by mRNA splicing, membrane potential, and Yme1L. *J Cell Biol*. (2007) 178:749–55. doi: 10.1083/jcb.200704110

47. Ehses S, Raschke I, Mancuso G, Bernacchia A, Geimer S, Tondera D, et al. Regulation of OPA1 processing and mitochondrial fusion by m-AAA protease isoenzymes and OMA1. *J Cell Biol.* (2009) 187:1023–36. doi: 10.1083/jcb.200906084

48. Head B, Griparic L, Amiri M, Gandre-Babbe S, van der Bliek AM. Inducible proteolytic inactivation of OPA1 mediated by the OMA1 protease in mammalian cells. *J Cell Biol.* (2009) 187:959–66. doi: 10.1083/jcb.200906083

49. Wang R, Mishra P, Garbis SD, Moradian A, Sweredoski MJ, Chan DC. Identification of new OPA1 cleavage site reveals that short isoforms regulate mitochondrial fusion. *Mol Biol Cell.* (2021) 32:157–68. doi: 10.1091/mbc.E20-09-0605

50. Cipolat S, Martins de Brito O, Dal Zilio B, Scorrano L. OPA1 requires mitofusin 1 to promote mitochondrial fusion. *Proc Natl Acad Sci USA.* (2004) 101:15927–32. doi: 10.1073/pnas.0407043101

51. Chen H, Chomyn A, Chan DC. Disruption of fusion results in mitochondrial heterogeneity and dysfunction. *J Biol Chem.* (2005) 280:26185–92. doi: 10.1074/jbc.M503062200

52. Chen H, McCaffery JM, Chan DC. Mitochondrial fusion protects against neurodegeneration in the cerebellum. *Cell.* (2007) 130:548–62. doi: 10.1016/j.cell.2007.06.026

53. Lee H, Smith SB, Yoon Y. The short variant of the mitochondrial dynamin OPA1 maintains mitochondrial energetics and cristae structure. *J Biol Chem.* (2017) 292:7115–30. doi: 10.1074/jbc.M116.762567

54. Chen H, Vermulst M, Wang YE, Chomyn A, Prolla TA, McCaffery JM, et al. Mitochondrial fusion is required for mtDNA stability in skeletal muscle and tolerance of mtDNA mutations. *Cell.* (2010) 141:280–9. doi: 10.1016/j.cell.2010.02.026

55. Hu C, Shu L, Huang X, Yu J, Li L, Gong L, et al. OPA1 and MICOS regulate mitochondrial crista dynamics and formation. *Cell Death Dis.* (2020) 11:940. doi: 10.1038/s41419-020-03152-y

56. Cogliati S, Frezza C, Soriano ME, Varanita T, Quintana-Cabrera R, Corrado M, et al. Mitochondrial cristae shape determines respiratory chain supercomplexes assembly and respiratory efficiency. *Cell.* (2013) 155:160–71. doi: 10.1016/j.cell.2013.08.032

57. Quintana-Cabrera R, Quirin C, Glytsou C, Corrado M, Urbani A, Pellattiero A, et al. The cristae modulator optic atrophy 1 requires mitochondrial ATP synthase oligomers to safeguard mitochondrial function. *Nat Commun.* (2018) 9:3399. doi: 10.1038/s41467-018-05655-x

58. Barrera M, Koob S, Dikov D, Vogel F, Reichert AS. OPA1 functionally interacts with MIC60 but is dispensable for crista junction formation. *FEBS Lett.* (2016) 590:3309–22. doi: 10.1002/1873-3468.12384

59. Glytsou C, Calvo E, Cogliati S, Mehrotra A, Anastasia I, Rigoni G, et al. Optic atrophy 1 is epistatic to the core MICOS component MIC60 in mitochondrial cristae shape control. *Cell Rep.* (2016) 17:3024–34. doi: 10.1016/j.celrep.2016.11.049

60. Patten DA, Wong J, Khacho M, Soubannier V, Mailloux RJ, Pilon-Larose K, et al. OPA1-dependent cristae modulation is essential for cellular adaptation to metabolic demand. *EMBO J.* (2014) 33:2676–91. doi: 10.15252/embj.201488349

61. Lee H, Smith SB, Sheu S-S, Yoon Y. The short variant of optic atrophy 1 (OPA1) improves cell survival under oxidative stress. *J Biol Chem.* (2020) 295:6543–60. doi: 10.1074/jbc.RA119.010983

62. Ban T, Heymann JAW, Song Z, Hinshaw JE, Chan DC. OPA1 disease alleles causing dominant optic atrophy have defects in cardiolipin-stimulated GTP hydrolysis and membrane tubulation. *Hum Mol Genet.* (2010) 19:2113–22. doi: 10.1093/hmg/ddq088

63. Bocca C, Kane MS, Veyrat-Durebex C, Chupin S, Alban J, Kouassi Nzoughet J, et al. The metabolomic bioenergetic signature of Opa1-disrupted mouse embryonic fibroblasts highlights aspartate deficiency. *Sci Rep.* (2018) 8:11528. doi: 10.1038/s41598-018-29972-9

64. Bocca C, Kane MS, Veyrat-Durebex C, Nzoughet JK, Chao de la Barca JM, Chupin S, et al. Lipidomics reveals triacylglycerol accumulation due to impaired fatty acid flux in Opa1-disrupted fibroblasts. *J Proteome Res.* (2019) 18:2779–90. doi: 10.1021/acs.jproteome.9b00081

65. Chao de la Barca JM, Fogazza M, Rugolo M, Chupin S, Del Dotto V, Ghelli AM, et al. Metabolomics hallmarks OPA1 variants correlating with their *in vitro* phenotype and predicting clinical severity. *Hum Mol Genet.* (2020) 29:1319–29. doi: 10.1093/hmg/ddaa047

66. Chao de la Barca JM, Arrázola MS, Bocca C, Arnauné-Pelloquin L, Iuliano O, Tcherkez G, et al. The metabolomic signature of Opa1 deficiency in rat primary cortical neurons shows aspartate/glutamate depletion and phospholipids remodeling. *Sci Rep.* (2019) 9:6107. doi: 10.1038/s41598-019-42554-7

67. Patten DA, McGuirk S, Anilkumar U, Antoun G, Gandhi K, Parmar G, et al. Altered mitochondrial fusion drives defensive glutathione synthesis in cells able to switch to glycolytic ATP production. *Biochim Biophys Acta Mol Cell Res.* (2021) 1868:118854. doi: 10.1016/j.bbamcr.2020.118854

68. Olichon A, Emorine LJ, Descoins E, Pelloquin L, Brichese L, Gas N, et al. The human dynamin-related protein OPA1 is anchored to the mitochondrial inner membrane facing the inter-membrane space. *FEBS Lett.* (2002) 523:171–6. doi: 10.1016/s0014-5793(02)02985-x

69. Satoh M, Hamamoto T, Seo N, Kagawa Y, Endo H. Differential sublocalization of the dynamin-related protein OPA1 isoforms in mitochondria. *Biochem Biophys Res Commun.* (2003) 300:482–93. doi: 10.1016/s0006-291x(02)02874-7

70. Griparic L, van der Wel NN, Orozco IJ, Peters PJ, van der Bliek AM. Loss of the intermembrane space protein Mgm1/OPA1 induces swelling and localized constrictions along the lengths of mitochondria. *J Biol Chem.* (2004) 279:18792–8. doi: 10.1074/jbc.M400920200

71. Ishihara N, Fujita Y, Oka T, Mihara K. Regulation of mitochondrial morphology through proteolytic cleavage of OPA1. *EMBO J.* (2006) 25:2966–77. doi: 10.1038/sj.emboj.7601184

72. Guillery O, Malka F, Landes T, Guillou E, Blackstone C, Lombès A, et al. Metalloprotease-mediated OPA1 processing is modulated by the mitochondrial membrane potential. *Biol Cell.* (2008) 100:315–25. doi: 10.1042/BC20070110

73. Griparic L, Kanazawa T, van der Bliek AM. Regulation of the mitochondrial dynamin-like protein Opa1 by proteolytic cleavage. *J Cell Biol.* (2007) 178:757–64. doi: 10.1083/jcb.200704112

74. Arnoult D, Grodet A, Lee YJ, Estaquier J, Blackstone C. Release of OPA1 during apoptosis participates in the rapid and complete release of cytochrome c and subsequent mitochondrial fragmentation. *J Biol Chem.* (2005) 280:35742–50. doi: 10.1074/jbc.M505970200

75. Kushnareva YE, Gerencser AA, Bossy B, Ju WK, White AD, Waggoner J, et al. Loss of OPA1 disturbs cellular calcium homeostasis and sensitizes for excitotoxicity. *Cell Death Differ.* (2013) 20:353–65. doi: 10.1038/cdd.2012.128

76. Lee Y, Jeong SY, Karbowski M, Smith CL, Youle RJ. Roles of the mammalian mitochondrial fission and fusion mediators Fis1, Drp1, and Opa1 in apoptosis. *Mol Biol Cell.* (2004) 15:5001–11. doi: 10.1091/mbc.e04-04-0294

77. Stephan T, Brüser C, Deckers M, Steyer AM, Balzarotti F, Barbot M, et al. MICOS assembly controls mitochondrial inner membrane remodeling and crista junction redistribution to mediate cristae formation. *EMBO J.* (2020) 39:e104105. doi: 10.15252/embj.2019104105

78. Olichon A, Landes T, Arnauné-Pelloquin L, Emorine LJ, Mils V, Guichet A, et al. Effects of OPA1 mutations on mitochondrial morphology and apoptosis: relevance to ADOA pathogenesis. *J Cell Physiol.* (2007) 211:423–30. doi: 10.1002/jcp.20950

79. Yamaguchi R, Lartigue L, Perkins G, Scott RT, Dixit A, Kushnareva Y, et al. Opa1-mediated cristae opening is Bax/Bak and BH3 dependent, required for apoptosis, and independent of Bak oligomerization. *Mol Cell.* (2008) 31:557–69. doi: 10.1016/j.molcel.2008.07.010

80. Jang S, Javadov S. OPA1 regulates respiratory supercomplexes assembly: the role of mitochondrial swelling. *Mitochondrion.* (2020) 51:30–9. doi: 10.1016/j.mito.2019.11.006

81. Fülöp L, Szanda G, Enyedi B, Várnai P, Spät A. The effect of OPA1 on mitochondrial Ca^{2+} signaling. *PLoS ONE.* (2011) 6:e25199. doi: 10.1371/journal.pone.0025199

82. Chen M, Chen Z, Wang Y, Tan Z, Zhu C, Li Y, et al. Mitophagy receptor FUNDC1 regulates mitochondrial dynamics and mitophagy. *Autophagy.* (2016) 12:689–702. doi: 10.1080/15548627.2016.1151580

83. Olichon A, Elachouri G, Baricault L, Delettre C, Belenguer P, Lenaers G. OPA1 alternate splicing uncouples an evolutionary conserved function in mitochondrial fusion from a vertebrate restricted function in apoptosis. *Cell Death Differ.* (2007) 14:682–92. doi: 10.1038/sj.cdd.4402048

84. Sun Y, Xue W, Song Z, Huang K, Zheng L. Restoration of Opa1-long isoform inhibits retinal injury-induced neurodegeneration. *J Mol Med (Berl).* (2016) 94:335–46. doi: 10.1007/s00109-015-1359-y

85. Lang A, Anand R, Altinoluk-Hambüchen S, Ezzahoini H, Stefanski A, Iram A, et al. SIRT4 interacts with OPA1 and regulates mitochondrial quality control and mitophagy. *Aging (Albany NY).* (2017) 9:2163–89. doi: 10.18632/aging.101307

86. Pidoux G, Witczak O, Jarnæss E, Myrvold L, Urlaub H, Stokka AJ, et al. Optic atrophy 1 is an A-kinase anchoring protein on lipid droplets that mediates adrenergic control of lipolysis. *EMBO J.* (2011) 30:4371–86. doi: 10.1038/emboj.2011.365

87. Rogne M, Chu D-T, Küntziger TM, Mylonakou M-N, Collas P, Tasken K. OPA1-anchored PKA phosphorylates perilipin 1 on S522 and S497 in adipocytes differentiated from human adipose stem cells. *Mol Biol Cell.* (2018) 29:1487–501. doi: 10.1091/mbc.E17-09-0538

88. Amati-Bonneau P, Guichet A, Olichon A, Chevrollier A, Viala F, Miot S, et al. OPA1 R445H mutation in optic atrophy associated with sensorineural deafness. *Ann Neurol.* (2005) 58:958–63. doi: 10.1002/ana.20681

89. Amati-Bonneau P, Milea D, Bonneau D, Chevrollier A, Ferré M, Guillet V, et al. OPA1-associated disorders: phenotypes and pathophysiology. *Int J Biochem Cell Biol.* (2009) 41:1855–65. doi: 10.1016/j.biocel.2009.04.012

90. Spinazzi M, Cazzola S, Bortolozzi M, Baracca A, Loro E, Casarin A, et al. A novel deletion in the GTPase domain of OPA1 causes defects in mitochondrial morphology and distribution, but not in function. *Hum Mol Genet.* (2008) 17:3291–302. doi: 10.1093/hmg/ddn225

91. Nochez Y, Arsene S, Gueguen N, Chevrollier A, Ferré M, Guillet V, et al. Acute and late-onset optic atrophy due to a novel OPA1 mutation leading to a mitochondrial coupling defect. *Mol Vis.* (2009) 15:598–608.

92. Bonifert T, Karle KN, Tonagel F, Batra M, Wilhelm C, Theurer Y, et al. Pure and syndromic optic atrophy explained by deep intronic OPA1 mutations and an intralocus modifier. *Brain.* (2014) 137:2164–77. doi: 10.1093/brain/awu165

93. Agier V, Oliviero P, Lainé J, L'Hermitte-Stead C, Girard S, Fillaut S, et al. Defective mitochondrial fusion, altered respiratory function, and distorted cristae structure in skin fibroblasts with heterozygous OPA1 mutations. *Biochim Biophys Acta.* (2012) 1822:1570–80. doi: 10.1016/j.bbadis.2012.07.002

94. Kao S-H, Yen M-Y, Wang A-G, Yeh Y-L, Lin A-L. Changes in mitochondrial morphology and bioenergetics in human lymphoblastoid cells with four novel OPA1 mutations. *Invest Ophthalmol Vis Sci.* (2015) 56:2269–78. doi: 10.1167/iovs.14-16288

95. Kane MS, Alban J, Desquiret-Dumas V, Gueguen N, Ishak L, Ferre M, et al. Autophagy controls the pathogenicity of OPA1 mutations in dominant optic atrophy. *J Cell Mol Med.* (2017) 21:2284–97. doi: 10.1111/jcmm.13149

96. Zhang J, Liu X, Liang X, Lu Y, Zhu L, Fu R, et al. A novel ADOA-associated OPA1 mutation alters the mitochondrial function, membrane potential, ROS production and apoptosis. *Sci Rep.* (2017) 7:5704. doi: 10.1038/s41598-017-05571-y

97. Millet AMC, Bertholet AM, Daloyau M, Reynier P, Galinier A, Devin A, et al. Loss of functional OPA1 unbalances redox state: implications in dominant optic atrophy pathogenesis. *Ann Clin Transl Neurol.* (2016) 3:408–21. doi: 10.1002/acn3.305

98. Fülöp L, Rajki A, Maka E, Molnár J, Spät A. Mitochondrial Ca^{2+} uptake correlates with the severity of the symptoms in autosomal dominant optic atrophy. *Cell Calcium.* (2015) 57:49–55. doi: 10.1016/j.ceca.2014.11.008

99. Napolitano F, Terracciano C, Bruno G, Nesti C, Barillari MR, Barillari U, et al. Intrafamilial "DOA-plus" phenotype variability related to different OMI/HTRA2 expression. *Am J Med Genet A.* (2020) 182:176–82. doi: 10.1002/ajmg.a.61381

100. Rowe RG, Daley GQ. Induced pluripotent stem cells in disease modelling and drug discovery. *Nat Rev Genet.* (2019) 20:377–88. doi: 10.1038/s41576-019-0100-z

101. Galera-Monge T, Zurita-Díaz F, Moreno-Izquierdo A, Fraga MF, Fernández AF, Ayuso C, et al. Generation of a human iPSC line from a patient with an optic atrophy "plus" phenotype due to a mutation in the OPA1 gene. *Stem Cell Res.* (2016) 16:673–6. doi: 10.1016/j.scr.2016.03.011

102. Zurita-Díaz F, Galera-Monge T, Moreno-Izquierdo A, Corton M, Ayuso C, Garesse R, et al. Establishment of a human DOA "plus" iPSC line, IISHDOi003-A, with the mutation in the OPA1 gene: c.1635C>A; p.Ser545Arg. *Stem Cell Res.* (2017) 24:81–4. doi: 10.1016/j.scr.2017.08.017

103. Hauser S, Schuster S, Theurer Y, Synofzik M, Schöls L. Generation of optic atrophy 1 patient-derived induced pluripotent stem cells (iPS-OPA1-BEHR) for disease modeling of complex optic atrophy syndromes (Behr syndrome). *Stem Cell Res.* (2016) 17:426–9. doi: 10.1016/j.scr.2016.09.012

104. Chen J, Riazifar H, Guan M-X, Huang T. Modeling autosomal dominant optic atrophy using induced pluripotent stem cells and identifying potential therapeutic targets. *Stem Cell Res Ther.* (2016) 7:2. doi: 10.1186/s13287-015-0264-1

105. Barboni P, Carbonelli M, Savini G, Foscarini B, Parisi V, Valentino ML, et al. OPA1 mutations associated with dominant optic atrophy influence optic nerve head size. *Ophthalmology.* (2010) 117:1547–53. doi: 10.1016/j.ophtha.2009.12.042

106. Jonikas M, Madill M, Mathy A, Zekoll T, Zois CE, Wigfield S, et al. Stem cell modeling of mitochondrial Parkinsonism reveals key functions of OPA1. *Ann Neurol.* (2018) 83:915–25. doi: 10.1002/ana.25221

107. Iannielli A, Bido S, Folladori L, Segnali A, Cancellieri C, Maresca A, et al. Pharmacological inhibition of necroptosis protects from dopaminergic neuronal cell death in Parkinson's disease models. *Cell Rep.* (2018) 22:2066–79. doi: 10.1016/j.celrep.2018.01.089

108. Iannielli A, Ugolini GS, Cordiglieri C, Bido S, Rubio A, Colasante G, et al. Reconstitution of the human nigro-striatal pathway on-a-chip reveals OPA1-dependent mitochondrial defects and loss of dopaminergic synapses. *Cell Rep.* (2019) 29:4646–56.e4. doi: 10.1016/j.celrep.2019.11.111

109. Caglayan S, Hashim A, Cieslar-Pobuda A, Jensen V, Behringer S, Talug B, et al. Optic atrophy 1 controls human neuronal development by preventing aberrant nuclear DNA methylation. *iScience.* (2020) 23:101154. doi: 10.1016/j.isci.2020.101154

110. Chiaradia I, Lancaster MA. Brain organoids for the study of human neurobiology at the interface of in vitro and in vivo. *Nat Neurosci.* (2020) 23:1496–508. doi: 10.1038/s41593-020-00730-3

111. Cowan CS, Renner M, De Gennaro M, Gross-Scherf B, Goldblum D, Hou Y, et al. Cell types of the human retina and its organoids at single-cell resolution. *Cell.* (2020) 182:1623–40.e34. doi: 10.1016/j.cell.2020.08.013

112. Yarosh W, Monserrate J, Tong JJ, Tse S, Le PK, Nguyen K, et al. The molecular mechanisms of OPA1-mediated optic atrophy in Drosophila model and prospects for antioxidant treatment. *PLoS Genet.* (2008) 4:e6. doi: 10.1371/journal.pgen.0040006

113. Shahrestani P, Leung H-T, Le PK, Pak WL, Tse S, Ocorr K, et al. Heterozygous mutation of Drosophila Opa1 causes the development of multiple organ abnormalities in an age-dependent and organ-specific manner. *PLoS ONE.* (2009) 4:e6867. doi: 10.1371/journal.pone.0006867

114. Tang S, Le PK, Tse S, Wallace DC, Huang T. Heterozygous mutation of Opa1 in Drosophila shortens lifespan mediated through increased reactive oxygen species production. *PLoS ONE.* (2009) 4:e4492. doi: 10.1371/journal.pone.0004492

115. Kanazawa T, Zappaterra MD, Hasegawa A, Wright AP, Newman-Smith ED, Buttle KF, et al. The *C. elegans* Opa1 homologue EAT-3 is essential for resistance to free radicals. *PLoS Genet.* (2008) 4:e1000022. doi: 10.1371/journal.pgen.1000022

116. Rolland SG, Lu Y, David CN, Conradt B. The BCL-2-like protein CED-9 of *C. elegans* promotes FZO-1/Mfn1,2- and EAT-3/Opa1-dependent mitochondrial fusion. *J Cell Biol.* (2009) 186:525–40. doi: 10.1083/jcb.200905070

117. Byrne JJ, Soh MS, Chandhok G, Vijayaraghavan T, Teoh JS, Crawford S, et al. Disruption of mitochondrial dynamics affects behaviour and lifespan in *Caenorhabditis elegans. Cell Mol Life Sci.* (2019) 76:1967–85. doi: 10.1007/s00018-019-03024-5

118. Chaudhari SN, Kipreos ET. Increased mitochondrial fusion allows the survival of older animals in diverse *C. elegans* longevity pathways. *Nat Commun.* (2017) 8:182. doi: 10.1038/s41467-017-00274-4

119. Zaninello M, Palikaras K, Naon D, Iwata K, Herkenne S, Quintana-Cabrera R, et al. Inhibition of autophagy curtails visual loss in a model of autosomal dominant optic atrophy. *Nat Commun.* (2020) 11:4029. doi: 10.1038/s41467-020-17821-1

120. Rahn JJ, Stackley KD, Chan SSL. Opa1 is required for proper mitochondrial metabolism in early development. *PLoS ONE.* (2013) 8:e59218. doi: 10.1371/journal.pone.0059218

121. Eijkenboom I, Vanoevelen JM, Hoeijmakers JGJ, Wijnen I, Gerards M, Faber CG, et al. A zebrafish model to study small-fiber neuropathy reveals a potential role for GDAP1. *Mitochondrion.* (2019) 47:273–81. doi: 10.1016/j.mito.2019.01.002

122. Alavi MV, Bette S, Schimpf S, Schuettauf F, Schraermeyer U, Wehrl HF, et al. A splice site mutation in the murine Opa1 gene features pathology of autosomal dominant optic atrophy. *Brain.* (2007) 130:1029–42. doi: 10.1093/brain/awm005

123. Davies VJ, Hollins AJ, Piechota MJ, Yip W, Davies JR, White KE, et al. Opa1 deficiency in a mouse model of autosomal dominant optic atrophy impairs mitochondrial morphology, optic nerve structure and visual function. *Hum Mol Genet.* (2007) 16:1307–18. doi: 10.1093/hmg/ddm079

124. Sarzi E, Angebault C, Seveno M, Gueguen N, Chaix B, Bielicki G, et al. The human OPA1delTTAG mutation induces premature age-related systemic neurodegeneration in mouse. *Brain.* (2012) 135:3599–613. doi: 10.1093/brain/aws303

125. Heiduschka P, Schnichels S, Fuhrmann N, Hofmeister S, Schraermeyer U, Wissinger B, et al. Electrophysiological and histologic assessment of retinal ganglion cell fate in a mouse model for OPA1-associated autosomal dominant optic atrophy. *Invest Ophthalmol Vis Sci.* (2010) 51:1424–31. doi: 10.1167/iovs.09-3606

126. Nguyen D, Alavi MV, Kim KY, Kang T, Scott RT, Noh YH, et al. A new vicious cycle involving glutamate excitotoxicity, oxidative stress and mitochondrial dynamics. *Cell Death Dis.* (2011) 2:e240. doi: 10.1038/cddis.2011.117

127. White KE, Davies VJ, Hogan VE, Piechota MJ, Nichols PP, Turnbull DM, et al. OPA1 deficiency associated with increased autophagy in retinal ganglion cells in a murine model of dominant optic atrophy. *Invest Ophthalmol Vis Sci.* (2009) 50:2567–71. doi: 10.1167/iovs.08-2913

128. Diot A, Agnew T, Sanderson J, Liao C, Carver J, Neves RP das, et al. Validating the RedMIT/GFP-LC3 mouse model by studying mitophagy in autosomal dominant optic atrophy due to the OPA1Q285STOP mutation. *Front Cell Dev Biol.* (2018) 6:103. doi: 10.3389/fcell.2018.00103

129. Chao de la Barca JM, Simard G, Sarzi E, Chaumette T, Rousseau G, Chupin S, et al. Targeted metabolomics reveals early dominant optic atrophy signature in optic nerves of Opa1delTTAG/+ mice. *Invest Ophthalmol Vis Sci.* (2017) 58:812–20. doi: 10.1167/iovs.16-21116

130. Perganta G, Barnard AR, Katti C, Vachtsevanos A, Douglas RH, MacLaren RE, et al. Non-image-forming light driven functions are preserved in a mouse model of autosomal dominant optic atrophy. *PLoS ONE.* (2013) 8:e56350. doi: 10.1371/journal.pone.0056350

131. González-Menéndez I, Reinhard K, Tolivia J, Wissinger B, Münch TA. Influence of Opa1 mutation on survival and function of retinal ganglion cells. *Invest Ophthalmol Vis Sci.* (2015) 56:4835–45. doi: 10.1167/iovs.15-16743

132. La Morgia C, Ross-Cisneros FN, Sadun AA, Hannibal J, Munarini A, Mantovani V, et al. Melanopsin retinal ganglion cells are resistant to neurodegeneration in mitochondrial optic neuropathies. *Brain.* (2010) 133:2426–8. doi: 10.1093/brain/awq155

133. Carelli V, Ross-Cisneros FN, Sadun AA. Mitochondrial dysfunction as a cause of optic neuropathies. *Prog Retin Eye Res.* (2004) 23:53–89. doi: 10.1016/j.preteyeres.2003.10.003

134. Yu-Wai-Man P, Griffiths PG, Chinnery PF. Mitochondrial optic neuropathies–disease mechanisms and therapeutic strategies. *Prog Retin Eye Res.* (2011) 30:81–114. doi: 10.1016/j.preteyeres.2010.11.002

135. Williams PA, Morgan JE, Votruba M. Opa1 deficiency in a mouse model of dominant optic atrophy leads to retinal ganglion cell dendropathy. *Brain.* (2010) 133:2942–51. doi: 10.1093/brain/awq218

136. Williams PA, Piechota M, von Ruhland C, Taylor E, Morgan JE, Votruba M. Opa1 is essential for retinal ganglion cell synaptic architecture and connectivity. *Brain.* (2012) 135:493–505. doi: 10.1093/brain/awr330

137. Li Z, Okamoto K-I, Hayashi Y, Sheng M. The importance of dendritic mitochondria in the morphogenesis and plasticity of spines and synapses. *Cell.* (2004) 119:873–87. doi: 10.1016/j.cell.2004.11.003

138. Chen L, Liu T, Tran A, Lu X, Tomilov AA, Davies V, et al. OPA1 mutation and late-onset cardiomyopathy: mitochondrial dysfunction and mtDNA instability. *J Am Heart Assoc.* (2012) 1:e003012. doi: 10.1161/JAHA.112.003012

139. Piquereau J, Caffin F, Novotova M, Prola A, Garnier A, Mateo P, et al. Down-regulation of OPA1 alters mouse mitochondrial morphology, PTP function, and cardiac adaptation to pressure overload. *Cardiovasc Res.* (2012) 94:408–17. doi: 10.1093/cvr/cvs117

140. Le Page S, Niro M, Fauconnier J, Cellier L, Tamareille S, Gharib A, et al. Increase in cardiac ischemia-reperfusion injuries in Opa1$^{+/-}$ mouse model. *PLoS ONE.* (2016) 11:e0164066. doi: 10.1371/journal.pone.0164066

141. Zhang Z, Wakabayashi N, Wakabayashi J, Tamura Y, Song WJ, Sereda S, et al. The dynamin-related GTPase Opa1 is required for glucose-stimulated ATP production in pancreatic beta cells. *Mol Biol Cell.* (2011) 22:2235–45. doi: 10.1091/mbc.E10-12-0933

142. Pereira RO, Tadinada SM, Zasadny FM, Oliveira KJ, Pires KMP, Olvera A, et al. OPA1 deficiency promotes secretion of FGF21 from muscle that prevents obesity and insulin resistance. *EMBO J.* (2017) 36:2126–45. doi: 10.15252/embj.201696179

143. Tezze C, Romanello V, Desbats MA, Fadini GP, Albiero M, Favaro G, et al. Age-associated loss of OPA1 in muscle impacts muscle mass, metabolic homeostasis, systemic inflammation, and epithelial senescence. *Cell Metab.* (2017) 25:1374–89.e6. doi: 10.1016/j.cmet.2017.04.021

144. Rodríguez-Nuevo A, Díaz-Ramos A, Noguera E, Díaz-Sáez F, Duran X, Muñoz JP, et al. Mitochondrial DNA and TLR9 drive muscle inflammation upon Opa1 deficiency. *EMBO J.* (2018) 37:e96553. doi: 10.15252/embj.201796553

145. Lehtonen JM, Forsström S, Bottani E, Viscomi C, Baris OR, Isoniemi H, et al. FGF21 is a biomarker for mitochondrial translation and mtDNA maintenance disorders. *Neurology.* (2016) 87:2290–9. doi: 10.1212/WNL.0000000000003374

146. Maresca A, Del Dotto V, Romagnoli M, La Morgia C, Di Vito L, Capristo M, et al. Expanding and validating the biomarkers for mitochondrial diseases. *J Mol Med (Berl).* (2020) 98:1467–78. doi: 10.1007/s00109-020-01967-y

147. Sarzi E, Seveno M, Piro-Mégy C, Elzière L, Quilès M, Péquignot M, et al. OPA1 gene therapy prevents retinal ganglion cell loss in a dominant optic atrophy mouse model. *Sci Rep.* (2018) 8:2468. doi: 10.1038/s41598-018-20838-8

148. Meglei G, McQuibban GA. The dynamin-related protein Mgm1p assembles into oligomers and hydrolyzes GTP to function in mitochondrial membrane fusion. *Biochemistry.* (2009) 48:1774–84. doi: 10.1021/bi801723d

149. Rujiviphat J, Meglei G, Rubinstein JL, McQuibban GA. Phospholipid association is essential for dynamin-related protein Mgm1 to function in mitochondrial membrane fusion. *J Biol Chem.* (2009) 284:28682–6. doi: 10.1074/jbc.M109.044933

150. Abutbul-Ionita I, Rujiviphat J, Nir I, McQuibban GA, Danino D. Membrane tethering and nucleotide-dependent conformational changes drive mitochondrial genome maintenance (Mgm1) protein-mediated membrane fusion. *J Biol Chem.* (2012) 287:36634–8. doi: 10.1074/jbc.C112.406769

151. Rujiviphat J, Wong MK, Won A, Shih Y-L, Yip CM, McQuibban GA. Mitochondrial genome maintenance 1 (Mgm1) protein alters membrane topology and promotes local membrane bending. *J Mol Biol.* (2015) 427:2599–609. doi: 10.1016/j.jmb.2015.03.006

152. DeVay RM, Dominguez-Ramirez L, Lackner LL, Hoppins S, Stahlberg H, Nunnari J. Coassembly of Mgm1 isoforms requires cardiolipin and mediates mitochondrial inner membrane fusion. *J Cell Biol.* (2009) 186:793–803. doi: 10.1083/jcb.200906098

153. Mishra P, Carelli V, Manfredi G, Chan DC. Proteolytic cleavage of Opa1 stimulates mitochondrial inner membrane fusion and couples fusion to oxidative phosphorylation. *Cell Metab.* (2014) 19:630–41. doi: 10.1016/j.cmet.2014.03.011

154. Ban T, Ishihara T, Kohno H, Saita S, Ichimura A, Maenaka K, et al. Molecular basis of selective mitochondrial fusion by heterotypic action between OPA1 and cardiolipin. *Nat Cell Biol.* (2017) 19:856–63. doi: 10.1038/ncb3560

155. Ge Y, Shi X, Boopathy S, McDonald J, Smith AW, Chao LH. Two forms of Opa1 cooperate to complete fusion of the mitochondrial inner-membrane. *Elife.* (2020) 9:e50973. doi: 10.7554/eLife.50973

156. Zhang D, Zhang Y, Ma J, Zhu C, Niu T, Chen W, et al. Cryo-EM structures of S-OPA1 reveal its interactions with membrane and changes upon nucleotide binding. *Elife.* (2020) 9:e50294. doi: 10.7554/eLife.50294

157. Faelber K, Dietrich L, Noel JK, Wollweber F, Pfitzner A-K, Mühleip A, et al. Structure and assembly of the mitochondrial membrane remodelling GTPase Mgm1. *Nature.* (2019) 571:429–33. doi: 10.1038/s41586-019-1372-3

158. Yan L, Qi Y, Ricketson D, Li L, Subramanian K, Zhao J, et al. Structural analysis of a trimeric assembly of the mitochondrial dynamin-like GTPase Mgm1. *Proc Natl Acad Sci USA.* (2020) 117:4061–70. doi: 10.1073/pnas.1919116117

159. Yu C, Zhao J, Yan L, Qi Y, Guo X, Lou Z, et al. Structural insights into G domain dimerization and pathogenic mutation of OPA1. *J Cell Biol.* (2020) 219:e201907098. doi: 10.1083/jcb.201907098

160. Civiletto G, Varanita T, Cerutti R, Gorletta T, Barbaro S, Marchet S, et al. Opa1 overexpression ameliorates the phenotype of two mitochondrial disease mouse models. *Cell Metab.* (2015) 21:845–54. doi: 10.1016/j.cmet.2015.04.016

161. Varanita T, Soriano ME, Romanello V, Zaglia T, Quintana-Cabrera R, Semenzato M, et al. The OPA1-dependent mitochondrial cristae remodeling pathway controls atrophic, apoptotic, and ischemic tissue damage. *Cell Metab.* (2015) 21:834–44. doi: 10.1016/j.cmet.2015.05.007

162. Wu W, Zhao D, Shah SZA, Zhang X, Lai M, Yang D, et al. OPA1 overexpression ameliorates mitochondrial cristae remodeling, mitochondrial dysfunction, and neuronal apoptosis in prion diseases. *Cell Death Dis.* (2019) 10:710. doi: 10.1038/s41419-019-1953-y

Leber's Hereditary Optic Neuropathy: A Report on Novel mtDNA Pathogenic Variants

Lorenzo Peverelli [1,2†], Alessia Catania [1†], Silvia Marchet [1], Paola Ciasca [3], Gabriella Cammarata [3], Lisa Melzi [3], Antonella Bellino [4], Roberto Fancellu [5], Eleonora Lamantea [1], Mariantonietta Capristo [6], Leonardo Caporali [6], Chiara La Morgia [6,7], Valerio Carelli [6,7], Daniele Ghezzi [1,8], Stefania Bianchi Marzoli [3] and Costanza Lamperti [1*]

[1] Unit of Medical Genetics and Neurogenetics, Fondazione IRCCS (Istituto di Ricovero e Cura a Carattere Scientifico) Istituto Neurologico Carlo Besta, Milan, Italy, [2] Neuromuscular and Rare Disease Unit, Department of Neuroscience, Fondazione IRCCS (Istituto di Ricovero e Cura a Carattere Scientifico) Ca' Granda Ospedale Maggiore Policlinico, University of Milan, Milan, Italy, [3] Neuro-Ophthalmology Service and Ocular Electrophysiology Laboratory, Department of Ophthalmology, Scientific Institute Auxologico Capitanio Hospital, Milan, Italy, [4] Neuromuscular Disorders Unit, Fondazione IRCCS (Istituto di Ricovero e Cura a Carattere Scientifico) Istituto Neurologico Carlo Besta, Milan, Italy, [5] Neurology Unit, IRCCS (Istituto di Ricovero e Cura a Carattere Scientifico) Ospedale Policlinico San Martino, Genoa, Italy, [6] IRCCS (Istituto di Ricovero e Cura a Carattere Scientifico) Istituto delle Scienze Neurologiche di Bologna, Unità Operativa Complessa (UOC) Clinica Neurologica, Bologna, Italy, [7] Department of Biomedical and Neuromotor Sciences, University of Bologna, Bologna, Italy, [8] Department of Pathophysiology and Transplantation, University of Milan, Milan, Italy

Leber's hereditary optic neuropathy (LHON) is due to missense point mutations affecting mitochondrial DNA (mtDNA); 90% of cases harbor the m.3460G>A, m.11778G>A, and m.14484T>C primary mutations. Here, we report and discuss five families with patients affected by symptomatic LHON, in which we found five novel mtDNA variants. Remarkably, these mtDNA variants are located in complex I genes, though without strong deleterious effect on respiration in cellular models: this finding is likely linked to the tissue specificity of LHON. This study observes that in the case of a strong clinical suspicion of LHON, it is recommended to analyze the whole mtDNA sequence, since new rare mtDNA pathogenic variants causing LHON are increasingly identified.

Keywords: Leber optic atrophy, mitochondrial respiratory chain, complex I, LHON, transmitochondrial cybrids

INTRODUCTION

Leber's hereditary optic neuropathy (LHON, OMIM #535000) is one of the most common inherited optic neuropathies causing bilateral loss of central vision. LHON is due to missense point mutations affecting mitochondrial DNA (mtDNA), usually found in the homoplasmic state, leading to mitochondrial dysfunction. Thus, LHON is maternally inherited but characterized by incomplete penetrance even in individuals carrying the same homoplasmic pathogenic mutation and with a clear male predilection (1).

Disease onset usually occurs during the second and third decades of life, but the age of onset can span from 2 to 87 (2). LHON typically presents as a painless, subacute, central vision loss in one eye, sequentially spreading to the other eye in weeks or months. Within 1 year, the large majority of affected patients have the second eye involved. Bilateral simultaneous onset occurs in about 25% of patients. During the acute phase, optic disc hyperemia, peripapillary-telangiectatic vessels, vascular tortuosity, and retinal nerve fiber layer (RNFL) pseudo-edema are often detected, even if these features may be subtle, with a slow progression toward blindness (3, 4).

Fundus changes can be accurately quantified by optical coherence tomography (OCT). In the acute phase, the RNFL initially thickens in the temporal and inferior quadrants and then

in the superior and nasal quadrants (5). OCT shows a global RNFL thinning as disease progresses. Visual evoked potentials (VEPs) and pattern electroretinograms (PERG) are typically abnormal, as they reflect optic nerve fiber degeneration (6). The visual prognosis in affected patients is usually poor, also depending on the underlying pathogenic mutation, ranging from individuals declared legally blind, to others who experience spontaneous recovery of visual acuity (7).

Molecular diagnosis currently shows that about 90% of all LHON cases are due to one of three common mtDNA point mutations, at nucleotide positions m.3460, m.11778, and m.14484, defined as "primary mutations." The diagnostic for other polymorphic variants for specific mtDNA backgrounds (haplogroup J) may be preferentially associated with some of the primary mutations (m.11778, and m.14484) exerting a synergistic modifying role; previously these variants were defined as "secondary mutations" (8). The most common is the m.11778G>A (*MT-ND4*, p.Arg340His) mutation, which accounts for ∼70% of all cases, whereas the m.14484T>C (*MT-ND6*,p.Met64Val) and m.3460G>A (*MT-ND1*, p.Ala52Thr) mutations account for ∼15% of cases (1). Recently, several rare or private mtDNA variants have been reported and validated, including the uncommon case of unique combinations of mtDNA polymorphic variants leading to a mild defect of complex I activity (9, 10). In view of these considerations, it has been proposed that, in case of evidence of maternal inheritance and clinical/OCT hallmarks of LHON, if none of the common primary mutations is found, the diagnostic gold standard should be the mtDNA complete sequence analysis (10).

In this report, we present eight patients affected by LHON belonging to five different and unrelated families of European descent, in which we identified five novel mtDNA variants, also providing some functional evidence of possible pathogenicity.

METHODS AND MATERIALS

Informed consent for a biological sample collection of fibroblast cell lines and DNA from blood to perform genetic studies was obtained from all patients involved, in agreement with the Declaration of Helsinki. The Ethical Committee of the Fondazione IRCCS Istituto Neurologico Carlo Besta, Milan, Italy, approved the study.

We have investigated five families with seven male individuals (patients 1, 3, 4, 5, 6, 7, and 8) and one female (patient 2) clinically affected by typical LHON but lacking any of the primary common mutations. A summary of the demographic, clinical, and genetic data is available in **Table 1** (see the **Supplementary Material** for more detailed information).

Fibroblast cultures were obtained from skin biopsies of patients 3, 5, and 6 and from age-matched control subjects. Fibroblast cell lines were cultured in Dulbecco's modified Eagle's

Abbreviations: LHON, Leber hereditary optic neuropathy; RNFL, retinal nerve fiber layer; OCT, optical coherence tomography; VEPs, Visual evoked potentials; PERG, pattern electroretinogram; DMEM, Dulbecco's modified Eagle's medium; FCS, fetal calf serum; OCR, Oxygen Consumption Rate; CS, citrate synthase; SD-OCT, Spectral Domain OCT Analysis; ctrls, controls.

medium (DMEM) supplied with 10% fetal calf serum (FCS) at 37°C in a 5% CO_2 atmosphere (11).

Trans-mitochondrial cybrids were generated from the fibroblasts of patient 6, as previously reported (12, 13).

Molecular analysis was performed on DNA extracted from peripheral blood lymphocytes of the eight patients and the unaffected individual. According to a standardized protocol (14) the entire mtDNA was PCR-amplified in eight overlapping fragments using a specific set of primer pairs. Each of the eight fragments was then sequenced, with four different "forward" primers, using a 3,100 ABI Prism Automated Sequencer. The mtDNA sequence was finally compared with the revised Cambridge reference mtDNA sequence.

Biochemical evaluation of OXPHOS complex activities was performed as previously described (14) in digitonin-treated skin fibroblasts from normal subjects and patients. The same measurements were performed in patient 6's cybrids and corresponding controls. The cells were cultured in a glucose-rich medium. The specific activity of each complex was normalized to citrate synthase activity, used as a standard mitochondrial mass marker.

The oxygen consumption rate (OCR) was measured in the fibroblasts of patients 3, 5, and 6 and in two controls using a SeaHorse FX-96 apparatus (Bioscience, Copenhagen, Denmark) as described in Invernizzi et al. (15) (data shown in **Supplementary Figure 3**). Cells were grown in a glucose-rich medium. Data are expressed as the mean ± SD, and comparisons were performed using a non-paired, two-tail Student *t*-test.

RESULTS

The complete sequence analysis of mtDNA from the eight subjects revealed five putative pathogenic LHON variants, one in each maternal lineage. All of them were absent in the mtDNA sequences from 100 healthy controls (screened and recorded in the in-house database from the Unit of Medical Genetics and Neurogenetics, The Foundation "Carlo Besta" Institute of Neurology). The m.13340 T>C (*MT-ND5*, p.Phe335Ser) variant was identified in patient 1 and in DNA from an affected first-grade female relative (patient 2) and the m.13379 A>G (*MT-ND5*, p.His348Arg) variant in patient 3 and his maternal relative (patient 4); both variants affect the ND5 subunit of complex I. Patient 5 and his asymptomatic first degree relative (subject 1) were shown to carry the m.3632C>T (*MT-ND1*, p.Ser109Phe) variant affecting the ND1 subunit of complex I. The relatives patient 6 and patient 7 carried the m.14538A>G (*MT-ND6*, p.Phe46Leu) variant in the ND6 subunit of complex I. Finally, we identified the m.10350C>A (*MT-ND3*,p.Leu98Met) variant in the ND3 subunit of complex I in patient 8. All variants were homoplasmic. The mtDNA haplogroup was determined for each family group using a specific provider (http//www.haplogrep.uibk.ac.at, not reported for privacy purposes, available on request).

All the identified variants affected evolutionarily highly conserved base pairs within the mitochondrial complex I subunits. More precisely, p.Phe335 and p.His348 are

TABLE 1 | Schematic summary of patients'clinical, instrumental, and molecular examinations (see also **Supplementary Material 1**).

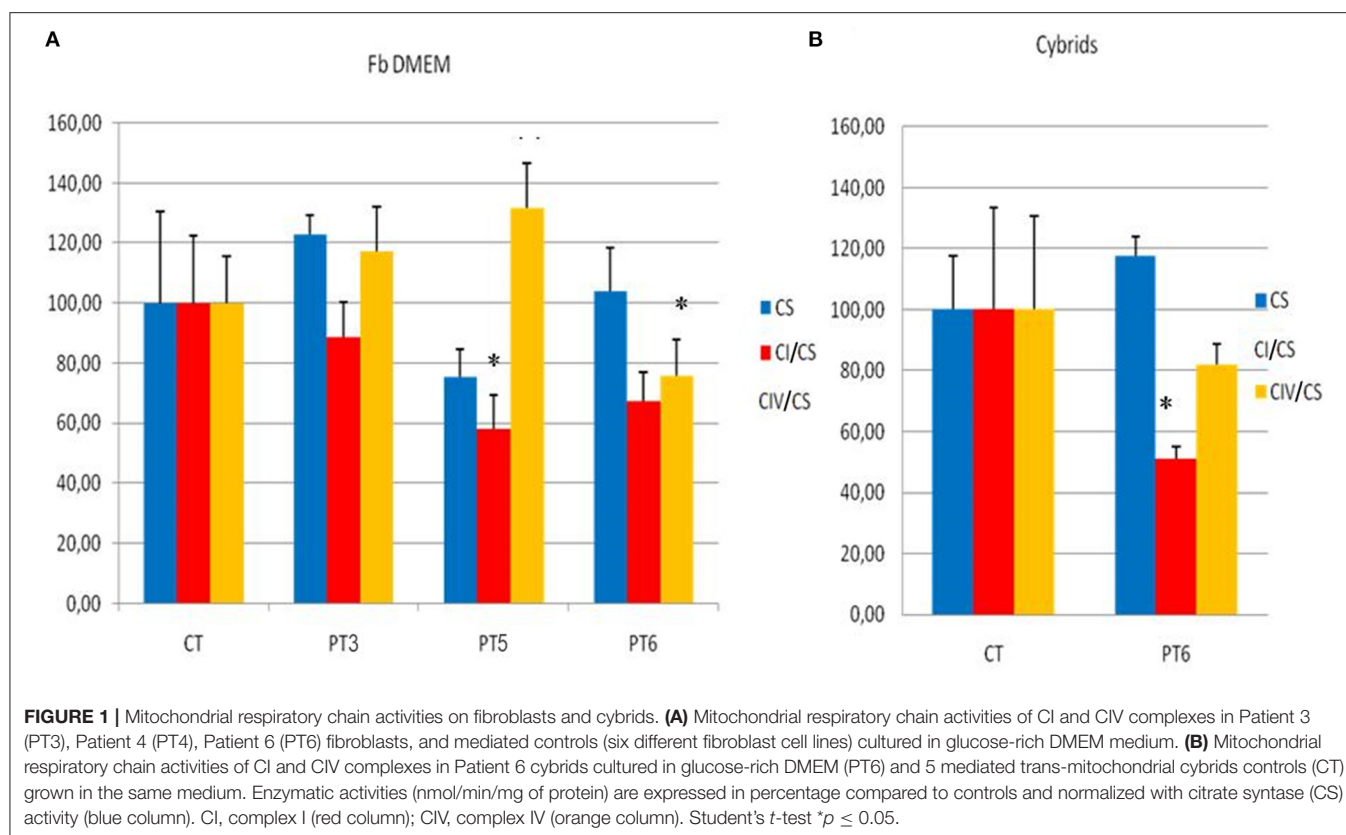|	Family 1		Family 2		Family 3		Family 4		Patient 8
	Patient 1	Patient 2	Patient 3	Patient 4	Patient 5	Subject 1	Patient 6	Patient 7	
Gender	M	F	M	M	M	F	M	M	M
Age range at onset	>40	>50	20–40	<20	20–40	20–40	20–40	20–40	>40
Affected eye	OU	LE	RE	UN	LE	NN	LE	OU	LE
Time to second eye involvement	NN	NN	Two months	UN	One month	NN	Three months	NN	One month
Clinical onset	Acute painless vision loss	Acute painless vision loss	Acute painless vision loss	Acute painless vision loss	Acute painless vision loss	NN	Acute painless vision loss	Acute painless vision loss	Acute painless vision loss
Alcoholic use Y/N	Y	N	N	UN	N	N	N	N	N
B12/folate bloodlevel	NR/NR	UN	NR/RD	NR/NR	NR/NR	NR/NR	NR/NR	NP	NR/NR
Smoke Y/N	Y	N	N	UN	Y	N	N	N	N
SD-OCT (average)	Normal PRNFL thickness OU (RE 108.25 LE 106.58 µm); Reduction of GCC thickness OU in perifoveal region (RE 84.43 LE 86.72 µm);	UN	PRNFL: RE focal increase of thickness in the superior pole (RE 120.06 µm); LE focal increase of thickness in the superior and inferior pole (LE 148.79 µm); diffused reduction of GCC in RE (63.12 µm), LE reduction in the perifoveal region (86.06 L µm)	UN	Reduction of PRNFL in OU In the inferior pole (RE 108.06 µm LE 92.50 µm); reduction of GCC thickness in OU (RE 86.63 µm; LE 92.62 µm)	NP	Reduction PRNFL in OU (RE 41.74 µm; L 42.54 µm); reduction of GCC thickness in OU in perifoveal region (RE 52.75 µm LE 56.99 µm)	Reduction of PRNFL in OU (RE 67.44 µm; LE 69.89 µm); reduction of GCC thickness in OU (RE 58.32 µm; LE 54.01 µm);	Reduction of PRNFL in OU (RE 76.69 µm; LE 72.96 µm); reduction of GCC thickness in OU in perifoveal region (RE 71.32 µm; LE 71.25 µm)
VEP	OU: Increased latency and RD amplitude, more evident with pattern stimulus 15′ (papillo-macular bundle)	UN	Did not show a replicable response	UN	RE 60′ Irregular morphology and reduced amplitude, 15′ : not replicable response; LE 60′ e 15′ not replicable response	NP	RD amplitude and delayed P100 OU sx > dx (60′ e 15′)	RD amplitude and increased latency OU at 60′ and 15′	RE increase in latency and RD amplitude (60′); not replicable response (15′). LE not replicable response (60′ e 15′)
PERG	OU RD amplitude of N95	UN	OU RD amplitude of N95	UN	OU RD amplitude of N95	NP	OU amplitude RD of N95	RE not detectable; LE RD amplitude of N95	OU amplitude reduction of N95

(Continued)

111

TABLE 1 | Continued

	Family 1		Family 2		Family 3		Family 4		Patient 8
	Patient 1	Patient 2	Patient 3	Patient 4	Patient 5	Subject 1	Patient 6	Patient 7	
Brain MRI	NR	NP	Enhancement of optic nerves bilaterally	NP	Bilateral hyperintensity of optic nerves, chiasm and part of the optical tracts.	NP	Unspecific, bilateral frontal white matter minimal alterations and bilateral thinning of optic nerves chiasm and optic tracts along with mild hyperintensity without enhancement.	Unspecific white matter lesions in T2-FLAIR infero-frontal lobe Left-side and anterior insular Right-side and iperT2 of the posterior part of the optic nerve without enhancement.	Mild swelling of the intraorbital ocular nerves portion.
Therapy (315 mg/die)	Idebenone (started 14 month after the exordium)	Idebenone (started 1 month after the onset)	Idebenone (started 5 month after the exordium)	NN	Idebenone (started 2 month after the exordium)	NN	Idebenone (started 8 month after the exordium)	Idebenone (started 12 years after the exordium)	Idebenone (started 4 month after the exordium)
Recovery	From finger count to 0.2 OU	NN	From finger count to 0.025 OU	NN	From 0.025 to 1 (RE) and 0.025 (LE) to 0.05 (RE) OS: 0.066 (LE)	NN	0.2 (RE), 0.1 (LE) without improvement	0.05 (RE) and 0.1 (LE) without improvement	From finger count (LE) and 0.6 (RE); to 0.025 (LE) and 0.025 (RE)
Mutation and localization	m. 13340 T>C, p.Phe335Ser on p.MT-ND5	m. 13340 T>C, p.Phe335Ser on p.MT-ND5	m.13379 A>G, p.His348Arg on p.MT-ND5	m.13379 A>G, p.His348Arg on p.MT-ND5	m.3632C>T, p.Ser109Phe on p.MT-ND1	m.3632C>T, p.Ser109Phe on p.MT-ND1	m.14538A>G, p.Phe46Leu on p.MT-ND6	m.14538A>G, p.Phe46Leu on p.MT-ND6	m.10350C>A, p.Leu98Met on p.MT-ND3

BL, Bilateral; GCC, macular ganglion cell layer; F, female; LE, Left Eye; M, male; MRI, Magnetic Resonance Image; N, no; NN, none; NP, Not Performed; NR, Normal; OU, Both eyes; PERG, pattern electroretinogram; PRNFL, peripapillary retinal nerve fiber layer; RD, reduced; RE, Right Eye; SD-OCT, Spectral Domain Optical Coherence Tomography Analysis; UN, Undetermined; VEPs, Visual evoked potentials; Y, yes.

FIGURE 1 | Mitochondrial respiratory chain activities on fibroblasts and cybrids. **(A)** Mitochondrial respiratory chain activities of CI and CIV complexes in Patient 3 (PT3), Patient 4 (PT4), Patient 6 (PT6) fibroblasts, and mediated controls (six different fibroblast cell lines) cultured in glucose-rich DMEM medium. **(B)** Mitochondrial respiratory chain activities of CI and CIV complexes in Patient 6 cybrids cultured in glucose-rich DMEM (PT6) and 5 mediated trans-mitochondrial cybrids controls (CT) grown in the same medium. Enzymatic activities (nmol/min/mg of protein) are expressed in percentage compared to controls and normalized with citrate syntase (CS) activity (blue column). CI, complex I (red column); CIV, complex IV (orange column). Student's *t*-test *$p \leq 0.05$.

conserved in 97 and 94%, respectively, of more than 5,000 p.MT-ND5 sequences from protists to humans (16); from the same database, p.Ser109 results conserved in 80%, and p.Leu98 in 94% homolog sequences. However, p.Phe46 is only conserved in 16% of more than 5,000 p.MT-ND6 sequences. All the affected amino acid residues are located in transmembrane domains or adjacent to them. These variants are reported as probably damaging by most of the commonly used prediction software (**Supplementary Table 1**), although the predictions were not fully consistent; notably, the same results were observed even for other known LHON mutations.

The mitochondrial respiratory chain activity in fibroblasts from three unrelated patients (patients 3, 5, and 6) harboring three different variants (p.His348Arg in *MT-ND5*, p.Ser109Phe in *MT-ND1*, and p.Phe46Leu in *MT-ND6*) showed a significant reduction in complex I activity in the fibroblasts from patients 5 and 6 (compared with age and sex-matched controls), whereas in patient 3 there was only a slight, nonsignificant reduction (**Figure 1A**). A statistically significant reduction of complex I activity was confirmed in cybrids of patient 6 compared with controls (**Figure 1B**).

Finally, the oxygen consumption rate (OCR) failed to show any clear difference in mitochondrial respiration rate in all patients analyzed (patients 3, 5, and 6) (see **Supplementary Figure 3**). SeaHorse respirometry was not performed on cybrids.

DISCUSSION

In this study, we report five putatively pathogenic mtDNA variants, all affecting ND subunits of complex I, in 8 patients form 5 unrelated families presenting with a classical LHON phenotype.

All of them are not present in diverse genomic databases (Mitomap, Ensembl, and Genome Browser) and were not present in the mtDNA from 100 healthy controls, suggesting a pathogenic association of these variants with LHON.

As further support to our hypotheses of pathogenicity, all these variants are extremely rare also in the set of 195,983 individuals from HelixMTdb (17) and 51,836 individuals from GenBank databases. In particular, m.3632C>T has been found only once in the heteroplasmic state in HelixMTdb and not once in GenBank databases; m.10350C>A has been found in the homoplasmic state only once in HelixMTdb and no individuals in Genbank; m.13340T>C has been found twice in the homoplasmic state and twice in the heteroplasmic state in HelixMTdb and in no individual from GenBank; m.13379A>G was not found in HelixMTdb nor in GenBank; finally, m.14538A>G was found once in the homoplasmic state in HelixMTdb and was not found in GenBank.

In silico prediction of pathogenicity using online resources classified the m.13340T>C, m.13379A>G, and m.3632C>T variants as functionally "deleterious"; the scores of pathogenicity were less consistent for the m.10350C>A variant and to a greater extent for the m.14538A>G variant. Four of them (m.13340

T>C, m.3632C>T, m.14538A>G, and m.10350C>A) have not previously been reported. Interestingly, the m.13379 A>G (*MT-ND5*) variant has been very recently found in an unrelated patient affected by typical LHON disease (18), thus representing an additional proof of its probable pathogenicity.

To further validate the pathogenicity of the mtDNA variants identified, we tested biochemical activity of respiratory complexes on both fibroblasts (from three patients) and cybrids (from one patient). We observed, to a variable extent, a reduction of complex I activity (**Figure 1**). SeaHorse respirometry, however, failed to show defective oxygen consumption. These results are not surprising; in fact, there is much evidence that even confirmed pathogenic LHON mutations may not display any detectable respiratory chain defect (19–22). High-resolution respirometry performed on fibroblasts from the recently described patient carrying the m.13379 A>G variant, gave ambiguous results, as well (15). The authors also report a high level of ROS production and a reduction of mitochondrial membrane potential (15).

It is worth considering that LHON is a tissue-specific disease, involving retinal ganglion cells and the optic nerve. Thus, the biochemical assessments performed on skin fibroblasts, a tissue not involved in the disease phenotype, may not necessarily mirror the respiratory activity of the tissue targeted by the disease. Besides, even for the three best-known primary mutations there is no validated biochemical method to prove their pathogenicity on fibroblasts.

The possible contribution of nuclear gene variants as molecular modifiers for the development of symptomatic LHON is not yet established and currently represents a challenging topic, worth further exploration. However, it has been previously reported that specific mitochondrial haplogroups, such as the haplogroup J, exert the role of penetrance modifiers in LHON (23). In fact, both LHON primary mutation m.11778G>A/*MT-ND4* and m.14484T>C/*MT-ND6*, when occurring on either a J1c or J2b mtDNA haplogroups, have increased risk of being symptomatic (23). In our cohort, one of the above-mentioned haplogroups was detected in patients 3 and 4. Notably, patient 3, despite Idebenone therapy, has been treated for more than 1 year but has not improved his visual function, supporting previous reports (23). Idebenone was administered to all affected patients (with exclusion of patient 4). All but patient 7, for whom therapy was started 12 years after the clinical onset due to misdiagnosis, received therapy roughly within the first year after onset. In five out of seven cases, idebenone treatment has been continued for more than 2 years with the exception of patient 2 (treated for slightly longer than 1 year) and patient 8, who has been treated for 5 months at the time of this study. We observed improvement in visual acuity in three out of six patients, stability in two, and a clear worsening in one (**Table 1**). In summary, therapy effectiveness for patients harboring these five novel mtDNA variants is in line with previously reported data on LHON due to "classic" mutations (1). Since the two patients in whom idebenone was ineffective carry the same m.14538A>G, we may speculate that this variant could be less responsive to therapy.

The peak age of disease onset was between the second and the third decades of life, and it is unusual for LHON patients to experience vision loss beyond 50 years of age, unless triggering factors have favored the disease onset as recently proposed (24). In relation to this observation, it is worth noticing that patients 1, 2, and 8 had late onset vision loss, the first around 50 and the third when he was almost 60. We may speculate that the variants in family 1 and patient 8 (m.13340 T>C and m.10350C>A) could be linked to phenotypes with later onset compared with classic LHON. Patient 1 was a heavy smoker and LHON vision loss occurred after at least 20 years of tobacco smoking and alcohol consumption (25, 26). However, familiar history supports pathogenicity of the identified variant, as a first-grade female relative (patient 2) affected by later onset LHON was found to be also positive for this variant. In patient 1 smoking and alcohol consumption could have contributed to accelerating the clinical onset. However, in patient 8, neither smoking nor alcohol abuse was reported; in this case, the identified variant (m.10350C>A) may be independently related to a later onset disease phenotype, or it could represent an additional predisposing factor within a specific genetic background or some other underrecognized triggering environmental/epigenetic influence. The latter is the most probable hypothesis, since we have an overall lower evidence of pathogenicity.

Possible variants on nuclear DNA have not been investigated in our group of patients because, with the exclusion of the recently reported *DNAJC30* gene (27), all the other nuclear genes have been associated with complex phenotypes rather than isolated Leber's hereditary optic neuropathy. *DNAJC30* has a "relevant" prevalence only in the Eastern European populations (none of our patients has such origins); moreover, it shows a recessive mode of inheritance that is not compatible with some of our pedigrees.

In conclusion, our study aims to emphasize the diagnostic relevance of running the whole mtDNA sequence analysis whenever LHON is documented on the clinical/OCT ground and the common mtDNA mutations are not detected, since rare or private mtDNA variants may be found (9). Besides, thanks to the advancement of the sequencing technologies, NGS is now widely available in most of the laboratories for mtDNA screening and is expected to become the method of choice for genetic analysis on mtDNA since it allows a rapid and cost-effective sequencing of the whole mtDNA with concurrent accurate quantification of heteroplasmy levels for point mutations (28). Remarkably, also, in our case series the novel mtDNA variants invariably affected ND subunits of complex I, and functional studies support a slight but detectable biochemical defect of complex I function in some of them. However, in all of them, we found relevant biological (low frequency of the identified variants in general population, evolutionary conservation, key location within complex I, and pathogenicity prediction) or clinical (typical course of disease and neuro-ophthalmological findings, family history) plausibility in support of their possible pathogenicity or potential contribution to pathogenicity in combination with other not yet determined genetic or extrinsic factors. Validation in further families will be necessary to consolidate the pathogenic role of these novel mtDNA variants in LHON. The possible role of other nuclear genes or environmental factors as disease modifiers needs to be further explored in future studies.

DATA AVAILABILITY STATEMENT

The original contributions presented in the study are publicly available. This data can be found here: https://zenodo.org/record/4683798#.YHfsV-gzaUk.

ETHICS STATEMENT

The studies involving human participants were reviewed and approved by the Ethical Committee of the Fondazione IRCCS Istituto Neurologico Carlo Besta, Milan. The patients/participants provided their written informed consent to participate in this study.

AUTHOR CONTRIBUTIONS

LP and AC performed neurologic evaluations and wrote the paper. SM, EL, and MC performed *in vitro* studies. RF helped with patients selection. PC, GC, and LM performed all neuro-ophthalmological evaluations and contributed to manuscript preparation. AB, LC, and CLM assisted in data analysis and manuscript preparation. VC, DG, SB, and CL led the overall effort. All authors contributed to the article and approved the submitted version.

SUPPLEMENTARY MATERIAL

The Supplementary Material for this article can be found online at: https://www.frontiersin.org/articles/10.3389/fneur.2021.657317/full#supplementary-material

REFERENCES

1. Yu-Wai-Man P, Griffiths PG, Chinnery PF. Mitochondrial optic neuropathies - disease mechanisms and therapeutic strategies. *Prog Retin Eye Res.* (2011) 30:81–114. doi: 10.1016/j.preteyeres.2010.11.002

2. Riordan-Eva P, Sanders MD, Govan GG, Sweeney MG, Da Costa J, Harding AE. The clinical features of Leber's hereditary optic neuropathy defined by the presence of a pathogenic mitochondrial DNA mutation. *Brain.* (1995) 2(118 Pt):319–37. doi: 10.1093/brain/118.2.319

3. Carelli V, Chan DC. Mitochondrial DNA: impacting central and peripheral nervous systems. *Neuron.* (2014) 84:1126–42. doi: 10.1016/j.neuron.2014.11.022

4. La Morgia C, Carbonelli M, Barboni P, Sadun AA, Carelli V. Medical management of hereditary optic neuropathies. *Front Neurol.* (2014) 5:141. doi: 10.3389/fneur.2014.00141

5. Barboni P, Carbonelli M, Savini G, Ramos CV, Carta A, Berezovsky A, et al. Natural history of Leber's hereditary optic neuropathy: longitudinal analysis of the retinal nerve fiber layer by optical coherence tomography. *Ophthalmology.* (2010) 117:623–7. doi: 10.1016/j.ophtha.2009.07.026

6. Ziccardi L, Sadun F, De Negri AM, Barboni P, Savini G, Borrelli E, et al. Retinal function and neural conduction along the visual pathways in affected and unaffected carriers with Leber's hereditary optic neuropathy. *Invest Ophthalmol Vis Sci.* (2013) 54:6893–901. doi: 10.1167/iovs.13-12894

7. Kirkman MA, Korsten A, Leonhardt M, Dimitriadis K, De Coo IF, Klopstock T, et al. Quality of life in patients with Leber hereditary optic neuropathy. *Invest Ophthalmol Vis Sci.* (2009) 50:3112–5. doi: 10.1167/iovs.08-3166

8. Caporali L, Maresca A, Capristo M, Del Dotto V, Tagliavini F, Valentino ML, et al. Incomplete penetrance in mitochondrial optic neuropathies. *Mitochondrion.* (2017) 36:130–7. doi: 10.1016/j.mito.2017.07.004

9. Achilli A, Iommarini L, Olivieri A, Pala M, Hooshiar Kashani B, Reynier P, et al. Rare primary mitochondrial DNA mutations and probable synergistic variants in Leber's hereditary optic neuropathy. *PLoS One.* (2012) 7:e42242. doi: 10.1371/journal.pone.0042242

10. Caporali L, Iommarini L, La Morgia C, Olivieri A, Achilli A, Maresca A, et al. Peculiar combinations of individually non-pathogenic missense mitochondrial DNA variants cause low penetrance Leber's hereditary optic neuropathy. *PLoS Genet.* (2018) 14:e1007210. doi: 10.1371/journal.pgen.1007210

11. Munaro M, Tiranti V, Sandonà D., Lamantea E, Uziel G, Bisson R, et al. A single cell complementation class is common to several cases of cytochrome c oxidase-defective Leigh's syndrome. *Hum Mol Genet.* (1997) 6:221–8. doi: 10.1093/hmg/6.2.221

12. King MP, Attardi G. Human cells lacking mtDNA: repopulation with exogenous mitochondria by complementation. *Science.* (1989) 246:500–3. doi: 10.1126/science.2814477

13. King MP, Attardi G. Isolation of human cell lines lacking mitochondrial DNA. *Methods Enzymol.* (1996) 264:304–13. doi: 10.1016/S0076-6879(96)64029-4

14. Bugiani M, Invernizzi F, Alberio S, Briem E, Lamantea E, Carrara F, et al. Clinical and molecular findings in children with complex I deficiency. *Biochim Biophys Acta.* (2004) 1659:136–47. doi: 10.1016/j.bbabio.2004.09.006

15. Invernizzi F, D'Amato I, Jensen PB, Ravaglia S, Zeviani M, Tiranti V. Microscaleoxygraphy reveals OXPHOS impairment in MRC mutant cells. *Mitochondrion.* (2012) 12:328–35. doi: 10.1016/j.mito.2012.01.001

16. Martín-Navarro A, Gaudioso-Simón A, Álvarez-Jarreta J, Montoya J, Mayordomo E, Ruiz-Pesini E. Machine learning classifier for identification of damaging missense mutations exclusive to human mitochondrial DNA-encoded polypeptides. *BMC Bioinformatics.* (2017) 18:158. doi: 10.1186/s12859-017-1562-7

17. Bolze A, Mendez F, White S, Tanudjaja F, Isaksson M, Jiang R, et al. A catalog of homoplasmic and heteroplasmic mitochondrial DNA variants in humans. *bioRxiv [Preprint].* (2020). doi: 10.1101/798264

18. Krylova TD, Sheremet NL, Tabakov VY, Lyamzaev KG, Itkis YS, Tsygankova PG, et al. Three rare pathogenic mtDNA substitutions in LHON patients with low heteroplasmy. *Mitochondrion.* (2020) 50:139–44. doi: 10.1016/j.mito.2019.10.002

19. Brown MD, Trounce IA, Jun AS, Allen JC, Wallace DC. Functional analysis of lymphoblast and cybrid mitochondria containing the 3460, 11778, or 14484 Leber's hereditary optic neuropathy mitochondrial DNA mutation. *J Biol Chem.* (2000) 275:39831–6. doi: 10.1074/jbc.M006476200

20. Hofhaus G, Johns DR, Hurkoi O, Attardi G, Chomyn A. Respiration and growth defects in transmitochondrial cell lines carrying the 11778 mutation associated with Leber's hereditary optic neuropathy. *J Biol Chem.* (1996) 271:13155–61. doi: 10.1074/jbc.271.22.13155

21. Majander A, Huoponen K, Savontaus M, Nikoskelainen EK, Wikstrom M. Electron transfer properties of NADH-ubiquinone the rarity of symptoms outside the optic pathways. The reductase in the NA1/3460 and the ND4/11778 mutations of the Leber hereditary optic neuroretinopathy (LHON). *FEBS Lett.* (1991) 292:289–92 doi: 10.1016/0014-5793(91)80886-8

22. Cock HR, Cooper JM, Schapira AHV. The 14484 ND6 mtDNA mutation in Leber hereditary optic neuropathy does not affect fibroblast complex I activity. *Am J Hum Genet.* (1995) 57:1501–2.

23. Carelli V, Achilli A, Valentino ML, Rengo C, Semino O, Pala M, et al. Haplogroup effects and recombination of mitochondrial DNA: novel clues

from the analysis of Leber hereditary optic neuropathy pedigrees. *Am J Hum Genet*. (2006) 78:564–74. doi: 10.1086/501236

24. Carelli V, d'Adamo P, Valentino ML, La Morgia C, Ross-Cisneros FN, Caporali L, et al. Parsing the differences in affected with LHON: genetic versus environmental triggers of disease conversion. *Brain*. (2016) 139(Pt 3):e17. doi: 10.1093/brain/awv339

25. Kirkman MA, Yu-Wai-Man P, Korsten A, Leonhardt M, Dimitriadis K, De Coo IF, et al. Gene-environment interactions in Leber hereditary optic neuropathy. *Brain*. (2009) 132(Pt 9):2317–26 doi: 10.1093/brain/awp158

26. Carelli V, Franceschini F, Venturi S, Barboni P, Savini G, Barbieri G, et al. Grand rounds: could occupational exposure to n-hexane and other solvents precipitate visual failure in leber hereditary optic neuropathy? *Environ Health Perspect*. (2007) 115:113–5. doi: 10.1289/ehp.9245

27. Wiggs JL. DNAJC30 biallelic mutations extend mitochondrial complex I-deficient phenotypes to include recessive Leber's hereditary optic neuropathy. *J Clin Invest*. (2021) 131:e147734. doi: 10.1172/JCI147734

28. Legati A, Zanetti N, Nasca A, Peron C, Lamperti C, Lamantea E, et al. Current and new Next-Generation Sequencing approaches to study mitochondrial DNA. *J Mol Diagn*. (2021) 1525–78. doi: 10.1016/j.jmoldx.2021.03.002. [Epub ahead of print].

Advantages of publishing in Frontiers

OPEN ACCESS
Articles are free to read
for greatest visibility
and readership

FAST PUBLICATION
Around 90 days
from submission
to decision

HIGH QUALITY PEER-REVIEW
Rigorous, collaborative,
and constructive
peer-review

TRANSPARENT PEER-REVIEW
Editors and reviewers
acknowledged by name
on published articles

Frontiers
Avenue du Tribunal-Fédéral 34
1005 Lausanne | Switzerland

Visit us: www.frontiersin.org
Contact us: frontiersin.org/about/contact

**REPRODUCIBILITY OF
RESEARCH**
Support open data
and methods to enhance
research reproducibility

DIGITAL PUBLISHING
Articles designed
for optimal readership
across devices

FOLLOW US
@frontiersin

IMPACT METRICS
Advanced article metrics
track visibility across
digital media

EXTENSIVE PROMOTION
Marketing
and promotion
of impactful research

LOOP RESEARCH NETWORK
Our network
increases your
article's readership